SVENSKA GEOFYSISKA FÖRENINGEN

VOLUME 4, NUMBER 4 **Tellus** NOVEMBER 1952

A QUARTERLY JOURNAL OF GEOPHYSICS

On the Content of Nitrogen in Atmospheric Precipiation in Sweden. II.

By ANDERS ÅNGSTRÖM and LINUS HÖGBERG
Swedish Meteorological and Hydrological Institute, Stockholm

(Manuscript received 3 November 1952)

Abstract

In the present paper an attempt is made to give a general idea of the geographical distribution of fixed nitrogen (NH_4-N) transferred to the soil through precipitation in Sweden. Further a map is given showing the distribution af α, a quantity proportional to the nitrogen concentration in the precipitation at the beginning of a rain and, it is assumed, representative for the content of fixed nitrogen in the atmosphere before the rain is falling.

A discussion of different causes of the concentration of fixed nitrogen in precipitation is presented and a photochemical process is suggested, which would explain the almost constant ratio between NH_4-N and NO_3-N frequently found within the temperate zones. It is evident, however, that other causes also are at work, especially at lower latitudes. The need of laboratory experiments is emphasized.

In our previous paper on this subject (ÅNGSTRÖM, HÖGBERG 1952), we reached the conclusion that the concentration of NH_4-N and NO_3-N in precipitation is dependent upon the amount of precipitation previously fallen. We further found a pronounced dependence of the concentration on the character of the air mass. Thus the tropical air contains between 10 and 30 per cent greater amount of nitrogen than the polar air, and almost double the amount found in the arctic air.

An attempt was made to express mathematically the change of concentration in its dependence of the quantity of precipitation fallen. The following expression was found valid:

$$s = \alpha \log (1 + P) \qquad (1)$$

where s is the quantity of nitrogen transferred through the precipitation P, and α is an arbitrary constant. The equation evidently implies that the concentration at a given moment in the falling precipitation is gradually decreasing. It has its largest value at the beginning of the rain, at which time the concentration has the value α. Referred to a certain given precipitation the quantity of nitrogen transferred is proportional to α.

For a given locality two quantities seem in this connection to be of a general importance, namely (1) the quantity of nitrogen, s, transferred through precipitation during the year and during different parts of it, and (2) the quantity α, denoting the nitrogen concentration at the beginning of precipitation. It seems reasonable to assume that α can be regarded as a measure on the nitrogen content of the atmosphere before the precipitation is beginning to fall.

Now the quantity s of nitrogen transferred in every individual case of precipitation has been measured only at Ultuna D and it is

Fig. 1. Station map.

from these measurements that the equation (1) and consequently also the value of α has been computed. At all other stations the quantity s measured refers only to the monthly sums, s_m. If we assume, which seems reasonable, that the transfer of nitrogen at all stations is connected to the precipitation already fallen through an equation of the general form (1) we can on the basis of this assumption and knowing the frequencies of different amounts of rain compute α for the different stations. We have namely then:

$$s_m = \Sigma s = \alpha \Sigma \log (1 + P_i) \qquad (2)$$

At this process of adding up, we have not taken account to the occurrence of different air masses or their trajectories; the coefficient α consequently corresponds to a mean value for cases where α has had rather different values. As the separation of one case of precipitation from another often meets with great difficulties, a simplified procedure has been applied, in the same way as in our previous paper: instead of taking the sum corresponding to all the separate precipitation values the terms have been referred to the separate daily totals. As it is not quite clear, without further, that this simplification does not include considerable differences between the results of the two methods of computation respectively, we have computed α_D for the station Ultuna D according to the more exact procedure — separate occasions of precipitation — and compared it with the α_A computed for the station Ultuna A, situated in the immediate vicinity of Ultuna D. In the former case we got a value: $\alpha_D = 0.0275$, in the latter one: $\alpha_A = 0.029$. For the purposes here in view it therefore seems reasonable to exchange the more cumbersome method, which it is not possible to apply at most stations, against the simplified one.

If we let n_i represent the frequency value for different intervalls within the daily precipitation observations and further P_i the corresponding mean value of the precipitation for the same intervall, we get, using ^{10}logaritms:

$$s_m = \alpha \sum_i n_i \log (1 + P_i) \qquad (3)$$

For daily precipitations above 40 mm the mean P_i has been evaluated to be 50 mm. The total precipitation and the number n_i of precipitation days are given in tables 1—2.

On the basis of these assumptions the table 3 has been computed. For comparison the tables 4—5 also are shown here. They refer to the content of NH_4-N alone. The reasons for not including NO_3-N also, will be given below.

Variation of s and α with the time of the year.

It is evident from the results already obtained that the quantity s is dependent not

only of α, the concentration when precipitation is starting, but also of the quantity of precipitation and of its frequency distribution. If we assume for a given station as well α as also the annual precipitation P to be given, the quantity s is still undetermined as we do not know the way in which P is distributed on more or less heavy rains. The more P is devided up on small quantities of precipitation, the larger we ought to expect s to be. On the other hand α, as it has been defined above, is independent as well of the amount of precipitations as of its frequency distribution. Its value therefore has a more fundamental character than s.

If we consider first the variation of α with the time of the year, we find for all stations a pronounced maximum in the spring and a minimum in the autumn or the winter. Exactly the same annual variation is in fact characteristic at the northern hemisphere for the content of solid or liquid particles in the air which give rise to the scattering of sun radiation. The cause of this variation may not be a single one. That the instability of the atmosphere, which reaches a maximum in the spring on account of the heating from below, must have en effect of permitting dust and pollen to be more freely carried from the earths surface to the atmosphere, seems rather evident. But it seems also probable that the effect of precipitation in washing out particles or molecules from the atmosphere ought to be least pronounced at the time of the year when the amount of precipitation itself has a minimum. The annual variation found to exist, seems on the other hand to speak against the electrical discharges in the atmosphere as producing to considerable extent the nitrogen ions here concerned. The electrical phenomena have on the northern hemisphere in general a pronounced maximum in the summer months July—August, a maximum not at all reflected in the variation neither of α or s. That thunderstorms, and electrical discharges in the atmosphere in general, must produce nitrogen ions, especially nitrogen oxides and related compounds, seems evident from other researches, but it seems on the other hand probable from the material here treated that phenomena must be of a secondary character as regards the causes of the nitrogen content in precipitation.

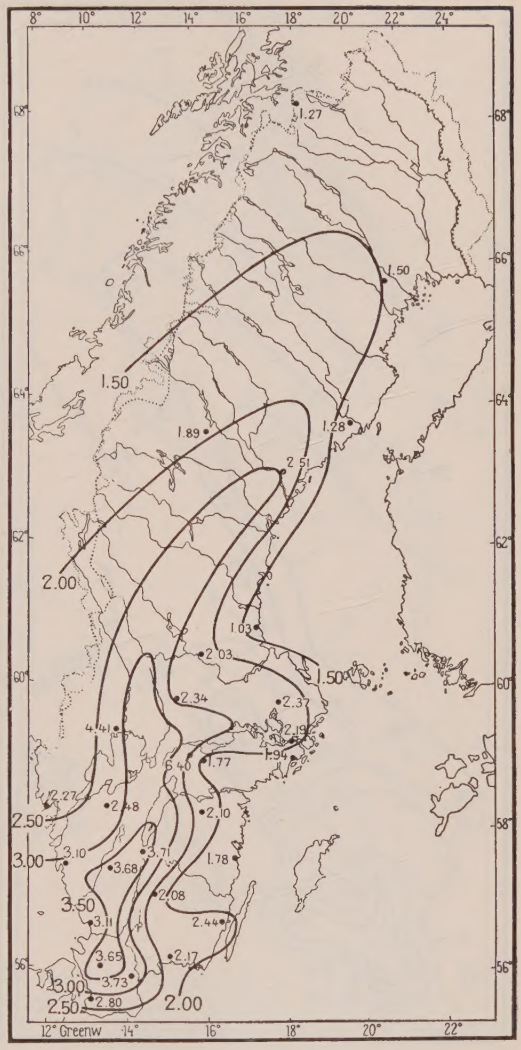

Fig. 2. Geographical distribution of annual amount of NH_4 in precipitation (kg per ha).

The annual variation of s as it appears from table 3 is evidently closely related to the amount of precipitation.

Geographical distribution of NH_4—N in precipitation.

The stations at which measurements have been made of the nitrogen concentration are not numerous enough to give more than a rather superficial idea of the geographical distribution. Yet, in figs. 2—3, an attempt is

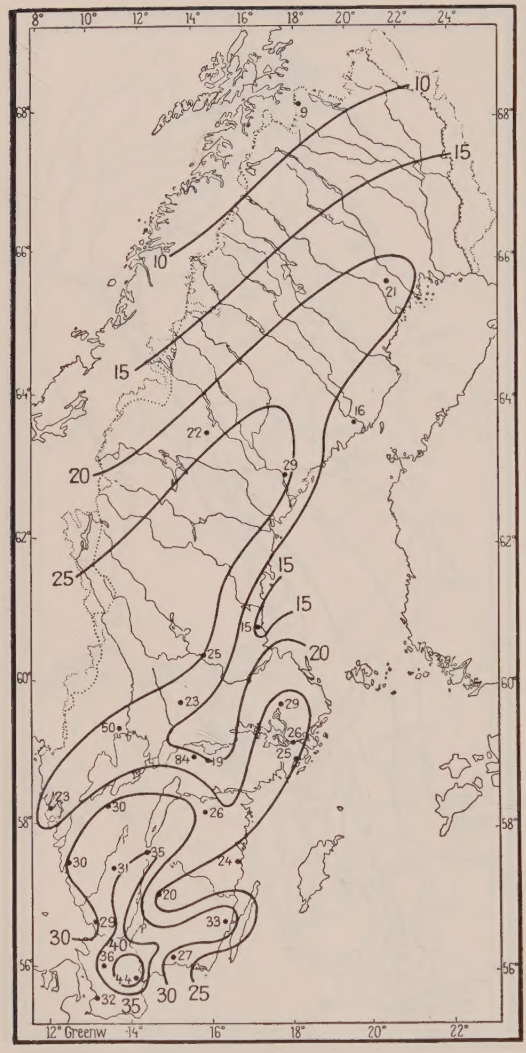

Fig. 3. Geographical distribution of average value of α for the year. The actual values of α are here multiplied by 10^3.

made to draw a map showing lines of equal α and s. If we make an exception for the station Kvarntorp, which will be discussed below, we generally find the quantity s to depend on the amount of precipitation, in the way that low values on the precipitation correspond also to low values for s and vice versa. There is, however, also a decided dependence on latitude, in the way that the nitrogen transfer through precipitation decreases with an increase in latitude. The highest values on s are found in the southwestern parts of Sweden, where its value in general is considerably higher than 3 kg per ha (10^4 m^2). Special attention must be given to the high values at the stations Kvarntorp and Varpnäs. As regards the former station the high value is undoubtedly a consequence of the industrial activity at that place. The same may be the case at Varpnäs.

As regards α there seems to be no decided dependence on the total precipitation. The most apparent characteristics as regards the general distribution seem to be the dependence on latitude, the values decreasing generally from south to north as illustrated in figs. 4—5.

Trying to find an equation satisfying these values in their dependence of latitude within Sweden, we get:

$$\alpha = 0.10 \cos^2\varphi \qquad (4)$$

$$\text{and} \quad s = 9.1 \cos^2\varphi \text{ kg/ha} \qquad (5)$$

As well α as s refer here to the NH_4-N alone. It could perhaps be expected that a similar treatment as that described above would give us the geographical and annual variation of α and s, referred to NO_3-N, which nitrogen element has also been measured in a similar way as NH_4-N. However, in the course of the treatment of the material of observations, it became clear, that only the momentary measurements of NO_3-N, referring to separate days or separate occasions of precipitation could be fully depended upon. The measurements referring to accumulated NO_3-N for the month or longer periods were affected, from causes still not clear, with considerable errors. Only the measurements of NO_3-N at Ultuna could therefore be regarded as reliable. In order to get an idea of the probable transfer of NO_3-N in its geographical and annual variation, we therefore were induced to base our considerations on the intimate correlation found to exist between NH_4-N and NO_3-N at Ultuna *D*. This correlation is clearly demonstrated in table 6. If we compute the correlation coefficient between the quantities of N transferred in the form of NH_4 and NO_3 respectively (in gram per ha), we get:

$$r = 0.777 \pm 0.025$$

The relationship can be well expressed through the linear equation:

$$s_{NO_3} = 0.48 s_{NH_4}$$

which implies that the quantity of nitrogen transferred to the ground in precipitation in the form of NO_3 is just about the half of the quantity transferred as NO_4.

Consequently, in order to get total quantity of nitrogen transferred through precipitation, we have to add 50 per cent to the values for NH_4 alone, viz to the values on the maps fig. 3 and in the table 4.

Remarks and suggestions

A historical survey on the investigations concerned with nitrogen in precipitation has been given by ERIK ERIKSSON (1952). Another very valuable survey has been presented by G. EVELYN HUTCHINSON (1945). Both papers together give a rather clear idea of the present state of the question. We may then limit ourselves to mention here some results of immediate bearing upon our present work.

In the first place some researches of A. H. WOODCOCK (1952) of SUGAWARA (1949), and of Y. MIYAKE and Y. SIGIURA (1950) to which our attention has been drawn after the writing of our first paper ought to be mentioned. These authors have all investigated the chloride concentration in rain, and they have obtained results similar to our own in the respect that the concentration generally decreases with time and with the intensity of rain. In fact the two last named authors in their common paper arrive at a formula for the concentration of chloride as a function of the precipitation previously fallen very similar to our own for combined nitrogen. Woodcock in his very interesting paper enters in detail into the process through which condensation takes place upon small salt particles and upon the way in which larger drops are assimilating smaller ones. Their results seem of great interest for the question concerning rain formation.

As regards chloride there seems to be no doubt that it enters the precipitation either as condensation nuclei or is caught in the form of particles or small drops at the falling of larger drops. In our present case the question is open as regards the way in which combined

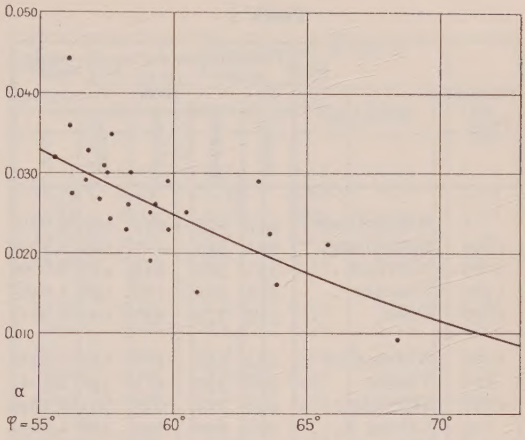

Fig. 4. Variation of α with latitude.

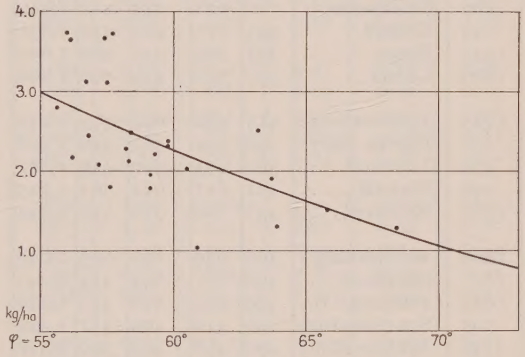

Fig. 5. Variation of annual amount of NH_4 (kg per ha) with latitude.

nitrogen is introduced in precipitation. Does it exist in a gaseous, liquid or solid state before the assimilation into drops of rain or cristals of snow? Perhaps the similarity between our results and those of the authors mentioned above, concerning the rate of decrease of concentration with amount of precipitation or intensity would suggest a similarity also of the form in which the salts are present, viz. we would be inclined to conclude that the nitrogen compounds here investigated are also *chiefly* present in form of particles or dissolved in small drops, in the way that the laws governing their entrance into precipitation will be the same as for the case of the chloride particles. This conclusion, however, must be put forward with great reserve, as it seems probable that nitrogen, especially as ammonia, is transferred to precipitation in several ways among

Table 1

Station Number	Station	Precipitation during the whole period $^{1}/_{10}$ 1947—$^{30}/_{9}$ 1950. mm				
		Spring	Summer	Autumn	Winter	Year
1	Riksgränsen	547	975	1,047	459	3,029
1539	Brännberg	391	345	401	365	1,502
2083	Norrfors	351	383	524	410	1,669
1469	Gisselås	375	562	326	348	1,610
1846	Offer	333	579	450	300	1,662
1273	Norrsundet	233	446	416	252	1,348
122	Vassbo	308	577	475	342	1,701
1897	Stjärnfors	408	722	621	503	2,254
209	Ultuna A_1	292	600	394	318	1,603
1345	Varpnäs	342	682	566	426	2,016
2014	Kvarntorp	271	618	442	292	1,623
1489	Stockholm	276	628	333	312	1,549
233	Högsjö	343	611	466	410	1,831
1433	Berga	324	565	427	380	1,697
1809	Lanna	307	550	434	306	1,598
1185	Kristineberg	415	592	672	563	2,242
270	Bjärka-Säby	348	522	360	348	1,578
570	Tovehult	360	443	440	439	1,682
246	Flahult	411	611	642	561	2,225
1976	Rossared	455	709	750	636	2,549
1806	Ambjörnarp	468	649	857	665	2,638
1817	Skärshult	396	671	643	533	2,243
1983	Halmstad fl.	449	533	678	556	2,217
305	Svartingstorp	266	416	409	331	1,422
1336	Bräkne-Hoby	270	478	405	366	1,518
358	Kolleberga	456	566	573	674	2,268
925	Ugerup	318	465	415	417	1,615
347	Alnarp	362	443	394	409	1,608

Table 2

Station number	Number of precipitation days during the whole period $^{1}/_{10}$ 1947—$^{30}/_{9}$ 1950					
	≧ 0.1 mm	≧ 1 mm	≧ 5 mm	≧ 10 mm	≧ 20 mm	≧ 40 mm
1	612	515	214	72	17	1
1539	386	262	102	38	5	
2083	346	280	104	47	10	3
1469	480	315	103	31	5	
1846	449	289	105	39	10	1
1273	373	234	90	40	5	1
122	355	289	112	50	12	
1897	488	359	151	61	16	
209	417	289	108	35	8	
1345	476	298	124	60	12	2
2014	351	278	105	49	8	2
1489	484	291	101	33	9	
233	477	306	119	56	9	1
1433	416	283	109	45	12	1
1809	438	299	99	40	5	
1185	410	338	157	74	14	
270	387	286	112	44	3	
570	400	278	118	54	6	
246	521	381	155	60	11	
1976	414	349	185	87	22	
1806	527	412	192	81	12	1
1817	492	368	159	57	8	1
1983	544	384	157	57	9	
305	401	283	88	33	7	
1336	384	311	100	29	5	1
358	463	360	164	64	10	
925	446	321	106	31	6	
347	490	317	115	31	7	

which absorption in the gasous state is certainly not to be totally neglected.

A great problem seems now to be concerned with the way in which the fixed nitrogen in precipitation is created. HUTCHINSON (1944) in his survey gives the following summary of the sources for combined nitrogen which can be imagined, namely:

a) From soil and the oceans
b) From fixation of atmospheric nitrogen
   (1) Electrically
   (2) Photochemically
   (3) In the trail of meteorites
c) From industrial contamination

It seems evident from what is well known concerning these phenomena, that they all to some extent are able to produce fixed nitrogen. The question, however, is: what must be regarded as a chief agent? Hutchinson excludes in this respect, as it seems on well founded reasons, c. This source gives fixed nitrogen to some degree but it is far from sufficient to explain the actual transfer.

If we consider only our own material of observations, here treated, we must state, that there is no indication that an electrical production plays an important part. If that would be the case we would expect the concentration to be rather large in summer, when thunder and atmospheric electrical discharges occur, and very small in autumn, winter and spring, at which times, in our climate, practically no such phenomena occur. Now, as we have shown, there is a pronounced maximum of the concentration in spring in

Table 3

Station Number	$\alpha_{NH_4\text{-}N}$				
	Spring	Summer	Autumn	Winter	Year
1	0.006	0.020	0.004	0.007	0.009
1539	0.022	0.022	0.021	0.018	0.021
2083	0.029	0.024	0.008	0.008	0.016
1469	0.032	0.025	0.018	0.012	0.022
1846	0.049	0.032	0.015	0.022	0.029
1273	0.021	0.014	0.012	0.015	0.015
122	0.047	0.020	0.018	0.022	0.025
1897	0.038	0.019	0.019	0.019	0.023
209	0.046	0.025	0.027	0.022	0.029
1345	0.092	0.043	0.050	0.025	0.050
2014	0.089	0.078	0.089	0.082	0.084
1489	0.036	0.022	0.026	0.022	0.026
233	0.038	0.016	0.015	0.011	0.019
1433	0.035	0.024	0.022	0.014	0.025
1809	0.038	0.032	0.023	0.027	0.030
1185	0.033	0.019	0.021	0.020	0.023
270	0.039	0.026	0.022	0.018	0.026
570	0.042	0.026	0.019	0.014	0.024
246	0.047	0.045	0.025	0.027	0.035
1976	0.039	0.027	0.025	0.030	0.030
1806	0.043	0.029	0.034	0.017	0.031
1817	0.025	0.027	0.017	0.013	0.020
1983	0.032	0.025	0.030	0.027	0.029
305	0.045	0.047	0.024	0.018	0.033
1336	0.057	0.024	0.020	0.016	0.027
358	0.037	0.060	0.038	0.015	0.036
925	0.047	0.059	0.041	0.031	0.044
347	0.036	0.033	0.038	0.019	0.032

Table 4

Station Number	Total amount of NH_4-N kg/ha				
	Spring	Summer	Autumn	Winter	Year
1	0.20	0.74	0.15	0.18	1.27
1539	0.40	0.37	0.38	0.35	1.50
2083	0.53	0.38	0.19	0.18	1.28
1469	0.61	0.63	0.41	0.24	1.89
1846	1.00	0.72	0.36	0.43	2.51
1273	0.31	0.28	0.23	0.21	1.03
122	0.68	0.51	0.42	0.42	2.03
1897	0.78	0.56	0.52	0.48	2.34
209	0.80	0.61	0.56	0.40	2.37
1345	1.56	1.11	1.24	0.50	4.41
2014	1.30	1.79	1.84	1.47	6.40
1489	0.64	0.57	0.55	0.43	2.19
233	0.68	0.42	0.41	0.26	1.77
1433	0.62	0.50	0.52	0.30	1.94
1809	0.65	0.76	0.56	0.51	2.48
1185	0.67	0.43	0.61	0.56	2.27
270	0.68	0.65	0.43	0.34	2.10
570	0.67	0.41	0.43	0.27	1.78
246	0.99	1.20	0.74	0.78	3.71
1976	0.80	0.73	0.73	0.84	3.10
1806	1.08	0.86	1.24	0.50	3.68
1817	0.55	0.71	0.52	0.30	2.08
1983	0.76	0.58	0.92	0.85	3.11
305	0.72	0.95	0.46	0.32	2.45
1336	0.84	0.53	0.44	0.36	2.17
358	0.81	1.36	1.02	0.46	3.65
925	0.84	1.27	0.91	0.71	3.73
347	0.73	0.71	0.91	0.45	2.80

our country. This speaks against an electrical source, even if we also have to consider that tropical air masses are coming from regions where other electrical conditions prevail.

In seeking for an explanation of the nitrogen content of precipitation within the temperate zones, it seems to us that there are chiefly two rather important facts, which ought to be kept in mind. The first one concerns the almost constant ratio of one against two, in which NO_3-N appears compared with NH_4-N. Hutchinson has given a graphical demonstration of this fact, largely based on a table by Miller. It is strongly supported by the observations here treated. The high correlation shows that it is in Sweden characterized by a rather high regularity.

The second fact which seems important concerns the similarity between the laws governing the decrease in concentration of nitrogen compounds in precipitation on the one side, and the chlorides on the other one. It suggests a similarity in the way in which the two kinds of compounds occur, viz. as some form of particles or drops.

The constant ratio seems to us to show that in our regions the productions of NH_4-N and NO_3-N are intimately bound to one another, and that when the one compound is produced the other automatically is produced also. The simplest way in which this would occur would be through a photochemical process, occurring for instance in small droplets, where the free nitrogen of the atmosphere, according to the laws of gaseous absorbtion of nitrogen in water, must be present to a concentration

Table 5

Station Number	Mean concentration of NH_4-N mg/L				
	Spring	Summer	Autumn	Winter	Year
1	0.11	0.23	0.04	0.12	0.13
1539	0.29	0.32	0.29	0.31	0.30
2083	0.43	0.30	0.10	0.12	0.22
1469	0.49	0.34	0.36	0.22	0.36
1846	0.84	0.37	0.22	0.43	0.44
1273	0.39	0.19	0.16	0.31	0.24
122	0.66	0.27	0.23	0.36	0.34
1897	0.57	0.23	0.25	0.30	0.32
209	0.83	0.30	0.41	0.38	0.44
1345	1.37	0.49	0.66	0.43	0.68
2014	1.44	0.87	1.30	1.52	1.20
1489	0.69	0.27	0.49	0.43	0.43
233	0.58	0.20	0.24	0.17	0.27
1433	0.57	0.27	0.35	0.24	0.34
1809	0.64	0.42	0.36	0.50	0.46
1185	0.49	0.22	0.26	0.28	0.30
270	0.59	0.37	0.33	0.31	0.40
570	0.66	0.35	0.31	0.23	0.38
246	0.76	0.59	0.34	0.43	0.51
1976	0.52	0.31	0.30	0.37	0.36
1806	0.66	0.40	0.40	0.24	0.41
1817	0.41	0.31	0.24	0.19	0.28
1983	0.51	0.36	0.41	0.44	0.43
305	0.80	0.68	0.36	0.33	0.54
1336	0.94	0.33	0.33	0.29	0.43
358	0.54	0.72	0.52	0.20	0.48
925	0.79	0.82	0.66	0.56	0.71
347	0.60	0.48	0.64	0.36	0.52

Table 6. Frequency numbers of simultaneous values of nitrogen amount *s* expressed in gr/ha. Totally 117 different cases.

NH_4-N \ NO_3-N	1—5	6—10	11—15	16—20	21—25	26—30	31—35	36—40	Σ
1—5	13								13
6—10	22	5	1						28
11—15	13	7	1						21
16—20	4	7	3	1					15
21—25	1	1	2	1					5
26—30		6	4	2	1				13
31—35		1	3	3	1				8
36—40			2	1					3
41—45			1			1			2
46—50					1	1	1		3
51—55				1	1		1		3
56—60									
61—65									
66—70					1				1
71—75									
76—80									
81—85				1					1
86—90								1	1
Σ	53	27	17	10	5	2	2	1	117

of about 15 mg/lit. A simple reaction according to the formula:

$$12\,N + 18\,H_2O = 4\,NH_4NO_3 + 4\,NH_4OH + O_2 \quad (6)$$

evidently gives us just the result found to exist, namely two times as much NH_4-N as NO_3-N in the drop. If such a process actually takes place it can occur in many ways, possibly with one or more intermediate steps. What here seems worth to point out is that in a water particle, either solid or liquid, all the material is already at hand if the agency able to produce such a reaction comes into play. The possibility of certain sea water salts acting as catalysers or even part-takers must be taken into consideration. The process suggested above only needs to transform about 3 per cent of the nitrogen present in the drop in free state, in order to give the concentration of fixed nitrogen found to exist in precipitation. Experiments are evidently needed in order to decide this question. If such a chemical action is found actually to be produced by some wave lengths of sun light entering the troposphere, such a result will evidently be of utmost importance. Not only will it explain the constant ratio relationship found at high latitudes, but it will also explain the similarity of the washing out process in the cases of chlorides on the one side and nitrogen compounds on the other. Further it will suggest the possibility of a new kind of cosmical influences on processes of biological nature through variations in the composition of sun radiation.

REFERENCES

HUTCHINSON, G. E., 1944: Nitrogen in Biochemistry of the Atmosphere. *American Scientist*, pp 178—195.

MIYAKE, Y. and SIGIURA, Y. 1950: The Mechanism of Dissolution of the Atmospheric Chloride into Rain Water. *Papers in Meteorology and Geophysics*, **1**, No. 2—4.

SUGAWARA, KEN, OANA, SHINYA and KOYAMA, TADASHIRO 1949: Separation of the Components of Atmospheric Salt and their Distribution. *Bulletin of the Chemical Society of Japan*, **22**, No. 2.

WOODCOCK, ALFRED H. 1952: Atmospheric salt particles and raindrops. *Journal of Meteorology*, **9**. No. 3.

ÅNGSTRÖM, A. and HÖGBERG, L. 1952: On the Content of Nitrogen (NH_4—N, and NO_3—N) in Atmospheric Precipitation. *Tellus*, **4**, No. 1.

Composition of Atmospheric Precipitation

II. Sulfur, chloride, iodine compounds. Bibliography

By ERIK ERIKSSON
Institute of Pedology and Institute of General and Inorganic Chemistry,
Royal Agricultural College of Sweden, Uppsala

(Manuscript received 30 October, 1952)
(Continuation from Vol 4, No 3)

C. Sulfur in rainwater

Unlike the nitrogen most sulfur determinations in rainwater have been carried out comparatively recently. The greater part of the investigations were carried out in the U.S.A. where an extensive survey of the contribution of atmospheric sulfur to the soil has been made for agricultural purposes.

1. Methods and analysis

The analytical procedure has mostly involved a precipitation of the sulfur compounds as $BaSO_4$. If properly done this is a satisfactory procedure. A division between sulfate sulfur and other forms of sulfur has rarely been done. If other forms of inorganic sulfur are present in rainwater they are generally rapidly oxidized by dissolved oxygen to sulfate.

The sampling of rainwater for sulfur analysis has mostly been done in metal containers which, as ALWAY et al. (8) pointed out in 1937 may give too large figures for the sulfur in rain. Most metals adsorb SO_2 directly from the air which is then oxidized to SO_3 and washed down into the containers with the rainwater as H_2SO_4. In areas of a high atmospheric pollution the contribution by this adsorbtion can amount to six times the sulfur actually present in rainwater.

It is obvious that under such circumstances most of the figures on the amount of sulfur in rainwater are too high. An absorption of SO_2 by the soil itself and even by the plants can, however, also occur. (THOMAS 283, 284.) Therefore the rainwater analysis may represent the total sulfur income by soil which from agricultural point of view is of most interest. But in the discussion on the origin of sulfur in precipitation they are of but little use.

The yearly averages from different states within the U.S.A. are shown in table 6 and results from other parts of the world are in table 7.

From table 6 it will be seen that the average yearly amounts of sulfur vary very much even within the same state due to differences in atmospheric pollution. There are also significant differences between different states (or probably better, between different investigations) which at least partly may be due to different sampling techniques (different sampling gauges). There are some striking differences between different states, compare e. g. Alabama, with Indiana. Both are fairly recent.

The U.S.A. investigations cover the eastern central area of the country.

The European figures are generally lower than those from the U.S.A. Some of the Russian figures are low and may therefore correspond to fairly uncontaminated air in continental areas. The New Zealand figures

Table 6. Sulfur in precipitation in the United States and Canada.

Ref.	Place	Period	Precipitation mm	mg S/l	kg S/ha
	Alabama				
294	Auburn	1940—1943	—	—	6.0
294	Birmingham	1940—1943	—	—	34.2
294	Block Belt Subst. Marion Jet	1940—1943	—	—	6.3
294	Exp. field Alexandria	1940—1943	—	—	6.3
294	» » Aliceville	1940—1943	—	—	5.6
294	» » Monroeville	1940—1943	—	—	4.8
294	» » Prattville	1940—1943	—	—	5.6
294	Gulf Coast Subst. Fairhope	1940—1943	—	—	6.5
294	Kinston	1940—1943	—	—	3.2
294	Sand Mountain Subst. Crossville	1940—1943	—	—	6.8
294	Wiregrass Subst. Headland	1940—1943	—	—	4.6
	Georgia				
294	Experiment	1940—1943	—	—	7.8
	Illinois				
95	Chicago	1921/22—1922/23	—	—	234
95	Liberty	1921/22—1922/23	—	—	61.6
279	Urbana	1913—1917	—	—	50.5
	Indiana				
26	Branchville	1946/47	—	—	34.0
26	Evansville	1946/47	—	—	32.5
26	Gary	1946/47	—	—	142
26	Indianopolis	1946/47	—	—	36.5
26	Lafayette	1946/47	—	—	24.3
26	Larwill	1946/47	—	—	26.0
26	Monterey	1946/47	—	—	30.6
26	Montgomery	1946/47	—	—	31.0
26	Orland	1946/47	—	—	28.9
26	Rising Sun	1946/47	—	—	33.2
	Iowa				
100	Ames	1921	—	—	16.7
15, 117, 161, 235, 246, 269, 290, 306, 313.	Mount Vernon (10 years)	1913/14—1931/32	—	—	22.7
	Kentucky				
153	Greenville	1921/22—1922/23	—	—	40.3
153	Lexington, center	1921/22—1922/23	—	—	46.1
153	» , 15 miles from center	1921/22—1922/23	—	—	26.6
153	Lincoln Inst. Shellbyville	1921/22—1922/23	—	—	19.1
153	Mayfield	1921/22—1922/23	—	—	29.0
153	Paducale	1921/22—1922/23	—	—	38.0
153	Russelville	1921/22—1922/23	—	—	40.3
	Minnesota				
8	Minneapolis, Weather Bureau	1936—1937	—	—	170
8	» , University Farm	1936—1937	—	—	31.1
8	Page	1936—1937	—	—	8.2
8	Bemidji	1936—1937	—	—	5.0
	Mississippi				
294	State College	1940—1943	—	—	5.8

Ref.	Place	Period	Precipitation mm	mg S/l	kg S/ha
	New York				
310	Alfred	1923/24—1924/25	—	—	55.6
310	Brockport	1923/24—1924/25	—	—	86.7
75	Geneva	1919—1928	—	—	46.2
308, 309, 310.	Ithaca	1915/16—1925/26	—	—	38.3
	Oklahoma				
132	Goodwell	1933—1934	—	—	6.5
132	Guthrie	1931—1939	—	—	9.0
132	Heavener	1934	—	—	19.0
132	Lone Grove	1934, 1936	—	—	10.8
132	Stillwater	1927—1942	—	—	9.9
	Tennessee				
195	Columbia	1919—1921	—	—	29.5
195	Copperhill,	1919—1921	—	—	260
195	» , 6 miles from center	1919—1921	—	—	80.9
195	Crossville	1919—1921	—	—	14.2
195	Jackson	1919—1921	—	—	66.2
294	Jackson	1940—1943	—	—	14.8
195	Knoxville, in town	1919—1920	—	—	103
195	» , University Farm	1917—1920	—	—	48.0
195	» , 7 miles from center	1917—1920	—	—	20.7
195	London	1919—1921	—	—	21.6
195	McGee	1919—1921	—	—	27.1
	Texas				
114	Angleton	1924—1928	—	—	10.6.
114	Balhorhea	1924—1928	—	—	4.6
114	Beaumont	1924—1928	—	—	17.2
114	Beeville	1924—1928	—	—	7.4
114	Chillicothe	1924—1928	—	—	11.2
114	College Sta. (Main)	1924—1928	—	—	14.2
114	Denton	1924—1928	—	—	13.2
114	Lubbock	1924—1928	—	—	13.4
114	Nacogdoches	1924—1928	—	—	13.4
114	San Antonio	1924—1928	—	—	9.2
114	Spur	1924—1928	—	—	9.0
114	Temple	1924—1928	—	—	10.0
114	Troup	1924—1928	—	—	10.2
114	Weslaco	1924—1928	—	—	17.4
	Virginia				
99	Blacksburg	1923—1928	—	—	18.9
	Wisconsin, Canada				
135	Madison	1910	—	—	7.8

are fairly representative of conditions in uncontaminated air in coastal places.

The yearly variation is as a rule greater in areas of a high degree of atmospheric pollution than in areas of a low.

The monthly variation is interesting from the point of view of the origin of sulfur in rainwater. In densely populated areas the winter months are highest in sulfur due to increased coal consumption during this season.

In the results from several years of investigation there are sometimes trends, the values increase during the period, indicating an in-

Table 7. Sulfur in precipitation in Europe and other countries except America.

Ref.	Place	Period	Precipitation mm	mg S/l	kg S/ha
	Europe				
27, 28	*France*: Paris	1931/32	(600)	16.0	(96)
27, 28	Grignon	1934/35	(600)	2.5	(15)
188	*Germany*: Müncheberg	1933/34	405	3.3	13.4
213	*Great Britain*: Rothamsted	1881/82—1886/87	760	1.0	7.9
81	Garforth	1907/08	720	1.4	10.2
312	*Russia*: Leningrad	1909/10	646	4.9	31.5
312	» outskirt of town	1909/10	669	4.8	31.7
	Pawlosk	1909/10	522	1.4	7.3
	Sapolje, Kreise Luga	1909/10	486	.9	4.3
	Smolensk	1909/10	660	.4	2.7
	Jekaterineslaw	1909/10	339	6.5	22.1
	Schotilowska, Tule distr.	1909/10	476	.8	3.7
	Borowoje, Ssarnara	1909/10	541	.4	2.3
	New Zealand				
125	Lincoln, Canterbury	1884—1887	750	.9	6.8
	Asia				
216	Tokio, Japan	1938	—	1.9	—

creasing degree of atmospheric pollution. This can be observed in the figures from Ithaca, N.Y. (310) where the yearly amount increases regularly from 1919—20 to 1925—26. In other places, e.g. in Stillwater, Oklahoma (132) no regular trend can be observed but rather periodic fluctuations. The variation in the yearly amounts in Ithaca and Stillwater is shown in fig. 7.

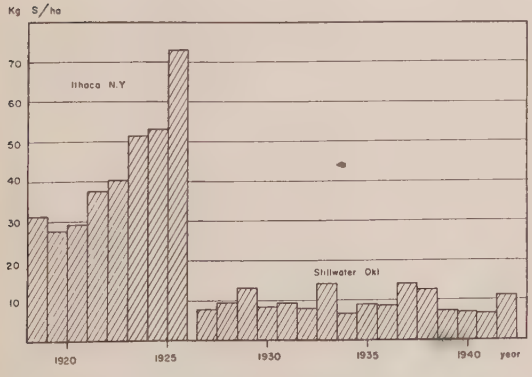

Fig. 7. The yearly amounts of sulfur in precipitation in Ithaca, N.Y. and Stillwater, Okl.

2. Origin of combined sulfur in the rainwater

As mentioned before sulfur present as sulfate has usually been estimated in the analytical procedure. In one instance (81) sulfide, sulfite and organic sulfur have also been determined besides sulfate sulfur. But then no division between sulfide, sulfite and organic sulfur was made.

There is probably very little of sulfide and sulfite present in rainwater, as H_2S is rather volatile and probably exists only as a gas in the air. Sulfite is rapidly oxidized to sulfate by dissolved oxygen in the rainwater but may be present in the air in appreciable concentrations.

There are several probable sources of sulfur in the atmosphere. One of these is coal which on combustion releases considerable amounts of sulfur. In industrial areas it has been noted that the yearly amounts of sulfur brought down by precipitation is very high. There are a number of recent investigations carried out to asses the degree of atmospheric pollution in industrial centres; but these will not be referred to in this paper. One of the earlier

investigations, however, of great agricultural interest was carried out in Leeds and its vicinity around 1910 by CROWTHER & RUSTON (81) (see also CROWTHER & STEWART 82). The results show very clearly that sulfur in precipitation is a very sensitive indicator of atmospheric pollution caused by industries. Even at 5 km distance from the centre of Leeds 170 kg S per hectare and year was brought down by precipitation and at 11 km distance it varied between 57 and 108 kg.

Apart from coal, sulfide ores used in industry certainly contribute to the sulfur content of the air.

Another source is organic matter which, on decay may give off hydrogen sulfide to the atmosphere which is oxidized to SO_3 and dissolved in the rainwater. The rate of delivery of hydrogen sulfide in this way will depend on the season. Hydrogen sulfide, formed by the reduction of sulfate in the sea is another source of atmospheric sulfur as suggested by CONWAY (78).

A great source for atmospheric sulfur is, no doubt, the sea. The sulfate is brought into the air by spray and precipitated by rain water. In coastal areas it is therefore interesting to study this contribution from the sea.

It is fairly well accepted that the main source for chloride in rainwater is the sea, and the only way it can be derived from there seems to be by spray. Comparing the ratio Cl/S in rainwater and in sea water in coastal districts, GRAY (125) in New Zealand observed, however, that this ratio was smaller for rainwater than for sea water. As the place where he collected the rainwater was situated on a small peninsula far from industries it could be expected that the ratio would be the same, as long as the proportion of chloride and sulfate is the same in the spray from the sea as in the sea water. In table 8 some values of the Cl/S ratio from different places are tabulated. It is seen that the New Zealand values come nearest to the expected values. There is also a seasonal variation, the winter and spring values being highest. This can be due to an accelerated liberation of H_2S during the summer and the autumn, not only from the soil but also from the sea.

It is remarkable that even the highest values of the Cl/S ratio in rainwater are only half as great as in sea water. Unless the washing out

Table 8. The ratio Cl/S in precipitation in some places.

Ref.	Place	Cl/S
125	Lincoln, Canterbury New Zealand	
	Sept. to Nov.	11.05
	Dec. to Febr.	9.86
	March to May	9.00
	June to Aug.	10.89
281	Sugashima, Japan at the see	5.85
281	Nagoya, » 4000 m from the sea	6.31
281	Matsumato, » 100 km » » »	.92
170	Holland 440 m from the sea	8.70
170	» 2280 » » » »	5.70
170	» 3000 » » » »	5.24
170	» 5600 » » » »	3.83
170	» 48000 » » » »	2.61
170	» 86000 » » » »	2.18
	Sea water	21.5

of the salts from the air is selective it can be inferred that only half of the sulfur in rainwater from this place is derived from the sea by the same mechanism as the chloride; the rest must have been delivered in another way.

The distance from the sea has a great influence on the Cl/S ratio as seen from the dutch values. In France, however, FARCY (105) has found a quite opposite trend, the Cl content being rather constant inland while the S was highest at the coast.

There is a recent investigation carried out in Australia by ANDERSON (13) on the composition of lake waters in arid districts compared to the composition of sea water (see table 9).

Table 9. The relative composition of some lake and river waters in south east Australia: Cl + Br = 100.

	Lake Corangamite		Woody Yallock River	Snarket Creek	Sea water
	Jan. 4 Low water level	June 12 Very low water level			
Cl+Br	100	100	100	100	100
Cl	—	99.84	99.86	99.86	99.85
Br	—	.16	.14	.14	.15
SO_4	2.99	2.89	6.5	8.2	10.26
CO_3	.91	.60	—	1.2	.45
HCO_2	.86	.54	7.1	5.0	
NO_3	—	—	.7	—	—
Ca	.29	.11	9.7	5.5	3.83
Mg	13.09	13.27	36.4	32.1	19.59
Na	86.26	87.00	65.7	74.7	85.17
K	3.95	3.21	3.8	2.4	1.82

The runoff from some of the lakes is very small and practically all their chlorides are derived from the sea, carried inland and precipitated by rain. He found, however, that the relative sulfate contents in these lake waters were less than in the sea; sulfate being lost in some way. Anderson suggested that this loss was due to the reduction of SO_4 to H_2S as there was a definite smell of H_2S around the lakes. It is also seen from the CO_3 and HCO_3 contents that the pH of the waters must have been quite high, apparently due to this reduction process. The loss of sulfate by reduction to H_2S in the lakes must have been very high and proportionally higher than in the sea as it can be expected that the rainwater carried relatively more sulfate than chloride from the sea.

An interesting investigation was carried out by Boss (46) on the south west coast of Africa. Due to a cold water current in the sea reaching the surface at this place there is a permanent fog in this district which is a desert. He found that the fog was relatively richer in sulfur than in chloride compared to sea water and that the proportion of sulfur increased inland. For an explanation he suggested a small sulfur cycle which took place in the following way. Both chlorides and sulfates are carried inland by the fog but the chlorides seems to be leached down into the soil much easier than the sulfates especially as most of the latter are in the form of $MgSO_4$. During dry weather fine particles of $MgSO_4$ are carried from the earth's surface to the air where they serve as condensation nuclei. Very little sulfate is actually lost in this way and the process leads to an enrichment of $MgSO_4$ in the top soil while chlorides are leached down into the subsoil. Perhaps such a small cycle of sulfur is partly responsible for the lower Cl/S ratio in rainwater compared to sea water.

To summarize it can be concluded that a great part of sulfur in precipitation is of oceanic origin either brought into the air by spray or as H_2S formed by reduction of sulfate in the sea. Another source of sulfur in rainwater is coal, sulfide ores and wood which, on combustion, liberate considerable quantities of sulfur. A third source is H_2S liberated from organic matter on decay, and a fourth may be of inorganic litospheric origin.

D. Chloride in precipitation

1. Results from different places

The first determinations of chloride in rainwater were made at the beginning of the nineteenth century but the first more systematic work was not published until 1851 when Arago (14) in Paris reported monthly amounts for a half year period. Another systematic investigation was carried out by Smith (277) who in 1872 published his well known "Air and Rain", where he has given analyses of rainwater collected at different places in the British Isles. Some of the chloride analyses in his work are given in table 11.

One of the longest series of analyses was carried out at Cirencester by Kinch (158, 159) covering a period of 26 years.

The determinations of chloride in rainwater has, of course, been made mostly for other reasons than agricultural. The salt transport from the sea may be of agricultural but is also often of technical value. In meteorology chloride in rainwater is of great interest as it can probably give a good indication of the origin of the air masses.

The amount and composition of chloride in rainwater from different places are tabulated in table 10. The European investigations are not so extensive as the corresponding ones for ammonia and nitrate and the American ones are also few, compared to the sulfur investigations. The New Zealand and Australian investigations are rather extensive because of the great practical importance of the salt transport from the sea by rain in these places.

The amounts and concentrations of Cl in rainwater do not vary very much in inland places whereas coastal places show a great variation. Remarkably high figures are however obtained from Iowa and Tennessee in the U.S.A., places which are really inland situated at great distances both from the Pacific Ocean and the Atlantic. For Iowa it has been assumed that all chloride in rain water is derived from the sea as no other likely sources exist in the neighbourhood.

2. Origin of chloride in precipitation

It was suggested long ago that the sea was the greatest source for chloride in rainwater as rainwater in coastal places contained by far the

Table 10. Chloride in precipitation at different places.

Ref.	Place	Period	Precipitation mm	mg Cl/l	kg Cl/ha
	Europe				
131	Denmark: Askov	1925/26	740	4.2	30.8
131	Blangsted	1925/26	000	4.7	20.3
131	Hornum	1925/26	495	5.8	28.0
131	Spangsbjerg	1925/26	730	12.4	00.9
14	France: Paris	1851	500	2.3	13.0
43	Nantes	1863	—	—	8.4
188	Germany: Müncheberg	1933.34	405	3.6	14.4
158, 159	Great Britain: Cirencester	1874—1900	775	3.2	24.0
213, 254	Rothamsted	1887/88-1915/16	740	2.4	18.0
81	Garforth	1907/08-1908/09	720	3.1	22.0
312	Russia: Leningrad	1909/10	046	3.6	23.0
312	» outside town	1909/10	000	2.4	15.8
312	Pawlowsk	1909/10	522	1.6	8.3
312	Sapolje, Kreise Luga	1909/10	486	3.0	14.0
312	Smolensk	1909/10	000	3.1	20.3
312	Jekaterieslaw	1909/10	330	3.8	12.8
312	Schotilowska, Tule distr.	1909/10	470	1.8	8.7
312	Borowoje, Ssarnara	1909/10	541	2.0	10.0
209	Spain: La Guardia (at the coast)	1892/93	1433	31.2	447
	America				
75	Geneva N.Y.	1919—1928	900	2.0 21	18
15, 117, 161, 235, 246, 269, 290, 306, 313	Iowa: Mont Vernon (8 years)	1913/14-1931/32	—	—	72
195	Tennessee: Knoxville	1022	—	—	140
195	» Univ. Farm	1022	—	—	70
288	Kansas: Madison	1915—1918	—	—	18
133	Barbados	1886—1886	-	8.1	-
133	British Guiana: Georgetown	1800—1805	-	4.0	—
	Asia				
216	Japan: Tokyo	1038	-	1.8	-
216	Kobe	1038	-	2.3	
216	Hamamatu	1038	—	2.4	—
18	India: Ceylon	1898 99	—	9.7	202
226	Bombay	1038	—	13.6	—
	Africa				
150	Bloemfontein, South Africa	1010 11-1011 12	550	9	5.1
150	Cedera, » »	1912	080	2.7	15.1
150	Durban, » »	1911—1912	010	8.2	73.5
150	Grahamstown, » »	1911 12	500	4.5	22.3
	New Zealand				
110	Rangatai 500 m from the sea	1948—1950	005	22.4	210
110	Baring Head 500 » » » »	1948—1950	820	20.2	200
110	Kelburn 6500 » » » »	1948—1950	1220	8.7	100
110	Pirinoa 6500 » » » »	1948—1950	840	11.8	96
110	Belmont Hills 8000 » » » »	1948—1950	1400	7.5	100
110	Levin 10000 » » » »	1948—1950	1000	4.6	50
110	Wallaceville 18000 » » » »	1948—1950	1270	5.8	74
110	Palmerston North 32000 » » » »	1948—1950	1040	4.8	50
110	Martinborough 32000 » » » »	1948—1950	700	7.6	80
110	Te Awa 48000 » » » »	1948—1950	1070	3.3	35
110	Waingawa 61000 » » » »	1948—1950	880	4.8	41
125	Lincoln, Canterbury	1884—1888	750	8.8	00.4

Ref.	Place	Period	Precipitation mm	mg Cl/l	kg Cl/ha
	Australia				
13	South Australia, York Pennisula	1923—1937	445	21.6	96
13	Victoria: O'Shamarsy	1923—1937	1620	2.7	44
13	East Camberwell	1923—1937	715	5.7	40
13	Yarra	1923—1937	1130	4.4	49
13	Upper Murray	1923—1937	840	1.6	8.4
13	Barrwan River Catchment	1923—1937	645	8.4	54
282	West Australia: Merredin	1933—1936	260	4.2	11.0
282	Salmon Gums	1933—1936	320	5.7	18.4
316	Esperance	1926	—	20.7	—
316	Geraldton	1926	—	28.7	—
316	Perth	1926	—	16.5	—
316	Coolgardie	1926	—	12.0	—
316	Cue	1926	—	9.6	—
316	Mundiwindi	1926	—	3.5	—
316	Rawlinna	1926	—	6.3	—
316	Wilunna	1926	—	4.0	—
316	Condon	1926	—	8.2	—

highest amounts of chloride. This is also clearly seen in table 11 where SMITH's data are tabulated. Special investigations have also been carried out in order to asses the influence of the sea. Recent investigation from New Zealand (119) shown in table 10 shows very clearly the influence of the sea. Another investigation which is of interest in this connection is that published in 1905 by JACKSON (151). He analysed spring waters in New England and New York and from his analysis he was able to draw isochlors for the whole area. These isochlors show very clearly the influence of the sea in this district. Later CONWAY (78) used his data to set up a mathematical relation between the chloride content in uncontaminated spring waters and the distance to the sea. The relation can be written

$$Cl = 5.7 \cdot e^{-0.0367\,x} + 0.55 \cdot e^{-0.00242\,x} \quad (D)$$

where Cl is expressed in mg/l and x is the distance from the sea in kilometers.

The first term represents a relatively rapid decrease of Cl inland while the second one, although small shows that after the first rapid decrease there is a much smaller decrease.

There is an investigation from Holland carried out by LEEFLANG (177) in 1938 of a similar kind as the New Zealand one although better suited for the calculation of a relationship of a similar type as (D) than the New Zealand investigation. The relationship corresponding to (D) from LEEFLANG's figures reads

$$Cl = 11.7 \cdot e^{-0.525\,x} + 3.0 \cdot e^{-0.0230\,x} + 3.0 \quad (E)$$

Also in this case the relation can be expressed by two exponential factors but it also involves a constant which is reasonable as there is always chloride in rainwater even very far

Table 11. Cl-content in precipitation in Great Britain from Smith's investigations (277).

Place	mg Cl/l
London, spec. for 1869	1.2
Birkenhead, Liverpool	3.1
Scotland, inland country places	3.3
» , near an alkali work	3.3
England, inland country places	3.9
Manchester, 1869—1870	5.7
Scotland, towns (not Glasgow)	5.7
Newcastle on Tyne	7.9
England, towns	8.5
Glasgow	8.7
St. Helen's	9.3
Liverpool	9.9
Scotland sea coast country places, west	11.9
Scotland sea coast country places, east and west	12.2
Scotland sea coast country places, east	12.6
Runcorn	25.0
Waterlow, near Liverpool	35.5
Ireland, Valentina	47.3
England, sea coast place, west	54.6

from the sea. The coefficients in (D) and (E) differ considerably. Firstly the initial Cl content seems to be higher in (E) than in (D) and the decrease in the first term is also much more rapid. The second term in (E) decreases, however, much faster than the same in (D). It is probable that the differences are significant and indicate differing meteorological conditions on the North American east coast and the European west coast.

The experimental points and relation (E) are shown graphically in fig. 8.

An investigation similar to that of Leeflang has also been carried out in France by FARCY (105) at different places on the road from Brest to Paris. As a rule the Cl contents are higher than the Dutch ones with a very slow decrease inland. In one serie the Cl content in rainwater at the sea was 19.0 mg per litre and 18.7 mg per litre at 24.3 km distance from the sea. It is thus seen that the conditions for the transport of chloride from the sea may vary considerably from place to place.

CONWAY (loc. cit.) has discussed the sources of Cl in detail. From equation (D) he calculated by integration over all coast lines that the total amount of Cl brought inland from the sea each year amounted to $0.69 \cdot 10^{14}$ g. Compared to other possible sources he mentions that the total salt production by human activities amounts to $0.09 \cdot 10^{14}$ g per year

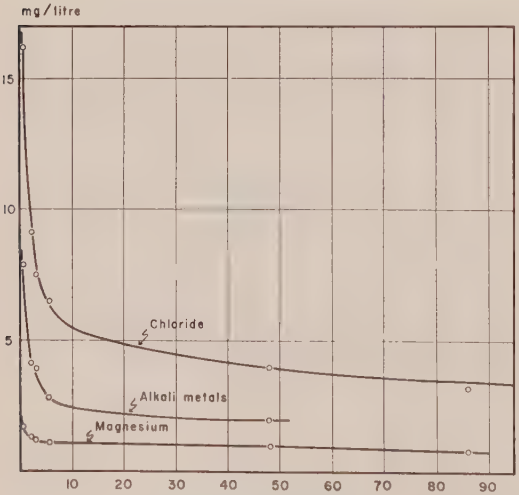

Fig. 8. The concentration of Cl, Mg and Ca in precipitation in Holland as a function of the distance to the sea.

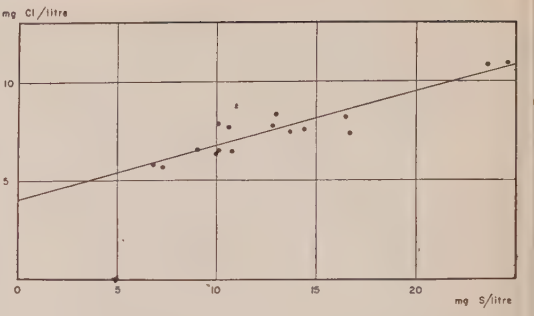

Fig. 9. The relation between the concentration of S and Cl in precipitation around Leeds, Great Britain.

while human secretion amounts to $0.05 \cdot 10^{14}$ g. Combustion of coal contributes only $0.015 \cdot 10^{14}$ g per year. From equation (D) and the French investigation mentioned it is obvious that the figure $0.69 \cdot 10^{14}$ g Cl per year may be far too small; obviously other sources of Cl in rainwater become insignificant compared to the sea.

In industrial places the Cl content of the rain may rise somewhat but compared to the increase in sulfur the increase in Cl is smaller. This is seen from an investigation by CROWTHER & STUART (82) who collected rainwater at different points around Leeds in England. From their data on S and Cl it is possible to get a linear relation between these two which reads

$$Cl = 4.06 + 0.275 \qquad (F)$$

This relation is shown diagrammatically in fig. 9. The correlation coefficient is equal to 0.925. It is seen that the increase in Cl is about one fourth of the increase in S due to atmospheric pollution. In other places it may be even less.[1]

Equation (F) is interesting as it shows that in absence of any industrial contamination the Cl content of rain should amount to 4.1 mg pro litre, a very reasonable figure for England (Cf. tab. 11 inland country places in England with 3.9 mg Cl pro litre).

In their final report of the Rothamsted investigations RUSSEL & RICHARD (254) mention that the Cl content in rainwater at

[1] The increase of Cl in this case can hardly be due to combustion of coal as the chloride content of coal is very low. It is probably connected to some chloride containing chemicals used in the industry.

Table 12. Cl in precipitation near volcanoes.

Place and date of sampling	Ref.	pH	Cl mg/l
Vesuvius, Italy			
March, 5, 1934	47	2.96	247
» , 17, »	47	3.16	193
May, 10, »	47	2.39	202
» , 18, »	47	2.82	105
June, 30, »	47	3.09	88
Paracutin, Michoacan, Mexico 1947 12 km N of the foot of the Volcano	55		440

Rothamsted had a tendency of increasing with time, a fact they attributed to the increased combustion of coal. In the Cirencester series (KINCH, 159) it is, however, impossible to detect any such trend.

Another source not mentioned before is Cl in volcanic gases. There are a couple of investigations which may be of interest in this connection. One is carried out near the Vesuvius volcano by BOTTINI (47) in 1934. The composition of 5 samples with respect to pH and Cl is shown in table 12, together with an analysis from the Paracutin volcano in Mexico (BULLARD, 59). It is seen that the chloride figures are very high and, further, that in the Vesuvius' figures at least part of the Cl is present as HCl as the pH is very low.

It is evident that some chloride may locally be of volcanic origin but the total contribution by volcanoes is insignificant compared to the contribution by the sea.

3. Meteorological factors influencing the Cl-content of rainwater

Some of these factors are obvious from the preceding discussion but as they have been pointed out in the literature they will be discussed here.

a. *Rainfall*

As in the case of other compounds there is generally an inverse relationship between the Cl-content and the amount of rainfall. As examples it can be mentioned that MILLER (213) using monthly averages calculated for Rothamsted the relationship to be approximately

$$Cl = 2+3/p$$

in winter

$$Cl = 0.5+3/p$$

in summer and

$$Cl = 1.25+3/p$$

for the whole year. In these expressions p is the monthly rainfall in inches.

The expressions indicate that there is a lower limit of concentration in the precipitation, and this limit is higher in winter than in summer.

SUGAWARA et al. (281) have recently (1946—47) analysed rainwater in Japan and found at Nagoya (4 km from the sea) also an inverse relationship between rainfall and Cl-concentration.

Also in a few other investigations an inverse relationship can be traced.

b. *Wind direction and wind strength*

It is a well known fact that near the sea the Cl concentration in rainwater is largely influenced by the wind direction at the time of rainfall. Also in inland places the Cl-concentration may be influenced by the wind direction, a fact which at least to a certain extent can give information as to the origin of the air masses.

In Leningrad WITUYNJ (312) found that the Cl content was higher in spring than in autumn depending on the westerly winds prevailing in the spring. In Denmark HANSEN (131) found that the Cl content even at inland places was highest during westerly winds. In Donnersberge in Germany MENZL (207) found that the Cl content of rime frost deposited under different wind directions was the following: N, 8.01; NE, 4.78; E, 3.43; W, 9.67 and NW, 10.53 mg/l. This shows that the air masses from north to west carried most Cl. In snow he (208) found about the same while rain from the west had the highest Cl concentration. In Haid also in Germany rain from SW had the highest Cl concentration followed by rain from NW. In Hohen Sonnblick in Austria at 3106 metres' altitude LAUSCHER & SCHWARZ (170) found that winds from north carried less chloride than winds from the south.

From this is seen that at lower altitudes the sea has still a noticable influence on the Cl

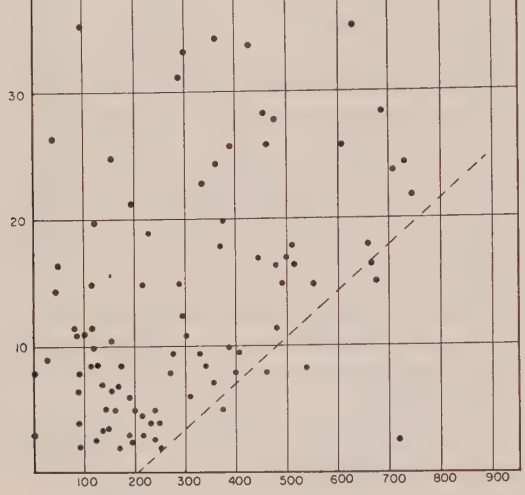

Fig. 10. The relation between the concentration of Cl and wind length at Perth, West. Australia.

concentration of atmospheric precipitation even in places far from the sea. At higher altitudes this influence is not so pronounced.

The wind strength when the winds come from the sea is reported to have some influence on the Cl content of rain. MIYAKE (216) in Japan found a strong correlation between Cl content and wind strength. WOOD & WILSMORE (316) in their research on the salinity of rain in Western Australia correlated the Cl content of rain at Perth with the total way the wind had travelled from the sea in 24 hours. It is a rather interesting relationship although the correlation is not very strong. In fig. 10 the Cl content of the rainfall has been plotted against their computed wind length sea wind in miles/24 hours.

From fig. 10 it is seen that the Cl content of the rain is independant of the wind strength up to a wind velocity of 200 miles pro 24 hours with a lower limit of 2 mg Cl pro litre. Above that velocity it can be stated that in general

$$Cl \geqq -7.2 + 0.036\, v \qquad (G)$$

where v is the wind length in 24 hours, this lower limit being indicated on the figure by the dashed sloping line. Deviation from this rule can, of course, occur on single occasions. The interpretation of this rule is simply that at high winds one cannot expect low Cl contents in the rains.

c. *Altitude*

There is an old investigation from France carried out by BOBIERRE (43) in Nantes in 1863 which may show differences at lower altitudes. He collected rainwater from two heights, 7 m and 50 m above the ground and analysed them. In the yearly averages there was no difference in the Cl contents but in winter the samples collected at 50 m contained more Cl than those collected at 7 m while the reverse was true during summer. The reason for this may be local.

There are, however, several investigations made at different altitudes where precipitation has been collected on mountains.

Analyses of rime frost on the Hohen Sonnblick in Austria made both by LIPP (192) and LAUSCHER & SCHWARZ (170) gave relatively low Cl values. LIPP found on 2962 m altitude an average of 1.1 mg Cl/l for 12 determinations with variations from 0.25 to 5.90. LAUSCHER & SCHWARZ found on 3106 m an average of 0.21 mg for 15 determinations with variations from 0.035 to 0.554 mg pro litre. In *Donnersberge* (207) on 853 m altitude the average for 17 determinations was, however, as high as 7.23, rain and snow containing about the same. Some analyses of water from lakes and rivers in the Haldde district in northern Norway presented by KÖHLER (167) indicate that the Cl content in general decreased with increasing altitude although there were variations, according to Köhler probably due to topographic conditions influencing the turbulence of the air.

The Cl content of precipitations thus seems to decrease with increasing altitudes. This has also been predicted by KÖHLER (166) from theoretical considerations.

d. *Seasonal variation*

The seasonal variation in the Cl concentration of precipitation seems to be entirely connected to the prevailing winds as can be expected and also to the general meteorological conditions such as wind strength. Such observations are reported from several places.

4. The "Köhler" distribution of Cl-concentrations

In 1925 KÖHLER (165) published a report on an investigation of the Cl concentration in white frost formed at high altitudes by precipitation and freezing of undercooled water particles in clouds. This type of frost will be called cloud frost here. From 49 analysis of collected cloud frost he found that the Cl concentration in the melted frost could be expressed by

$$Cl = 3.523 \cdot 2^n \text{ mg pro litre}$$

where n is a positive or negative integer. Of course there was some variation within each group but the group formation was quite obvious and statistically significant.

The distribution of Cl concentrations will be called the "Köhler" distribution here. It is of interest as he had earlier found that the masses of cloud particles also showed a group formation which could be written

$$m = B \cdot n$$

where B is a base number and n so far has been shown to take the values 2, 3, 4, 5, 6, 7, 8, 10 and 12.

A surprising fact from this frost analysis was, however, that no correlation between the masses of the cloud particles and their Cl concentrations was found.

The explanation offered by Köhler for the observed Cl distribution is that the weight of the spray particles, which leave the sea is distributed in the same way as the Cl concentrations, but the reason for such a distribution in the spray is, of course, difficult to give.

On basis of further investigations in the same place (the Haldde district in northern Norway) he found that the most common particle size had a radius of $8.82 \cdot 10^{-4}$ cm. As the most common Cl concentration was 3.523 mg/l the most common amount of sea salts in a particle is $1.847 \cdot 10^{-14}$ g but that smaller or greater amounts could occur. For comparison it can be mentioned that ALIVERTI (6, 7) in an investigation from Pavia in Italy found that the average amount of salt in condensation nuclei was $0.075 \cdot 10^{-14}$ which corresponds to a value of n in Köhler's formula between —4 and —5, if the particles had the same masses.

Investigations similar to Köhler's were later carried out by LIPP (192) and LAUSHER & SCHWARZ (170) in the Hohen Sonnblick and by MENZL (207) in Donnersberge. The data of LIPP and LAUSCHER & SCHWARZ are, however, too few to detect any "Köhler" distribution. The Cl values from Donnersberge are surprisingly high, varying from 3.43 to 15.33 mg Cl/l.

There are some other investigations of Cl in rainwater where distinct "Köhler" distributions of Cl concentrations are found. In these the rainfalls are, of course, analysed separately. In *Leiden* in Holland (4 km from the sea) ISRAËL (150) found that the Cl content of rainwater could be expressed by

$$Cl = 3.42 \cdot 2^n \text{ mg pro litre}$$

where $n = 0$ and 1 seemed to be the most common values.

The West Australian investigation mentioned before (WOOD & WILSMORE 316) show also weak signs of the "Köhler" distribution as well as MENZL's (208) on rainwater from Donnersberge.

In an investigation from Japan MIYAKE (216) also found "Köhler" distributions of Cl concentrations in rainwater although the base numbers varied somewhat. In Tokyo he found

$$Cl = 2.10 \cdot 2^n \text{ mg Cl/l}$$

and in Kobe

$$Cl = 1.89 \cdot 2^n \text{ mg Cl/l}$$

and in Hamamatu

$$Cl = 4.0 \cdot 2^n \text{ mg Cl/l.}$$

The most pronounced "Köhler" distribution of Cl contents in rainwater is found in the analysis from Mont Vernon in Iowa, U.S.A. The investigations are extended over 10 years with analysis of separate rainfalls. The analyses are, however, apparently carried out by different workers under the supervision of N. KNIGHT at the Mont Vernon University (For references see 15, 117, 161, 234, 246, 269, 290, 306 and 318). In most of the reports only the total amount of Cl/acre is given. The author has therefore recalculated the Cl concentrations from these amounts and the listed rainfalls.

Table 13. The distribution of Cl-concentrations of the rainfalls at Mont Vernon, Iowa. Cl = 0.355 · *s*.

s	1	3	7	8	10	13	14	15	16	18	20	22	23	24	25	26	27	
Frequ.	1	1	1	3	30	1	2	3	7	2	94	4	1	5	4	5	3	167
s	28	29	30	32	33	34	35	36	40	43	45	48	49	50	52	60	70	
Frequ.	1	1	71	2	1	2	3	5	14	1	3	1	1	1	1	4	2	114
s	73	88	92	140														
Frequ.	1	1	1	1														4
Total Frequ.																		285

From the total number of analysis it can be concluded that the analyses of Cl were carried out with a precision of 0.355 mg Cl pro litre as practically all the figures can be represented by the formula

$$Cl = 0.355 \cdot s$$

where *s* is a positive integer ranging from 1 to 140. The number of Cl analysis for different *s* is shown in tab. 13.

In connection with KÖHLER's work it is of interest to note the high frequency of *s* equal to 10, 20 and 40. These are well represented by Köhler's formula with the base number 3.5 and *n* equal to 0, 1 and 2. On the other hand the high frequency of the figure 10.65 ($s = 30$) indicates a deviation from the "Köhler" distribution, 10.65 being the sum of $3.55 \cdot 2^0$ and $3.55 \cdot 2^1$.

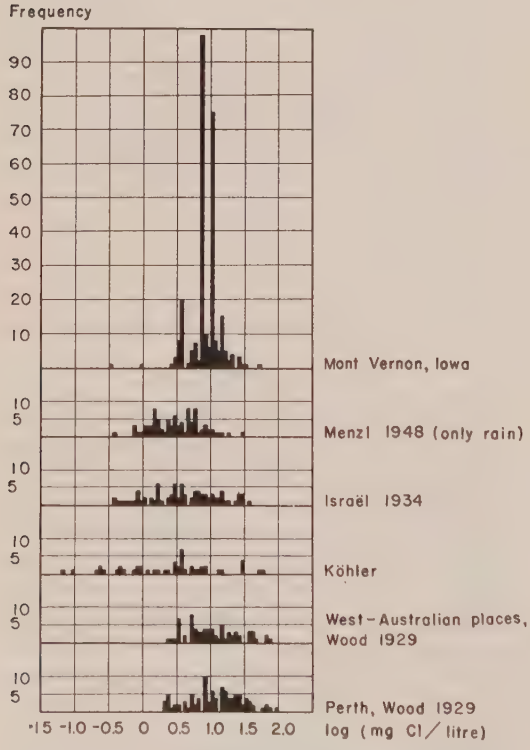

Fig. 11. The distribution of log (mg Cl/l) for some places.

The distribution of log (mg Cl pro litre) for Perth and some other places in Australia (WOOD & WILSMORE, 316) Haldde (KÖHLER, 165) Leiden (ISRAËL, 150) Donnersberge and Haid (MENZL, 208), and from Mont Vernon, Iowa is shown in fig. 11. The intervals have been taken equal to 0.05 units. It is seen that the Haldde series shows the widest distribution and very distinct frequency groups. This is also quite distinct in the Leiden series as well as in the Donnesberge-Haid series. In the Mont Vernon series this frequency group formation is very pronounced. The Australian series have, at least, a tendency of frequency group formation. The base values for this series seems, however, to differ from the European and American series, a fact which is of interest in connection with the earlier mentioned Japaneese observations.

A frequency group formation can also be traced in the figures published by HEYMANN (140) from Oosterveld in Holland which has been mentioned earlier. On the other hand the Zeeveld figures do not show any such tendency. As Zeeveld is close to the sea the figures may be influenced by sea spray which has precipitated straight into the rain gauge.

It should be mentioned that HOUGHTON & BENRIS (142) did not find any frequency group formation in the Cl values from cloud water collected on Mount Washington. However, they did not give any details of their work.

Table 14. See the text.

Catchment area	Area	Rainfall	Ratio Discharge to Rainfall	Mean conc. of Cl.		
				Rain-water	River water	
					calc.	Actual
	km²	mm				
Upper Murray, Vic.	26600	842	0.283	1.0	3.5	3.4
O'Shannany River, Vic.	121	1620	0.520	2.7	5.2	4.75
Yarra River, Vic.	2530	1110	0.311	4.4	14.2	15.3
Barwon River, Vic.	3710	642	0.075	8.4	112	134
Helena River, West. Austr.	1480	713	0.034	6.7	197	203

From all the results shown it seems quite evident that a frequency group formation of the Cl content in precipitation does exist.

5. Practical importance of the transport of oceanic salts inland

In arid places the transport of sea salts inland has a very great practical importance. In western Australia the transport of sea salts inland has caused an increase in the salt content of the soil, the streams and the water reservoirs (Wood, 315). In 1914 Weller (303) found that the Mundering reservoir catchment area (about 1400 square km) received around 90 kg of oceanic salts pro hectare and year and as there is practically no outlet from this area to the sea the salinity of the reservoir water has been steadily increasing. Wood (315) also mentions that in many of the water reservoirs for the railways in Western Australia the salinity of the water had increased to such a degree that the water could not be used for the locomotives. This process has been enhanced in many places by the clearing of land from natural vegetation thereby causing a rapid runoff of water to the reservoir, the runoff water carrying the accumulated salts in the soil.

A more recent Australian investigation mentioned earlier (Anderson, 13) concerns arid parts of the State of Victoria. He found from analysis of river waters from different catchment areas that, knowing the rainfall, runoff and the salt content of the rainfall, it was possible to calculate the composition of the river waters. Comparison between calculated and found values shows a very good agreement. (See table 14.) As mentioned earlier he also found that the composition of some lake waters in this district was very similar to that of sea water.

It is obvious that under arid conditions where the percentage evaporation is high an accumulation of salts must occur in the soils. This is, no doubt, a very common cause of saline soils in desert and semidesert district although some saline soils may be due to salt lenses in the soil at greater depths and a high evaporation.

The salt transport seems to be of some importance also in New Zealand (119) where, in some places, the soil processes appear to be effected by the accumulation of oceanic salts.

A concentration of oceanic salts in the soil water seems also to take place in humid areas. Warington (295) published an account of analysis of drain and well waters in Rothamsted in 1887. He found that the Cl content of drain water from unfertilized plots was higher than in rainwater. This, he explained, was due to the evaporation which takes place during summer. This fact suggests an indirect method of estimating loss of water by evaporation from uncultivated soils. This, however, is possible only where no well waters containing Cl can reach the upper layers of the soil.

E. Iodine in precipitation and air

The presence of iodine in atmospheric precipitation is mainly of medical interest in connection with goitre and most of the more recent investigations seem to have had, as a purpose, the making of a survey of existing sources which can deliver iodine to the air.

As early as in 1852 Marchand (197) showed that rain, snow and hail contained considerable amounts of iodine and bromine. At about the same time Chatin (71) found in analysis of rain and spring waters from Guiana in South America 5 μg iodine/l and in Nice 4 μg/l. In an investigation from Pisa around 1860 de Luca (193) found iodine both at 54 and 18 m

height above the ground. (The samples were taken from the famous leaning tower.) On the other hand CHAIRY (70) in 1884 did not find any iodine in rainwater collected in Algiers despite the fact that the content of oceanic salts in the water was quite high.

More systematic work was started by VON FELLENBERG (107, 108) who in 1926 published a paper about the iodine cycle in nature. Most of his work is concerned with analysis for iodine in the air.

In 1927 HEYMANN (140) in Holland published analyses of air, rain and drainwater. A few air analyses from Leiduna (6 km from the sea) in 1924—25 are given below.

Wind direction	E	SW	SW	E	SO	SSW	NW
μg I/l	0.5	1.0	0.2	1.5	0.1	0.05	0.2

The rain analysis were carried out in Oosterveld and Zeeveld. He found an average of 3.6 μg for Oosterveld and 3.7 μg for Zeeveld. The distribution of the values are given below

	μg I pro litre	1	2	3	4	5	6
Frequency at	Oosterveld ...	5	0	7	7	5	1
	Zeeveld	3	6	3	4	8	1

	μg I pro litre	7	8	9	10	11	12
Frequency at	Oosterveld ...	3	1	1	0	0	0
	Zeeveld	1	2	1	0	0	1

There is as seen no difference in the iodine content of rain from these two places. The average Cl content in Oosterveld was 12.6 and in Zeeveld 28.8 mg Cl/l, Zeeveld being at only 0.4 km distance from the sea. Further there was no correlation between the Cl and the iodine figures. This suggests a different mechanism by which iodine is brought from the sea which in this case was the only possible source.

Further the ratio Cl/I in the samples was very much lower than in sea water as sea water contains only 20 μg/l. HEYMANN further observed a great difference in the behaviour of Cl and iodine. From his drain water analysis he found that while Cl was higher in the drain water than in the rain (due to evaporation) the reverse was true for iodine. A loss of iodine must have occured in the soil. VON FELLENBERG (108) found a little later that water containing iodide lost iodide when in contact with air. He suggested that iodide is oxidized to iodine which is volatile and escapes from the water to the air. Further he found that the air in spas which used iodine rich ground water contained a high concentration of iodine, up to 5 γ pro cubic metre, a fact which supported his theory.

In a series of investigations CAUER (63, 64, 65, 66) continued VON FELLENBERG's work. He also analysed air at high altitudes 3000 m for iodine and found about the same concentration as near the ground, i.e., it varied between 0.1 and 1.4 μg/cubic metre. This is also different from Cl which seems to decrease at higher altitudes.

CAUER developed a theory that the oxidation of iodide to iodine was done by ozone, present in the air, and he showed that ultraviolet radiation of iodide containing water caused great losses of iodine. The iodine cycle in nature is thus more complicated than the chloride cycle.

The sea is thus a great source of iodine which is partly brought to the air by spray and partly by oxidation of iodide to iodine. Iodide carried to the soil by rain may also be brought to the atmosphere by this oxidation.

An important source of iodine in air in the western Europe is iodine released in the process of burning seaweed as practiced to a great extent in Bretagne in France. Seaweed contain rather great amounts of iodine and Cauer estimated that about 6 per cent was lost during the burning process. In 1933 and 1934 this amount was equal to 65 tons a year, an amount which he considered to be sufficient to raise the iodine content of the air in western Germany up to 2 μg pro cubic metre.

Another source is from coal used in industry but this contribution is very small.

F. Other inorganic compounds in precipitation

Occasionally rain and snow has been analyses for other compounds than those discussed. Some old analyses are given by PIERRE (237), ARAGO (14), BARRAL (20), DE LUCA (193) and ROBINET (248). Of these that of ARAGO is of greatest interest. He collected rainwater in Paris from July to December 1851 and analysed for Ca and Mg. The average for this time is 6.5 mg CaO and 2.1 mg MgO/l.

More recently MAC INTYRE & YOUNG (195) made analysis for Ca, Mg, K and Na in rainwater collected at some points in Tennessee in

U.S.A. The atmospheric pollution was, however, quite strong at these places due to industrial activities.

In Europe some recent data on Ca and Mg in rainwater have been given by FARCY (105). He collected rainwater in the neighbourhood of Brest in France. He concluded from his analysis that part of Ca and Mg in the rainwater was of litospheric origin. FARCY also found Mn in the rainwater on some occasions. He believed that it had been carried over the Atlantic from America.

In a series of papers from 1943 to 1947 BERTRAND (29—35) gives some data on Ca and Mg in rainwater collected at Grignon and at Paris in France. In Paris he found as an average a Mg/Ca ratio of 0.089 (the soluble part) and in Grignon 0.049. The same ratio in sea water is 3.16. Most of the Ca must then have been of litospheric origin while at least part of the Mg was derived from the sea.

In Holland LEEFLANG (177) analysed rainwater collected at different distances from the sea also for Ca and Mg. The results are shown below

Distance from the sea in km	0.44	2.28	3.0	5.6	48.0	86.0	Sea water
Ca mg/l	2.5	1.9	1.7	1.7	1.7	1.7	
Mg „	1.7	1.3	1.2	1,1	1.0	1.8	
Mg/Ca	.68	.68	:70	.65	.59	.47	3.16
Mg/Cl	.105	.143	.160	.169	.250	.250	.068
Ca/Cl	.154	.209	.226	.262	.425	.532	.021

and are shown graphically in fig. 8.

It is seen that Mg decreases regularly inland whereas Ca remains comparatively constant. The Mg/Cl ratio increase 2.5 times inland but is of the same order of magnitude as in sea water near the coast. The ratio Ca/Cl is much higher in the rainwater than in the sea even near the coast. It is about 25 times higher far from the coast.

A recent work from Japan gives similar results as those of LEEFLANG. From rainwater analyses during 1946—49 SUGAWARA et al. (281) reported the following ratios.

Place	Suga-shima	Na-goya	Matsu-moto	Sea water
Distance from the sea in km	0	4	100	
Na/Cl	.05	.55	.58	.55
Mg/Cl	.080	.109	.344	.068
Ca/Cl	.138	.172	3.76	.021

The Na/Cl ratio is remarkably constant but the Mg/Cl and Ca/Cl ratios shows about the same trend as mentioned before.

SUGAWARA et al. offer an interesting explanation for the variation in these ratios. They regard the salts in rainwater as derived from the sea but they are washed down selectively, the most hygroscopic salts being washed down near the coast. Salts like $CaSO_4$ which are non-hygroscopic can be carried far inland, thus raising the Ca/Cl ratio considerably as chlorides of Mg and Ca are much more hygroscopic than corresponding sulfates and are precipitated near the coast. They found a similar trend in the ratios in a vertical direction by analysing precipitation, rain and snow from different altitudes. Also LIPP (192) found a considerable enrichment of Mg over Cl in rime frost on Hohen Sonnblick in Austria.

BERTRAND (36, 38, 39) also determined K in some rainwater samples collected in Paris. He found 0.22 mg K/l in 1942 in a sample and 0.42 in another. The corresponding Mg figures were 0.19 in the first sample. The potassium is thus relatively high. Part of it may be derived from coal by combustion.

In a recent work INGHAM (148) found that vegetation can adsorb comparatively large quantities of Ca from air which is washed down by rain. It is possible that non-hygroscopic salt can be adsorbed from the air in this way and thus be brought to the soil.

A few other compounds have been reported occasionally in rainwater. Small amounts of P_2O_5 have been found (MOORE et al., 217; TRIESCHMANN, 290; DE LUCA, 199). INGHAM (148) found in rain 0.34 mg P_2O_5/l and in drip from tree leaves during rain 2.0 mg/l. These figures are indeed very high compared to earlier estimates.

There is also an analysis on As in rainwater reported by XHORIS (317). The rainwater was collected near Liege and contained 3.07 mg As pro 100 g dry matter from the rainwater. He suggested industrial origin.

G. Miscellaneous

Atmospheric precipitation invariably contains insoluble substances of different origin. These have not been studied very much; on a few occasions with exceptional high contamination they have been investigated mostly in order to determine their origin.

Volcanoes often give rise to local contaminations. Sometimes the dust from eruptions can travel long distances. A well known example is the dust rain which occurred in northern Europe in 1875 when the volcano Askja on Iceland was in action. The distribution of ash and dust from this occasion has been reviewed by THORARINSSON (285).

In the Mediterranean coloured rain may occur. This is due to solid particles from arid regions. By the action of wind the particles are brought up into the air and can be carried long distances before they are precipitated by rain. MENIER (210) found on one occasion in Palermo in Italy that a sample of such dust contained 59.14 per cent sand, 23.91 per cent $CaCO_3$ and 8.58 per cent clay. He suggested as origin the Sahara Desert.

A real dustrain occurred in 1892 in May (NORDENSKIÖLD, 229, 230), the rain falling over parts of Germany, Denmark, Sweden and Finland. It was brought down in appreciable quantities in a comparatively narrow strip from northwestern Germany to Finland. The dust consisted mainly of mineral fragments.

The radioactivity of precipitation has also been investigated. It is reported (77) that snow has an induced radioactivity which disappears after a couple of hours.

Erratum

In part I of this paper, page 231, the eleventh row below the subheading no. 8 stands "cm³". Should read "cm²".

BIBLIOGRAPHY

1. ACKROYD, W., 1901: Researches on Moorland waters. Part II. On the origin of combined chlorine. *Trans. Chem. Soc.* **79,** 673.
2. ADEL, A., 1939: Note on the atmospheric oxides of nitrogen. *Astroph. J.*, **90,** 627.
3. — 1946: A possible source of atmospheric N_2O. *Science*, **103,** 280.
4. — 1951: Atmospheric nitrous oxide and the nitrogen cycle. *Ibid.*, **113,** 624—625.
5. ALBRECHT, F., 1925: Wolkenuntersuchungen auf dem Hohen Sonnblick in Sommer 1924. *Jahresber. des Sonnblicks-Vereines*, 1924, 11—15.
6. ALIVERTI, G., 1941: La condensazione del vapor d'acqua nell'atmosfera. *Ricerca sci.* **12,** 1251—1260.
7. — 1946. La salinità delle precipitazioni a Pavia nel periodo Ottobre 1944—Ottobre 1945. *Ricerca sci. e ricostruz.* **16,** 929—931.
8. ALWAY, F. J., MARSCH, A. W., & METHLEY, W. J., 1937: Sufficiency of atmospheric sulfur for maximum crop yield. *Proc. Soil Sci. Soc. Amer.*, **2,** 229—238.
9. ALWAY, F. J., 1940: A nutrient element slighted in agricultural research. *J. Amer. Soc. Agron.* **32,** 913—921.
10. ANDERLIND, L., 1898: Mitteilungen über die Abhängigkeit der Menge des in den wässrigen Niederschlägen enthaltenen Stickstoffs von den Land- und Seewinden. *Die Landw. Versuchsst.* **50,** 159.
11. ANDERSON, V. G., 1914: The influence of weather conditions upon the amount of nitric acid and nitrous acid in the rainfall near Melbourne. *Chem. News*, **110,** No. 2859.
12. — 1915: The influence of weather conditions upon the amount of nitric acid and nitrous acid in the rainfall near Melbourne. *Quart. Journ. Roy. Met. Soc. London.* **41,** 99—122.
13. — 1945: Some effects of atmospheric evaporation and transpiration on the composition of natural waters in Australia. *Journ. Proc. Australian Chem. Inst.* **12,** 41—68, 83—98.
14. ARAGO, F., 1852: Rapport sur un travail de M. Barral, intitulé: Premier mémoire sur les eaux de pluie recuellies à l'Observatoire de Paris. *Compt. Rend.*, **34,** 824—834.
15. ARTIS, B., 1916: Nitrogen, chlorin and sulfates in rain and snow. *Chem. News*, **113,** No. 2928, 3—5.
16. ATKINS, W. R. G., 1947: Electrical conductivity of river, rain and snow water. *Nature*, **159,** 674.
17. AUFRAY, 1909: Nitric acid and ammonia in the rainfall at Tonkon. *Bull. Econ. Ind. China*, n. ser. 12.
18. BAMBER, M. K., 1900: *Report on Ceylon tea soils.* Colombo.
19. BARBADOS: Composition of Barbados rainfall. *Rpt. Agr. Work Barbados. Imp. Dept. Agr. West Indies.* The Years 1901 to 1908.
20. BARRAL, 1853: Note sur l'analyse d'eaux de pluie recueillies et distillées dans du platine. *Compt. rend.*, **36,** 184—187.
21. BASILE, G., 1895: Analisi delle acqua meteoriche cadute a Catania du tutto giugna 1888 a tutto settembre 1889. *Staz. Sper. Agrar. Ital.*, **28,** 545—574.
22. BATTA, G., & LECLERC, ED., 1934: Note sur la composition des eaux résultant de la foute des neiges. *Bull. Soc. Chim. Belg.*, **43,** 320—326.
23. BEAR, F. E., 1922: Nitrogen economy in soils. *J. Amer. Soc. Agron.*, **14,** 136—152.
24. BECHI, E., 1876: *Saggi di esperienze agrarie.* Florence 1870—76.
25. BERTOLANI, M., 1946: La neve rossa caduta nel gennaia 1946 sulla zona dell'Abetone. *Atti. Soc. Nat. e Mat. Modena.*, **77,** 123—129.
26. BERTRAMSON, G. R., FRIED, M., & TISDALE, S. L., 1950: Sulfur studies of Indiana soils and crops: *Soil Sci.*, **70,** 27—41.
27. BERTRAND, G., 1935: A propos des apports atmos-

phériques de soufre combiné aux terres arables. *Compt. Rend. Acad. Agr. France.*, **21,** 1015—1018.
28. — 1935: Observations à propos des apports atmosphériques de soufre aux terres arables. *Compt. Rend.*, **201,** 309—312.
29. — 1943: Sur le magnésium contenu dans l'eau de pluie récoltée à Grignon. *Ann. Agron.*, **13,** 109—116.
30. — 1943: Sur le magnésium contenu dans l'eau de pluie récoltée à Paris. *Ann. Agron.*, **13,** 221—232.
31. — 1943: Sur le magnésium contenu dans l'eau de pluie récoltée à Grignon. *Ann. de l'Institute Pasteur*, **69,** 294—302.
32. — 1943: Sur le magnésium de l'eau de pluie récoltée à Grignon. *Compt. Rend.*, **216,** 364—367.
33. — 1943: Sur le magnésium et le calcium de l'eau de pluie recoltée à Paris. *Compt. Rend.*, **216,** 701—704.
34. — 1944: Origin multiple du magnésium de l'eau de pluie. *Compt. Rend.*, **219,** 14—16.
35. — 1944: Sur le magnésium contenu dans l'eau de pluie récoltée à Paris. *Ann. de l'Institute Pasteur*, **70,** 234—247.
36. — 1945: Le potassium dans l'eau de pluie. *Compt. Rend.*, **220,** 865—868.
37. — 1945: Sur l'origine multiple de magnésium contenu dans l'eau de pluie. *Ann. Agron.*, **15,** 153—160.
38. — 1946: Sur le potassium de l'eau de pluie. *Ann. de l'Institute Pasteur*, **72,** 621—630.
39. — 1947: Démonstration biologique de la présence du magnésium et du potassium dans l'eau de pluie. *Compt. Rend.*, **225,** 169—172.
40. — 1947: Sur une démonstration par voie biologique de l'existence du magnésium et du potassium dans l'eau de pluie. *Ann. Agron.*, **17,** 639—642.
41. Bineau, A., 1852: Recherches sur la composition chimique des eaux de pluie recueillies dans l'hiver de 1851—52 à l'Observatoire de Lyon. *Compt. Rend.*, **34,** 357—359.
42. Bleyer, B., Schweibold, J., & Harder, B., 1932: Beiträge zur Kenntnis des Jodumlaufes in der Natur. *Biochem. Zeitschr.*, **251,** 87—100.
43. Bobierre, 1864: Recherches sur la composition chimique de l'eau pluviale recueillie dans les villes à diverses altitudes. *Compt. Rend.*, **58,** 755.
44. Boname, P., 1895: *Rapport Annuel de la Station Agronomique pour 1895.* Mauritius.
45. Bordas, F., & Desfemmes, A., 1928: Pluies de poussières et pluies de sel. *Compt. Rend.*, **185,** 603—605.
46. Boss, G., 1941: Niederschlagsmenge und Salzgehalt des Nebelwassers an der Küste Deutsch-Südwestafrikas. *Bioklim. Beiblätter.*, **8,** 1—15.
47. Bottini, O., 1935: Fattori pedogenetici particolari della regione vesuviana. Gas e sublimazioni vulcaniche. *Ann. Osservatorio Vesuviano.*, **3,** 141—151.
48. — 1939: (Corrosive rains in the Vesuvius region.) *Ann. chim. applicata*, **29,** 425—433. Ref. C. A., **34,** 1783.
49. Boussingault, J. B., 1882: Recherches sur la présence de l'acide nitrique et de l'ammoniaque dans le eaux et la neige, recueillies dans les glaciers des Alpes par M. Civilale. *Compt. Rend.*, **95,** 1121—1123.
50. — 1858: Recherches sur la quantité l'acide nitrique contenue dans la pluie, le brouillard, la rosée. *Compt. Rend.*, **46,** 1123—1130, 1175—1183.
51. Braadlie, O., 1930: Inneholdet av ammoniak og nitratkvelstoff i nedbøren ved Trondhjem. *Kgl. Norske Vids. Selskaps Forhandl.*, **3,** no. 20.
52. Braarud, T., & Klem, A., 1931: Hydrographical and chemical investigations in the coastal waters off Møre. *Hvalrad. Skr.* no. 1.
53. Bretschneider, P., 1872: *Ueber den Regenfall zu Ida-Marienhütte in den Jahren 1865—1872 und der Gehalt des meteorischen Wassers an Stickstoff in Form von Ammoniak und Salpetersäure.* Breslau 1872.
54. — 1872: Ueber die Quantitäten Ammoniak welche die hauptsächlichsten Konstituenten des Kulturbodens aus der Atmosphäre innerhalb eines Jahres auf gemessener Fläche absorbieren. *Der Lantwirt*, **8,** 225, 234, 238 & 241.
55. Brown, H. T., 1870: On the estimation of ammonia in atmospheric air. *Proc. Roy. Soc., London*, **18,** 286—288.
56. Brünnish, J. C., 1909: Fertilizing value of rainwater. *Ann. Rep. Dept. Agric. Queensland*, 1908—09, p. 59—60.
57. Buch, K., 1920: Ammoniakstudien an Meer- und Hafenwasserproben. *Kemistsamfundets Meddelanden* 1920, p 57—74.
58. Buenos Aires, 1906: The climate of Buenos Aires. *Statis. Ann. City Buenos Aires*, **16,** 3—8.
59. Bullard, F. M., 1947: Studies on Paracutin volcano, Michoacan, Mexico. *Bull. Geol. Soc. Amer.*, **58,** 433—450.
60. Capus, G., 1914: The economical value of tropical rainfall. *Ann. Geogr.*, **23,** 109—126.
61. Carmody, P., 1902: *Ann. Rep. Govt. Analyst for 1901—2* (Trinidad 1902.)
62. Casoli, A., 1901: L'ammoniaca nelle acqua meteoriche e la pioggia sanguinante. *Staz. Sper. Agr. Ital.* **34,** 833—848.
63. Cauer, H., 1931: Das Jod der Luft im Hochgebirge. *Jahresber. des Sonnblicks-Vereines*, 1931, p 20—27.
64. — 1933: Das Jod der Luft, sein chemisches Verhalten und seine bioklimatische Bedeutung. *Veröff. Med. Verw.*, **39,** 466—584.
65. — 1937: Chemisch-bioklimatische Studien in der Bretagne. *Biochem. Zeitschr.*, **292,** 116.
66. — 1938: Einiges über den Einfluss des Meeres auf den Chemismus der Luft. *Der Balneologe.*, **5,** 409—415.
67. — 1941: Chemische Studien über die Bedeutung der Gesteinsstaubteilchen als Sublimationskerne in der freien Atmosphäre. *Bioklim. Beibl.* no. 3—4, 90—92.
68. Cavalcanti, A. B. U.: *Aquas Pluviales.* Inst. Agron. Estado Sao Paulo em Campinas Colleccao dos trabalhos agricolas extrahidos dos Relatorios. *Annuaes* de 1888—1893, p 135—137.
69. Chabrier, 1871: Dosage des acides nitreux et nitriques dans les eaux de pluie. *Compt. Rend.*, **73,** 485—488, 1273—1274.
70. Chairy, 1884: Sur les eaux de pluie de la ville d'Algier. *Compt. Rend.*, **99,** 869—871.
71. Chatin, A., 1853: Présence de l'iode dans les eaux pluviales, les eaux courantes, et les plantes des Antilles et des côtes de la Méditerranée. *Compt. Rend.*, **37,** 958.
72. Clarke: The data of geochemistry. *U. S. Geol. Survey Bull.* 770.
73. Cloëz, S., 1861: Note sur la présence de l'acide nitrique libre et des composés nitreux oxygénés dans l'air atmospherique. *Compt. Rend.*, **52,** 527.
74. Collins, W. D., & Williams, K. T., 1933: Chloride

and sulfate in rain water. *Ind. Eng. Chem.*, **25**, 944—945.
75. Collison, J. B., & Mensching, J. E., 1932: Composition of rain water at Geneva, N.Y., for a 10-years period. *N. Y. State Sta. Techn. Bull.*, **193**, 19 pp.
76. Conrad, J. P., 1950: Sulfur fertilization in California and some related factors. *Soil Sci.*, **70**, 43—54.
77. Constanzo, G., & Negro, C., 1906: Über die Radioaktivität des Regens und Schnees. *Physikal. Zeitschr.*, **7**, 350—352, 921—924.
78. Conway, E. J., 1942: Mean geochemical data in relation to oceanic evolution. *Proc. Roy. Irish Acad.* **48**, 119—159.
79. Cooper, L. H. N., 1937: The nitrogen cycle in the sea. *J. Mar. Biol. Ass.*, **22**, 183—204.
80. Corbet: See Koch 1941.
81. Crowther, Ch., & Ruston, H. G., 1911: The nature, distribution and effects upon vegetation of atmospheric impurities in and near an industrial town. *J. Agr. Sci.*, **4**, 25—55.
82. Crowther, Ch., & Stuart, D. W., 1913: The distribution of atmospheric impurities in the neighbourhood of an industrial city. *J. Agr. Sci.*, **5**, 391—408.
83. Cultrera, R., 1946: (Photochemical oxidation of H_4N^+ to NO_2^- in soils.) *Ann. Chim. Appl.* **36**, 245—253. Ref. *Soil & Fert.*, **10**, 423.
84. Dalton, J., 1825: Salin impregnation of rain. *Edinburgh J. Sci.*, **2**, 176.
85. Daniel, H. A., Elwell, H. M., & Parker, H. Y., 1938: Nitrate nitrogen content of rain and runoff water from plots under different cropping systems on soils classified as Vernon fine sandy loam. *Proc. Soil Sci. Amer.*, **3**, 230—233.
86. Das, A. K., Sen, G. C., &, Pal, C. K., 1933: The composition of the rain water of Sylhet. *Indian J. Agr. Sci.*, **3**, 353—359.
87. Dauvillier, 1933: Sur l'origine de l'ozone atmosphérique. Recherches faites au Scoresby Sund durant l'Année polaire. *Compt. Rend.*, **197**, 1339.
88. Deacon, G. E. R., 1933: A general account of the hydrology of the southern oceans. *Discovery Rep.*, **7**.
89. Dhar, N. R., & Ram, A., 1933: Variation in the amounts of ammonical and nitric nitrogen in rain water of different countries and the origin of nitric nitrogen in the atmosphere. *J. Ind. Chem. Soc.*, **10**, 125—133.
90. Dhar, N. R., & Seshacharyulu, E. V., 1939: Nitrogen fixation in soil not wholly a bacteriel process. *J. Ind. Chem. Soc.*, **16**, 557—562.
91. Dhar, N. R., 1946: New aspects of nitrogen fixation in soils and origin of soil nitrogen. *Proc. Nat. Acad. Sci. India.*, **15**, 15—53.
92. Djalma, H., 1929: The composition of rainwater of Rio de Janeiro. *Rev. Bras. Chim.*, **1**, 51—52.
93. Dole, R. B., 1914: Chlorine content of rainwater at Tortugas, Fla. *Washington Acad. Sci. Journ.*, **4**, 3—4.
94. Dole, M., 1949: The history of oxygen. *Science*, **109**, 77—81.
95. Eaton, S. V., & Eaton, J. H., 1926: Sulfur in rain water. *Plant Physiology*, **1**, 77—87.
96. Ehrenberg, P., 1907: Die Bewegung des Ammoniakstickstoffs in der Natur. Kritische Monographie aus dem Kreislauf des Stickstoffs. *Mitt. Landw. Inst. Königl. Univ. Breslau*, **4**, 254 pp.
97. Eichhorn, W., 1866: Bericht der Central-Kommission für das agrikulturchemische Versuchswesen über die in den Jahren 1864—65 ausgeführten Messungen, der mit dem Regenwasser niederfallenden Ammoniak- und Salpetersäuremengen, an den Minister für die landwirtschaftlichen Angelegenheiten Herrn von Selchow. *Ann. Landwirtschaft.*, **24**, 97—141.
98. — 1867: See ref. 97. *Ann. Landwirtschaft.*, **25**, 249—278.
99. Ellet, W. B., & Hill, H. H., 1929: Effect of lime materials on the outgo of sulfur from Hagerstown silt loam soil. *J. Agr. Res.*, **38**, 697—711.
100. Erdman, L. W., 1922: The sulfur of rainwater. *Soil Sci.*, **14**, 363—367.
101. Ernst, W., 1938: Über pH-Wertmessungen von Niederschlägen. *Der Balneologe*, **5**, 545—549.
102. Erwin, R. W., 1893: Nitrogen in rainwater. *Utah Sta. Rpt.* 1893, p. 252—253.
103. Eugling, W., 1877: Ueber den Gehalt an Ammoniak und Salpetersäure in den atmosphärischen Niederschlägen. *Ber. über die Tätigheit d. lantw. chem. Versuchsstation des Landes Vorarlberg*, 1876—1877.
104. Failyer, G. H., & Willard, J. T., 1889: Ammonia and nitric acid in atmospheric waters. *Sec. Ann. Rpt. Kansas Agr. Exp. Sta.* p. 123—132.
105. Farcy, L., 1931: La composition des eaux de pluie de la région de Brest et du Nord finistère. *Ann. Hyg.*, **9**, 504.
106. von Feilitzen, H., & Lugner, I., 1910: Undersökningar över de mängder bundet kväve, som tillföres jorden med nederbörden. *Kgl. Lantbr. Akad. handl. o. tidskrifter.* 1910, p 151.
107. von Fellenberg, T., 1926: *Das Vorkommen, der Kreislauf und der Stoffwechsel des Jods.* München 1926.
108. — 1930: Joduntersuchungen in Bad Hall in Oberösterreich. *Mitt. Geb. Lebensmitt. Unters. und Hygiene*, **21**, 188—204.
109. Filhol, E., 1855: Note sur la composition chimique de l'eau de pluie tombée aux environs de Toulouse pendant le premier semestre de l'année 1855. *Compt. Rend.*, **41**, 838—839.
110. Finell, H. H., & Houghton, H. W., 1931: Soil nitrogen income from rainwater. *Oklahoma Panhandle Sta. Panhandle Bull.*, **23**, 7—24.
111. — 1932: Nitrogen content of rainwater. Ibid. **34**, 3—8.
112. Finnberg, F. V., 1923: Einige Bestimmungen des Gehaltes der atmosphärischen Niederschläge an Stickstoffverbindungen, ausgeführt in Storkyrö (Finnland), 1921—22. *Soc. Sci. Fennica Commentations Physica-Math.* I nr 28, 1—9.
113. Fodor, J., 1881: *Hygienische Untersuchungen über Luft, Boden und Wasser. I. Die Luft.* Braunschweig. 1881.
114. Fraps, G. S., 1930: Possibilities of sulfur as a soil amendment. *Texas. Agr. Exp. Sta. Bull.*, **414**, 56 pp.
115. Freeman, Y. F., 1924: Nitrogen in the rainwater of different points in Kentucky. *J. Amer. Soc. Agron.*, **16**, 356—358.
116. Fried, M. J., & Jackson, M. L., 1947: Sulfur collection in precipitation by means of an all-weather noncorrosive rain and snow gauge. *Science* **106**, 19—20.
117. Fries, H. S. J., 1923: Substances dissolved in rain and snow. *Chem. News*, **126**, 113.
118. Gehrcke, E., 1933: Warum hat Ägyptien eine

braune Farbe? *Forschung und Fortschritte* no 34, p 489.
119. Gibbs, H. S., & Blakemore, L., 1952. (On cyclic salts.) *N. Z. J. Sci. Techn.* In the press.
120. Goppelschröder, F. R., 1870: Ueber Schwankungen im Gehalte der Trinkwasser an Salpetersäure und über deren Gemenge in den atmosphärischen Niederschlägen. *Zeitschr. Anal. Chem.* **9,** 177—178.
121. — 1871: Mitteilungen. *Journ. Prakt. Chem.* (N.F.), **4,** 139—159.
122. — 1871: Bestimmungen des Salpetersäuregehaltes in Regenwasser, Quell-, Fluss- und Seewässern. *Ibid.* **4,** 383—388.
123. — 1871: Beitrag zur Kenntnis der Chemie der atmosphärischen Niederschlägen, mit besonderen Berücksichtigung deren Gehaltes an Salpeter. *Zeitschr. Anal. Chem.*, **10,** 259—277.
124. — 1872: Beitrag zur Kenntnis der Chemie der atmosphärischen Niederschlägen (Fortsetzung) und des Salpetersäure- resp. Nitratgehaltes verschiedener Quell-, Bach-, Fluss- und Seewässern. *Ibid.*, **11,** 16—22.
125. Gray, G., 1888: On the dissolved matter contained in the rainwater collected at Lincoln, Canterbury, New Zealand. *Proc. Austr. Ass. Sydney.* 138—152.
126. — 1910: On the dissolved matter contained in rainwater, collected at Lincoln, New Zealand. *Canterbury Agr. Coll. Mag.*, **24,** 1910, Nov.
127. Günther, C., 1914: Wasser und Wasserversorgung. *Eulenburg Real Encyklopädie der Gesamte-Heilkunde.* 4. Aufl. Berlin 1914.
128. Hall, A. D., & Miller, N. H. J., 1908: The nitrogen compounds of the fundamental rocks. *J. Agr. Sci.*, **2,** 343—345.
129. — 1911: On the absorption of ammonia from the atmosphere. *J. Agr. Sci.* **4,** 56—68.
130. Hansen, F., 1926: Om bestemmelse av nitratkvælstoff i regnvand, drænvand og jord. *Tidskr. f. Planteavl.*, **32,** 69—120.
131. — 1931: Undersøgelser av regnvand. Ibid. **37,** 123—150.
132. Harper, H. J., & College, M., 1943: Sulfur content of Oklahoma rainfall. *Proc. Oklahoma Acad. Sci.*, **23,** 73—82.
133. Harrison, J. B., & Williams, J. 1897: The proportions of chlorine and of nitrogen as nitric acid and as ammonia in certain tropical rain waters. *J. Amer. Chem. Soc.*, **19,** 1—9.
134. Harrison, J. B., 1912: Composition of rainwater. *Rpt. Exp. Agr. Rpt. Sci. & Agr.* 1904—10, p. 15—18.
135. Hart, E. B., & Peterson, W. H., 1911: Sulfur requirements of farm crops in relation to the soil and air supply. *Wisc. Agr. Exp. Sta. Research Bull.*, **14,** 21 pp.
136. Harvey, H. W,. 1931: The fertility of the sea. *Finska Kemistsamfundets Medd.*, **40,** 63—66.
137. Hayman, J. M., 1906: Amount and composition of drainage waters, rain, dew and canal waters collected during the years 1903—04, 1904—05, and 1905—06. *Rpt. Cawnpore India Agr. Sta.* 1906, p. 23—29.
138. Heinrich, R., 1881: Ueber die Ammoniakmengen welche der Atmosphäre im Lauf eines Jahres durch Salzsäure entzogen werden. *Wollnys Forschungen,* **4,** 446—452.
139. Heller, V. G., 1938: The chemical content of Oklahoma rainfall. *Oklahoma Sta. Techn. Bull.*, **1,** 23 pp.
140. Heymann, J. A., 1927: Het jodiumgehalte van duin- en regenwater. *Nederland. Tijdschr. Geneeskunde,* **71,** 640.
141. Höll, K., 1935: Ueber die Trinkwasserversorgung der Insel Helgoland und über Vorkommen von bleihaltigen Trinkwasser daselbst. *Arch. Hygiene, Bakteriologie,* **113,** 283—295.
142. Houghton, H. G., &, Benris, A. C., 1939: Cloud particle studies on Washington. *Bull. Met. Soc. Amer.* **20,** 400—401.
143. Houzeau, A., 1883: Sur les causes capables d'influe sur la teneur en ammoniaque des eaux de pluviales. *Compt. Rend.*, **96,** 259—261.
144. Hudig, J., 1912: The amounts of nitrogen as ammonia and as nitric acid (and nitrous) in the rainwater collected at Vithuizermeeden, Groningen. *J. Agr. Sci.*, **4,** 260—269.
145. Hutchinson, G. E., 1944: Nitrogen in the biogeochemistry of the atmosphere. *Amer. Sci.* **32,** 178—195.
146. Ilkov, V., 1925: (Nitrogen compounds in atmospheric precipitation.) *Spisanic na zemedelskite opitni inst. v. Bulgarija.*, **3,** 325—328. Ref. in *Exp. Sta. Rec.*, **54,** 615.
147. Ingham, G., 1940: Fallowing in relation to nitrogen supply. *J. South African Chem. Inst.*, **23,** 52—54.
148. — 1950: Effect of materials adsorbed from the atmosphere in maintaining soil fertility. *Soil Sci.* **70,** 205—212.
149. Ingle, H., 1905: Amounts of nitrogen as ammonia and nitrates in rainwater collected at Pretoria. *Transvaal Agr. Journ.*, **4,** 104—105.
150. Israël, H., 1934: Ueber den Chlorgehalt des Regenwassers. *Bioklimatische Beiblätter* 1934. 53—57.
151. Jackson, D. D., 1905: The normal distribution of chlorine in natural waters of New York and New England. *U. S. Geol. Surv. Water Supp. and Irrig. Paper* nr 144.
152. Jacobs, W. C., 1937: Preliminary report on a study of atmospheric chlorides. *Mo. Weather Rev.* **65,** 147—151.
153. Johnson, E. M., 1924: Sulfur in rainwater in Kentucky. *J. Amer. Soc. Agron.*, **16,** 353—356.
154. — 1925: Analysis of rainfall from a protected and an exposed gauge for sulfur, nitrate nitrogen and ammonia. *Ibid.*, **17,** 589—591.
155. Jorissen, W. P., 1906: Het chloorgehalte van regenwater. *Chem. Weekbl.*, **3,** 647—649.
156. Juritz, C. F., 1914: Chemical composition of rain in the Union of South Africa. *South African J. Sci.*, **10,** 170—193.
157. Kellner, O., Savano, J., Yoshii, T., & Makina, R., 1886: I. Untersuchungen über der Gehalt den Atmosphärishen Niederschlägen an Stickstoffverbindungen. II. Ueber das Maximum an gebundenen Stickstoff welches des Ackerboden der Atmosphäre zu entziehen vermag. *Lantwirtschaftliche Jahrb.*, **15,** 701—711.
158. Kinch, E., 1887: The amount of chlorine in rainwater collected at Cirencester. *Trans. Chem. Soc. London.* **51,** 92—94.
159. —, 1900: Amount of chlorine in rainwater collected at Cirencester. *Ibid.*, **77,** 1271.

160. KNIGHT, N., 1911 and 1913: Nitrogen in rain and snow. *Proc. Iowa Acad. Sci.*, **18,** 75—77, **20,** 189—191.
161. KNOX, W. K., 1915: Nitrogen and chlorine in rain and snow. *Chem. News.*, **111,** 61—62.
162. KOCH, D. E. V., 1941 and 1943: The nitrogen content of Ceylon rain. *Trop. Agr.* (Ceylon) **97,** 74—77, **99,** 18—19.
163. KOSSOVICK, P. S., 1913: (On the circulation of sulfur and of chlorine on the earth, and on the importance of this process in the evolution of soil in the plant world.) *Zhur. Opytoi. Agron.* **14,** 181—228. Ref. in *Exp. Sta. Rec.* **30,** 422.
164. KUDRIN, S. A., 1948: (Nitrogen in rain in the serozem zone.) *Potchvovedenje,* **10,** 608—611.
165. KÖHLER, H., 1925: Untersuchungen über die Elemente des Nebels und der Wolken. *Medd. Stat. Meteor. Hydrogr. Anst. Stockholm,* **2,** nr 5.
166. — 1932: Vattenångans kondensation i atmosfären och molnens konstitution. *Kosmos,* **10,** 101—140.
167. — 1937: Studien über Nebelfrost und Schneebildung, und über den Chlorgehalt des Nebelfrostes, des Schnees und des Seewassers im Halddegebiet. *Bull. Geol. Inst. Uppsala,* **26,** 279—308.
168. — 1941: An experimental investigation on sea water nuclei. *Nova Acta Reg. Soc. Sci. Uppsaliensis.*, **12,** 55.
169. — 1946: Vatten i atmosfären. *Medd. nr 9 från Meteorologiska Inst. vid Kungl. Universitetet, Uppsala.*
170. LAUSCHER, F., & SCHWARZ, K., 1933: Ueber den Chlorgehalt des Nebelfrostes auf dem Sonnblick. *Jahresber. des Sonnblicksvereins.* 1931. 32 pp.
171. LAWES, J. B., & GILBERT, J. H., 1851: On agricultural chemistry. *J. Roy. Agr. Soc.*, **12,** 1—40.
172. — 1854: On the amount of, and methods of estimating ammonia and nitric acid in rainwater. *British Assoc. Reports,* 1854, p. 70—71.
173. LAWES, J. B., GILBERT, J. H., & WARINGTON, R. 1881. On the amount and composition of the rain- and drainage waters collected at Rothamsted. *J. Roy. Agr. Soc.*, **17,** 241—279, 311—350.
174. — 1883: New determinations of ammonia, chlorine and sulfuric acid in the rain water collected of Rothamsted. *Ibid.*, **19,** 313—331.
175. LEATHER, J. W., 1906: Composition of Indian rain and dew. *Mem. Dep. Agr. India. Chem.* Ser. 1. No. 1. 11 pp.
176. LECLERC, A., 1877: Analyse de pluies tombées à Methroy en 1877. *Bull. Soc. Agric. France.*, **9,** 302, **10,** 77 & 163.
177. LEEFLANG, K. W. H., 1938: De chemische Samenstelling van den Neerslag in Nederland. *Chem. Weekbl.*, **35,** 658—664.
178. LEVY, A. A., 1877: Dosages d'ammoniaque dans l'air et les eaux meteoriques faits à Montsouris. *Compt. Rend.*, **84,** 273—276.
179. — 1880: Ammoniaque de l'air et des eaux. *Ibid.* **91,** 94—97.
180. — 1888: *Annuaire de l'observatoire de Montsouris pour l'an 1887.* 180 pp.
181. — 1902: *Annales de l'Observatoire de Montsouris,* **3,** 362.
182. LIEBIG, J., 1847: *Farmer's Magazine,* **16,** 511.
183. LIEBIG, J., 1851: *Letters on chemistry,* 1851, 3rd ed. p. 519.
184. — 1863: Natural laws of husbandry. Chapt. XI.
185. LIESEGANG, W., 1927: Chemische Ermittlungen auf dem Gebiete der Lufthygiene. *Kleine Mitt. Mitgl. Ver. Wasser-, Boden und Lufthygiene.*, **3,** 9.
186. — 1927, 1928 and 1929: Die Untersuchung atmosphärischer Niederschläge. *Ibid.*, **3,** 317—327, **4,** 178—182, 261—265, 329—330, **5,** 84—86.
187. — 1933: Untersuchungen über die Mengen der in Niederschlagswässern enthaltenen Verunreinigungen. *Ibid.*, **9,** 306—321.
188. — 1934: *Ibid.*, **9,** 350—355,
189. LINCOLN, R., 1934: Report of the Chemical Division. *Dept. Agr. Mauritus, Ann. Rept.* 1934, 27—28.
190. — 1937: Chlorine in rainwater in Mauritius. *Mauritius Dept. Agr. Leaflet.* **41,** 12 pp.
191. — 1938: Report of the Chemical Division. *Dept. Agr. Mauritius, Ann. Rept.* 1938, p. 55—56.
192. LIPP, H., 1933: Ueber die chemische Zusammensetzung des Nebelfrostes auf der Zugspitze. *Jahresber. des Sonnblicksvereins.* 1937, p 27.
193. DE LUCA, S., 1861: Recherches sur les matières organiques et minerales des eaux de pluie. *Compt. Rend.*, **53,** 153—156.
194. MACH, E., 1888: Ueber den Gehalt des Regenwassers in St. Michele an Ammoniak und Salpetersäure. *Tiroler Landw. Be.*, **7,** 16—17.
195. MAC INTYRE, W. H., & YOUNG, J. B, 1923: Sulfur, calcium, magnesium and potassium content and reaction of rainfall of different points in Tennessee. *Soil Sci.*, **15,** 205—227.
196. MARCANO, V., MÜNTZ, A., & LÉVY, A., 1891. Ammoniaque dans l'atmosphère et dans les pluies d'une region tropicale. *Compt. Rend.* **113,** 779—781.
197. MARCHAND, E., 1852: Sur la constitution physique et chimique des eaux naturelles. *Compt. Rend.*, **34,** 54—56.
198. MARIMPIETRI, L., & SIMONCELLI, F.: Il pH e il contenuto in azote delle precipitazioni meteoriche vute in Roma nel triennio 1929—31. *Pubblicazioni della R. Stazione Chimico-Agraria di Roma.* Pubbl. N. 299.
199. MARR, T., 1891: Over Nitreuse Stiktof in het Regenwater. *East Java Exp. Sta. Contr.* **38.**
200. —, 1893: Stickstoffgehalt des Regenwassers in Java. *Zuckerindustri,* **18,** 1521.
201. — 1893: Over den Regenval en het Stikstofgehalte van het Regenwater. *East Java Exp. Sta. Contr.* **47,** 63—67.
202. MASON, O., ANDERSON, V. G., AVERY, D., & HUNT, H. A., 1915: The influence of weather conditions upon the amount of nitric acid and nitrous acid in the rainfall near Melbourne. *Rep. Brit. Assoc. Adv. Sci.*, **85,** 87—94.
203. MASON, O., 1916: The influence of weather conditions upon the amount of nitric acid and nitrous acid in the rainfall near Melbourne. *Ibid.*, **86,** 128—129.
204. MATTSON, S., SANDBERG, G., &, TERNING, P. E., 1944: Electrochemistry of soil formation: VI. Atmospheric salts in relation to soil and peat formation and plant composition. *Ann. Agric. Coll. Sweden* **12,** 101—118.
205. MAYER, A., 1889: Stickstoffsgehalt verschiedenen Wassersorten in der Umgegend der Versuchstation Wageningen. *J. Landw.* 1889. p. 39—41.
206. MENZL, O., 1944: Ueber den Chlorgehalt der Niederschläge. *Bioklimatische Beiblätter,* **11,**

207. —, 1948: Nebelfrostuntersuchungen auf dem Donnersberge. *Wetter und Klima*, **1**, 88—92.
208. — 1948: Ueber den Chlorgehalt der Niederschläge. *Zeischr. Meterorologi*, **2**, 289—295.
209. Merino, B., 1894: Algunas indicaciones sobra el cloro y ammoniaco contenido en la lluvia del ano 1893 y parte de 1894. *Observatorio Meterologico del Colegio de la Campania de Jesus en la Guardia Cuaderno Tercero* p. 37. Tuy' 1894.
210. Meunier, S., 1901: Sur la pluie de sang observée à Palerme dans la nuit du 9 au 10 Mars 1901. *Compt. Rend.*, **132**, 894—896.
211. Meyrac, V., 1852: Observations sur les eaux de pluie, des neiges et de rosées. *Compt. Rend.*, **34**, 714—717.
212. Miller, H. B., 1924: Economy through smoke abatement. *Ind. Eng. Chem.*, **16**, 1049—1051.
213. Miller, N. H. J., 1902: The amounts of nitrogen as ammonia and as nitric acid and chlorine in the rainwater collected at Rothamsted. *J. Agr. Sci.*, **1**, 280—303.
214. — 1913: The composition of rainwater collected in the Hebrides and in Iceland. *J. Scot. Met. Soc.*, **3**, 141—158.
215. Miquel, P., 1908: Eaux d'alimentation de Paris. Premier semestre 1908. *Ann. Obs. Munic. Montsouris*, Paris 1908 nr 1—2, p. 29—62.
216. Miyake, Y., 1939: The chemistry of rainwater. *J. Met. Soc. Japan*, **17**, 20—37.
217. Moore, W. A., & Browning, G., 1921: The substances dissolved in rain and snow. *Chem. News* **122**, 51—52.
218. Mrose, H., 1940: Chemische Untersuchung von Raureifschmelzwasser in Thüringen. *Zeitschr. f. angew. Met. (Das Wetter)*, **57**, 241—254.
219. Müntz, A., & Aubin, E., 1882: De la distribution de l'ammoniaque dans les météores aqueux aux grandes altitudes. *Compt. Rend.*, **95**, 788.
220. — 1882: Sur la nitrification atmospherique. *Ibid.* **95**, 919—921.
221. — 1883: Sur les origines de l'azote combiné existant à la surface de la terre. *Ibid.*, **97**, 240—243.
222. Müntz, A., & Marcano, V. 1889: Sur la proportion de nitrates contenus dans les pluies des regions tropicales. *Ibid.*, **108**, 1062—1064.
223. — 1892: Ammoniaque dans l'atmosphere et dans les pluie. *Ibid.*, **114**, 184.
224. Müntz, A., & Lainé, E., 1911: Les nitrates dans l'atmosphere des regions australes. *Ibid.*, **152**, 166—169.
225. — 1911: L'ammoniaque dans les pluies et les neiges des stations d'observation de la Mission Charcot. *Ibid.*, **153**, 749—750.
226. Narayanaswami, R., 1939: Measurements of the chloride, nitrate and nitrite present in the water of monsoon rains of Bombay. *Proc. Indian Acad. Sci.*, **9A**, 518—525.
227. Newman, I. V., 1948: Aerobiology on commercial air routes. *Nature*, **161**, 275—276.
228. Nichols, R. L., 1941: Atmospheric oxygen and the volcanic gases. *Trans. Amer. Geophys. Union.* Part II. 505—506.
229. Nordenskiöld, A. E., 1893: Om stoftfallet i Sverige och angränsande länder den 3:dje maj 1892. *Geol. För. Förh. Stockholm*, **15**, 417—459.
230. — 1894: Ueber den grossen Staubfall in Sweden und angrenzenden Länder an 3 Mai 1892. *Met. Zeitschr.*, **11**, 201—218.
231. Olson, G. A., & St. John, J. L., 1921: An investigation of sulfur as a plant food. *Wash. Agr. Exp. Sta. Bull.*, **165**.
232. Passerini, N., 1889: (Soluble compounds in rainwater in 1888 and 1889.) *L'agric. Ital.* 189. Fasc. 15. Ref. in *Ztbl. Agrik. Chem.* 1892, 291
233. — 1891: Sui materiali disciolti nell'acqua piovana precipitata negli anni 1888, 1889, 1890. Ricerche chimiche instituite presso la stazione meteorologica della Scuola Agraria di Scandicci (Firenze). *Bol. Soc. Met. Ital.* 1891 p. 11.
234. Peck, E. L., 1917: Nitrogen, chlorine and sulfates in rain and snow. *Chem. News*, **116**, 283—284.
235. Petermann, A., & Graftian, J., 1893: Combinaisons azotées contenues dans les eaux météoriques. *Bull. Stat. Agron. Gembloux.*, **53**.
236. — 1896: Recherches sur la composition de l'atmosphere. II. Combinaisons azotées contenues dans les eaux météoriques. *Mem. Cour. Acad. de Belgique*, **49**, 28 pp.
237. Pierre, J., 1851: Note relative a l'emploi du sel sur les terres. Du sel contenu dans les terres non réputées terres salées et dans les eaux de pluie. *Ann. Agron.*, **1**, 466—475.
238. Pfaff, G., 1937: Ueber Lysimeter-Versuche. *Der Forschungsdienst*, Sonderheft, **6**, 102—114.
239. Posnjakov, A., 1904: (Investigations on the chemical composition of atmospheric precipitations as dependant upon meteorological factors). *Zhur. Opytoi. Agron.*, **5**, 787. Ref. in *Ztbl. Agrik. Chem.* **34**, 289—290.
240. Potter, H. C., 1930: Hydrion concentration of rain and potable waters. *Nature*, **126**, 434—435.
241. Quitmann, E., & Cauer, H., 1933: Verfahren zur chemischen Analyse der Nebelkerne der Luft. *Zeitschr. Anal. Chem.*, **116**, 81—94.
242. Rakestraw, N. W., & Carrit, D. E., 1940: Some seasonal changes in the open ocean. *J. Marine Research* (Sears Found.), **7**, no. 3, 362—369.
243. Ram, A., 1934: Origin of combined nitrogen in the atmosphere. The analysis of tropical rain and its importance im agriculture. *Proc. Acad. Sci.* (United Prov. Agr. Oudh. India) **4**, 147—158.
244. Rao, G., Gapalo, & Dhar, N. R., 1931: Bildung von Stickstoffverbindungen in Luft und im Boden unter dem Einfluss des Lichtes. *Zeitschr. Anorg. Allgem. Chem.*, **199**, 422—426.
245. Regener, V. H., 1938: Neue Messungen der vertikalen Ozonverteilung in der Atmosphäre. *Naturwiss.* 1938, p. 155.
246. Ribble, H., & Bowman, P., 1926: Substances in rain and snow. *U. S. Mo. Weather Rev.*,. **54**, no. 10, 424.
247. Riffenburg, H. B., 1925: Chemical character of ground waters of the northern great plains. *U. S. Geol. Survey.* Water-Supply Paper 560-B.
248. Robinet, 1863: Quelques faits pour servir a l'étude de l'eau de pluie. *Compt. Rend.*, **57**, 493—494.
249. Robinson, W. O., 1936: Composition and origin of dust in the fall of red snow. *U. S. Mo. Weather Rev.*, **64**, 86.
250. Roelofsen, P. A., 1941: Stikstof in Regenwater. *Natuurv. Tijdschr. Nederland. Indie*, **101**, 179—180.
251. Romell, L. G., 1946: Organic dust in the air and

the ammonia found in atmospheric waters. *Svensk Bot. Tidskr.*, **40**:1, 1—8.

252. Rosing, A., & Wankel, G., 1870: Ammoniakmängden i Regn, Sne, Kilders, Floders og Søers Vand samt Havvandet. *Kongl. Norsk Videnskab. Selsk. Skr.*, **6**, 5—28.
253. Rousseau, E., 1928: (The colored rain of October 30, 1926.) *Rev. vit.* **69**, 283—286.
254. Russel, E. J., & Richards, E. H., 1919: The amounts and composition of rain and snow falling at Rothamsted. *J. Agr. Sci.*, **9**, 309—337.
255. Scharrer, K., & Schropp, W., 1940: Ueber den Stickstoffgehalt der Niederschläge. *Forschungsdienst*, **5**, 469.
256. Scharrer, K., & Fast, H., 1951: Untersuchungen über die dem Boden durch die Niederschläge zugeführten Pflanzenernährstoffe. *Zeitschr. Pflanzenernähr. Düngung. Bodenkunde*, **55**, (**100**) 97—106.
257. Schlösing, T., 1875: Sur l'ammoniaque de l'atmosphère. *Compt. Rend.*, **80**, 175—178.
258. — 1875: Dosage de l'ammoniaque atmosphérique. *Ibid.*, **80**, 265—268.
259. — 1875: Sur les lois de échanges d'ammoniaque entre les mers, l'atmosphére et les continents. *Ibid.*, **81**, 81.
260. — 1875: Sur les échanges d'ammoniaque entre les eaux naturelles et l'atmosphère. *Ibid.*, **81**, 1252—1254.
261. Schlösing, T., 1876: Sur les échanges d'ammoniaque entre les eaux naturelles et l'atmosphère. *Ibid.*, **82**, 747—775, 846—849, 969—972. 1105—1108
262. — 1878: Ueber die Gesetze des Ammoniak-Austauches zwischen dem Meere, der Atmosphäre und dem Festlande. *Zblt. Agrik. Chem.*, **7**, 162—177.
263. — 1888: *Contributions à l'étude de la chimie agricole 1888.*
264. — 1890: Sur l'absorbtion de l'ammoniaque de l'atmosphère par les terres végétales. *Compt. Rend.* **110**, 429—435, 499—504.
265. — 1890: Remarques au sujet des observations de M. Berthelot sur les réactions entre la terre végétale et l'ammoniaque atmosphérique. *Ibid.*, **110**, 612—613.
266. Schneidewind, W., 1910: Versuche über die Stickstoffverluste des Schwefels. Ammoniak und Kalkstickstoffs bei Oberflächendüngung. *Lantw. Jahrb.*, **39**, Erg.-bd III, 221—117.
267. Schmaus, A., & Wiegand, A., 1929. *Die Atmosphäre als Kolloid.* Braunschweig 1929.
268. Schroeder, J., 1915: Composition of rainfall at Montevideo 1909—12. *Rev. Assoc. Rural Uraguay*, **49**, 381—391.
269. Shaffer, S., 1922: Substances dissolved in rain and snow. *U. S. Mo. Weather Rev.*, **49**, 404—405.
270. Shipley, J. W., 1919: Ammonia and nitrous nitrogen in the rain water of south Alaska. *Ohio. Journ. Sci.*, **19**, 230—234.
271. Shutt, F. T., 1908: The fertilizing value of snow. *Chem. News*, **97**, 243—244.
272. — 1909—1924: The fertilizing value of rain and snow. *Can. Exp. Farms Rep.* 1907: 173—176, 1909: 190—192, 1910: 216—218, 1911: 99—100, 200—201, 1912: 164—166, 1913: 225, 265—268, 1915: 160—162, 1916: 174—178, 1918: 19, 1919: 51, 1920: 54—55, 1921: 13—16, 1923: 11—12, 1924, 8—10, 1925: 68—74.
273. — 1910 and 1914: The nitrogen compounds in rain and snow. *Proc. Trans. Roy. Soc. Canada. Sec. III.*, **4**, 55—59, **8**, 83—87.
274. Shutt, F. T., & Dorrance, R. L., 1917: The nitrogen compounds in rain and snow. *Ibid.*, **11**, 63—71.
275. Shutt, F. T., & Hedley, B., 1925: The nitrogen compounds in rain and snow. *Ibid.*, **19**, 1—10.
276. Slobod, R. L. &, Krogh, M. E., 1950: Nitrous oxide as a constituent of the atmosphere. *J. Amer. Chem. Soc.*, **72**,, 1175—1177.
277. Smith, A. R., 1872: *Air and Rain.* London. 1872.
278. Sricantia, C., 1930: Combined nitrogen in rain water. *Half-Yearly Mysore Univ.*, **4**, 195—198.
279. Stewart, R., 1920: Sulfur in relation to soil fertility. *Ill. Agr. Exp. Sta. Bull.*, **227**, p. 1:7.
280. Stoklasa, J., 1987: Gehalt der atmosphärischen Niederschläge an Ammoniak und Salpetersäure im Jahre 1883—84. *Ztlb. Agrik. Chem.*, **16**, 361—362.
281. Sugawara, K., Oana, S., & Kayama, T., 1949. Separation of the components of atmospheric salt and their distribution. *Bull. Chem. Soc. Japan*, **22**, 47—52.
282. Teakle, J. H., 1937. The salt (sodium chloride) content in rain water. *J. Dept. Agr. W. Australia*, **14**, 115—123.
283. Thomas, M D., & Hill, G. R., 1935: Absorption of sulfur dioxide by alfalfa in its relation to leaf injury. *Plant Physiology*, **10**, 291—307.
284. — 1937: Relation of sulfur dioxide in the atmosphere to photosynthesis and respiration of alfalfa. *Ibid.* **12**, 309—383.
285. Thorarinsson, S., 1944: *Tefrokronologiska studier på Island.* Köpenhamn, 1944.
286. Thoulet, J., 1903: Absorbtion de l'ammoniaque par l'eau de mer. *Compt. Rend.* **136**, 477—478.
287. Tissiander, G., 1875: Corpuscules aériens et matières salines contenues dans la neige. *Ibid.*, **80**, 58—61.
288. Tottingham, W. E., 1919: A preliminary study of the influence of chlorides on the growth of certain agricultural plants. *J. Amer. Soc. Agron.*, **11**, 1—32.
289. Tracy, S. M., 1895: Ammonia in rainwater. *Miss. Agr. Exp. Sta. 8th Ann. Rpt.*, p. 102.
290. Trieschmann, J. E., 1919: Nitrogen and other compounds in rain and snow. *Chem. News*, **119**, 49.
291. Tuxen, C. F. A., 1890: Undersøgelser over Regnens Betydning her i Landet som Kvælstofkilde for Kulturplanterna. *Tidskr. f. Landsøkonomi*, **9**, 325—350.
292. Viner, V., 1909: (Nitrogen compounds in rainwater.) *Otchet Shatilov Selsk. Khoz. Opuitn. Santzir.* **4**, 44—63. Ref. in *Exp. sta. Rec.*, **24**, 22.
293. Vogel, A., 1872: Ueber den Ammoniakgehalt des Schnewassers. *Chem. Ztbl. 3. Folge*, p. 506.
294. Volk, N. J., Tidmore, J. W., & Meadows, D. T., 1945: Supplements to high- analysis fertilizers with special reference to sulfur, calcium, magnesium and limestone. *Soil. Sci.*, **60**, 427—435.
295. Warington, R., 1887: A contribution to the study of well-waters. *Trans. Chem.* Soc., **51**, 500—552.
296. — 1889: The amounts of nitric acid in rainwater of Rothamsted, with notes on the analysis of rainwater. *Ibid.*, **60**, 537—545.
297. Wattenberg, H., 1931: Der chemische Aufbau

des atlantischen Ozeans. *Finska Kemistsamfundets Medd.*, **40**, 67—78.

298. Way, J. T., 1855: The atmosphere as a source of nitrogen to plants being an account of recent researches on this subject. *J. Roy. Agr. Soc. Engl.*, **16**, 249—267.
299. — 1856: On the composition of the waters of land drainage and of rain. *Ibid.*, **17**, 123—162.
300. — 1856: On the quantity of nitric acid and ammonia in the rain water. *Ibid.*, **17**, 618—621.
301. Welbel, B. M., 1889—1905: *Rep. Ann. Sta. Exp. Agron. Ploty.* 1899, 1900, 1902, 1903, and 1905.
302. — 1903: (The nitrogen content of atmospheric precipitaions.) *Zurn. Opytnoi. Agron.*, **4**, 194.
303. Weller, W. K., 1926: Note on the salinity in the Mundaring reservoir. *Austr. Ass. Adv. Sci.*, **18**, 633—674.
304. Weedon, T., 1909: Fertilizing value of rain water. *Ann. Rpt. Dept. Agr. and Stock.* (*Queensland*) 1908—09, pp 77—78.
305. Wiesner, G. H., 1914: Nitrogen and chlorine in rain and snow. *Chem. News.*, **109**, 85—87.
306. Williams, S. F., & Beddow, O. K., 1932: Analysis of the precipitation of rains and snows at Mont Vernon, Iowa. *Chem. News*, **145**, 40—43.
307. Wilson, B. D., 1921: Nitrogen in the rainwater of Ithaca, N. Y. *Soil Sci.*, **11**, 101—110.
308. Wilson, B. D., 1921: Sulfur supplied to the soil in rainwater. *J. Amer. Soc. Agron.*, **13**, 226—229.
309. — 1923: The quantity of sulfur in rainwater. *Ibid.*, **15**, 453—456.
310. — 1926: Nitrogen and sulfur in rainwater in New York. *Ibid.*, **18**, 1108—1112.
311. Witz, G., 1885: Sur la presence de l'acide sulphureux dans l'atmosphère des villes. *Compt. Rend.*, **100**, 1385—1388.
312. Wituynj, J., 1911: Die Mengen von Cl und SO_2, die in den Boden mit den atmosphärischen Niederschlägen gelangen. *J. Exp. Landw.* (*Russia.*), **12**, 20—30.
313. Woehlk, J. H., 1923: Nitrogen and other substances in rain and snow. *Chem. News*, **127**, 30.
314. Wollny, E., 1896: Untersuchungen über das Verhalten des atmosphärischen Niederschläge zur Pflanze und zum Boden. *Wollnys Forschungen*, **19**, 267—286.
315. Wood, W. E., 1924: Increase of salt in soil and streams following the destruction of native vegetation. *J. Roy. Soc. W. Australia*, **10**, 35—47.
316. Wood, W. E., & Wilsmore, N. T. M., 1929: Salinity of rain in Western Australia. Final Report to the Royal Society of Western Australia. *Ibid.* **15**, 12—30.
317. Xhoris, R., 1945: Sur la présence d'arsinic dans l'eau de pluie. *Bull. Soc. Roy. Sci. Liége*, **14**, 479—480.

Molecular Nitrogen Fixation and Nitrogen Cycle in Nature

By ARTTURI I. VIRTANEN, Biochemical Institute, Helsinki, Finland

(Manuscript received 10 November, 1952)

Abstract

The origin of nitrogen oxides in the atmosphere is discussed. Evidently only a small proportion of the nitrate- and nitrite-nitrogen found in the precipitation is formed through electric discharges from molecular nitrogen, photochemical nitrogen fixation being probably of greater importance. Formation of nitrate nitrogen through atmospheric oxidation of nitrous oxide (N_2O) evaporating from the soil is also considered likely.

Determination of nitrogen compounds at different altitudes is indispensable for gaining information of the N_2-fixation in the atmosphere and, in general, of the origin of nitrogen oxides and their decomposition. International co-operation is needed for this as well as for the quantitative determination of the nitrogen compounds removed from the soil by leaching and brought by waters into the seas.

In a recent issue of this journal ÅNGSTRÖM and HÖGBERG (1952) have dealt with the concentration of NH_4-N and NO_3-N in atmospheric precipitation and its dependence on the character of the air mass, in the light of the observations made in Sweden during recent years. At the request of Prof. Rossby I shall present in this paper some aspects of the nitrogen cycle which also may be of interest to meteorologists.

The atmosphere, with its 77,000 tons of molecular nitrogen per ha, is the nitrogen store of the earth, and the fixed nitrogen in the soil — also in good cultivated soil a few or at most some tens of tons per ha — originates chiefly from the nitrogen fixation by microorganisms (so-called biological nitrogen fixation). Without this process the earth would not have its present plant and animal kingdom. The most intensive nitrogen fixation takes place in the leguminous root nodules. A good lucerne or clover field fixes 150—400 kg N_2 per ha per summer. The amounts of nitrogen fixed by the action of free-living nitrogen-fixing microorganisms are much more modest varying perhaps from some kilograms to a few tens of kilograms per ha. N_2-fixation is not known to take place in soil independent of living cells. The share of industrial fertilizers in the nitrogen contained in the annual crops of the cultivated plants of the globe is only some two per cent. In regard to nitrogen fixation I refer to my recent lecture (VIRTANEN, 1952).

Nitrogen fixation can be expected in the atmosphere by electric discharges and photochemically. There is no reliable information as to how extensive is the N_2-fixation in the atmosphere. The studies have mostly been directed to the determination of nitrogenous compounds brought to the earth by precipitation. In this way, however, no elucidation can be obtained of the N_2-fixation in the atmosphere as will be seen from the following:

1. The precipitation contains more NH_4-N than NO_3-N. There is reason to assume that NH_4-N originates from the soil, for ammonia synthesis does not seem likely under atmos-

pheric conditions. Organic nitrogen which is found in the rain water originates from dust particles, insects and microorganisms in the air.

2. NO_3-N present in the rain water (and NO_2-N which also is found to some extent) can be formed by N_2-fixation. It must be assumed that some nitrogen oxides are derived from electric discharges connected with thunderstorms, a conclusion which follows from the knowledge of the conditions of N_2-oxidations. FINNELL and HOUGHTON (1932) have tried to estimate the increase in the nitrate nitrogen of rain effected by thunderstorms in Goodwell (Oklahoma), and HUTCHINSON (1944) has calculated on the basis of the values reported that at most 140—350 g N_2 is fixed per ha in temperate regions through electric discharges. Since the annual precipitation contains about one kilogram NO_3-N per ha, electric discharges would, on the average, have no great part in the production of this nitrate.

It is quite possible that most of the N_2-fixation in the atmosphere is photochemical. The conditions for this fixation exist probably in the ozonosphere, at altitudes of over 10 km, where both oxygen and nitrogen have great energy. Ozone oxidizes the nitrogen oxide formed to nitrogen pentoxide which has been spectroscopically found by ADEL and LAMPLAND (1938) in the ozonosphere, in amounts of about 1 mol. per 100 mol. ozone. The downward moving nitrogen pentoxide may be brought with rain to the earth's surface, the rising nitrogen pentoxide becomes exposed to a more and more energetic radiation which causes the molecules to decompose. The observations of ELVEY (1942) on the spectral bands of NO at altitudes of about 90—140 km is in accord with this.

There is, however, no certainty that all the NO_3-N in the precipitation is produced by N_2-fixation. On the contrary, it is very possible that a part of it is formed through oxidation of NH_4-N. Nitrous oxide N_2O, which evaporates from the soil and is liberally formed, in addition to N_2, in the decomposition of nitrate by bacteria (denitrification), also may be partly oxidized in the atmosphere to higher nitrogen oxides. ADEL (1939, 1951) was the first to find N_2O in the atmosphere. According to him, N_2O is decomposed

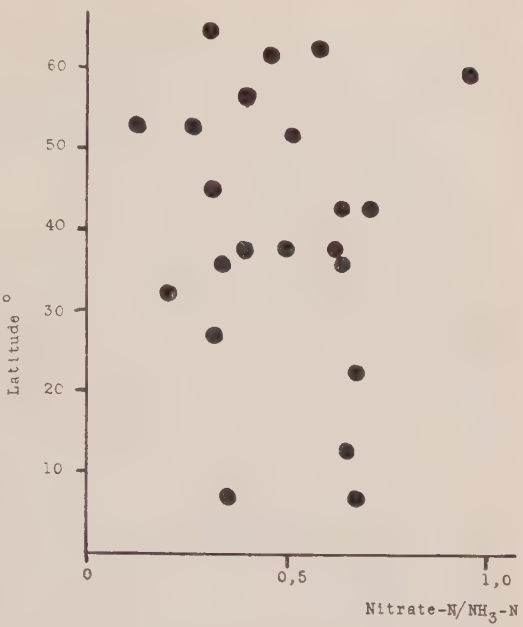

Fig. 1. Inter-relationship between nitrate-N and ammonium-N in precipitation at different latitudes.

photochemically to N_2, O_2, and NO by $\lambda <$ 2,000 A in the upper atmosphere. The latter product is further dissociated photochemically to N_2 and O_2. While NO is being brought to the lower atmosphere it may, however, be oxidized to NO_2 and even further to higher nitrogen oxides (author's opinion). Consequently, there is a possibility that a part of the NO_3-N found in the precipitation may originate from the N_2O evaporated from the soil.

The amount of nitrogen compounds in the atmosphere is nowadays also very much affected by man. In industrial centres and densely populated districts as a whole, both nitrogen oxides (mainly NO_2) and ammonium nitrogen are brought to the atmosphere as products of burning solid and liquid fuels. This makes explicable the enormous amounts of NO_3-N and NH_4-N (12.3 kg and 15.9 kg per ha respectively) found by SCHARRER and FAST (1952) in the annual precipitation near Giessen in Germany. (In Iceland RUSSEL and RICHARDS (1919) found 0.912 kg. NH_4-N and 0.292 kg. NO_3-N in precipitation per ha; in East Bothnia, Finland, FINNBERG (1923) found 1.8 kg. NH_4-N, 0.825 kg. NO_3-N,

and 0.025 kg. NO_2-N in precipitation per ha). It must also be borne in mind that some N_2-fixation obviously also takes place in internal combustion engines and that with the increasing number of automobiles, tractors etc. nitrogen oxides may be brought to the atmosphere, although their amount is relatively insignificant.

ÅNGSTRÖM and HÖGBERG consider on the basis of the Swedish data, that the annual precipitation at Uppsala contains normally 1.90 kg. NH_4-N and 0.91 kg. NO_3-N per ha. Hence the ratio of NO_3-N to NH_4-N would be almost constant, about 0.5, which seems to suggest a common origin. However, such a ratio is not regularly found in the analyses of precipitation reported in the literature. Fig. 1 gives the inter-relationship of NO_3-N and NO_4-N in precipitation at different latitudes in the northern hemisphere computed from values found in the literature.

The personal opinion of the author is that the analyses of the precipitation do not give full information of the atmospheric nitrogen compounds, of their origin, and of the possible participation of nitrogen oxides in the chemical reactions in the atmosphere. It would be necessary to obtain quantitative data of the different nitrogen compounds in various layers of the atmosphere from the ground level to high altitudes. Such determinations would probably give a definite idea of the formation of nitrogen oxides from N_2 and of their decomposition at different altitudes, as well as of the nitrogen compounds evaporating from the earth's surface. The nitrogen cycle in nature would thus become more defined. This work is difficult in method, but as far as I can see there is no other way.

In order to get elucidation on the nitrogen status of the earth and changes therein, systematic analytical work would be needed for determination of the amounts of different nitrogen compounds which are annually brought by waters into the seas. Nitrogen analyses should be made at definite intervals in different parts of the world at the mouth of representative rivers, both large and small. In order to obtain a realiable picture of the quantitative side of the nitrogen cycle international cooperation is indispensable. If the nitrogen analyses of the riverwaters are accompanied by determinations of phosphate, potassium, and calcium (and possibly other elements), material will be obtained which will be of immense significance to the agriculture and forestry of the world, in other words, for the living possibilities of man.

REFERENCES

ADEL, A., 1939: Note on the atmospheric oxides of nitrogen. *Astrophys. J.* **90**, p. 627.

ADEL, A., 1951: Atmospheric nitrous oxid and the nitrogen cycle. *Science* **113**, pp. 624—625.

ADEL, A., and LAMPLAND, C. O., 1938: A new band in the absorption spectrum of the earth's atmosphere. *Astrophys. J.* **87**, pp. 198—203.

ÅNGSTRÖM, A., and HÖGBERG, L., 1952; On the content of nitrogen (NH_4-N, and NO_3-N) in atmospheric precipitation. *Tellus* **4**, pp. 31—42.

ELVEY, C. T., 1942: The light of the night sky. *Rev. Modern Phys.* **14**, pp. 140—150.

FINNBERG, F. V., 1923: Einige Bestimmungen des Gehaltes der atmosphärischen Niederschläge an Stickstoffverbindungen aufgeführt in Storkyrö (Finnland) 1921—22. *Soc. Sci. Fennica, Commentationes Phys Math.* **1**, No. 28.

FINNELL, H. H., and HOUGHTON, H. W., 1932: Nitrogen content of rain water. *Panhandle Bull.* **34**, pp. 3—8.

HUTCHINSON, E., 1944: Nitrogen in the biogeochemistry of the atmosphere. *Am. Scientist* **32**, pp. 178—195.

RUSSEL, E. J. and RICHARDS, E. H., 1919: The amount and composition of rain falling at Rothamsted. *J. Agr. Sci.* **9**, pp. 309—337.

SCHARRER, K., and FAST, H., 1952: Untersuchungen über die dem Boden durch die Niederschläge zugeführten Pflanzennährstoffe. *Z. Pflanzenernähr. Düngung u. Bodenkunde* **55** (100), pp. 97—106.

VIRTANEN, A. I., 1952: Atmosphärischer Stickstoff als Aufrechterhalter des Lebens. *Angew. Chemie* (in press).

The Chemical Denudation of the Soil

By O. ARRHENIUS, Kagghamra

(Manuscript received October 28, 1952)

Abstract

The chemical denudation plays a greater role in our climate than the mechanical erosion. The Swedish well waters contain 3—4 times more soluble salts than those rivers which are fed by them. The chemical denudation therefore must be much greater than formerly calculated. A map shows the salt concentration of the well waters of Sweden. The amount of nitrogen accumulated per annum in a district of central Sweden seems to amount to 3—6 kg N per har.

The symposium is supposed to deal with the nitrogen in the atmosphere. It is, however, of great interest to follow up the problems regarding the balance between soil-water and also to try to show the general problem which is of the greatest practical interest: the denudation of the soil.

One of the most discussed items just now is the soil erosion in connection with the possibilities to nourish the ever increasing population of the earth (BENNET, 1939). In all the books published on this subject we find the wind and water erosion, thus the mechanical erosion, mentioned but never the chemical erosion, the soil denudation. In humid climate, like ours, the chemical denudation is more destructive to the soil than the erosion.

Every country which neglects its soil giving it a prey to denudation and erosion is doomed to decline and fall. We may look at the Roman Empire. The country round Rome was a fertile land giving good yields of wheat nourishing the capital. The land was neglected, Rome lived on import goods, and the area turned very acid (pH below 5), denuded of its nutrients, giving low yields. And costing immense sums to reclaim.

About A.D. 400 the farmers of Gotland probably because of a change in rainfall moved their dwellings from the lower, clayey soils to the sandy parts of the island. Within some centuries these soils were depleted and the population had to live as merchants and sailors. When these latter possibilities were throttled in the 12th century an era of poverty and famine was reigning until the lowerlying areas were reclaimed in the 16th century.

On a still larger scale similar things have happened in the U.K. The soils in large districts have been neglected, and denudation has carried away much of the plant nutrients. The food question has been one of the difficulties with which the english people has had to struggle lately.

What is then denudation. The precipitating water percolates the soil layers dissolving the nutrients carrying them down to deeper layers or to the ground water. The ground water feeds the rivers which carry the dissolved salts to the sea. On the way from the well to the sea certain amounts disappear being taken up by plants or precipitated in lakes or rivers.

Certain powers counteract the denudation. The plants evaporating the water diminishes the strength of the down current. Plants have

an ability to take up salts even from very diluted solutions. HARVEY (1926) has shown that organisms living in the sea are able to take up nitrates from solutions at such a low concentration as 10 mg/m³. The plants, thus, take up the nutrients and concentrate them, often thousandfold. When shedding leaves and needles, when the plant dies, wholly or to a certain part, the offall forms the humuslayer on the top of the soil and this layer is rich in light soluble nutrients. In this way the top soil is re-enriched.

By studying the ground water—well water composition and knowing the amount of percolating water it is possible to estimate the amounts of different salts carried away from the upper soil layers. The map shows the concentration of total salts dissolved. The clay districts show high figures, the sand districts and Norrland are on the other hand very poor. From the map is also seen that the deviations within the districts are rather small. (Fig. 1).

The average composition of the water is the same, the concentration only differs. The composition of the percolating water we know but the amount of percolating water is only an assumption. We guess that 30—35 % of the rainfall is not evaporated. And we assume that the percolating water is of the same amount as what we find the rivers carrying off to the sea.

We may therefore compare the concentration of well water with that of river water and that will throw a light on the denudation problem. All earlier investigations on soil

The concentration of soluble inorganic substance sulphates, chlorides and nitrates in some Swedish rivers and in the well waters feeding the different rivers.

From the rivers we have no data with regard to nitrates. Judged from other analyses the nitrate content in the river waters seems to be very low and would in this table be = 0. It is easily seen that not only the total inorganics diminish from the well to the river waters but also SO_4, Cl and NO_3.

		SO_4	Inorg. subst.	Cl	NO_3
Skellefteälv	River water	0.9	21.2	3.1	—
	Well »	1.0	8	13	—
Umeälv	River water	1.5	20.9	3.3	—
	Well »	6	102	14	—
Öreälv	River water	—	26.0	3.2	—
	Well »	6	54	3	—
Ångerman-älven	River water	1.7	20.9	2.5	—
	Well »	4	107	11	9
Indalsälven	River water	2.1	32.6	4.5	—
	Well »	5	170	9	3
Ljungan	River water	1.2	28.4	3.0	—
	Well »	5	131	15	—
Ljusnan	River water	1.6	24.6	2.5	—
	Well »	1	54	7	5
Dalälven	River water	2.0	25.3	2.8	—
	Well »	28	150	10	—
Närkes Svartå	River water	9.6	43.9	4.9	—
	Well »	10	103	9	5
Nyköpingsån	River water	12.7	58.0	6.2	—
	Well »	2.5	258	31	12
Mjölnaån	River water	27.9	138.4	9.6	—
	Well »	35	416	58	28
Stångån	River water	7.9	49.6	7.1	—
	Well »	9	233	31	17
Emån	River water	7.1	40.1	6.8	—
	Well »	9	153	21	12
Mörrumsån	River water	5.3	30.6	7.9	—
	Well »	16	157	28	18
Helgeån	River water	7.4	51.0	11.7	—
	Well »	35.0	215	33	38
Tommarpsån	River water	33.6	202.5	14.2	—
	Well »	50	410	39	58
Kävlingeån	River water	30.7	210.7	18.7	—
	Well »	50	498	74	35
Rönneån	River water	14.9	94.1	15.0	—
	Well »	45	316	51	27
Lagan	River water	4.9	27.9	6.8	—
	Well »	9	126	20	17
Nissan	River water	6.9	33.3	7.0	—
	Well »	9	105	21	13
Ätran	River water	5.3	36.8	7.4	—
	Well »	5	97	15	19
Viskan	River water	7.9	48.7	10.9	—
	Well »	9	116	9	9
Klarälven	River water	2.5	22.6	3.2	—
	Well »	5	59	9	5
Ölman	River water	—	49.5	5.5	—
	Well »	4	163	27	7
Gullspångs-älven	River water	2.9	21.8	4.3	—
	Well »	5	95	8	8
Tidan	River water	13.4	81.6	9.6	—
	Well »	20	213	28	19
Lidan	River water	37.9	193.2	16.6	—
	Well »	22	370	50	18

denudation have used the amount of salts emptied into the sea by the rivers as a measure of denudation (BAULIG, 1910, ERIKSSON, 1929). In the table we find the amount of total salts, Cl, SO_4 and NO_3 of the well waters of different rivers in Sweden.

From this we see that the amount washed-out of the soil is much greater than that

Fig. 1. The concentration (salinity) of well waters of Sweden. The figures give the concentration in mg/litre. The analyses obtained by the courtesy of the Institute of Public Health.

emptied into the sea. The salts must thus be precipitated or absorbed either in the subsoil (the deeper layer) or in the rivers and lakes. It is interesting to see that from the poor waters more is precipitated than from the rich ones.

The total amount of the chemical denudation amounts to about 20 mill. tons a year or 500 kgs per ha.

In the investigations regarding the composition of river water from Sweden by JOEL ERIKSSON (1929), no analyses were made of the content of nitrates. It is therefore impossible to make a comparison like that for the other salts but I have examined all data published by HOFMAN-BANG (1902—03) and SONDÉN (1914) and from this is seen that practically all river waters are free from nitrates. Here probably the organisms of the rivers have assimilated the total amount of the nitrates.

On the other hand the rivers carry large amounts of nitrogen to the sea. It is very probable that this consists of colloidal and suspended peat and humus (ERIKSSON, 1929, HOFMAN-BANG, 1902—03). At least this is often the case in Swedish rivers. But we know rather little of this problem. One may estimate the denudation with the rivers to 3 kg N ha and year. The nitrates of the ground water will amount to 11 kg N per ha. and year.

The question then arises: will there be anything left of nitrogen in the soil or have we to expect a depletion. Dalecarlia has recently been very closely investigated geologically. On the basis of the investigation made we have a humuslayer chiefly in peat bogs in average containing about 30,000 kg N/ha. We may assume that this accumulation has gone on for the last 5—10 thousand years. This would be a net accumulation of 3—6 kg N/ha. and year.

As the nitrogen is the most scarce and most essential nutrient of the soil such an investigation as that discussed here is of the utmost practical interest. Are we able to enrich the soil with nitrogen we may produce more on the soil.

But we still lack essential data about

1) nitrogen fixed

2) the amounts of nitrogen denuded and carried off to the sea

3) the amount of water percolating through the soil.

4) An investigation with regard to nitrogen similar to that which Joel Eriksson has published regarding other water properties must be made.

REFERENCES

BAULIG, HENRI, 1910: Écoulement fleuvial et denudation. *Annales de Géographie* XIX.

BENNET, H. H., 1939: *Soil conservation.* Mc. Graw Hill Book Co. New York and London.

ERIKSSON, JOEL, 1929: Den kemiska denudationen i Sverige. *Meddelanden från Statens Meteorologiska-Hydrografiska Anstalt,* 5.

HARVEY, H. W., 1926: Nitrates in the sea. *Marine Biol. Ass. U.K.,* Plymouth.

HOFMAN-BANG, O., 1902—03: Studien über schwedische Fluss- und Quellwasser. *Bull. of the Geological Institution of the University of Upsala.* VI.

Meddelanden från Statens Meteorologiska Hydrografiska Anstalt 1914—51, 1—14: De svenska vattendragens arealförhållanden.

SONDÉN, KLAS, 1914: Anteckningar rörande svenska vattendrag. I. II. Stockholm.

ULE, WILLI, 1925: *Physiographie des Süsswassers. Encyclopädie der Erdkunde.* Leipzig und Wien.

A Laboratory Study of the Wind-driven Ocean Circulation.[1]

By WILLIAM S. VON ARX

Woods Hole Oceanographic Institution, Woods Hole, Massachusetts

(Manuscript received 10 August 1952)

Abstract

Experiments with rotating oceanographic models are being attempted in the laboratory at Woods Hole in the hope that some information may be gained which will help to close the gap between recent theories of ocean circulation and the observed nature of the circulation. Recent theoretical descriptions by STOMMEL (1948) and MUNK (1950) indicate the broad features of the climatological mean circulation pattern. In contrast, observations usually allow description of possibly transient situations in only relatively small regions. The major observational problem at the moment, short of synoptic measurements over large areas, is to learn how the observations made from moving ships fit into the pattern of very large scale fluid processes.

Some insight has already been gained through the search for atmospheric counterparts initiated by Dr C.-G. Rossby, and it is hoped that a wind-driven model of the oceans may offer additional clues. It is recognized that ocean models cannot be scaled in every particular and that the scales taken into account may lead to error since processes of verification, ordinarily used to test the suitability of hydraulic models, cannot be applied. Thus the behavior of a rotating model can bear a limited resemblance only to contemporary ideas of what the primary ocean circulation may be like.

In terms of these ideas, however, it has been possible to reproduce westward intensification of the primary circulations in compartments shaped like the North Atlantic and North Pacific basins. Sargasso Sea-like features and several details have also appeared which are qualitatively like contemporary views of the major motions of the sea. These major, and some minor features of the circulation develop rapidly under wind-stress applied to homogeneous water.

1. Description of the apparatus

A basin having the internal form of a paraboloid of revolution was chosen because it provides a Coriolis parameter which varies with latitude, and a free liquid surface which is accessible for the application of wind stress, heat, light, and tracer materials. In a paraboloid of reasonable depth, however, the Coriolis parameter does not ordinarily approach zero at the rim. Therefore, experiments are generally limited to extratropical regions unless geometrical and dynamical distortions of various sorts are allowed. Figure 1 shows the arrangement of parts.

a) The mechanical system

The paraboloidal basin now in use is 2 meters in diameter and has a focal length of 0.5 meter. The paraboloid rises from the vertex to the latus rectum, then enters a toroidal section and is terminated in a cylindrical

[1] Contribution No. 622, from the Woods Hole Oceanographic Institution. This work has been supported by the Office of Naval Research under Contract No. N6onr-27701 (NR-083-004) with the Woods Hole Oceanographic Institution.

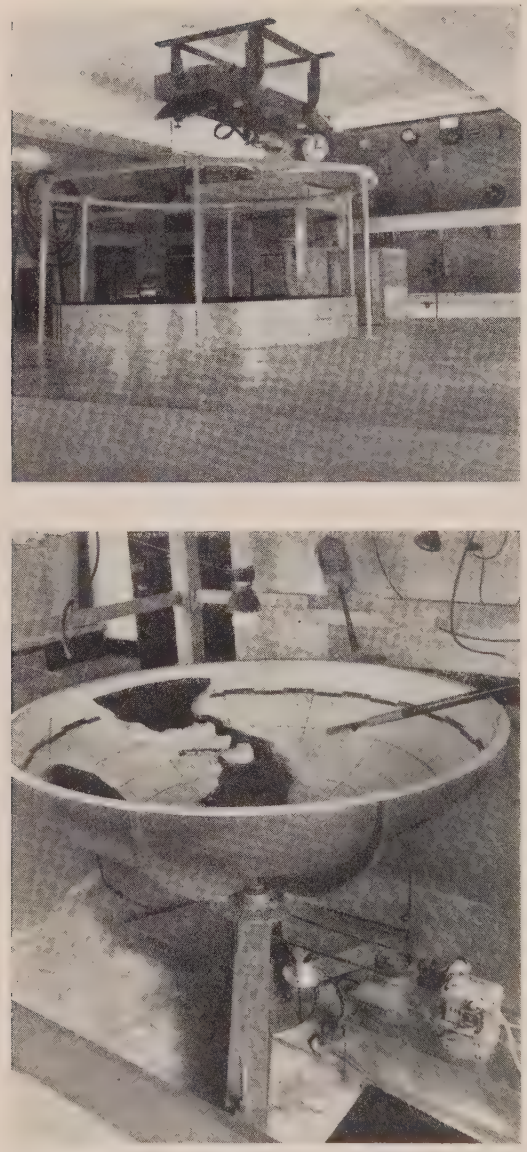

Fig. 1. General arrangement of the rotating basin apparatus. The control panel at the extreme right is accessible from the observers desk at the eye end of the optical train. The basin itself is mounted in a concrete sump below the observation platform. The drive machinery can be seen at the lower right. The main light at the effective center of curvature of the basin and the blowers around the basin are suspended from the platform. The continental modeling is 6 cm high and cemented in place.

section extended high enough to prevent a layer of water 10 cm deep from overflowing at the equilibrium rate of rotation. The basin is made of fiberglass bonded with a plastic. Eight ribs are bonded to the basin and to a stainless hub at the vertex. The basin weighs about 80 kilograms and will support a 500 kilograms load of water.

The basin is mounted on the end of a vertical shaft 10 cm diameter by 0.6 meter high, fitted snugly into two self-aligning radial-thrust bearings in a heavy, welded steel tripod which is secured to a concrete slab by nuts on three leveling screws embedded in the slab. The drive for the basin consists of a 1 H.P. capacitor-starting synchronous motor which drives the basin through a variable-ratio V-belt speed controller and a worm gear speed reducer. The basin shaft is coupled to the drive by a V-belt which has proven satisfactory when run with considerable slack. Once the basin has been accelerated to speed, it runs nearly free of the drive machinery except for the small amounts of power required to overcome friction and air resistance. The equilibrium rate of rotation of the basin is 3.13 radians per second, hence the tangential velocity of the rim is over 3 meters per second. Even so, the water in the basin remains quiet and the free surface is smooth except for the wind ripples which become noticeable in the zone within 20 to 35 cm of the rim. These ripples can be damped out by means of a detergent on the free surface. To avoid seiches the vertical shaft carrying the basin must be quite plumb.

b) The optical system

The optical system for observing the circulation in the basin and illuminating it requires consideration. In the Woods Hole installation, where there is only limited head-room, the entrance pupil of the optical system was, o necessity, placed 2.5 meters above the vertex of the paraboloid, hence a true field of 60° was required. This was accomplished by viewing the basin through the "wrong end" of a surplus M71H tank telescope having a 65° apparent field, focused so as to produce a beam of parallel rays emerging from the objective end. This places the image of the basin at infinity. Derotation of the image is accomplished with a Dove prism. This component, mounted in precision ball bearings, was placed in emergent beam and rotated by means of a selsyn repeater motor driven by a

similar selsyn motor linked to the basin shaft by a rubber belt. The sheave ratio at the basin shaft was made 1/3 and the sheave ratio at the Dove prism 6/1, so that the Dove prism revolves at one-half of the basin rate regardless of the angular velocity of the basin, while the selsyns themselves turn over at a more efficient rate. It was found expedient to provide the Dove prism sheave with a cylindrical face and the repeater selsyn sheave with a 90° groove so that small changes required to adjust the ratio of these two sheaves could be effected by changing the tension of the round rubber belt connecting them.

A Dove prism must be placed in a beam of parallel light, so that the aberrations introduced at the first refracting face are exactly cancelled by the second. A Schmidt prism, or an equivalent system of plane mirrors, may be used if parallel light cannot be managed. Both prisms offer an odd number of internal reflections (one in the Dove prism and five in the Schmidt prism) so that an additional reflection is required to revert the image. This added reflection was obtained from a plane first-surface mirror ahead of the entrance pupil. This proved to be a convenient way to change the axis of the optical system from vertical to horizontal under low head-room conditions.

The parallel beam emerging from the Dove prism provides a stationary, real image at infinity which has only a small angular size due to the negative magnification of the reversed telescope. This image can be examined comfortably through a second telescope or photographed directly if lenses of suitably long focal length are used to cause the image to fill the frame. Exposures longer than one second have been possible. The light losses in the optical train amount to about 60 per cent.

Time lapse motion pictures have been made through this optical system which are synchronized with the rotation of the basin. A microswitch trips the camera electrically as it is engaged by combinations of 16 pins of different lengths concentrically arranged on a disc turning with the basin shaft. Of the 16 pins, one is longest, one is located at 180° from the first and is made a little shorter, two at 90° to the first pair are equal in length but shorter than the second mentioned, four still shorter pins are located at the 45° positions, and the eight shortest pins are located at the 22.5° positions. Thus by simply raising and lowering the micro-switch the camera can be tripped 1, 2, 4, 8, and 16 times per basin revolution regardless of the angular velocity of the basin. A small light mounted at rest in the field of view appears as a streak in each exposure indicating the angular motion during and between exposures. The duration of exposures and time elapsed between them can be measured in this way.

The main source of illumination is a 2000 watt lamp. The lamp is placed at the effective radius of curvature of the paraboloid so that the illumination is quite uniform and reflections from the free surface are returned to the light source.

The optical system is supported independently so that the vibrations of machinery do not disturb it, and the activities of the observer do not change its alignment with the axis of rotation of the basin.

c) The pneumatic system

The air streams over the model which are used to simulate atmospheric circulations are produced by three tank-type vacuum cleaners operating wrong-end-to as blowers, and spaced 120° apart around the basin. When equipped with nozzles these blowers can be aimed at limited zones of the paraboloid to increase or decrease the local relative motion of air beyond that due to the rotation of the basin. A variac controls the speed of all three blowers simultaneously. Suitable wind torques can be achieved either by directing the blowers so as to produce westerlies in temperate latitudes or easterlies in the trade wind zone. The latter requires smaller discharge velocities from the blowers and is more generally used.

d) Tracers

The matter of tracers for the detection and measurement of water motion is unsettled. Neutrally buoyant ink, potassium permanganate, aluminum tristearate, n-butyl phthalate and xylene, aluminum foil and several other substances (including cranberries) have been used at different times. The ink-potassium permanganate combination is useful since the ink stays near the surface and the permanganate crystals sink to the bottom to produce trails of color. In regions of upwelling the

permanganate solution oxidizes the ink and changes the color of the mixture. The latter three tracers are essentially particulate but none has a high enough albedo to permit satisfactory streak photographs to be made with the present apparatus. An interesting alternative to streak photographs has been proposed; namely, if the two instantaneous photographs taken at slightly different times, the stereoscopic relief of displaced particles or dye fronts would be proportional to the velocity. In this manner a velocity solid might be visualized or constructed.

e) Comments on design

The design of the mechanical and optical systems for this rotating basin apparatus was exploratory, and can be improved in many ways. For example: ultra-wide field astronomical optical systems exist which, with a Schmidt prism for derotation, would be an improvement over the rather crude optical system now in use. Similarly, the frequency controlled synchronous telescope drives already in use in some observatories could be adapted to the basin drive to afford not only a steadier motion but better control and measurement of the angular velocity. Wind stresses should be applied in a more elegant manner than at present, and should be subject to better quantitative control. The matter of suitable tracers for the detection and measurement of circulation at all levels requires more study.

2. Scaling and modeling

An oceanographic model requires that certain elementary properties of the lithosphere, hydrosphere, and atmosphere be represented together. Since the hydrosphere is the principal object of study, the functions of the lithosphere and atmosphere are of consequence only where they touch the hydrosphere. Thus it is sufficient to model in the coastlines and ocean bed, and to reproduce the surface winds over the ocean areas.

The original choice of the diameter and focal length of the paraboloid imposes limits on the scale and degree of similarity attainable. If the diameter of the basin is equal to four times the focal length, the rim makes an angle of 45° with the axis of rotation and limits the variation of the Coriolis parameter from 0.707 f at the rim to f at the vertex, or pole.

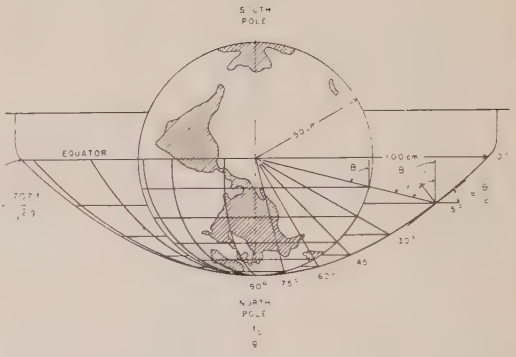

Fig. 2. Gnomic projection of the landmasses of the northern hemisphere on the interior of the paraboloidal basin. The variation of the Coriolis parameter at the equilibrium speed of rotation and the change of the combined gravitational and centrifugal accelerations are indicated.

The absolute magnitude of the Coriolis parameter is determined by the rate of rotation of the basin, which cannot (for practical reasons) depart from the equilibrium rate by more than a few per cent. This rate, in effect, also fixes the time scale of the model. For the Woods Hole basin, T_r is approximately 2.3×10^{-5}.

Despite the limitation that the Coriolis parameter cannot approach zero at the rim, the topography of the entire northern hemisphere has been projected on the interior of the paraboloid as an experiment, by the method shown in Figure 2. The projection was made gnomonically from the center of a sphere having a radius equal to the focal length of the paraboloid, placed so as to be tangent to the paraboloid at the vertex. The north pole of the sphere and the vertex of the paraboloid coincide. The resulting scale of the projection on the basin is the same as that of the sphere at the pole but increases toward the equator at the rim to $2\sqrt{2}$ times the north-south dimensions and 2 times the east-west dimensions of the sphere. This distortion is not objectionable to the eye.

Assuming that the length of a quadrant on the paraboloid is a characteristic length, the ratio L_r becomes 0.8×10^{-7} approximately, with respect to a quadrant on the earth. From this and the estimate of the time scale, T_r, the coefficient of lateral eddy diffusivity may be scaled by the ratio $(L_r)^2/T_r$, or 0.3×10^{-9}.

If a representative value for the lateral eddy diffusivity is in the order 10^8 cm^2/sec. the scaled value for the basin becomes about 1 cm^2/sec. which can be maintained experimentally.

The depth of water in the model may be exaggerated to allow for the nearly 100:1 inequality of the vertical and horizontal values of eddy diffusivity in the real ocean. If oceans are in the order of one thousand times wider than they are deep, an appropriate depth of water in the model is as much as one-tenth of the model ocean width. This can be accommodated, but departures from this ratio seem experimentally to produce very little effect.

Two other distortions exist in the paraboloid which are different from the situation on the earth; namely, the variation in the effective acceleration of gravity from g at the pole to $g\sqrt{2}$ at the rim, and the fact that at the equilibrium rate of rotation the depth of water measured normal to the free surface decreases as the cosine of the parabolic latitude. The increase of g and decrease of normal depth at the equilibrium rate of rotation cause the water to exert equal pressures on equal areas of the basin itself, but for the isobaric surfaces above the bottom to diverge poleward. This has an extraordinary effect which was explained by Dr C.-G. Rossby, that under these circumstances the cyclonic vorticity tendency associated with the horizontal convergence of the stretching water columns transferred from the rim to the pole is exactly equal and opposite to the anticyclonic vorticity tendency associated with the northward change in latitude. As a result, westward intensification of the circulation does not occur at the equilibrium rate of rotation. Having the effective planetary vorticity adjustment of the tendency under experimental control through meridional change in the depth of water in the model it becomes possible to study the changes in the broad pattern of the circulation under different combinations of the planetary, wind-stress and frictional vorticities. When the effective planetary vorticity tendency is increased by increasing the rate of rotation of the basin so that the normal depth at the rim is about 1.7 times that at the pole, the normal westward intensification of the circulation appears. If the rate of rotation

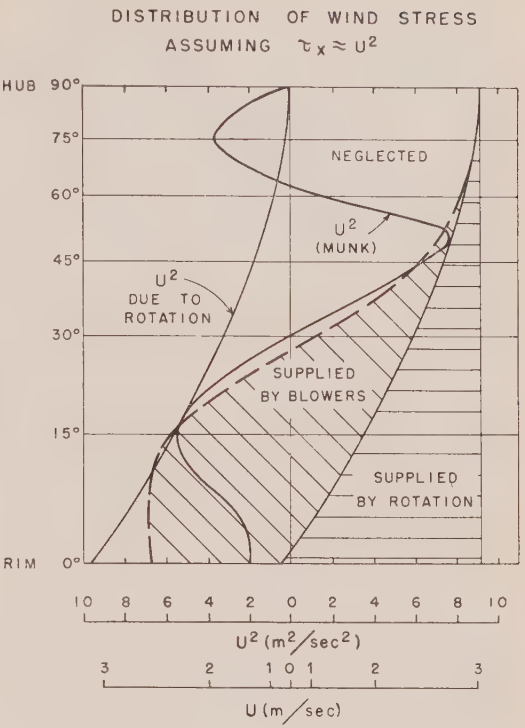

Fig. 3. Experimental distribution of zonal wind stress (dashed line) compared with that derived by Munk (1950) (solid line) from records of the average zonal wind stress over the earth.

is made correspondingly less than the equilibrium rate of rotation the sign of the planetary vorticity tendency is reversed, the circulation pattern is rotated 180°, so that the intensified circulation follows the eastern margins of the ocean basins. This occurs without any change in the intensity or distribution of wind torque. Theoretically the normal westward intensification should occur in the model when the depth normal to the free surface at the rim is $(1 + 1/\sqrt{2})$ times greater than that at the pole. The rate of rotation necessary to achieve the proper ratio of depths is, of course, a function of the average depth.

Figure 3 represents the experimental distribution of wind stress superimposed on that determined by Munk from average winds over the earth. The experimental curve approximates the natural one only in mid-latitudes. Experimentally the latitude of the inflection point seems to be more significant

than the latitudes of the wind stress maxima, therefore attention has been concentrated on this adjustment for the time being. It is considered at the moment that a first approximation of the proper intensity of wind torque has been reached when the current velocities in the water approach the velocity scale L_r/T_r or 0.4×10^{-2}. The magnitude of the wind torque required to bring the velocity of the Gulf Stream nearly in scale is approximately 0.007 dyne/cm^2.

Because wavelets produce turbulent mixing at the coastlines, the wind stresses on the basin have been kept as small as possible. Wavelets, it is found, can be damped out to a great extent by covering the water surface with a film of Aerosol (a laboratory detergent). This film seems to have no important effect on the ratio of a given wind velocity to the water velocity produced. KEULEGAN (1951) reports similar results using Glim.

Modeling of the land masses has been done in commercial grade sponge rubber. This material permits the carving to be done originally on flat sheets which are easily bent to conform with the paraboloidal shape of the basin. The modeling was cemented in place. Besides being convenient to use, the sponge rubber modeling presents a rough surface along the margins of the ocean basins in contrast to the glassy smooth finish of the plastic of the basin which forms the bottom surface. The lateral roughness is of theoretical as well as experimental importance and can be changed through a wide range by either serrating the rubber, cutting it smoothly with sharp tools, or filling the pores with paint so as to be almost as smooth as the plastic surface of the basin. It is found that the roughness of the order of pore size in the rubber is of less consequence to the circulation than the large scale roughness of the geography of the continental masses themselves.

3. Some oceanographic results

The rotating basin experiments at Woods Hole have been in progress only a few months, so that this discussion is both qualitative and subject to change. It is regretted that no instantaneous photographs of the circulation, such as Figure 4 (opposite p. 318) can represent the changing occurrences that may be seen during an hour's operation of the basin. The description that follows has been written with the realization that others might have described or interpreted the same experimental results in other ways.

When the model is rotated at the optimum angular velocity for normal westward intensification, the circulation in both the North Atlantic and North Pacific compartments is dominated by a swift, narrow current flowing along the western margin of each compartment. The current in the North Atlantic compartment follows a course similar in many ways to present ideas of the course of the Gulf Stream. This current is composed of water from the south central North Atlantic area; from the slow drift of water upwelling in the lee of the West African bulge, and from the swift and relatively narrow Guiana current flowing northwestward along the northern coast of South America. Water from these sources flows through the Caribbean and through the Straits of Florida with very little transverse mixing. There is a pulsation of the flow through the Florida Straits which influences both the anticyclonic sweep of a small fraction of the flow into the eastern part of the Gulf of Mexico and the steadiness of the flow downstream as far as the Grand Banks. The similarity of this flow to the Gulf Stream extends to such details as the persistent anticyclonic bend over the Blake Plateau, and the oscillating cyclonic and anticyclonic curvature of flow east of Cape Henry. Meander structures of standing or slowly progressive (downstream) waves have occurred in the region between Cape Hatteras and the Grand Banks in recent experiments. These are similar to the actual meander structures that have been described by ISELIN and FUGLISTER (1948) and FUGLISTER and WORTHINGTON (1951) except that the wavelength is too long by a factor of about three.

FUGLISTER (1951) has also described some branches of the Gulf Stream system in the vicinity of the Grand Banks. Branching has been observed in the basin current in this region but the character of the circulation appears to be different. Multiple currents in the basin consist in stagnating streamers on the southeast side of the main current. A sudden discontinuity may occur in the flow which causes the active current to pass the older segment on the

left. If the new thrust does not branch in the cyclonic circulation of the Labrador Sea it may penetrate northeastward as far as the coast of Norway before stagnating and being itself wedged aside by the next active thrust.

The circulations produced in the rotating basin resemble the ocean surface circulations best in the western regions of intense currents and sharply bounded water masses. In order to obtain a pattern of circulation along the eastern borders of the North Atlantic that resembles the patterns thought to exist, and for the North Atlantic Current to make its way toward the British Isles and to turn into the Arctic Ocean along the Norwegian coast, it is necessary in the model to vent the Arctic Ocean basin and return this discharge to the vicinity of the Gulf of Guinea. This artifice may be equivalent to the sinking of water in the northern North Atlantic, and the return, as either equivalent to upwelling off the coast of West Africa or possibly to the penetration of surface water northward across the equator from the South Atlantic Ocean.

The circulation of the North Pacific Ocean resembles some contemporary ideas of the actual circulation in several respects. In the model the Kuroshio is shorter than the Gulf Stream. It develops from the North Equatorial Current in the latitude of the Philippines north of Mindanao, accelerates steadily on its way past Formosa and the Ryikyu archipelago, is both swiftest and narrowest as it skirts the southern coast of Japan. During some experiments the Kuroshio stands off the southern coast of Japan, resembling to some extent the cyclonic bend described by Uda (1949), (1951). Beyond the 140° E meridian the Kuroshio decays rapidly, as does the Gulf Stream when it merges into the North Atlantic Current, and the circulation becomes quite sluggish. The equivalent of the Sargasso Sea in the Pacific is a very small patch of relatively motionless water directly south of the Kuroshio.

The prolongation of the Kuroshio Extension across the northern Pacific as the North Pacific Current is a slow, persistent movement which has no well defined boundaries but which accelerates slightly along the California coast and weakens again before joining the North Equatorial Current formed by the confluence of this water with the circulation northwestward along the west coast of Central America. The North Pacific Current crosses the mouth of the Gulf of Alaska and either contributes to, or sets up, a slow cyclonic circulation in the Gulf between Queen Charlotte Island and the beginning of the Aleutian archipelago. A similar cyclonic circulation appears east of the Kuril Islands, and a current flows southeastward along that chain which corresponds in a general way to the Oyashio. In certain experiments strong eddies develop in the region where the Kuroshio Extension and Oyashio meet off the coast of northern Japan, but in others the confluence is smooth or the Oyashio itself does not appear.

Within the main body of the North Pacific there is a slow general motion southward and southeastward from the paths of the strongest currents in the northwest which carries the complex filaments developed in the north toward the North Equatorial Current. The major contributions of water from the North Pacific to the North Equatorial Current appear to occur in the region between the coast of Central America and the 150° W meridian.

While the circulation within the North Pacific Ocean compartment is similar to that in the North Atlantic compartment, there are marked dissimilarities of detail. These may be due as much to the effects of northern seas on the Atlantic circulation as to the difference in shape and size of the two oceans in the temperate and equatorial latitudes.

4. In prospect

In none of the experiments with ocean compartments of realistic shape has it seemed desirable to include bottom topography other than that of the continental shelves to the level of the 200 meter isobath. Deeper topographic features such as major ridges and swells alter the circulation too much, and yet some modification of the otherwise featureless bottom seems to be needed. The surface circulation is thought to be represented in the basin and since, in nature, this is largely confined to the levels above the main thermocline, it may be that this interface is of importance to the wind-driven circulation. Experimentally a bottom surface having the topography of the main

thermocline would influence the local changes in the planetary vorticity tendency and may alter the circulation pattern in instructive ways. In past experiments this has been considered as only a simple function of latitude.

Attempts to develop a density interface similar to that at the thermocline, through the solution of crystalline table salt dropped to the bottom of the basin, have failed. This failure is presumed to result from the halocline adjusting to an isobaric surface in which case the planetary vorticity tendency is canceled for motions in the upper less saline layer.

In homogeneous water, however, the Coriolis force is balanced only by the pressure gradient due to elevation of the free surface. Near the bottom, where velocities are small, the pressure gradient is greater than the Coriolis force. Therefore, there is marked anticyclonic motion in the bottom layer beneath the surface dome of the Sargasso Sea area. A line of weaker horizontal divergence extends northeastward from this point into the northern North Atlantic. There is a similar but weaker bottom circulation in the Pacific compartment. Presumably this mode of motion would not occur were it possible to establish a two layer system without losing experimental control of the planetary vorticity adjustment, except during periods of rapid acceleration due to increased wind torque. This problem and a study of the circulation resulting from equatorial heating and polar cooling in the absence of wind is of present interest, as are the circulation systems of the southern hemisphere.

REFERENCES

Fuglister, F. C., 1951: Multiple Currents in the Gulf Stream System. *Tellus* **4**, 230—233.

Fuglister, F. C., and Worthington, L. V., 1951: Some results of a multiple ship survey of the Gulf Stream. *Tellus* **3**, 1—14.

Iselin, C. O'D., and Fuglister, F. C., 1948: Some recent developments in the study of the Gulf Stream. *Jour. Mar. Res.* **8**, 317—329.

Keulegan, G. H., 1951: Wind set-up in small closed channels. *Jour. Mar. Res. Natl. Bur. Stds.* **46** (5), 358—381.

Munk, W. H., 1950: On the wind-driven ocean circulation. *Jour. of Meteorology*, **7**, 79—93.

Stommel, Henry, 1948: The westward intensification of wind-driven ocean currents. *Trans. Amer. Geophys. Union*, **29**, 202—206.

Uda, M., 1949: On the correlated fluctuation of the Kuroshio current and the cold water mass. *Oceanog. Mag.* (Tokyo) **1**, 1—12.

— 1951: On the fluctuations of the main stream axis and its boundary line of Kuroshio. *Jour. Oceanogr. Soc. Japan* **6**, 181—189.

Fig. 4.

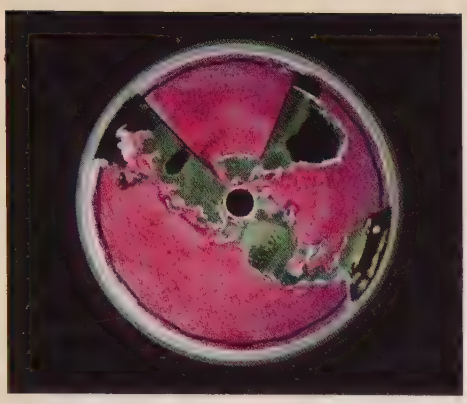

a) Color streamers from potassium permanganate crystals scattered on the bottom of the basin rotating at 3.18 radians/sec. Average depth of water 4 cm. Revolutions from start 24.

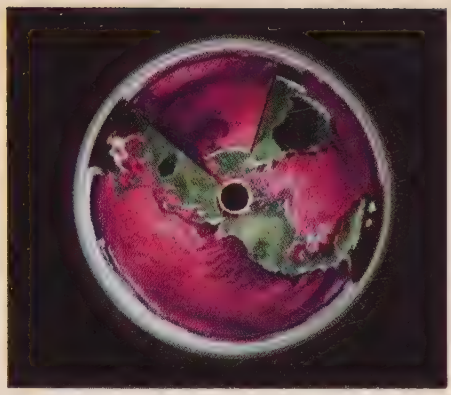

b) Same as (a) 150 revolutions from start. Color rises to the surface and occupies full depth of water in the regions of the coastal water masses.

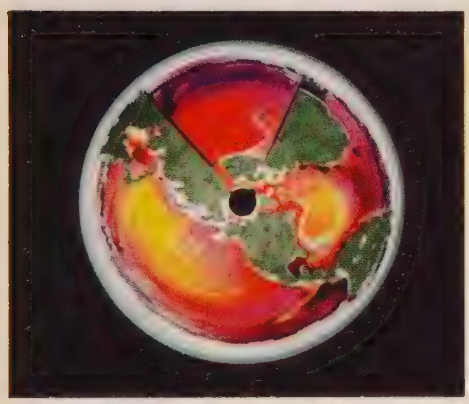

c) Occurence of patches of water on the right of the Gulf Stream system between Cape Hatteras and Grand Banks which may be similar to the patches of unusually warm water associated with the Gulf Stream.

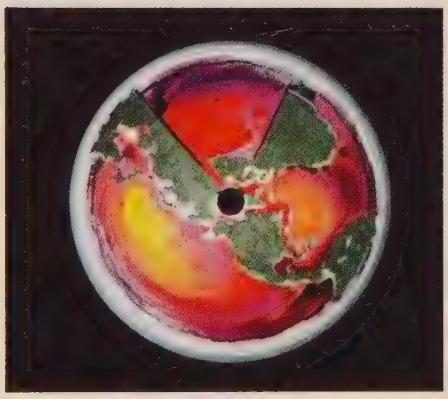

d) An example of the type of multiple current in the Gulf Stream system in the vicinity of Grand Banks revealed in the basin. This differs from the description of the natural occurrence given by FUGLISTER (1951) and may not be the same phenomen.

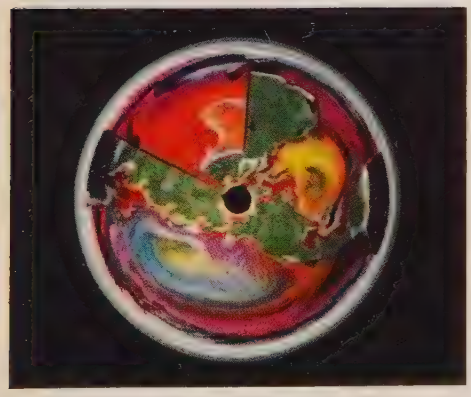

e) Structure of the Gulf Stream and Kuroshio current systems 400 revolutions after the introduction of potassium permanganate crystals on the bottom and blue ink on the surface. The pulsating character of the flow of the Gulf Stream can be recognized, and the cyclonic bend of the Kuroshio described by UDA (1949), (1951) is suggested.

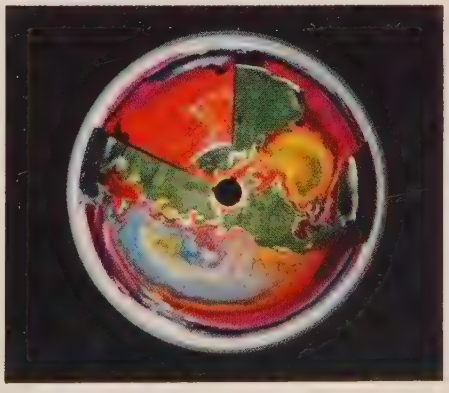

f) Further developments of the experiment shown in (e) at 450 revolutions. The small amount of lateral mixing along the course of the intensified western circulation is shown as well as the relative areas of the Sargasso Sea and its equivalent in the Pacific.

The quadrilateral compartment in the middle of Asia can be used as a control. The boundaries of this compartment are straight sided and uniformly smooth. In all of the photographs the Arctic ocean is permitted

Determination of the Sense of Polarization of the Magneto-Ionic z-Component

By BJÖRN LANDMARK, the Norwegian Defence Research Establishment

(Manuscript received 28 August 1952)

Abstract

The sense of polarization of the third magneto-ionic component, the z-component, was determined in a number of cases at the Auroral Observatory at Tromsö during October 1951. The observations showed without exception that the z-component was polarized in the same way as the ordinary component.

1. Introduction

The third magneto-ionic component, the z-component, was first reported by ECKERSLEY (1933). Today the z-component is a well known phenomenon at all stations at high latitudes. Thus at the Norwegian Defence Research Establishment at Kjeller (60° N, 11° E), recordings of both E- and F-layer triple splits are common, and at the Auroral Observatory at Tromsö (70° N, 19° E), the z-component is almost a daily returning phenomenon.

In the last years the magneto-ionic triple splitting has been treated theoretically by a number of writers. The z-wave may be explained as due to a coupling of the usual ordinary mode to the isolated extraordinary mode. The most complete treatment of the problem has perhaps been given by RYDBECK (1951). He shows that for even a smooth ionosphere at moderately high geomagnetic latitudes a z-wave is excited by the vertically incident ordinary wave in the neighbourhood of and at the ordinary reflection level.

According to the theory, the z-component should be polarized in the same way as the ordinary component. HOGARTH (1951), has published a single observation showing that this is the case. The purposes of the present paper is to present additional observations of the effect.

2. Experimental method

Different methods have been used in order to determine the state of polarization of radio waves. In 1932 APPLETON and WATSON-WATT, (WATSON-WATT, 1946) introduced the cathode ray direction-finding technique.

By this technique, the reflected echo is resolved into two components, at right angles, by a crossed loop receiving antenna system. The two components are connected, through identical HF-amplifiers, to the x- and y-plates of a cathode ray tube. If IF-amplification is used, the local oscillator must be common. If an elliptically polarized wave is reflected vertically from the ionosphere, the ellipse of polarization will be directly visible on the screen of the cathode ray oscilloscope.

A detailed study of the state of polarization can only be made if the echos appearing on the screen can be isolated. Appleton and Watson-Watt solved this problem by introducing a circular timebase on the screen with a timebase frequency equal to the pulse repetition frequency of the emitted waves. This solution does not utilize the screen to its full extent and the accuracy is therefore limited. By a time selection technique (gating) it is possible to remedy this difficulty. The cathode ray tube is opened by electronic gate-impulses in

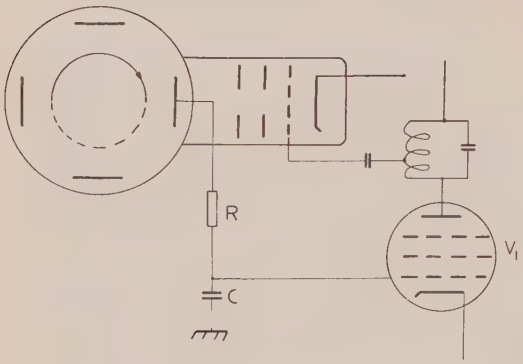

Fig. 1. Determination of the sense of polarization.

synchronism with the wanted signals, otherwise it remains closed.

Appleton and Watson-Watt determined the sense of polarization (sense of rotation of the field vectors) by studying the alterations of the ellipse on the screen when altering the trimming capacity in one of the HF-amplifiers, thus introducing a known phase shift. This method is somewhat difficult since the ellipses undergo constant and rapid fluctuations. In Fig. 1 is illustrated another method by which this difficulty was overcome. As before the x- and y-plates of the cathode ray tube are fed from the two loops respectivily, with conservation of phase relationship. The signal on the x-plates is shifted 90° in phase by the resistor R and the condenser C, and the phase-shifted signal is amplified in the pentode V_1, the anode circuit of which is tuned to the signal frequency. The phase-shifted signal is fed to the grid of the cathode ray tube via a condenser. When the gating signal from the pentode is positive, the brilliancy of the cathoderay tube will increase; when the signal is negative, the brilliancy will decrease. The gating signal goes positive 90° before the signal on the x-plates. This will make visible the upper or the lower part of the ellipse during each cycle according to the sense of rotation of the field vectors. Thus, the sense of polarization can be easily determined, as illustrated in Fig. 1, even if the ellipse of polarization be rapidly varying in size and shape.

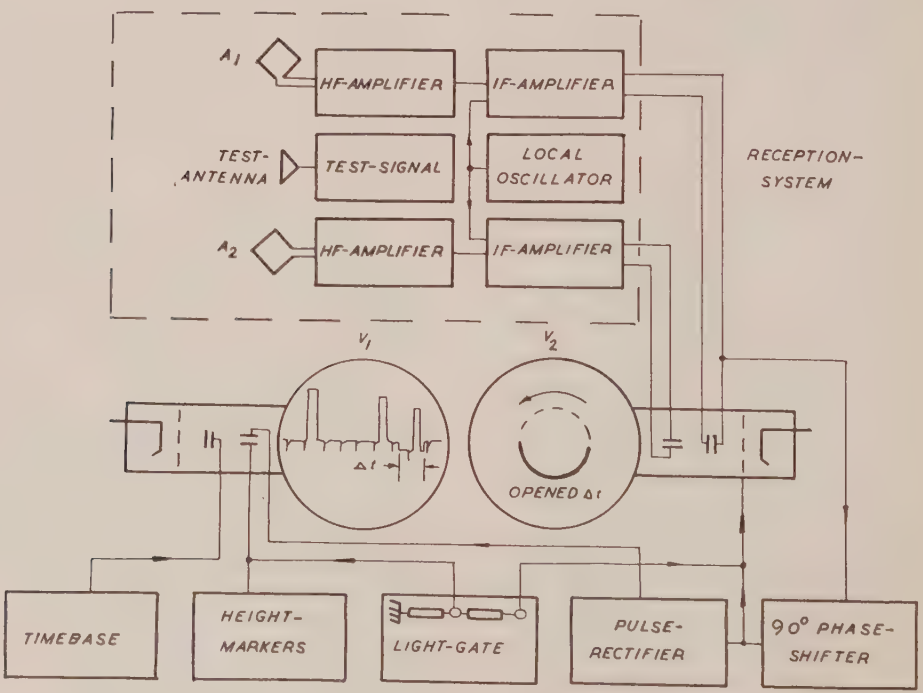

Fig. 2. Block-diagram of the radio polaritmer.

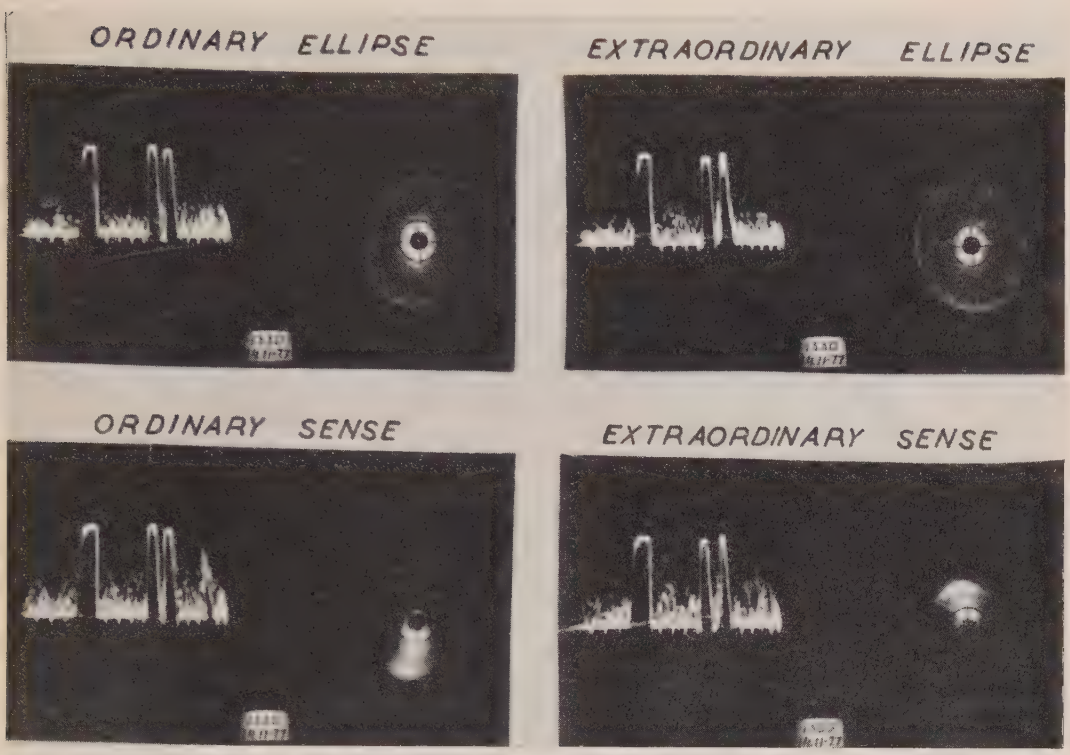

Fig. 3. The complete determination of the state of polarization for an ordinary and an extraordinary echo from the F_2-layer. The observations were made at the Norwegian Defence Research Establishment, Kjeller, on November 14th at 1330 MET on a frequence of 7.7 Mc/s.

In Fig. 2 is illustrated the basic principles of the radio polarimeter. The reception system consists of an HF-direction-finder of standard naval type, described by DE WALDEN, ROCKE and BARRAT (1947). V_1 and V_2 are two cathode ray tubes. V_1 gives the usual echopattern. A timebase is fed to the x-plates, and the signal together with height marks (each 50 km apparent height) is fed to the y-plates. V_2 is opened by an intensity modulation gate-impulse. This gate-voltage is also in reduced form fed to the y-plates of V_1, thus marking by a small pedestal on the trace the intervals in which V_2 is open. By altering the phase and width of the gate-impulse, the wanted signal may be selected. The signals from the two frame aerials are fed to the x- and y-plates of V_2 with conservation of phase relationship. In addition, the signal from the x-plates is shifted 90° in phase, and by superimposing this shifted signal on the gating-impulse of V_2, the sense of rotation may be determined as described above.

3. Results

The radio polarimeter described in section (2) has proved to be well suited for the study of the polarization ellipse, and also for the determination of the sense of rotation of the field vectors.

In Fig. 3 the complete determination of the state of polarization of an ordinary echo as well as an extraordinary one from the F_2-layer is shown.

In Fig. 4 an example is given which shows how the sense of polarization of the z-component is determined. The observation was made on October 24th at 0915 MET on a frequency of 4.4 Mc/s at the Auroral Observatory. In Fig. 4 the h'f-registration is also given which was obtained at 0900 MET. From Figs. 3 and 4 it appears that the *z-component is*

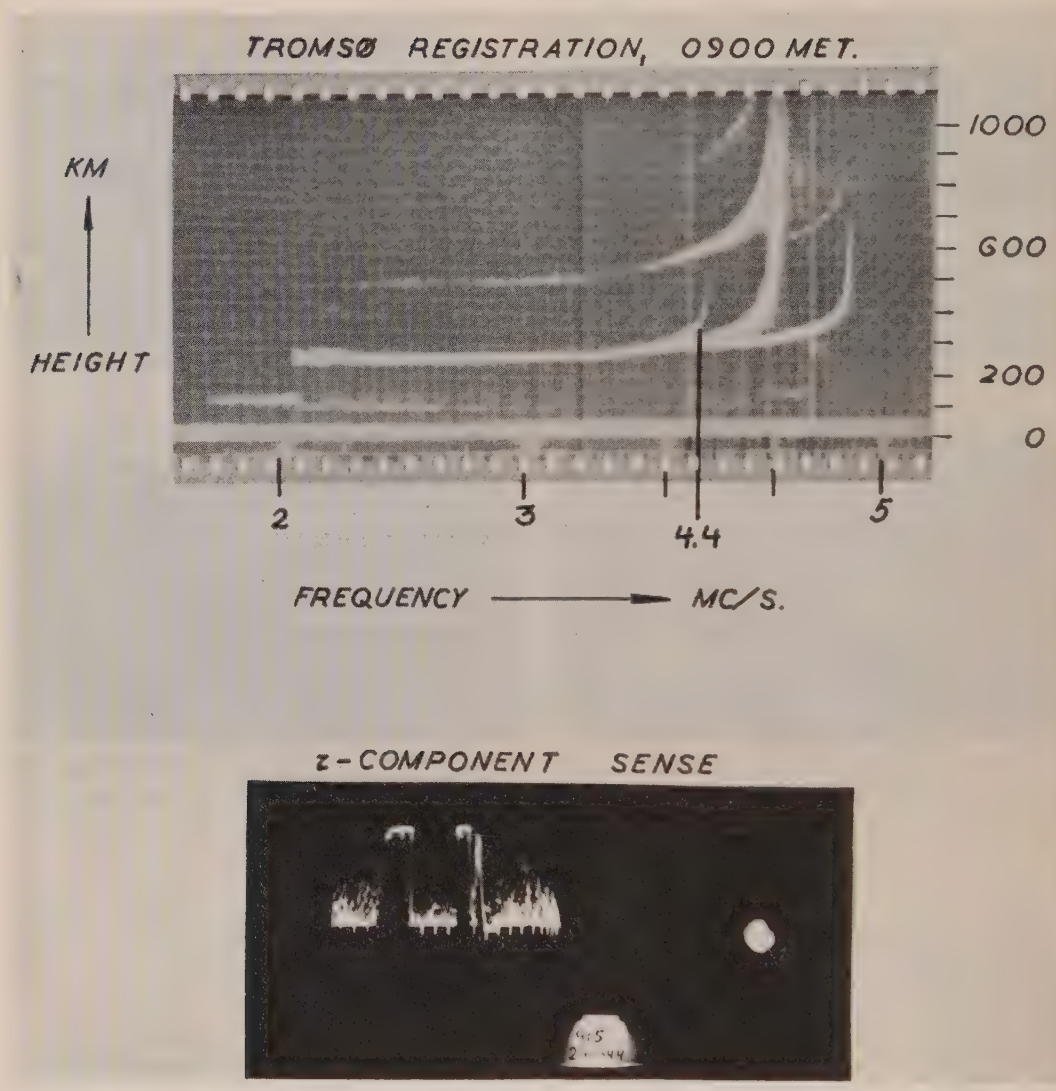

Fig. 4. Determination of the sense of polarization of the z-component. The observation was made at the Auroral Observatory, Tromsö, on October 24th at 0915 MET on a frequency of 4.4 Mc/s. The h'f-registration obtained at 0900 MET is also given.

polarized in the same way as the ordinary component.

The sense of polarization of the z-component was observed regularly during October 1951 at the Auroral Observatory. The observations showed without exception that the z-component was polarized in the same way as the ordinary component. This means that the field vectors is rotating from North to West on the Northern hemisphere.

Acknowledgements

The radio polarimeter was constructed at the Norwegian Defence Research Establishment as a part of the program of the Division of Telecommunication. The observations were made at the Auroral Observatory at Tromsö.

The author is indepted to Dr L. Harang, under whose supervision the present work was done, and to Mr F. Lied for inspiring discussions and suggestions.

REFERENCES

ECKERSLEY, T. L., 1933: *Proc. Roy. Soc.*, A, **141**, 710.

RYDBECK, O. E. H., 1951: The Theory of Magneto Ionic Triple Splitting, Rep. No. 14, *Research Laboratory of Electronics, Trans. Chalmers Univ. of Technology*, **101**.

HOGARTH, J. E., 1951: Polarization of the Z-Trace, *Nature*, **167**, 943.

DE WALDEN, S., ROCKE, A. F. L., BARRATT, J. O. G., and PITTS, W. J., 1947: The development of a High-Frequency Cathode-Ray Direction — Finder for Naval Use, *Journal I.E.E.*, **94**, Part IIIA, 823.

WATSON-WATT, R. A., 1946: Applications of the Cathode Ray Oscillograph in Radio Research. *Published by His Majesty's Stationary Office*, London.

On the Budget of Angular Momentum in the Zone between Equator and 30° N

By E. PALMÉN and M. A. ALAKA, University of Chicago

(Manuscript received 3 October 1952)

Abstract

A complete budget of angular momentum in the atmosphere is possible only by considering both the eddy transfer of angular momentum and the transport due to "mean meridional circulations". An attempt has been made in the present paper to achieve such a complete budget for the zone 20—30°N using the data available. The mean mass transport in the tropical circulation cell accumulates high relative momentum (W wind) in the upper atmosphere of this belt, whereas the eddy transport distributes it northwards and downwards from this subtropical jet.

1. Introduction

Several attempts have recently been made to explain the maintenance of the zonal atmospheric circulation as a result of horizontal and vertical flux of relative angular momentum primarily due to large-scale eddies (MINTZ, 1951; PRIESTLEY, 1951; STARR, WHITE, 1952; WIDGER, 1949). Whereas these attempts seem to give rather satisfactory results at higher latitudes, they have encountered considerable difficulties in the tropical and subtropical belts. As shown by meridional cross sections (MINTZ, 1951; PETTERSSEN, 1950), the strongest westerlies aloft during winter are, on the average, located around latitude 25°—30° N. According to Y. MINTZ (1951) and W. K. WIDGER (1949), this latitude is a zone where the northward angular-momentum flux due to large-scale eddies results in a momentum flux divergence. These eddies therefore tend to destroy the mean hemispheric "jet stream". Other mechanisms of momentum transfer are thus required to compensate for this divergence. In order to avoid this dilemma, Widger postulates the existence of an upward eddy flux of momentum in the subtropical belt.

As pointed out by PRIESTLEY (1951) and (PALMÉN 1951), a complete momentum budget necessitates the inclusion of a mean meridional circulation. Such a circulation, if existing, is instrumental in transforming absolute angular momentum ("ω-angular momentum") into relative angular momentum ("u-angular momentum") of the subtropical jet stream. The further poleward transport of u-momentum from the belt of strong zonal motion along the poleward margin of the tropical circulation cell can then primarily be regarded as some kind of eddy flux, in agreement with principles developed by V. P. STARR (1948), J. BJERKNES (1948), and others.

The aim of the present paper is to investigate the effect of various mechanisms of momentum transfer operating in the lower latitudes. Since no new empirical data are presented here, the paper should be regarded primarily as an attempt to discuss the principles of a complete momentum budget by considering

empirical data already in existence. Further, since the best data available are for the month of January, we shall limit our discussion to this month. The general principles, however, can presumably be extended to other months of the year.

Our budget will consider the balance between the following quantities in the belt 0—30° N:

a. The horizontal and vertical flux of angular momentum due to the mass transport resulting from a mean meridional circulation.

b. The horizontal and vertical eddy flux of angular momentum.

c. The angular momentum transfer from earth to atmosphere due to the surface stress of the wind.

2. Mass transport in the tropical circulation cell

Although the mean meridional circulation plays an essential role in all classical theories of the general circulation, very few attempts have been made to compute the mass transport in this mean circulation from real wind data. The discrepancy between the results achieved by C. H. B. Priestley (1951) and by V. P. Starr and R. M. White (1952) concerning the net meridional air flow in the free atmosphere indicates that the network of upper wind stations probably is not good enough for that purpose. By use of surface wind data, however, reasonably good values of the mass transport in the surface layer of the tropical and subtropical belts of both hemispheres can be computed, as H. Riehl and T. C. Yeh (1950) have shown. The greatest difficulty, however, arises when one wants to estimate the change of this horizontal mass transport along the vertical.

In order to obtain a minimum estimate of the masses involved in the meridional circulation, Riehl and Yeh assumed that the mean equatorward wind component decreases linearly with height and vanishes at 1 km. They, however, pointed out that the meridional circulation, computed under that assumption, obviously gives too small values.

Several investigations indicate that the meridional wind component does not essentially decrease from the surface up to about 950 or 900 mb. A study by Riehl and collaborators (1951) showed this to be the case in the trade-wind zone of the eastern Pacific. Also, an investigation by K. M. Nagler, not yet published, gives similar indications. In order to estimate the mass transport involved, we shall therefore use the values of the surface flow during January, given by Riehl and Yeh in the above-mentioned paper. But concerning the vertical extension, we shall adopt two tentative assumptions:

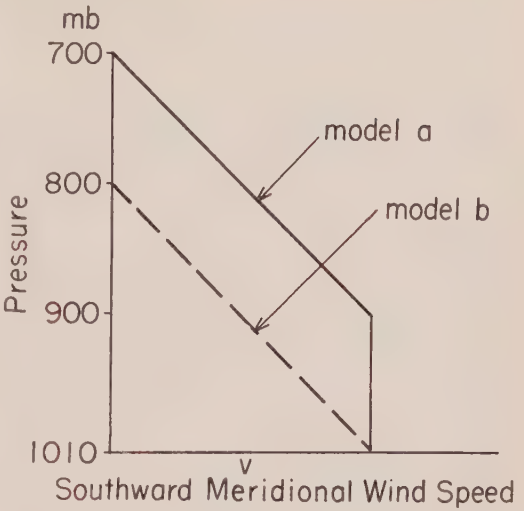

Fig. 1. Model (a) and (b) for the meridional wind component between 1010 and 700 mb.

Model a: The surface meridional wind as computed by Riehl and Yeh is constant up to 900 mb and decreases then linearly to zero at 700 mb.

Model b: The surface meridional wind decreases linearly with height and reaches the value zero at 800 mb.

The mass transport $[m]_\varphi$ across a given latitude φ between the isobaric surfaces p_1 and p_2 is

$$[m]_\varphi = \frac{2\pi a \cos\varphi}{g} \int_{p_2}^{p_1} v\,dp. \qquad (1)$$

Here g is the acceleration of gravity, a the earth's radius, and v the mean meridional wind component at an arbitrary isobaric surface at latitude φ. If $\bar{v}$ denotes a "mean value" of the meridional component between the isobaric surfaces p_1 and p_2 the mass transport between these isobaric surfaces can be expressed by

$$[m]_\varphi = \frac{2\pi a \cos\varphi}{g} \bar{v}(p_1 - p_2). \qquad (2)$$

Fig. 1 gives the profiles of the meridional wind for our two schematic models (a) and (b). The quantity $\bar{v}(p_1 - p_2)$ is determined by the area between the wind profiles and the coordinate axes. If we assume that the mean surface pressure is 1010 mb, it is easy to see that in model (a) the equatorward mass flux is two times that corresponding to model (b). Since no schematic assumption can exactly describe the distribution of meridional wind with height in the total belt Equator — 30° N, the above assumptions were selected in order to give a simple comparison.

Table 1 gives values of the southward mass transport at different latitudes computed on the basis of model (a), if the surface wind v_0 is assumed to be equal to the values for January computed by RIEHL and YEH (1950).

Table 1: Southward mass transport $[m]_\varphi$ (unit 10^6 tons/sec.) in the layer between 1010 and 700 mb in the belt 30—0° N computed on the basis of model (a).

Latitude	30°	25°	20°	15°	10°	5°	0°
$[m]_\varphi$	58	84	126	183	190	134	67

The vertical mass flux through the upper boundary can be determined by the difference in horizontal flux across the parallels of two latitudes, if one assumes that there is no change in mass distribution. The vertical mass transports through the 700-mb surface are presented in Table 2:

Table 2: Vertical mass transport $[m]_\varphi$ (unit 10^6 tons/sec.) through the isobaric surface 700 mb in the belt 30—0° N computed on the basis of model (a).

Latitude	30—25°	25—20°	20—15°	15—10°	10—5°	5—0°
$[m]_\varphi$	— 26	— 42	— 57	— 7	56	67

The mass fluxes according to model (b) can be obtained from Tables 1 and 2 by dividing the corresponding values by two. In this case, of course, the horizontal mass transport will be for the layer between the surface and 800 mb, and the vertical mass transport will be that across the 800-mb surface.

3. Flux of angular momentum due to meridional circulation

If we multiply the quantities in Tables 1 and 2 by the total angular momentum per unit mass

$$\Omega = \omega a^2 \cos^2\varphi + u a \cos\varphi \qquad (3)$$

we obtain the horizontal and vertical transport of angular momentum across the horizontal and vertical boundaries in question. The angular momentum transport can be expressed as the sum of two terms, one giving the transport of ω-angular momentum, the other that of u-angular momentum. In view of the observed zonal wind speeds, the second term is small compared to the first.

Since we assume a steady state, the southward mass transport in the lower layers must be compensated by an equal northward mass transport above the level of reversal of the meridional circulation (700 mb in model [a], and 800 mb in model [b]). Consequently, if we neglect the small effect of the variation in the distance from the earth's axis, the intensity of flow of ω-angular momentum must be the same, though its direction is opposite, in the two layers. The net transport of ω-angular momentum across each latitude circle is therefore approximately zero when summed from the earth's surface to the upper limit of the atmosphere; any net poleward transport of angular momentum across an arbitrary latitude is then determined solely by the flow of u-angular momentum.

The angular momentum budget due to the meridional circulation computed from model (a) is presented in Figure 2. The arrows showing the horizontal and vertical fluxes of angular momentum point in the direction of the mean air movement. The erect figures give the flux of ω-momentum and the slanting figures the flux of u-momentum. In computing the latter values the distribution of zonal wind according to MINTZ (1951) was used. Since Mintz' computation was not extended to the upper limit of the atmosphere and to the

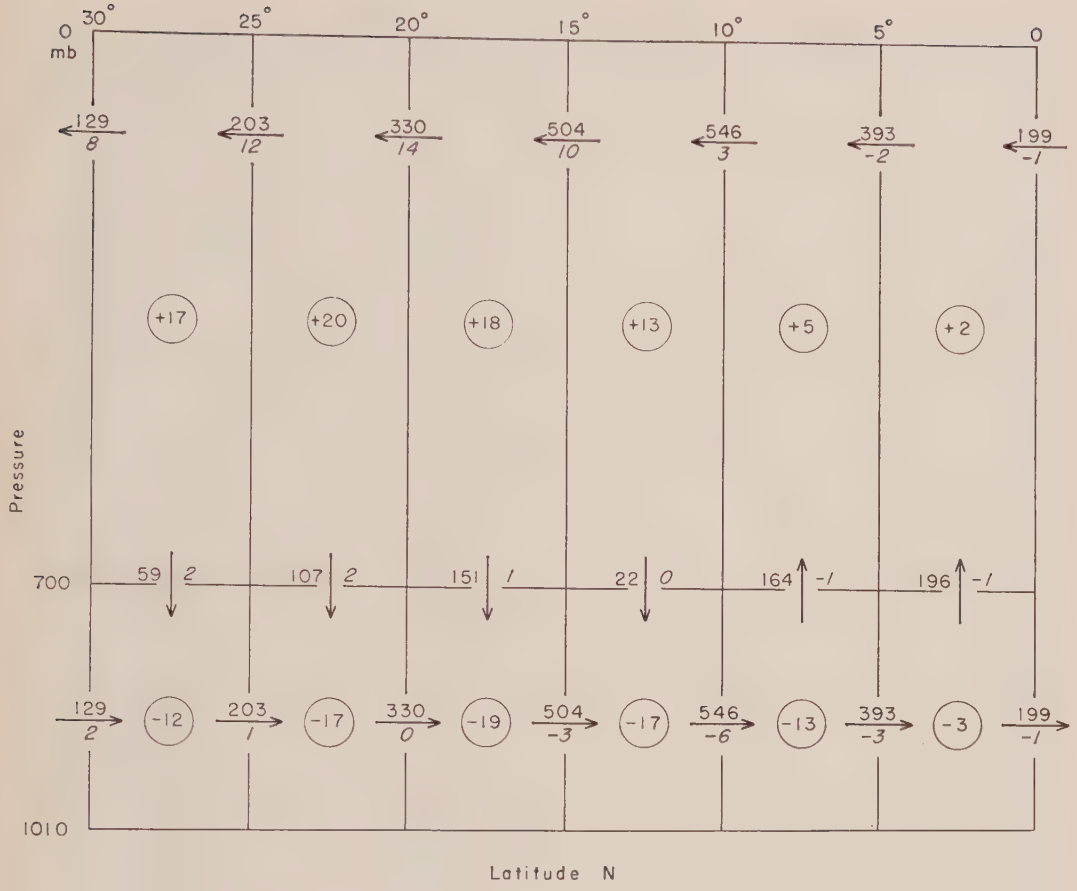

Fig. 2. Flux of ω-angular momentum (erect figures) and u-angular momentum (slanting figures) due to the meridional circulation computed from model (a) in Fig. 1. Encircled figures give the surplus or deficit of angular momentum in each block. Unit: 10^{25} g cm^2 sec^{-2}.

Equator, the missing data were extrapolated. The possible errors made in the extrapolation are of relatively minor importance. If u is negative (east wind) the positive transport of momentum is naturally in a direction opposite to the arrows. All values in Figure 2 are given in units of 10^{25} g cm^2 sec^{-2}. The encircled figures in the different blocks represent the difference between inflow and outflow of angular momentum; thus, they represent the generation or loss of angular momentum in each block as a result of the meridional circulation.

The following conclusions can be drawn from Figure 2:

1) The total deficit of angular momentum in the whole lower layer, represented by the sum of the encircled negative numbers is 81×10^{25} g cm^2 sec^{-2}, while the total surplus in the upper layer is 75×10^{25} g cm^2 sec^{-2}. The difference, 6×10^{25} g cm^2 sec^{-2}, represents the net flux of angular momentum due to meridional drift of air at latitude 30° N. The same result can be obtained by subtracting the slanting figures in the upper and lower layers at latitude 30° N.

2) The angular momentum transferred from the earth to the atmosphere in the belt 30°—0° N, due to the wind stress in the easterlies, is, according to PRIESTLEY (1951) and WIDGER (1949), much greater than the net northward flux of momentum of 6×10^{25} g

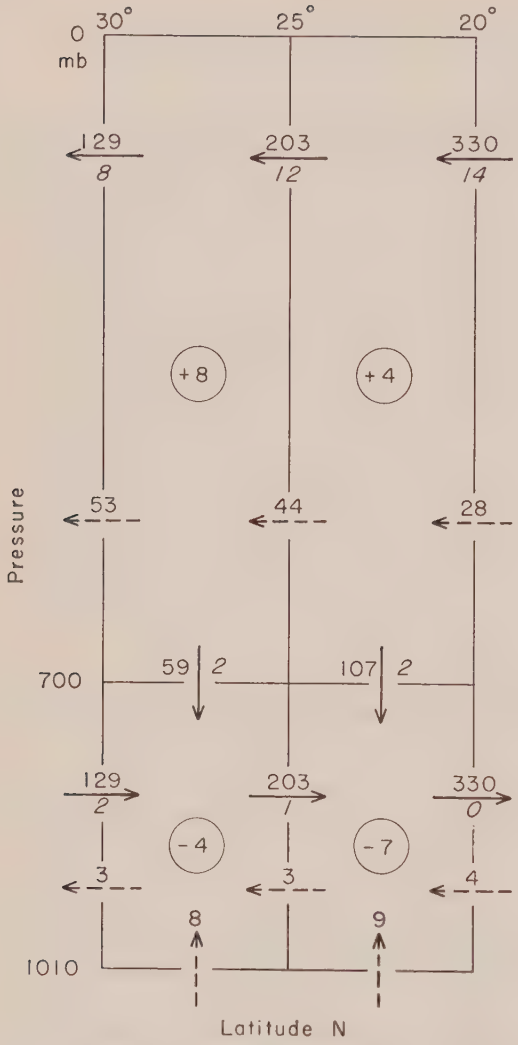

Fig. 3. Budget of angular momentum in the belt 30—20°N computed by use of model (a) and considering the horizontal eddy flux of angular momentum according to Mintz and the transfer from earth according to Widger. Encircled figures give the surplus or deficit of angular momentum if the vertical eddy flux is not considered. Unit: 10^{25}g cm² sec⁻².

cm² sec⁻². Thus, one can conclude that the meridional circulation computed from our model (a) does not give any satisfactory angular momentum budget. The same can naturally be said about every circulation with weaker mass transport, e.g., our model (b). This negative result is in good agreement with conclusions recently made by Starr and White (1952).

4. Total budget of angular momentum

In order to obtain a satisfactory momentum budget we have to add to the data presented in Figure 2 the horizontal and vertical eddy flux of angular momentum, and also the transfer of angular momentum due to the zonal stress of the surface wind. For the horizontal eddy transfer the data recently published by Mintz (1951) can be used. These data, which were computed on the assumption that the geostrophic wind approximates the real wind in the free atmosphere, are restricted to the north of latitude 20° N. For the transfer of angular momentum from earth to atmosphere, values computed by Widger (1949) are utilized. These values are based on a constant ratio between the geostrophic wind, as determined from the surface isobars, and the actual wind. As shown by C. L. Jordan (1952), this assumption is quite satisfactory southwards to around latitude 20° N.

In view of the above, we shall confine our complete momentum budget to the zone 30—20° N. Since the data for the geostrophic horizontal transfer of angular momentum computed by Mintz do not extend above 100 mb, the remaining transport above this level has been extrapolated. By this extrapolation we assumed that the flux of angular momentum linearily approaches zero at the 0-mb surface.

In Figure 3 the total budget, with the exception of the vertical eddy flux, is represented on the basis of model (a). The horizontal eddy fluxes and the transports from earth to atmosphere are here represented by broken arrows. In the lower layer between latitude 30 and 20° N the deficit of angular momentum amounts to 11×10^{25} g cm² sec⁻². If our budget is exact, this should correspond to the excess of angular momentum in the upper layer and represent the vertical eddy flux of momentum downwards across the 700-mb surface. Figure 3 shows that the excess in the upper layer is 12×10^{25} g cm² sec⁻². Thus, in spite of the approximate nature of all data used, a very close balance is obtained.

Of great interest is the fact that throughout the belt considered, the vertical eddy flux of momentum is directed downwards across the 700-mb surface, i.e., in the direction from higher to lower u-momentum. This result

should be compared with the streamlines for angular momentum flux given by WIDGER (1949). It might be pointed out that our value of the vertical eddy flux of angular momentum is computed from continuity considerations and that it therefore includes everything from molecular viscosity to the effect of large-scale atmospheric disturbances. If A denotes the area of the latitude belt 30—20° N the vertical transfer of angular momentum $[M]_z$ can be written

$$[M]_z = \overline{\varrho u' w'}\, A\, a\, \cos\varphi, \qquad (4)$$

or if we use a coefficient of eddy viscosity μ,

$$[M]_z = -\mu \overline{\frac{\partial u}{\partial z}}\, A\, a\, \cos\varphi. \qquad (5)$$

In Equation (4) u', w' denote the fluctuations in zonal and vertical velocity. Using the mean value of 11.5×10^{25} g cm^2 sec^{-2} for the downward eddy transfer of angular momentum through the 700-mb surface we get for the coefficient μ the value 120 g cm^{-1} sec^{-1} if $\frac{\partial u}{\partial z} = 4 \times 10^{-3}$ sec^{-1}

This value is considerably smaller than the value computed by RIEHL and collaborators (1951) for the trade wind belt of the Eastern Pacific Ocean. By order of magnitude it is, however, in agreement with the latter and also with values generally accepted for the free atmosphere above the frictional layer.

There are indications of a positive correlation between u' and w' in the large-scale eddies represented by cyclones, anticyclones, long waves and so on. Such a correlation would, according to Equation (4), result in upward momentum transfer. It is, however, easy to see that such an organized motion could hardly transport upwards more than a relatively small part of the angular momentum transferred from the earth, which according to Widger, amounts to 17×10^{25} g cm^2 sec^{-2}.

From this, it follows that there must be a lower limit of the meridional circulation determined by the possible vertical eddy flux of momentum, if we assume that all other quantities are approximately right. This is illustrated by Figure 4 which is computed on the basis of model (b). The horizontal eddy fluxes are nearly the same as in Figure 3 in all

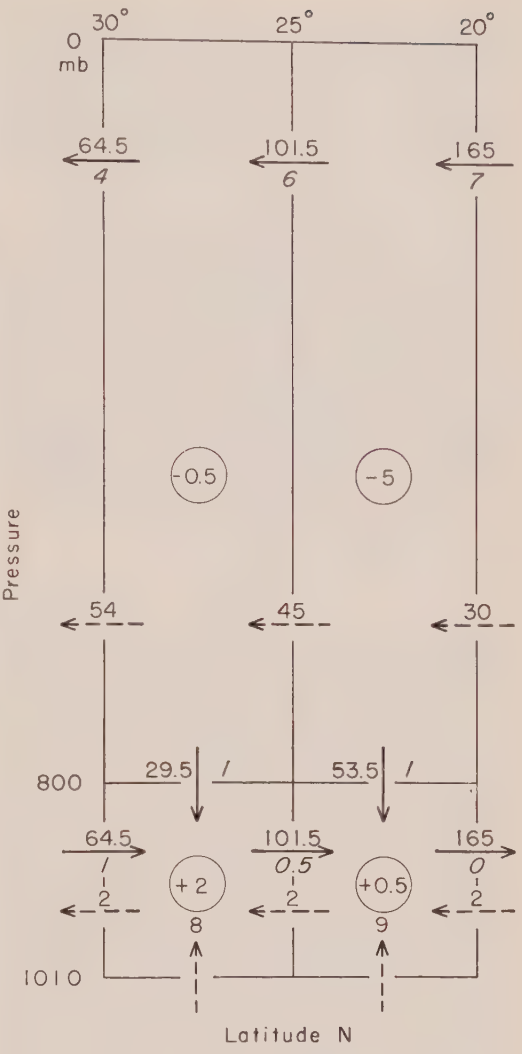

Fig. 4. Budget of angular momentum in the belt 30—20°N computed from model (b) and considering the horizontal eddy fluxes and the fluxes from earth according to Mintz and Widger. Meaning of figures the same as in Fig. 3.

blocks, now separated by the 800-mb surface, but the fluxes due to the meridional mass circulation are reduced to one half of the values in Figure 3. This gives a deficit of 5.5×10^{25} g cm^2 sec^{-2} in the upper layer and a surplus of 2.5×10^{25} g cm^2 sec^{-2} in the lower layer, requiring an upward eddy transfer of momentum across the 800-mb surface. This seems to indicate that the meridional circulation necessary for a complete balance probably

should be stronger than according to model (b), but perhaps a little weaker than according to model (a). A decision concerning the strength of the meridional circulation is possible only if exact values of both the horizontal and vertical eddy transport of momentum, including the transfer earth →atmosphere, could be computed.

Figure 3 reveals another interesting fact. Whereas the flux of angular momentum due to the assumed meridional circulation results in convergence of momentum in the upper layer and divergence of momentum in the lower layer, the horizontal eddy transport, according to Widger and Mintz, has the opposite effect. The net gain or loss of angular momentum in the upper layer, especially in the uppermost part of the troposphere, therefore depends on whether the former or latter transport is preponderant.

It should be remembered that Figure 3 represents the mean conditions for January assuming a complete balance between the different components of angular momentum flux. Such a balance does not necessarily prevail at all times. It is conceivable that all quantities involved undergo changes with time. At

period when the meridional circulation is etronger than usual, the horizontal and vertical addy fluxes are not vigorous enough to drain all the momentum surplus in the upper troposphere. Continuous accumulation of angular momentum then means strengthening of the upper subtropical jet. This in turn will increase the eddy flux of momentum and act to restore the balance. The opposite is true at periods with subnormal meridional circulation. Thus, although the quantities involved in our mean budget are in balance, instantaneous situations may show pronounced deviations from this balance. This departure from and return to balanced conditions could be responsible for the fluctuations in the intensity of the subtropical jet stream.

The total momentum flux from the tropics to higher latitudes across the parallel circle 30° N is 62×10^{25} g cm^2 sec^{-2}, according to Figure 3. This value appears quite reasonable considering that Widger computed a contribution of 17×10^{25} g cm^2 sec^{-2} from the earth in the belt 30—20°N and that the area between 20° N and the Equator is likely to yield more than twice this amount. Priestley (1951) recently estimated the surface torque to be at least 10^{34} g cm^2 sec^{-1} per annum in both hemispheres between the Equator and 30°. He pointed out, however, that the real torque probably is considerably greater. Presumably this is the case, since Priestley's estimate corresponds to only about 50 per cent of the flux given in Figure 3.

The total flux of angular momentum from earth to atmosphere in the belt Equator—30° N can also be estimated from Figure 2. The sum of the negative encircled figures in all blocks in the layer between 1010 and 700 mb is -81×10^{25} g cm^2 sec^{-2}. If we reduce this value by the downward eddy flux of momentum, the remaining value must be balanced by the momentum transfer from the earth and the eddy influx across 30°N and the Equator. In the belt 30—20°, we estimated the vertical downward eddy flux at 11.5×10^{25} g cm^2 sec^{-2}. Since the vertical wind shear decreases equatorwards from about latitude 30—25°N, we can assume that the contribution of the vertical eddy flux in the total belt 20°—Equator hardly could be larger than the contribution between 30 and 20° N. If we thus estimate the total downward eddy flux through the 700-mb surface to be about 20×10^{25} g cm^2 sec^{-2} and assume that the horizontal eddy flux is small in the layer in question (compare Fig. 3), the transfer of angular momentum from the earth to the atmosphere due to the surface wind stress in the total belt would amount to 61×10^{25} g cm^2 sec^{-2}, which is in agreement with the total flux of angular momentum across latitude 30° N which, as shown above, amounts to 62×10^{25} g cm^2 sec^{-2}. If all these rather crude estimates are approximately valid, no great net exchange of angular momentum between both hemispheres is necessary, at least in January.

It could also be of interest to compare the net northward flux of angular momentum due to the assumed meridional circulation with the eddy flux. From Figure 3, we get the following values:

The contribution from the circulation is very small compared with the eddy flux at latitude 30° N, but increases both absolutely and relatively equatorwards. This result seems to be in qualitative agreement with results recently achieved by Starr and White (1952).

Table 3: Total northward flux of angular momentum due to meridional circulation and large-scale eddies in January (unit: 10^{25} g cm^2 sec^{-2}).

Latitude	30°	25°	20°
Circulation transport	6	11	14
Eddy transport	56	47	32
Ratio in per cent	11	23	44

Conclusions: In spite of our doubts concerning the different empirical values used here, we feel that our discussion of the maintenance of the zonal motion in the atmosphere could be of interest. The data presented above show, in our opinion, that a total angular momentum budget for the atmosphere can be derived following the principles outlined here. Until more complete observational data are available the different terms in the momentum budget naturally have to be regarded as extremely approximate.

Acknowledgment: This paper is a report on research conducted under contracts between the Office of Naval Research, United States Navy, and the University of Chicago. The authors are indebted to Dr H. Riehl, University of Chicago, for many helpful discussions and suggestions. We also wish to express our gratitude to Mr K. M. Nagler, U.S. Weather Bureau, who permitted us to use results from a paper not yet published.

REFERENCES

Bjerknes, J., 1948: Réunion d'Oslo 1948, Programme et Résumé des Mémoires, pp. 13—14.

Jordan, C. L., 1952: A Comparison Between Observed and Geostrophic Winds in Low Latitudes. (To be published.)

Mintz, Y., 1951: The Geostrophic Poleward Flux of Angular Momentum in the Month of January, 1949. *Tellus*, **3**, pp. 195—200.

Palmén, E., 1951: The Role of Atmospheric Disturbances in the General Circulation. *Quart. J. Roy. Met. Soc.*, **77**, pp. 337—354.

Petterssen, S., 1950: Some Aspects of the General Circulation of the Atmosphere. *Quart J. Roy. Met. Soc.*, Cent. Proc., pp. 120—155.

Priestley, C. H. B., 1951: Physical Interactions Between Tropical and Temperate Latitudes. *Quart. J. Roy. Met. Soc.*, **77**, pp. 200—214.

Riehl, H., and Yeh, T. C., 1950: The Intensity of the Net Meridional Circulation. *Quart. J. Roy. Met. Soc.*, **76**, pp. 182—188.

Riehl, H., et al., 1951: The North-east Trade of the Pacific Ocean. *Quart. J. Roy. Met. Soc.*, **77**, pp. 598—627.

Starr, V. P., 1948: An Essay on the General Circulation of the Earth's Atmosphere. *J. of Met.*, **5**, pp. 39—43.

Starr, V. P., and White, R. M., 1952: Meridional Flux of Angular Momentum in the Tropics. *Tellus*, **4**, pp. 118—125.

Widger, W. K., 1949: A Study of the Flow of Angular Momentum in the Atmosphere. *J. of Met.*, **5**, pp 291—299.

Two Years of Momentum Flux Data for 31° N

By V. P. STARR, Massachusetts Institute of Technology
and R. M. WHITE, U.S.A.F. Cambridge Research Center, Mass.

(Manuscript received October 20, 1952)

At various times during the past two years, the authors have had occasion to report upon the results of an investigation of the angular momentum balance of the atmosphere as deduced from actual wind measurements distributed over the northern hemisphere (STARR and WHITE 1951, 1952a, 1952b). The meteorological implications of the results of these studies have been discussed in these papers. A further investigation for a period of one additional year has now been completed for 31° N, in order to verify the previous conclusions with independent data. A continuous two-year period has thus been analysed and represents a concluded phase of the investigation for this latitude.

For the second year, computations were made at the standard pressure levels. In combining the data for the first year with those of the second the 2, 6, 10, 20, 30, 40, and 55 thousand foot levels are identified with the 1000, 850, 700, 500, 300, 200, and 100 mb pressure levels respectively. For purposes of record Table I presents the final array of results, while Table II presents a frequency distribution of all available observations for the two year period. The form of these tables is identical with that of the corresponding ones given by STARR and WHITE (1952a, 1952b), to which papers the reader is referred for details of notation.

It is worthy of note that the vertical average of $[\overline{v}]$ with respect to pressure between 1000 and 100 mb is only —1.31 cm sec^{-1}.

Table I. Percentage of total possible observations at each level for each station.

Stations	Pressure levels in mb.						
	1000	850	700	500	300	200	100
Qrendi	20	57	58	52	52	33	18
Bahrein	22	63	62	61	57	47	22
Hyderabad	50	0	94	78	34	0	0
Debrugarh	80	0	87	46	17	0	0
Tokyo	91	92	97	95	85	58	24
Midway	81	79	74	66	53	42	21
Honolulu	93	88	80	73	60	46	26
Weather Ship (a)	77	84	85	82	71	59	22
Santa Maria	99	99	99	97	87	74	38
Big Spring	4	99	99	94	76	58	21
New Orleans	99	98	96	89	70	48	11
Miami	100	100	99	93	90	78	30
Kindley Field	87	87	83	68	36	13	1
Weather Ship (b)	85	79	81	74	55	40	15
Lagens	83	88	87	80	65	41	9
North Front	69	71	68	61	51	23	7
Habbaniya	25	54	52	53	49	43	29
Hong Kong	55	45	40	34	23	18	11
Farouk	32	58	58	55	38	16	2

Table II. Numerical analysis for the period Feb. 1949 to Jan. 1951 inc. The levels are given in mb. All velocities are in m sec.$^{-1}$.

Internal consistency of figures given is limited by rounding-off approximations.

1	2	3	4	5	6	7	8
Level	$\overline{[u]}$	$\overline{[v]}$	$\overline{[u]}\,\overline{[v]}$	$\overline{[u\ v]}$	$\overline{[u]}\,\overline{[v]}$	$\overline{[u]'\,[v]'}$	$\overline{[u'\,v']}$
100	+ 8.8	—0.05 ±0.39	— 2 ± 6	+ 14 ± 8	0	— 2	+16 ±4
200	+17.6	—0.27 ±0.39	— 5 ± 9	+ 40 ± 12	— 5	0	+45 ±7
300	+14.5	0.00 ±0.24	— 1 ± 5	+ 33 ± 7	0	— 1	+35 ±5
500	+ 8.7	+0.03 ±0.14	0 ± 2	+ 14 ± 3	0	— 1	+14 ±2
700	+ 3.8	—0.01 ±0.10	0 ± 1	+ 5 ± 1	0	0	+ 5 ±1
850	+ 1.2	+0.23 ±0.12	+ 1 ± 0	+ 4 ± 1	0	+ 1	+ 3 ±1
1000	— 0.7	—0.28 ±0.09	+ 1 ± 0	+ 4 ± 1	0	0	+ 3 ±1
Integral (10^7 CGS units)				+ 14.5	— 0.4	— 0.3	+ 15.1

	9	10	11	12	13	14	15
Level	n	$\{u\}$	$\{v\}$	$\{u\ v\}$	$\{uv\} - \{u\}\,\{v\}$	r	N
100	564	+ 7.8	+ 0.06	+ 15	+ 14	+ 0.14	2123
200	727	+ 15.9	— 0.11	+ 43	+ 44	+ 0.19	5351
300	730	+ 14.0	— 0.01	+ 33	+ 34	+ 0.19	7793
500	730	+ 8.6	— 0.01	+ 13	+ 13	+ 0.14	9912
700	730	+ 3.9	— 0.02	+ 5	+ 5	+ 0.10	10941
850	730	+ 1.2	+ 0.14	+ 4	+ 4	+ 0.09	9806
1000	730	— 0.7	— 0.30	+ 4	+ 3	+ 0.13	9043
Integral (10^7 CGS units)				+ 14.7	+ 14.8	Sum	54969

REFERENCES

Starr, V. P., and White, R. M., 1951: A hemispherical study of the atmospheric angular-momentum balance. *Quart. J. R. Met. Soc.*, **77**, 215—225.

Starr, V. P., and White, R. M., 1952a: Note on the seasonal variation of the meridional flux of angular momentum. *Quart. J. R. Met. Soc.*, **78**, 62—69.

Starr, V. P., and White, R. M., 1952b: Meridional flux of angular momentum in the tropics. *Tellus*, **4**, no. 2, 118—125.

Energy Conversions in the Atmosphere on the Scale of the General Circulation

By JACQUES VAN MIEGHEM, University of Brussels[1]

(Manuscript received 10th June 1952)

Abstract

From the equations of balance established for the different forms of energy (potential, kinetic and internal energies), the energy fluxes, the rates of energy production and conversion are deduced. Provided weighted mean values are considered the zonally averaged value of the kinetic energy may be decomposed into kinetic energy of the mean motion and the mean kinetic energy of the large-scale eddies. The corresponding equations of balance are established. The axial symmetry with respect to the earth's axis allows the introduction of the kinetic energy of the zonal motion and of the motion in the meridional planes. Their equations of balance are given. The conversions between the different species of mechanical energies are envisaged and the influence of the inertial stability on the conversion of "meridional" eddy-kinetic energy into "zonal" eddy-kinetic energy is pointed out. The definition of the large-scale eddy diffusion of heat is deduced from the first law of thermodynamics. This definition contains the flux of "sensible heat" and of "latent heat" as an approximation. Neglecting viscosity and small-scale turbulence, the general formulas are applied to the large atmospheric disturbances. A tentative formulation of the second law of thermodynamics is given.

1. Introduction

For the investigation of the different possible energy conversions in the atmosphere, on the scale of the general circulation, it is necessary to introduce a state of mean motion such that the averaged quantities vary slowly from one point (x^1, x^2, x^3) to another and from one instant (t) to another. This condition is fulfilled when the averages are taken for a one-, two- or three-dimensional domain of space, or for a time interval, or for a space-time domain, which is large with respect to the volume and the local lifetime of the perturbations (large-scale eddies) imbedded in the mean flow.

In this article only mean values along latitude circles will be considered. Let $\overline{X}\ (x^2, x^3, t)$ be the zonal mean value of the function $X\ (x^1, x^2, x^3, t)$ where x^1 designates the longitude λ. The corresponding weighted mean value $\hat{X}$ is defined by $\overline{\varrho}\ \hat{X} = \overline{\varrho X}$, ϱ being the specific mass of the air. The fluctuations X' and X'' of X with respect to the mean values $\overline{X}$ and $\hat{X}$ are given by $X = \overline{X} + X' = \hat{X} + X''$, with the conditions $\overline{X'} \equiv 0$, $\overline{\varrho X''} \equiv 0$, $X'' = \overline{X''} + X'$ and $-\overline{\varrho} \overline{X''} = \overline{\varrho' X''} = \overline{\varrho' X'} = \overline{\varrho X'} = \overline{\varrho' X}$, (Van Mieghem, 1949).

[1] At present at the Institute of Meteorology of the University of Stockholm.

Following a general method outlined elsewhere (VAN MIEGHEM, 1949) we establish successively the equations of balance of the kinetic, potential and internal energies of the zonally averaged motion and of the mean kinetic energy of the large-scale eddies. In the atmosphere of a rotating planet, the concepts of "zonal" and "meridional" kinetic energies are introduced and the equations of balance for these energies are also given. From the divergence form of the first member of an equation of balance, the flux of the envisaged property is deduced. The second member of the equation of balance defines the rate of production of that property. The rate of production of any of the above mentioned energy forms may be expressed as a sum of terms such that each of them appears also in the rate of production of only one other energy form, but with the opposite sign. Such a term may then be interpreted as a rate of conversion between the two energy forms (energy transformation function of J. E. MILLER, 1950).

Finally, evidence is given of the influence of the inertial stability on the conversion between the "zonal" and the "meridional" kinetic energy of the large-scale eddies.

2. Equations for non-averaged properties

The system of coordinates which is most appropriate for the study of the general circulation is one of non-local coordinates, symmetric with respect to the earth's axis. Let x^1 be the azimuthal coordinate (the longitude λ) and (x^2, x^3) arbitrary coordinates in the meridional plane, $\gamma_{ij} \equiv \gamma_{ji}$ the coefficients of the metric form in the variables x^i $(i, j = 1, 2, 3)$, γ^{ij} the algebraic minor of γ_{ij} divided by the determinant $\gamma \equiv \|\gamma_{ij}\|$, $v^i \equiv \frac{dx^i}{dt}$ and $v^i = \gamma_{ij} v^j$ respectively the contravariant and components of the air velocity $\mathbf{v}$ with respect to the earth, ω the angular speed of the earth, $\emptyset$ the geopotential, T^{ij}, T_{ij}, T^i_j respectively the contravariant, covariant and mixed components of the internal stresses. We know that $T_{ij} \equiv -p\gamma_{ij} + P_{ij} + R_{ij}$, where p is the pressure, $P_{ij} \equiv P_{ji}$ the Stokes (1842)—Navier (1822) viscosity stresses and $R_{ij} \equiv R_{ji}$ the Reynolds stresses (1895) due to small-scale turbulence.

It should be noted that the coefficients γ_{12} and γ_{13} are identically equal to zero, and that the four other γ's (namely: γ_{11}, γ_{22}, γ_{23}, γ_{33}) and the geopotential $\emptyset$ are independent of time t and longitude $x^1 \equiv \lambda$.

The coefficient γ_{11} represents the square of the distance to the earth's axis; the coefficients γ_{22} and γ_{33} define the linear elements $\sqrt{\gamma_{22}}\,\delta x^2$ and $\sqrt{\gamma_{33}}\,\delta x^3$ of the coordinate lines $x^3 = \text{constant}$ and $x^2 = \text{constant}$ in the meridional planes and γ_{23} the angle α between these lines $(\sqrt{\gamma_{22}\,\gamma_{23}}\cos\alpha = \gamma_{23})$.

In spherical coordinates: $x^1 \equiv \lambda$, $x^2 \equiv \varphi$, $x^3 \equiv r$, so that we have $\gamma_{11} \equiv r^2\cos^2\varphi$, $\gamma_{22} \equiv r^2$, $\gamma_{33} \equiv 1$, $\gamma_{ij} \equiv 0$ when $i \neq j$, and $\gamma \equiv r^4\cos^2\varphi$. The usual zonal, meridional and vertical components (u, v, w) of the air velocity $\mathbf{v}$ are:

$$u \equiv r\cos\varphi\, v^1 \equiv r\cos\varphi\frac{d\lambda}{dt} \equiv \frac{v_1}{r\cos\varphi},\quad v \equiv r v^2 \equiv r\frac{d\varphi}{dt} \equiv \frac{v_2}{r},\quad w \equiv v^3 \equiv \frac{dr}{dt} \equiv v_3.$$

The coordinate components of the tensor $\mathbf{T}$ in the usual zonal, meridional and vertical axis x, y, z in an arbitrary point are:

$$T^x_x \equiv T^1_1,\ T^y_y \equiv T^2_2,\ T^z_z \equiv T^3_3,\ T^x_y \equiv T^y_x \equiv \cos\varphi\ T^1_2 \equiv \frac{T^2_1}{\cos\varphi},\ T^y_z \equiv T^z_y \equiv r\ T^2_3 \equiv \frac{T^3_2}{r},$$

$$T^z_x \equiv T^x_z \equiv r\cos\varphi\ T^1_3 \equiv \frac{T^3_1}{r\cos\varphi}.$$

In axially symmetric coordinates (x^1, x^2, x^3) the equations of motion assume the form:

$$\begin{cases} \varrho \dfrac{d v_1}{dt} = -\omega \gamma_{11,\alpha}\ \varrho v^\alpha + T^i_{1\cdot i}, & (1) \\ \varrho \dfrac{d v_\delta}{dt} - \dfrac{1}{2}\gamma_{\alpha\beta,\delta}\ \varrho v^\alpha v^\beta = \dfrac{1}{2}\gamma_{11,\delta}(2\omega + v^1)\varrho v^1 + T^i_{\delta\cdot i} - \varrho \dfrac{\partial \Phi}{\partial x^\delta}, & (2) \end{cases}$$

$$(i = 1, 2, 3;\ \alpha, \beta\ \delta = 2, 3)$$

where the point before the suffix i indicates the covariant derivation with respect to x^i and where $\dfrac{d}{dt} \equiv \dfrac{\partial}{\partial t} + v^i \dfrac{\partial}{\partial x^i}$ and $\gamma_{ij,\alpha} \equiv \dfrac{\partial \gamma_{ij}}{\partial x^\alpha}$.

In spherical coordinates we have

$$\begin{cases} \dfrac{1}{r\cos\varphi} T^i_{1\cdot i} \equiv \dfrac{\partial T^x_x}{\partial x} + \dfrac{1}{\cos^2\varphi}\dfrac{\partial(\cos^2\varphi\, T^y_x)}{\partial y} + \dfrac{1}{r^3}\dfrac{\partial(r^3 T^z_x)}{\partial z}, \\ \dfrac{1}{r} T^i_{2\cdot i} \equiv \dfrac{\partial T^x_y}{\partial x} + \dfrac{1}{\cos\varphi}\dfrac{\partial(\cos\varphi\, T^y_y)}{\partial y} + \dfrac{1}{r^3}\dfrac{\partial(r^3 T^z_y)}{\partial z} + T^x_x \dfrac{\operatorname{tg}\varphi}{r}, \\ T^i_{3\cdot i} \equiv \dfrac{\partial T^x_z}{\partial x} + \dfrac{1}{\cos\varphi}\dfrac{\partial(\cos\varphi\, T^y_z)}{\partial y} + \dfrac{1}{r^2}\dfrac{\partial(r^2 T^z_z)}{\partial z} - (T^z_z + T^y_y)\dfrac{1}{r}, \end{cases}$$

where $\dfrac{\partial}{\partial x} \equiv \dfrac{1}{r\cos\varphi}\dfrac{\partial}{\partial\lambda}$, $\dfrac{\partial}{\partial y} \equiv \dfrac{1}{r}\dfrac{\partial}{\partial\varphi}$, $\dfrac{\partial}{\partial z} \equiv \dfrac{\partial}{\partial r}$.

In order to make a clear distinction between "zonal" and "meridional" quantities, two sets of indices are used systematically: $i, j, k, \ldots = 1, 2, 3$ and $\alpha, \beta, \delta, \ldots = 2, 3$, the last set designating only coordinates and components in the meridional planes.

After multiplication of (1) by v^1, of (2) by v^δ, summation with respect to δ $(= 2, 3)$ and substitution of the equation of continuity

$$\frac{\partial \varrho}{\partial t} + \frac{1}{\sqrt{\gamma}}\frac{\partial(\sqrt{\gamma}\,\varrho v^i)}{\partial x^i} = 0 \qquad \text{or} \qquad \frac{\partial \varrho}{\partial t} + (\varrho v^i)_{\cdot i} = 0, \tag{3}$$

one obtains the equations of the "zonal" $\left(k_\xi \equiv \frac{1}{2} v_1 v^1\right)$ and "meridional" $\left(k_\mu \equiv \frac{1}{2} v_\alpha v^\alpha\right)$ kinetic energies

$$\frac{\partial(\varrho k_\xi)}{\partial t} + \frac{1}{\sqrt{\gamma}}\frac{\partial}{\partial x^i}\left[\sqrt{\gamma}\,(\varrho k_\xi v^i - T^i_1 v^1)\right] = -\frac{1}{2}\gamma_{11,\alpha}(2\omega + v^1)\varrho v^1 v^\alpha - T^i_1 \frac{\partial v^1}{\partial x^i}, \tag{4}$$

$$\begin{cases} \dfrac{\partial(\varrho k_\mu)}{\partial t} + \dfrac{1}{\sqrt{\gamma}}\dfrac{\partial}{\partial x^i}\left[\sqrt{\gamma}\,(\varrho k_\mu v^i - T^i_\alpha v^\alpha\right] = \\ \qquad \dfrac{1}{2}\gamma_{11,\alpha} v^\alpha \left[(2\omega + v^1)\varrho v^1 - T^{11}\right] - T^\beta_\alpha v^\alpha_{\cdot\beta} - T^1_\alpha \dfrac{\partial v^\alpha}{\partial x^1} - g\varrho w, \end{cases} \tag{5}$$

$$(i = 1, 2, 3;\ \alpha = 2, 3)$$

and by addition of (4) and (5), the equation of balance of the total kinetic energy $k \equiv k_\xi + k_\mu \equiv \frac{1}{2} v_i v^i$,

$$\frac{\partial(\varrho k)}{\partial t} + \frac{1}{\sqrt{\gamma}} \frac{\partial}{\partial x^i} \left[\sqrt{\gamma} (\varrho k v^i - T^i_j v^j)\right] = - T^i_j v^j{}_{,i} - g \varrho w. \tag{6}$$

Further, the equation of balance for the potential energy may be written

$$\frac{\partial(\varrho \Phi)}{\partial t} + \frac{1}{\sqrt{\gamma}} \frac{\partial}{\partial x^i} (\sqrt{\gamma} \varrho \Phi v^i) = \varrho \frac{\partial \Phi}{\partial x^\alpha} v^\alpha \cong g \varrho w, \tag{7}$$

where Φ is the geopotential (or the potential energy per unit of mass), g the acceleration of gravity and w the vertical cartesian component of the air velocity $\mathbf{v}$.

Finally, multiplying (1) by v_β and (2) by v_1 adding and substituting (3), the equation of the tensor component $\varrho v_1 v_\delta$ is easily obtained:

$$\frac{\partial}{\partial t} (\varrho v_1 v_\delta) + \left[\varrho v_1 v_\delta v^i - T^i_1 v_\delta - T^i_\delta v_1\right]_{,i} = - \omega (\gamma_{11,\alpha} \varrho v^\alpha v_\delta - \gamma_{11,\delta} \varrho v^1 v_1) -$$
$$- (T^i_1 v_{\delta,i} + T^i_\delta v_{1,i}) - \varrho \frac{\partial \Phi}{\partial x^\delta} v_1. \tag{8}$$

In the same way, an equation for the tensor component $\varrho v_\alpha v_\beta$ may be established.

3. Equations for the averaged properties

The averaged motion being defined by the zonal mean values $\bar{\varrho}$ and $\overline{\varrho v^i}$ of the specific mass ϱ and of the contravariant components of the relative linear momentum $\varrho \mathbf{v}$, is independent of longitude λ or x^1. In order to take full advantage of this circumstance, we shall consider all the possible transformations of coordinates in the meridional plane only, thus keeping the longitude λ as independent variable. Then it is obvious that v^1, v_1, γ_{11}, γ^{11}, T_{11}, T^{11} and T^1_1 are invariants, v^α, T^α_1, $\gamma^{\alpha\beta}$ and $T^{\alpha\beta}$ contravariant, and v_α, T^1_α, $\gamma_{\alpha\beta}$ and $T_{\alpha\beta}$ covariant quantities with respect to any change of variables x^2 and x^3. Hence, both $k_{\xi m} \equiv \frac{1}{2} \hat{v}_1 \hat{v}^1$ and $k_{\mu m} \equiv \frac{1}{2} \hat{v}_\alpha \hat{v}^\alpha$ are independent of longitude and invariant with respect to any change of meridional variables; this justifies the introduction of the "zonal" and "meridional" energies of the mean motion.

Every equation in connection with the zonally averaged motion will be written in such a way that all terms have a variance with respect to the transformations of the meridional coordinates only.

From the averaged equation (7), we deduce the components $C^\alpha(\Phi)$ of the meridional flux and the rate of production $\sigma(\Phi)$ of the potential energy Φ of the mean motion:

$$C^\alpha(\Phi) \equiv \Phi \overline{\varrho v^\alpha} = \Phi (\bar{\varrho} \bar{v}^\alpha + \overline{\varrho' v'^\alpha}) \quad \text{and} \quad \sigma(\Phi) \equiv g \overline{\varrho w} = g (\bar{\varrho} \bar{w} + \overline{\varrho' w'}). \tag{9}$$

In most cases, the correlation between ϱ' and w' is negative, and the correlation between ϱ' and v' is negative in the troposphere, but positive in the stratosphere. Consequently, the flux $\overline{\varrho' \mathbf{v}'}$ is generally directed toward the earth, both in the stratosphere and in the troposphere, toward the pole in the stratosphere, and toward the equator in the troposphere. The second term $g \overline{\varrho' w'}$ of $\sigma(\Phi)$ is generally negative so that it represents a destruction of potential energy of the mean motion. From the first term of $\sigma(\Phi)$, it follows that

production of potential energy of the mean motion occurs in the ascending branch ($\overline{w} > 0$), and destruction of potential energy in the descending branch ($\overline{w} < 0$) of the mean meridional circulation ($\overline{v}, \overline{w}$).

Using the equations of the zonally averaged motion [instead of (1) and (2)] and the equation of continuity of the mean motion

$$\frac{\partial \overline{\varrho}}{\partial t} + \frac{1}{\sqrt{\gamma}} \frac{\partial}{\partial x^\alpha} (\sqrt{\gamma}\, \overline{\varrho}\, \hat{\mathrm{v}}^\alpha) = 0, \tag{10}$$

instead of (3), equations of balance for the "zonal" $\left(k_{\xi m} \equiv \frac{1}{2} \hat{\mathrm{v}}_1 \hat{\mathrm{v}}^1\right)$ and "meridional" $\left(k_{\mu m} \equiv \frac{1}{2} \hat{\mathrm{v}}_\alpha \hat{\mathrm{v}}^\alpha\right)$ kinetic energies of the mean motion, similar to (4) and (5), are obtained:

$$\frac{\partial}{\partial t} (\overline{\varrho}\, k_{\xi m}) + \frac{1}{\sqrt{\gamma}} \frac{\partial}{\partial x^\alpha} \left[\sqrt{\gamma}\, \overline{\varrho}\, k_{\xi m} \hat{\mathrm{v}}^\alpha - \overline{T}_1^\alpha \hat{\mathrm{v}}^1 + \overline{\varrho\, \mathrm{v}_1'' \mathrm{v}''^\alpha} \hat{\mathrm{v}}^1\right] = \tag{11}$$

$$= -\frac{1}{2} \gamma_{11,\alpha} (\hat{\mathrm{v}}^1 + 2\omega)\, \overline{\varrho}\, \hat{\mathrm{v}}^1 \hat{\mathrm{v}}^\alpha - \overline{T}_1^\alpha \frac{\partial \hat{\mathrm{v}}^1}{\partial x^\alpha} + \overline{\varrho\, \mathrm{v}_1'' \mathrm{v}''^\alpha} \frac{\partial \hat{\mathrm{v}}^1}{\partial x^\alpha},$$

and

$$\frac{\partial}{\partial t} (\overline{\varrho}\, k_{\mu m}) + \frac{1}{\sqrt{\gamma}} \frac{\partial}{\partial x^\alpha} \left[\sqrt{\gamma}\, (\overline{\varrho}\, k_{\mu m} \hat{\mathrm{v}}^\alpha - \overline{T}_\beta^\alpha \hat{\mathrm{v}}^\beta + \overline{\varrho\, \mathrm{v}_\beta'' \mathrm{v}''^\alpha} \hat{\mathrm{v}}^\beta\right] = \tag{12}$$

$$= \frac{1}{2} \gamma_{11,\alpha} \hat{\mathrm{v}}^\alpha \left[(\hat{\mathrm{v}}^1 + 2\omega)\, \overline{\varrho}\, \hat{\mathrm{v}}^1 - \overline{T}^{11} + \overline{\varrho\, \mathrm{v}''^1 \mathrm{v}''^1}\right] - \overline{T}_\alpha^\beta \hat{\mathrm{v}}^\alpha_{\cdot\beta} + \overline{\varrho\, \mathrm{v}''^\beta \mathrm{v}_\alpha''} \hat{\mathrm{v}}^\alpha_{\cdot\beta} - g\, \overline{\varrho w},$$

where $-\overline{\varrho\, \mathrm{v}_i'' v''^j}$ represent the Jeffreys-stresses (1926) due to the large-scale eddies.

Averaging equations (4) and (5) along the latitude circles and subtracting from them the equations (11) and (12), one obtains the equations of balance of the "zonal" $\left(k_{\xi e} \equiv \frac{1}{2} \mathrm{v}''^1 \mathrm{v}_1''\right)$ and "meridional" $\left(k_{\mu e} \equiv \frac{1}{2} \mathrm{v}''^\alpha \mathrm{v}_\alpha''\right)$ kinetic energies of the large-scale eddying motion:

$$\frac{\partial}{\partial t} (\overline{\varrho\, k_{\xi e}}) + \frac{1}{\sqrt{\gamma}} \frac{\partial}{\partial x^\alpha} \left[\sqrt{\gamma}\, (\overline{\varrho\, k_{\xi e}} \hat{\mathrm{v}}^\alpha + \overline{\varrho\, k_{\xi e} \mathrm{v}''^\alpha})\right] =$$

$$= -\frac{1}{2} \gamma_{11,\alpha} \left\{\left[2 (\omega + \hat{\mathrm{v}}^1)\, \overline{\varrho\, \mathrm{v}''^1 \mathrm{v}''^\alpha} + \overline{\varrho\, \mathrm{v}''^1 \mathrm{v}''^1 \mathrm{v}''^\alpha}\right] + \overline{\varrho\, \mathrm{v}''^1 \mathrm{v}''^1}\, \hat{\mathrm{v}}^\alpha\right\} - \tag{13}$$

$$- \overline{\varrho\, \mathrm{v}_1'' \mathrm{v}''^\alpha} \frac{\partial \hat{\mathrm{v}}^1}{\partial x^\alpha} + \overline{T^i_{1\cdot i}\, \mathrm{v}''^1},$$

and

$$\frac{\partial}{\partial t} (\overline{\varrho\, k_{\mu e}}) + \frac{1}{\sqrt{\gamma}} \frac{\partial}{\partial x^\alpha} \left[\sqrt{\gamma}\, (\overline{\varrho\, k_{\mu e}} \hat{\mathrm{v}}^\alpha + \overline{\varrho\, k_{\mu e} \mathrm{v}''^\alpha})\right] = \tag{14}$$

$$= \frac{1}{2} \gamma_{11,\alpha} \left[2 (\omega + \hat{\mathrm{v}}^1)\, \overline{\varrho\, \mathrm{v}''^1 \mathrm{v}''^\alpha} + \overline{\varrho\, \mathrm{v}''^1 \mathrm{v}''^1 \mathrm{v}''^\alpha}\right] - \overline{\varrho\, \mathrm{v}''^\alpha \mathrm{v}_\beta''} \hat{\mathrm{v}}^\beta_{\cdot\alpha} + \overline{T^i_{\alpha\cdot i}\, \mathrm{v}''^\alpha}.$$

Finally, addition of (11) and (12), and of (13) and (14), leads to the equations of balance of the kinetic energy $\left(k_m \equiv k_{\xi m} + k_{\mu m} \equiv \frac{1}{2}\,\hat{v}_i\,\hat{v}^i\right)$ of the mean motion and of the kinetic energy $\left(k_e \equiv k_{\xi e} + k_{\mu e} \equiv \frac{1}{2}\,v''_i\,v''^i\right)$ of the large-scale eddying motion:

$$\frac{\partial}{\partial t}(\bar{\varrho}\,k_m) + \frac{1}{\sqrt{\gamma}}\frac{\partial}{\partial x^\alpha}\left[\sqrt{\gamma}\,(\bar{\varrho}\,k_m\,\hat{v}^\alpha - \bar{T}^\alpha_i\,\hat{v}^i + \overline{\varrho\,v''_i\,v''^\alpha}\,\hat{v}^i\right] = -\,\bar{T}^i_j\,\hat{v}^j_{\cdot i} + \overline{\varrho\,v''^i\,v''_j}\,\hat{v}^j_{\cdot i} - g\,\overline{\varrho\,w}, \quad (15)$$

and

$$\frac{\partial}{\partial t}(\overline{\varrho\,k_e}) + \frac{1}{\sqrt{\gamma}}\frac{\partial}{\partial x^\alpha}\left[\sqrt{\gamma}\,(\overline{\varrho\,k_e}\,\hat{v}^\alpha + \overline{\varrho\,k_e\,v''^\alpha})\right] = \overline{T^i_{j\cdot i}v''^j} - \overline{\varrho\,v''^i\,v''_j}\,\hat{v}^j_{\cdot i}. \quad (16)$$

$$(\alpha = 2, 3;\ i, j = 1, 2, 3)$$

All these equations assume the form of a balance:

$$\frac{\partial}{\partial t}(\bar{\varrho}\,k) + \frac{1}{\sqrt{\gamma}}\frac{\partial}{\partial x^\alpha}\left[\sqrt{\gamma}\,C^\alpha(k)\right] = \sigma(k),$$

where the meridional flux $C^\alpha(k)$ and the rate of production $\sigma(k)$ of the different energy forms k appear in the divergence term and in the second member of equations (11) to (16) respectively. These equations may be given the following interpretation.

The kinetic energies $\bar{\varrho}\,k_{\xi m}$, $\bar{\varrho}\,k_{\mu m}$ and $\bar{\varrho}\,k_m$ in a fixed unit of volume may change in consequence of:

a) transport of air across the boundary: $\bar{\varrho}\,k_{\xi m}\,\hat{v}^\alpha$, $\bar{\varrho}\,k_{\mu m}\,\hat{v}^\alpha$ and $\bar{\varrho}\,k_m\,\hat{v}^\alpha$;

b) performance of boundary work by the internal stresses: $-\left(\bar{P}^\alpha_1 + \bar{R}^\alpha_1\right)\hat{v}^1, \bar{p}\,\hat{v}^\alpha - -\left(\bar{P}^\alpha_\beta + \bar{R}^\alpha_\beta\right)\hat{v}^\beta$ and $\bar{p}\,\hat{v}^\alpha - \left(\bar{P}^\alpha_i + \bar{R}^\alpha_i\right)\hat{v}^i$;

c) large-scale eddy flux of momentum through the boundary:

$$\overline{\varrho\,v''_1\,v''^\alpha}\,\hat{v}^1,\ \overline{\varrho\,v''_\beta\,v''^\alpha}\,\hat{v}^\beta,\ \overline{\varrho\,v''_i\,v''^\alpha}\,\hat{v}^i,\ \text{(Van Mieghem, 1949 a)};$$

d) production within the volume at the rate:

$$\left.\begin{aligned}
\sigma(k_{\xi m}) &\equiv \frac{1}{2}\,\gamma_{11,\alpha}\,(2\omega + \hat{v}^1)\,\varrho\,\hat{v}^1\,\hat{v}^\alpha - \left(\bar{P}^\alpha_1 + \bar{R}^\alpha_1\right)\frac{\partial \hat{v}^1}{\partial x^\alpha} \\
&\quad + \overline{\varrho\,v''^\alpha\,v''_1}\,\frac{\partial \hat{v}^1}{\partial x^\alpha}, \\
\sigma(k_{\mu m}) &\equiv -\frac{1}{2}\gamma_{11,\alpha}\,(2\omega + \hat{v}^1)\,\bar{\varrho}\,\hat{v}^1\,\hat{v}^\alpha - \left(\bar{P}^\beta_\alpha + \bar{R}^\beta_\alpha\right)\hat{v}^\alpha_{\cdot\beta} - \frac{1}{2}\,\gamma_{11,\alpha}\,\hat{v}^\alpha\left(\bar{P}^{11} + \bar{R}^{11}\right) + \\
&\quad + \bar{p}\ \mathrm{div}\,\hat{\mathbf{v}} + \overline{\varrho\,v''^\beta\,v''_\alpha}\,\hat{v}^\alpha_{\cdot\beta} + \frac{1}{2}\,\gamma_{11,\alpha}\,\hat{v}^\alpha\,\overline{\varrho\,v''^1\,v''^1} - g\,\overline{\varrho\,w}, \\
\sigma(k_m) &\equiv -\left(\bar{P}^i_j + \bar{R}^i_j\right)\hat{v}^j_{\cdot i} \\
&\quad + \bar{p}\ \mathrm{div}\,\hat{\mathbf{v}} + \overline{\varrho\,v''^i\,v''_j}\,\hat{v}^j_{\cdot i} - g\,\overline{\varrho\,w},
\end{aligned}\right\} \quad (17)$$

where $$\mathrm{div}\,\hat{\mathbf{v}} \equiv \frac{1}{\sqrt{\gamma}}\frac{\partial}{\partial x^\alpha}\left(\sqrt{\gamma}\,\hat{v}^\alpha\right) \equiv \frac{\partial \hat{v}}{\partial y} + \frac{\partial \hat{w}}{\partial z} - \frac{\hat{v}}{r}\,\mathrm{tg}\,\varphi + 2\,\frac{\hat{w}}{r}.$$

The mode of redistribution of kinetic energy due to the boundary work of the Stokes-Navier and Reynolds mean stresses $(\overline{P}^i_j + \overline{R}^i_j)$ may be disregarded outside the boundary layer.

The production of kinetic energy $k_{\xi m}$ of the zonal mean motion results from the meridional eddy flux $\overline{\varrho\, v''_1 v''^{\alpha}}$ of relative angular momentum $\varrho\, v_1$ and the meridional shears $\frac{\partial \hat{v}^1}{\partial x^\alpha}$ of the mean zonal wind (Kuo, 1951). The kinetic energy of the meridional mean motion is produced by:

a) the meridional eddy flux $\overline{\varrho\, v''_\alpha v''^{\beta}}$ of relative meridional mean momentum $\varrho\, v_\alpha$ and the shears of the mean wind in the meridional planes;

b) the expansion (div $\hat{\mathbf{v}} > 0$) of the air (Starr, 1948);

c) the destruction of potential energy, $(g\,\overline{\varrho\, w} < 0)$.

It should be noted that the destruction (production) of a certain amount of potential energy of the mean motion entails *ipso facto* the production (destruction) of an equal amount of kinetic energy. For instance, as a consequence of the negative correlation between the fluctuations of density and vertical velocity, the term $-g\,\overline{\varrho' w''}$ represents a rate of effective production of kinetic energy of the mean motion.

The action of the viscous and turbulent frictional stresses $\Big[$represented by $(\overline{P}^\alpha_1 + \overline{R}^\alpha_1)\,\frac{\partial \hat{v}^1}{\partial x^\alpha}$, $(\overline{P}^\beta_\alpha + \overline{R}^\beta_\alpha)\,\hat{v}^\alpha_{\cdot\beta} + \frac{1}{2}\,\gamma_{11,\alpha}\,(\overline{P}^{11} + \overline{R}^{11})\,\hat{v}^\alpha$ and $(\overline{P}^i_j + \overline{R}^i_j)\,\hat{v}^j_{\cdot i}\Big]$ consists of a dissipation. It is well known that the Rayleigh (1873) dissipation function $P^i_j v^j_{\cdot i}$ is a positive quadratic form o the wind shears and that the same is *generally* true for the dissipation function $R^i_j v^j_{\cdot i}$ for small-scale turbulence.

Finally the term $\frac{1}{2}\,\gamma_{11,\alpha}\,(2\,\omega + \hat{v}^1)\,\bar{\varrho}\,\hat{v}^1\hat{v}^\alpha$ represents the rate of conversion of kinetic energy of the zonal mean motion into kinetic energy of the meridional mean motion. This term drops out in the expression of the rate of production of the kinetic energy $k_m \equiv k_{\xi m} + k_{\mu m}$ of the mean motion.

The kinetic energies $\overline{\varrho\, k_{\xi e}}$, $\overline{\varrho\, k_{\mu e}}$ and $\overline{\varrho\, k_e}$ in a fixed unit of volume may change in consequence of:

a) meridional transport of air across the boundary: $\overline{\varrho\, k_{\xi e}}\,\hat{v}^\alpha$, $\overline{\varrho\, k_{\mu e}}\,\hat{v}^\alpha$ and $\overline{\varrho\, k_e}\,\hat{v}^\alpha$;

b) large-scale meridional eddy diffusion across the boundary: $\overline{\varrho\, k_{\xi e}\, v''^{\alpha}}$, $\overline{\varrho\, k_{\mu e}\, v''^{\alpha}}$ and $\overline{\varrho\, k_e\, v''^{\alpha}}$;

c) production within the volume at the rate:

$$
\left\{
\begin{aligned}
\sigma(\hat{k}_{\xi e}) \equiv\ & -\frac{1}{2}\,\gamma_{11\,\alpha}\left[2\,(\omega+\hat{v}^1)\,\overline{\varrho\, v''^1 v''^\alpha} + \overline{\varrho\, v''^1 v''^1 v''^\alpha}\right] - \overline{\varrho\, v''_1 v''^\alpha}\,\frac{\partial \hat{v}^1}{\partial x^\alpha} - \\
& -\frac{1}{2}\,\gamma_{11,\alpha}\,\hat{v}^\alpha\,\overline{\varrho\, v''^1 v''^1} + \overline{T^i_{1\cdot i}\, v''^1}, \\
\sigma(\hat{k}_{\mu e}) \equiv\ & \frac{1}{2}\,\gamma_{11,\alpha}\left[2\,(\omega+\hat{v}^1)\,\overline{\varrho\, v''^1 v''^\alpha} + \overline{\varrho\, v''^1 v''^1 v''^\alpha}\right] - \overline{\varrho\, v''_\beta\, v''^\alpha}\,\hat{v}^\beta_{\cdot\alpha} \\
& + \overline{T^i_{\alpha\cdot i}\, v''^\alpha}, \\
\sigma(\hat{k}_e) \equiv\ & -\overline{\varrho\, v''^i v''_j}\,\hat{v}^j_{\cdot i} \\
& + \overline{T^i_{j\cdot i}\, v''^j}.
\end{aligned}
\right. \tag{18}
$$

The terms $\overline{T^i_{1\cdot i}\,v''^1}$, $\overline{T^i_{\alpha\cdot i}\,v''^\alpha}$ and $\overline{T^i_{j\cdot i}\,v''^j}$ represent the mean values of the work, per unit volume and time, performed by the pressure forces and by the viscous and turbulent frictional forces along the large-scale eddying motion parallel to the latitude circles, in meridional planes and in the three dimensional space respectively. The energy per unit volume and time expressed by $\overline{T^i_{j\cdot i}\,v''^j}$ may be interpreted as an *instability energy* (Van Mieghem, 1949 b). According to the sign of the instability energy, the large-scale eddying motion is stable or unstable. When $\overline{T^i_{j\cdot i}\,v''^j} > 0$, the large-scale eddies do work: the large-scale eddying motion is unstable and $\overline{T^i_{j\cdot i}\,v''^j}$ represents, per unit volume and time, the instability energy released by the large-scale eddies. On the other hand, when $\overline{T^i_{j\cdot i}\,v''^j} < 0$, the large-scale eddies have work done on them at the expense of the energy of the surroundings and therefore the large-scale eddying motion is stable in that case. It should be noted that the inequality $\sigma(\hat{k}_e) > 0$ expresses a necessary condition for the maintenance of the large-scale eddying motion (generalization of the Richardson criterion).

Finally, the term $\frac{1}{2}\,\gamma_{11,\alpha}\left[2\,(\omega+\hat{v}^1)\,\overline{\varrho\,v''^1 v''^\alpha}+\overline{\varrho\,v''^1 v''^1 v''^\alpha}\right]$ represents the rate of conversion of kinetic energy $k_{\xi e}$ of the zonal eddying motion into kinetic energy $k_{\mu e}$ of the meridional eddying motion. This term drops out in the expression of the rate of production of the eddy kinetic energy $k_e \equiv k_{\xi e} + k_{\mu e}$.

4. Conversions involving mechanical energies only

In the formulas (17) and (18) of the rates of production, certain terms appear twice with opposite signs. As already mentioned in the introduction such a term may be considered as a rate of energy conversion. In spherical coordinates, these terms assume the form:

$$\Gamma_m \equiv -\frac{1}{2}\,\gamma_{11,\alpha}\,(2\omega+\hat{v}^1)\,\hat{v}^1\,\overline{\varrho\,v^\alpha} = \left(2\omega\sin\varphi+\frac{\hat{u}}{r}\,\mathrm{tg}\,\varphi\right)\hat{u}\,\overline{\varrho\,v}-\left(2\omega\cos\varphi+\frac{\hat{u}}{r}\right)\hat{u}\,\overline{\varrho\,w}$$

$$\Gamma_e \equiv -\frac{1}{2}\,\gamma_{11,\alpha}\left[2\,(\omega+\hat{v}^1)\,\overline{\varrho\,v''^1 v''^\alpha}+\overline{\varrho\,v''^1 v''^1 v''^\alpha}\right] =$$

$$= 2\left(\omega+\frac{\hat{u}}{r\cos\varphi}\right)\left(\overline{\varrho\,u''v''}\sin\varphi-\overline{\varrho\,u''w''}\cos\varphi\right)+\frac{1}{r\cos\varphi}\left(\overline{\varrho\,u''u''v''}\sin\varphi-\overline{\varrho\,u''u''w''}\cos\varphi\right),$$

$$\chi_\mu \equiv \overline{\varrho\,v''^\beta v''_\alpha}\,\hat{v}^\alpha_{\cdot\beta} = \overline{\varrho\,v''v''}\left(\frac{\partial\hat{v}}{\partial y}+\frac{\hat{w}}{r}\right)+\overline{\varrho\,w''w''}\,\frac{\partial\hat{w}}{\partial z}+\overline{\varrho\,v''w''}\left(\frac{\partial\hat{v}}{\partial z}+\frac{\partial\hat{w}}{\partial y}-\frac{\hat{v}}{r}\right),$$

$$\chi_\xi \equiv \overline{\varrho\,v''_1 v''^\alpha}\,\frac{\partial\hat{v}^1}{\partial x^\alpha} = \overline{\varrho\,u''v''}\left(\frac{\partial\hat{u}}{\partial y}+\frac{\hat{u}}{r}\,\mathrm{tg}\,\varphi\right)+\overline{\varrho\,u''w''}\left(\frac{\partial\hat{u}}{\partial z}-\frac{\hat{u}}{r}\right),$$

$$\chi_{\mu\xi} \equiv \frac{1}{2}\,\gamma_{11,\alpha}\,\hat{v}^\alpha\,\overline{\varrho\,v''^1 v''^1} = \overline{\varrho\,u''u''}\left(-\frac{\hat{v}}{r}\,\mathrm{tg}\,\varphi+\frac{\hat{w}}{r}\right).$$

Hence,

$$\left\{\begin{array}{l} \sigma(\varnothing) \equiv \quad g\,\bar{\varrho}\,\overline{w}+g\,\overline{\varrho'w''}\,, \\ \qquad\qquad\quad \updownarrow \qquad \downarrow \\ \sigma(k_m) \equiv -g\,\bar{\varrho}\,\overline{w}-g\,\overline{\varrho'w''}+\chi_{\mu\xi}+\chi_\xi+\chi_\mu+\ldots, \\ \qquad\qquad\qquad\quad\ \updownarrow \quad \updownarrow\uparrow \quad \updownarrow \\ \sigma(\hat{k}_e) \equiv \qquad\qquad -\chi_{\mu\xi}-\chi_\xi-\chi_\mu+\ldots, \end{array}\right. \tag{19}$$

and

$$\left\{\begin{array}{lllll} \sigma(k_{\xi m}) \equiv & \Gamma_m & +\chi_\xi & & +\dots, \\ \sigma(k_{\mu m}) \equiv & -\Gamma_m + \chi_{\mu\xi} & & +\chi_\mu - g\overline{\varrho w} & +\dots, \\ \sigma(\hat{k}_{\xi e}) \equiv & \Gamma_e - \chi_{\mu\xi} & -\chi_\xi & & +\dots, \\ \sigma(\hat{k}_{\mu e}) \equiv & -\Gamma_e & & -\chi_\mu & +\dots, \end{array}\right. \tag{20}$$

where the dots indicate terms which, as we shall see in section 6, correspond to conversions between kinetic energy and internal energy as well as kinetic energy of microturbulence.

The arrows in (19) and (20) indicate all the possible conversions between the mechanical energies. As a rule, in low and middle latitudes: $\overline{\varrho u'' v''} > 0$ and $\overline{\varrho u'' w''} < 0$. Consequently $\Gamma_e > 0$, so that Γ_e expresses always a conversion of $k_{\mu e}$-energy into $k_{\xi e}$-energy, the terms $\overline{\varrho u'' u'' v''}$ and $\overline{\varrho u'' u'' w''}$ being presumably of less importance. Kuo (1951) has shown that the two terms of χ_ξ have opposite signs, the first being positive and of the right order of magnitude to account for the frictional dissipation of kinetic energy at the earth's surface. The rate of conversion $\chi_{\mu\xi}$ between the $\hat{k}_{\xi e}$ and the $\hat{k}_{\mu m}$-energy is very small because it depends only on the normal and geodesic curvatures of the parallel circles and may therefore be neglected ($\chi_{\mu\xi} \cong 0$). Finally, there is no conversion possible between the $k_{\xi m}$ and the $k_{\mu e}$ energy.

5. Influence of the inertial stability on the conversion of "meridional" eddy-kinetic energy into "zonal" eddy-kinetic energy

Averaging the equation (8) along the latitude circles and subtracting from this averaged equation the corresponding equation for the mean motion, one finds, after some calculations,

$$\frac{\partial}{\partial t}\left(\overline{\varrho v_1'' v_\delta''}\right) = -\left(\omega\gamma_{11,\beta} + \frac{\partial \hat{v}_1}{\partial x^\beta}\right)\overline{\varrho v_\delta'' v''^\beta} + \dots\dots\dots, \tag{21}$$

$$(\beta, \delta = 2, 3)$$

where the dots designate terms which do not contain the Jeffreys stresses $-\overline{\varrho v_\delta'' v''^\beta}$.

The local change $\frac{\partial \Gamma_e}{\partial t}$ of the rate of conversion $\Gamma_e\,(>0)$ of "meridional" kinetic energy into "zonal" kinetic energy of the large-scale eddying motion has the following expression:

$$\frac{\partial \Gamma_e}{\partial t} = -\gamma_{11,\alpha}(\omega + \hat{v}^1)\frac{\partial}{\partial t}\left(\overline{\varrho v''^1 v''^\alpha}\right) + \dots\dots\dots \tag{22}$$

Multiplication of (21) by $\gamma^{11}\gamma^{\alpha\delta}$ and subsequent substitution in (22), give

$$\frac{\partial \Gamma_e}{\partial t} = \gamma_{11,\alpha}\gamma^{11}\left(\omega\gamma_{11,\beta} + \frac{\partial \hat{v}_1}{\partial x^\beta}\right)(\omega + \hat{v}^1)\overline{\varrho v''^\alpha v''^\beta} + \dots\dots\dots, \tag{23}$$

or, in spherical coordinates,

$$\frac{\partial \Gamma_e}{\partial t} = 2\left\{\left(\omega \sin\varphi + \frac{\hat{u}}{r}\operatorname{tg}\varphi\right)\left(2\omega\sin\varphi - \frac{\partial \hat{u}}{\partial y} + \frac{\hat{u}}{r}\operatorname{tg}\varphi\right)\overline{\varrho v'' v''} - \right.$$

$$- \left[\left(\omega\sin\varphi + \frac{\hat{u}}{r}\operatorname{tg}\varphi\right)\left(2\omega\cos\varphi + \frac{\partial \hat{u}}{\partial z} + \frac{\hat{u}}{r}\right) + \left(\omega\cos\varphi + \frac{\hat{u}}{r}\right)\left(2\omega\sin\varphi - \right.\right. \quad (23\,a)$$

$$\left.\left. - \frac{\partial \hat{u}}{\partial y} + \frac{\hat{u}}{r}\operatorname{tg}\varphi\right)\right]\overline{\varrho v'' w''} + \left(\omega\cos\varphi + \frac{\hat{u}}{r}\right)\left(2\omega\cos\varphi + \frac{\partial \hat{u}}{\partial z} + \frac{\hat{u}}{r}\right)\overline{\varrho w'' w''}\left.\right\} + \ldots,$$

or, in vector form,

$$\frac{\partial \Gamma_e}{\partial t} = 2\,\overline{\varrho\,(\mathbf{v}'' \times \Omega)_x \cdot (\mathbf{v}'' \times \operatorname{curl}\mathbf{U})_x} + \ldots, \quad (23\,b)$$

where Ω represents the absolute angular speed about the earth's axis and $\mathbf{U}$ the absolute linear velocity along the latitude circles.

In the atmosphere, $(\mathbf{v}'' \times \Omega)_x$ and $(\mathbf{v}'' \times \operatorname{curl}\mathbf{U})_x$ have the sign of $\left(\omega\sin\varphi + \frac{\hat{u}}{r}\operatorname{tg}\varphi\right)v''$ and $\left(2\omega\sin\varphi - \frac{\partial \hat{u}}{\partial y} + \frac{\hat{u}}{r}\operatorname{tg}\varphi\right)v''$ respectively.

When the large-scale eddying motion is inertially stable, $\frac{\partial \hat{u}}{\partial y} < 2\omega\sin\varphi + \frac{\hat{u}}{r}\operatorname{tg}\varphi$, or $(\mathbf{v}'' \times \Omega)_x \cdot (\mathbf{v}'' \times \operatorname{curl}\mathbf{U})_x > 0$, (Van Mieghem, 1951); consequently the inertial stability contributes to the local increase with time of the rate of conversion Γ_e. On the other hand, the inertial instability contributes to the local decrease with time of the rate of conversion Γ_e of "meridional" into "zonal" eddy kinetic energy.

6. The first law

The first law of thermodynamics expresses the conservation of the *total energy* of the system envisaged. In the case considered here, the total energy u, per unit of mass, is equal to the sum of the potential energy $\emptyset$, the kinetic energy k, the kinetic energy $\varkappa$ of microturbulence and the internal energy e per unit of mass ($u \equiv \emptyset + k + \varkappa + e$).

The equation of balance of the kinetic energy $\varkappa$ of microturbulence assumes the form (Van Mieghem, 1949 b):

$$\frac{\partial}{\partial t}(\varrho\varkappa) + \frac{1}{\sqrt{\gamma}}\frac{\partial}{\partial x^i}\left[\sqrt{\gamma}\,(\varrho\varkappa \mathrm{v}^i + K^i)\right] = \varrho\triangle + R^i_j\,\mathrm{v}^j_{.i} > 0, \quad (24)$$

$$(i, j = 1, 2, 3)$$

where K^i designates the flux due to small-scale turbulent diffusion, $\triangle$ the instability energy released per unit mass and time along the small-scale eddying motion, and $R^i_j\,\mathrm{v}^j_{.i}$ the amount of kinetic energy available per unit of volume for conversion into kinetic energy of small-scale turbulence. It is *generally* accepted that $R^i_j\,\mathrm{v}^j_{.i} > 0$. When the small-scale eddying motion is stable, $\triangle < 0$ and $\triangle$ represents the amount of kinetic energy of small-scale turbulence converted per unit mass into heat; when $\triangle > 0$, the small-scale eddying motion is unstable and $\triangle$ represents the amount of heat converted per unit mass and time into kinetic energy of small scale turbulence. The Richardson number h^2 of the small-scale turbulence may be defined as $h^2 \equiv \varrho\,|\triangle| : (R^i_j\,\mathrm{v}^j_{.i})$ (Van Mieghem 1949 b, 1950 a). The inequality in (24) expresses the necessary condition for the maintenance of small-scale turbulence ($h^2 < 1$).

In virtue of (6), (7) and (24), the flux $C^i(u)$ of the total energy u is given by

$$C^i(u) \equiv \varrho u v^i - T^i_j v^j + K^i + W^i,$$

where W^i represents the flux of heat due to radiation, conduction and convection (the effect of conduction is negligible in the atmosphere), hence the balance

$$\frac{\partial(\varrho u)}{\partial t} + \frac{1}{\sqrt{\gamma}} \frac{\partial(\sqrt{\gamma}\, C^i(u))}{\partial x^i} = 0, \tag{25}$$

the rate of production of the total energy being equal to zero as a result of the conservation of the total energy, ($\sigma(u) = 0$, VAN MIEGHEM, 1949).

Averaging equation (25) along latitude circles and subtracting the equations (15), (16) and the averaged equations (7) and (24), one obtains the equation of balance of the averaged internal energy

$$\frac{\partial \overline{\varrho e}}{\partial t} + \frac{1}{\sqrt{\gamma}} \frac{\partial}{\partial x^\alpha} \left[\sqrt{\gamma}\left(\overline{\varrho e}\,\hat{v}^\alpha + \overline{\varrho h v''^\alpha} - \overline{P^\alpha_i v''^i} + \overline{W^\alpha}\right)\right] = \tag{26}$$

$$= -\overline{\varrho \triangle} - \bar{p}\ \mathrm{div}\,\hat{\mathbf{v}} + \bar{P}^i_j \hat{v}^j_{.i} - \overline{\left(-\frac{\partial p}{\partial x^i} v''^i + P^i_{j.i} v''^j\right)},$$

where h designates the specific enthalpy ($\varrho h \equiv \varrho e + p$).

It should be noted that the averaged equation of balance (24) may be written

$$\frac{\partial(\overline{\varrho \varkappa})}{\partial t} + \frac{1}{\sqrt{\gamma}} \frac{\partial}{\partial x^\alpha}\left[\sqrt{\gamma}\left(\overline{\varrho \varkappa}\,\hat{v}^\alpha + \overline{\varrho \varkappa v''^\alpha} + \overline{K^\alpha} - \overline{R^\alpha_j v''^j}\right)\right] = \overline{\varrho \triangle} + \bar{R}^i_j \hat{v}^j_{.i} - \overline{R^i_{j.i} v''^j}. \tag{27}$$

The zonally averaged internal energy $\overline{\varrho e} = \bar{\varrho}\,\hat{e}$ in a fixed unit of volume changes in consequence of:

a) transport of air across the boundary: $\bar{\varrho}\,\hat{e}\hat{v}^\alpha$;

b) large-scale eddy-diffusion of heat: $W^\alpha_{(e)} \equiv \overline{\varrho h v''^\alpha} - \overline{P^\alpha_i v''^i}$;

c) heat flux $\overline{W^\alpha}$ (radiation + convection);

d) production within the volume at the rate:

$$\sigma(\hat{e}) \equiv -\bar{p}\ \mathrm{div}\,\hat{\mathbf{v}} + \bar{P}^i_j \hat{v}^j_{.i} - \overline{\left(-\frac{\partial p}{\partial x_i} + P^j_{i.j}\right) v''^i} - \overline{\varrho \triangle}. \tag{28}$$

Finally, grouping in one table the rates of energy production $\sigma(\Phi)$, $\sigma(k_m)$, $\sigma(\hat{k}_e)$, $\sigma(\hat{\varkappa})$ and $\sigma(\hat{e})$, the possible conversions between the five considered energy forms appear immediately:

$$\left.\begin{array}{lllll}
\sigma(\Phi) \equiv & g\overline{\varrho w}, & & & \\
\sigma(k_m) \equiv & -g\overline{\varrho w} + \bar{p}\ \mathrm{div}\,\hat{\mathbf{v}} - \bar{P}^i_j \hat{v}^j_{.i} - \bar{R}^i_j \hat{v}^j_{.i} + \overline{\varrho v''_j v''^i}\,\hat{v}^j_{.i}, & & & \\
\sigma(\hat{k}_e) \equiv & & -\overline{\varrho v''_j v''^i}\,\hat{v}^j_{.i} + \overline{\left(-\frac{\partial p}{\partial x_i} + P^j_{i.j}\right) v''^i} & + \overline{R^i_{j.i} v''^j}, & \\
\sigma(\hat{\varkappa}) \equiv & & \bar{R}^i_j \hat{v}^j_{.i} + \overline{\varrho \triangle} & & - \overline{R^i_{j.i} v''^j}, \\
\sigma(\hat{e}) \equiv & -\bar{p}\ \mathrm{div}\,\hat{\mathbf{v}} + \bar{P}^i_j \hat{v}^j_{.i} & - \overline{\varrho \triangle} & - \overline{\left(-\frac{\partial p}{\partial x^i} + P^j_{i.j}\right) v''^i} &
\end{array}\right\} \tag{29}$$

$(i, j = 1, 2, 3)$

The corresponding energy fluxes in the meridional planes assume the form:

$$\left.\begin{aligned}
C^{\alpha}(\varnothing) &\equiv \varnothing\,\overline{\varrho\,v}^{\alpha},\\
C^{\alpha}(k_m) &\equiv (k_m + R\hat{T})\,\overline{\varrho\,v}^{\alpha} - \left(\overline{P}_i^{\alpha} + \overline{R}_i^{\alpha} - \overline{\varrho\,v_i''\,v''^{\alpha}}\right)\hat{v}^i,\\
C^{\alpha}(\hat{k}_e) &\equiv \hat{k}_e\,\overline{\varrho\,v}^{\alpha} + \overline{\varrho\,k_e\,v''^{\alpha}},\\
C^{\alpha}(\hat{\varkappa}) &\equiv \hat{\varkappa}\,\overline{\varrho\,v}^{\alpha} + \overline{\varrho\,\varkappa\,v''^{\alpha}} - \overline{R}_i^{\alpha}\,\overline{v}^{i} + \overline{K}^{\alpha},\\
C^{\alpha}(\hat{e}) &\equiv \hat{e}\,\overline{\varrho\,v}^{\alpha} + \overline{\varrho\,h\,v''^{\alpha}} - \overline{P}_i^{\alpha}\,\overline{v}^{i} + \overline{W}^{\alpha},
\end{aligned}\right\} \quad (30)$$

$$(i = 1, 2, 3;\ \alpha = 2, 3)$$

where $R\hat{T} = \bar{p} : \bar{\varrho}$, R being the specific ideal gas constant for air and T the absolute temperature.

7. Large-scale eddy-diffusion of heat

In section 6, we have established that the large-scale eddy-diffusion is responsible for the heat flux

$$W_{(e)}^{\alpha} \equiv \overline{\varrho\,h\,v''^{\alpha}} - \overline{P}_i^{\alpha}\,\overline{v''^{i}} \quad (31)$$

$$(\alpha = 2, 3;\ i = 1, 2, 3)$$

in the meridional planes. The last term in (31) due to the viscosity may be neglected, consequently

$$W_{(e)}^{\alpha} \cong \overline{\varrho\,h\,v''^{\alpha}} = \overline{\varrho\,h''\,v''^{\alpha}}, \quad (31\,a)$$

where (Van Mieghem and Dufour 1948)

$$h = \tau_a\,h_a + \tau_v\,h_v + \tau_w\,h_w, \quad (32)$$

h_a, h_v, h_w, being the specific enthalpies of dry air, water vapour and liquid water respectively and τ_a, τ_v, τ_w the corresponding mass-proportions. It is easily seen that

$$\tau_v = \varepsilon_v\,\frac{1 - \varepsilon}{1 - \varepsilon_v}, \quad (33)$$

where $\varepsilon_v \equiv \dfrac{\tau_v}{\tau_a + \tau_v}$ is the specific humidity and $\varepsilon \equiv \tau_v + \tau_w \equiv 1 - \tau_a$. Finally substituting (33) and the classical formula $L_v = h_v - h_w$ for the heat of vaporization of water into (32), one obtains for the fluctuation h'' of h the following expression:

$$h'' \equiv (1 - \varepsilon)\,h_a'' + \varepsilon\,h_w'' + (1 - \varepsilon)\left(\frac{\varepsilon_v L_v}{1 - \varepsilon_v}\right)'', \quad (34)$$

account being taken of the fact that the fluctuation ε'' of ε is practically equal to zero ($\varepsilon'' \cong 0$).

In the atmosphere, one may, with a very good approximation, neglect ε and ε_v with respect to 1 and assume the constancy of the specific heats c_{pa}, c_{pv} and c_w; hence, the approximate relation

$$h'' \cong c_p\,T'' + (\varepsilon_v L_v)'', \quad (34\,a)$$

where T'' designates the fluctuation of the absolute temperature T with respect to its weighted zonal mean value $\hat{T} = \overline{\varrho T} : \bar{\varrho}$, and where $c_p = c_{pa} + \varepsilon\,c_w \cong c_{pa}$. Moreover for

the fluctuations ε_v'' and L_v'' of ε_v and L_v with respect to the weighted zonal mean values $\hat{\varepsilon}_v$ and $\hat{L}_v$, it is easy to verify the inequality[2] $(L_v'' : \hat{L}_v) \ll \varepsilon_v'' : \hat{\varepsilon}_v$, so that one obtains the approximate formula (PRIESTLEY 1948)

$$h'' \cong c_p T'' + L_v \varepsilon_v'' \tag{34 b}$$

in which L_v is considered as being a constant.

Finally, substitution of (34 b) in (31 a) gives the expression of the heat flux due to the correlation between the fluctuations h'' and v''^{α} of the enthalpy h and the meridional components (v^2, v^3) of the air velocity $\mathbf{v}$, namely

$$W^{\alpha}_{(e)} \cong \overline{\varrho h'' v''^{\alpha}} \cong c_p \overline{\varrho T'' v''^{\alpha}} + L_v \overline{\varrho \varepsilon_v'' v''^{\alpha}}, \qquad (\alpha = 2, 3) \tag{31 b}$$

where, according to PRIESTLEY (1948), the first term represents the flux of "sensible" heat and the second, the flux of "latent" heat.

8. Application to the large disturbances

Neglecting viscosity and small-scale turbulence, the expressions (29) and (30) for the rates of energy production and for the energy fluxes assume simplified forms. Thus for the rates:

$$\left\{\begin{aligned} \sigma(\varnothing) &\equiv g \overline{\varrho w} \\ \sigma(k_m) &\equiv -g \overline{\varrho w} + \chi + \bar{p} \operatorname{div} \hat{\mathbf{v}}, \\ \sigma(\hat{k}_e) &\equiv -\chi - \overline{\nabla p \cdot \mathbf{v}''}, \\ \sigma(\hat{e}) &\equiv -\bar{p} \operatorname{div} \hat{\mathbf{v}} + \overline{\nabla p \cdot \mathbf{v}''}, \end{aligned}\right. \tag{35}$$

where

$$\chi \equiv \overline{\varrho u'' u''} \left(-\frac{\hat{v}}{r} \operatorname{tg} \varphi + \frac{\hat{w}}{r}\right) + \overline{\varrho v'' v''} \left(\frac{\partial \hat{v}}{\partial y} + \frac{\hat{w}}{r}\right) + \overline{\varrho w'' w''} \frac{\partial \hat{w}}{\partial z} +$$

$$+ \overline{\varrho v'' w''} \left(\frac{\partial \hat{v}}{\partial z} + \frac{\partial \hat{w}}{\partial y} - \frac{\hat{w}}{r}\right) + \overline{\varrho u'' w''} \left(\frac{\partial \hat{u}}{\partial z} - \frac{\hat{u}}{r}\right) + \overline{\varrho u'' v''} \left(\frac{\partial \hat{u}}{\partial y} + \frac{\hat{u}}{r} \operatorname{tg} \varphi\right) \cong$$

$$\cong \overline{\varrho u'' v''} \left(\frac{\partial \hat{u}}{\partial y} + \frac{\hat{u}}{r} \operatorname{tg} \varphi\right) + \overline{\varrho u'' w''} \frac{\partial \hat{u}}{\partial z}, \tag{36}$$

and for the fluxes:

$$\left\{\begin{aligned} C^{\alpha}(\varnothing) &\equiv \varnothing \overline{\varrho v^{\alpha}}, \\ C^{\alpha}(k_m) &\equiv (k_m + R\hat{T}) \overline{\varrho v^{\alpha}} + \overline{\varrho v_i'' v''^{\alpha}} \hat{v}^i, \\ C^{\alpha}(\hat{k}_e) &\equiv \hat{k}_e \overline{\varrho v^{\alpha}} + \overline{\varrho k_e v''^{\alpha}}, \\ C^{\alpha}(\hat{e}) &\equiv \hat{e} \overline{\varrho v^{\alpha}} + \overline{\varrho h v''^{\alpha}} + \overline{W}^{\alpha}. \end{aligned}\right.$$

[2] This inequality is not necessarily satisfied in the case of small-scale turbulence.

Hence, for each of the above mentioned energy forms, the equation of balance for an axially symmetric volume may be written:

$$\frac{\partial}{\partial t}\iint_{(\alpha)} r\cos\varphi\,\bar{\varrho}\bar{f}\,\delta\alpha = -\oint_{(s)} r\cos\varphi\,C_N(f)\,\delta s + \iint_{(\alpha)} r\cos\varphi\,\sigma(f)\,\delta\alpha, \tag{37}$$

where α is the meridional section of the volume envisaged and s the closed curve limiting the area α, and N the external normal to s.

Applying the balance (37) to the kinetic energy of the zonally averaged motion, the friction at the earth's surface should not be overlooked when a portion of s coincides with the mean meridional profile of the earth's surface.

It should be noted that 1) $k_m \cong \frac{1}{2}(\hat{u})^2$ and 2) k_m may be neglected with respect to $R\hat{T}$ (STARR 1949).

For the very large atmospheric disturbances, the following assumptions are justified:

a) hydrostatic equilibrium along the vertical z: $\frac{\partial\bar{p}}{\partial z} + g\bar{\varrho} \cong 0$;

b) $\operatorname{div}\hat{\mathbf{v}} \cong -\frac{\hat{w}}{\bar{\varrho}}\frac{\partial\bar{\varrho}}{\partial z}$, (CHARNEY 1948, VAN MIEGHEM 1950 b);

c) quasi-homogeneity: $\left(\varrho'\frac{\hat{d}\hat{\mathrm{v}}_\delta}{dt} - \frac{1}{2}\gamma_{\alpha\beta,\delta}\varrho'\hat{\mathrm{v}}^\alpha\hat{\mathrm{v}}^\beta - \frac{1}{2}\gamma_{11,\delta}(2\omega+\hat{\mathrm{v}}^1)\varrho'\hat{\mathrm{v}}^1\right)$, (38)

where $\frac{\hat{d}}{dt} \equiv \frac{\partial}{\partial t} + \hat{\mathrm{v}}^\alpha\frac{\partial}{\partial x^\alpha}$, may be neglected, $(\alpha, \beta, \delta = 2, 3)$;

d) the terms $\varrho'\cdot\overline{[\varrho\,\mathrm{v}''^i\mathrm{v}''_\delta]}_{\cdot i}$ and $\overline{\mathrm{v}''^i\frac{\partial p'}{\partial x^i}}$ may be deleted.

As a consequence of the assumptions (38) *a* and *b* and of the identity $\frac{1}{\hat{\Theta}}\frac{\partial\hat{\Theta}}{\partial z} \equiv \frac{c_v}{c_p}\frac{1}{\bar{p}}\frac{\partial\bar{p}}{\partial z} - \frac{1}{\bar{\varrho}}\frac{\partial\bar{\varrho}}{\partial z}$, where $\hat{\Theta}$ is the weighted zonally averaged value of the potential temperature $\hat{\Theta}$, one obtains

$$\bar{p}\,\operatorname{div}\hat{\mathbf{v}} \cong \left[\frac{\bar{p}}{\bar{\varrho}}\frac{1}{\hat{\Theta}}\frac{\partial\hat{\Theta}}{\partial z} + \frac{c_v}{c_p}g\right]\overline{\varrho w} \cong \frac{c_v}{c_p}g\,\overline{\varrho w}, \tag{39}$$

the first of the terms in brackets being one order of magnitude less than the other. On the other hand substitution of the equations of the zonally averaged meridional motion, namely

$$\bar{\varrho}\frac{\hat{d}\hat{\mathrm{v}}_\delta}{dt} - \frac{1}{2}\gamma_{\alpha\beta,\delta}\bar{\varrho}\hat{\mathrm{v}}^\alpha\hat{\mathrm{v}}^\beta - \frac{1}{2}\gamma_{11,\delta}(2\omega+\hat{\mathrm{v}}^1)\overline{\varrho\mathrm{v}}^1 = -\frac{\partial\bar{p}}{\partial x^\delta} - \overline{(\varrho\,\mathrm{v}''^i\mathrm{v}''_\delta)}_{\cdot i} - \bar{\varrho}\frac{\partial\Phi}{\partial x^\delta}$$

in

$$-\overline{\mathrm{v}''^i\frac{\partial p}{\partial x^i}} = -\overline{\mathrm{v}''^i\frac{\partial p'}{\partial x^i}} - \overline{\mathrm{v}''^\delta}\frac{\partial\bar{p}}{\partial x^\delta},$$

leads to

$$-\overline{\mathbf{v}''\bigtriangledown p} \equiv -\overline{\mathrm{v}''^i\frac{\partial p}{\partial x^i}} \cong -g\,\overline{\varrho' w'} \equiv -g\,\overline{\varrho' w''}, \tag{40}$$

in virtue of (38) *c* and *d* and of $-\bar{\varrho}\,\overline{\mathrm{v}''^\alpha} = \overline{\varrho'\,\mathrm{v}'^\alpha} = \overline{\varrho'\,\mathrm{v}''^\alpha}$.

After substitution of (36), (39) and (40) in (35), one obtains the approximate expressions of the rates of energy production, namely:

$$\left\{\begin{array}{lll} \sigma(\varnothing) \equiv & g\overline{\varrho' w''} & + g\bar{\varrho}\,\bar{w} \\ \sigma(k_m) \cong & \overline{\varrho u'' v''}\left(\dfrac{\partial \hat{u}}{\partial y} + \dfrac{\hat{u}}{r}\operatorname{tg}\varphi\right) - \dfrac{c_p - c_v}{c_p} g\overline{\varrho' w''} & + \overline{\varrho u'' w''}\dfrac{\partial \hat{u}}{\partial z} - \dfrac{c_p - c_v}{c_p} g\bar{\varrho}\,\bar{w} \\ \sigma(\hat{k}_e) \cong & -g\overline{\varrho' w''} - \overline{\varrho u'' v''}\left(\dfrac{\partial \hat{u}}{\partial y} + \dfrac{\hat{u}}{r}\operatorname{tg}\varphi\right) & - \overline{\varrho u'' w''}\dfrac{\partial \hat{u}}{\partial z} \\ \sigma(\hat{e}) \cong & + \dfrac{c_p - c_v}{c_p} g\overline{\varrho' w''} & - \dfrac{c_v}{c_p} g\bar{\varrho}\,\bar{w} \end{array}\right. \qquad (41)$$

where, as a rule, $\overline{\varrho' w'} = \overline{\varrho' w''} < 0$.

As already pointed out in section 4, the rate of conversion $\overline{\varrho u'' v''}\left(\dfrac{\partial \hat{u}}{\partial y} + \dfrac{\hat{u}}{r}\operatorname{tg}\varphi\right)$ of k_e into $k_m \cong \frac{1}{2}(\bar{u})^2$ is more important than the rate of conversion $\overline{\varrho u'' w''}\dfrac{\partial \hat{u}}{\partial z}$ of k_m into k_e, the difference being presumably of about one order of magnitude.

As a result of the negative correlation between the fluctuations of specific mass ϱ and vertical velocity w, internal energy e is converted into kinetic energy k_m of the zonally averaged motion and simultaneously, at a rate at least three times $\left(\dfrac{c_p - c_v}{c_p} \cong 0.3\right)$ higher than the rate of conversion of e into k_m, potential energy $\varnothing$ is converted into kinetic energy k_e of the large-scale disturbances. FJØRTOFT (1951) has recently stressed the importance of the conversion of potential energy into kinetic energy for the maintenance of the disturbances.

In the ascending branch ($\bar{w} > 0$) of the mean meridional circulation ($\bar{v}$, $\bar{w}$), internal energy is transformed into kinetic energy of the mean motion, and kinetic energy of the mean motion into potential energy. In the descending branch ($\bar{w} < 0$), however, the reversed conversions take place. As a consequence of these energy conversions "potential + internal" energy is transformed into kinetic energy of the mean motion, or vice versa, depending upon the sign of w. For these energy conversions, we may write

$$\sigma(k_m) \equiv -\sigma(\varnothing + \hat{e}) \cong -g\,\frac{c_p - c_v}{c_p}\,\bar{\varrho}\,\bar{w} > 0$$

when $\bar{w} < 0$, and $\sigma(k_m) < 0$ when $\bar{w} > 0$.

For the energy conversions due to the large-scale eddy motion only, we have

$$\sigma(\hat{k}) \equiv \sigma(k_m + \hat{k}_e) = -\sigma(\varnothing + \hat{e}) > 0.$$

This inequality indicates a permanent conversion of "potential + internal" energy into kinetic energy of the air flow. The necessary brake in the steady increase of kinetic energy in the atmosphere is provided by the friction at the earth's surface.

Combining the results (20) and (41), we finally obtain:

$$\sigma(\varnothing) \cong \qquad g\,\overline{\varrho' w''},$$

$$\sigma(k_m) \equiv \begin{cases} \sigma(k_{\xi m}) \cong \left(\dfrac{\partial \hat{u}}{\partial y} + \dfrac{\hat{u}}{r}\operatorname{tg}\varphi\right)\overline{\varrho u'' v''} + \left(\dfrac{\partial \hat{u}}{\partial z} - \dfrac{\hat{u}}{r}\right)\overline{\varrho u'' w''} + \left(2\omega + \dfrac{\hat{u}}{r\cos\varphi}\right)\left(\overline{\varrho' v''}\sin\varphi - \overline{\varrho' w''}\cos\varphi\right)\hat{u}, \\ + \\ \sigma(k_{\mu m}) \cong -\dfrac{c_p - c_v}{c_p}\, g\,\overline{\varrho' w''} \qquad\qquad -\left(2\omega + \dfrac{\hat{u}}{r\cos\varphi}\right)\left(\overline{\varrho' v''}\sin\varphi - \overline{\varrho' w''}\cos\varphi\right)\hat{u}, \end{cases}$$

$$\sigma(\hat{k}_e) \equiv \begin{cases} \sigma(\hat{k}_{\xi e}) \cong \left(2\omega\sin\varphi - \dfrac{\partial \hat{u}}{\partial y} + \dfrac{\hat{u}}{r}\operatorname{tg}\varphi\right)\overline{\varrho u'' v''} - \left(2\omega\cos\varphi + \dfrac{\partial \hat{u}}{\partial z} + \dfrac{\hat{u}}{r}\right)\overline{\varrho u'' w''}, \\ + \\ \sigma(\hat{k}_{\mu e}) \cong -g\,\overline{\varrho' w''} - 2\left(\omega + \dfrac{\hat{u}}{r\cos\varphi}\right)\left(\overline{\varrho u'' v''}\sin\varphi - \overline{\varrho u'' w''}\cos\varphi\right), \end{cases} \tag{42}$$

$$\sigma(\hat{e}) \cong \qquad \frac{c_p - c_v}{c_p}\, g\,\overline{\varrho' w''},$$

where the terms due to the mean meridional circulation $(\bar{v}, \bar{w})$ have been omitted consistently.

From (41) and (42), it seems reasonable to conclude that the two most important energy transformations on the scale of the general circulation are:

a) for the maintenance of the large disturbances, the conversion of potential energy into kinetic energy of the large-scale eddies, as a result of the negative correlation between density and vertical velocity fluctuations (or positive correlation between temperature and vertical velocity fluctuations);

b) for the maintenance of the zonally averaged motion ($\cong$ mean zonal motion), the conversion of kinetic energy of the large-scale disturbances into kinetic energy of the mean motion $\left(k_m \cong \frac{1}{2}(\hat{u})^2\right)$, due to the lateral Jeffreys-stress $-\overline{\varrho u'' v''}$ and the meridional shear of the mean zonal wind $\hat{u}$.

9. The second law

Let us assume that the zonally averaged physical state of the atmosphere has a mean specific entropy s_m which is a function of the mean internal energy $\hat{e}$ and of the mean specific mass $\bar{\varrho}$ $[s_m \equiv s_m(\hat{e}, \bar{\varrho})]$, satisfying the Gibbsian equation

$$\hat{T}\frac{\hat{d}s_m}{dt} = \frac{\hat{d}\hat{e}}{dt} - \frac{\bar{p}}{(\bar{\varrho})^2}\frac{\hat{d}\bar{\varrho}}{dt},$$

where $\dfrac{\hat{d}}{dt} \equiv \dfrac{\partial}{\partial t} + \hat{v}^\alpha \dfrac{\partial}{\partial x^\alpha}$, $(\alpha = 2, 3)$. It should be noted that the functions $\bar{p}$, $\bar{\varrho}$, $\hat{e}$, $\hat{T}$ and s_m are independent of longitude λ. Upon substituting (26) and (10) into (43), we find the equation of balance

$$\frac{\partial \bar{\varrho} s_m}{\partial t} + \frac{1}{\sqrt{\gamma}}\frac{\partial}{\partial x^\alpha}\left[\sqrt{\gamma}\left(\bar{\varrho} s_m \hat{v}^\alpha + \frac{\overline{W}^\alpha + W^\alpha_{(e)}}{\hat{T}}\right)\right] = \tag{44}$$

$$= -\frac{\overline{W}^\alpha + W^\alpha_{(e)}}{(\hat{T})^2}\frac{\partial \hat{T}}{\partial x^\alpha} + \frac{\overline{P^i_j}\hat{v}^j{}_{\cdot i} - \overline{\varrho \triangle}}{\hat{T}} - \frac{1}{\hat{T}}\overline{\left(-\frac{\partial p}{\partial x^i} + P^j_{i\cdot j}\right)v''^i},$$

$$(\alpha = 2, 3;\ i, j = 1, 2, 3)$$

where the second member represents the rate of production $\sigma(s_m)$ of entropy. The second law states that the entropy production is real, $(\sigma(s_m) > 0)$.

The contribution of small-scale turbulence and thermo-convection to the entropy production has been examined elsewhere (VAN MIEGHEM 1949 b).

Neglecting viscosity and small-scale turbulence, we shall consider here the entropy production due to large-scale turbulence only. Large-scale turbulence generates entropy at the rate

$$\sigma_e(s_m) = -\frac{W^{\alpha}_{(e)}}{(\hat{T})^e}\frac{\partial \hat{T}}{\partial x^{\alpha}} + \frac{1}{\hat{T}}\overline{\frac{\partial p}{\partial x^i}\,v''^i}, \tag{45}$$

or, after substitution of (31 b),

$$\sigma_{(e)}(s_m) \cong \frac{1}{\hat{T}}\,\overline{\mathbf{v}''.\nabla p} - \frac{c_p}{(\hat{T})^2}\,\overline{\varrho\, T''\mathbf{v}''}.\nabla \hat{T} - \frac{L_v}{(\hat{T})^2}\,\overline{\varrho\,\varepsilon''_v\mathbf{v}''}.\nabla \hat{T}. \tag{45 a}$$

Introducing the fluctuation Θ'' of Θ with respect to the weighted mean value $\hat{\Theta}$ into (40) and (45 a),

$$\psi'' \equiv \frac{\Theta''}{\hat{\Theta}} \equiv -\frac{\varrho'}{\bar{\varrho}} + \frac{c_v}{c_p}\frac{p'}{\bar{p}} \equiv \frac{T''}{\hat{T}} - \frac{R}{c_p}\frac{p'}{\bar{p}} \cong -\frac{\varrho'}{\bar{\varrho}} \cong \frac{T''}{\hat{T}}. \tag{46}$$

where $\psi \equiv \lg \Theta$, we find

$$\overline{\mathbf{v}''.\nabla p} \cong g\,\overline{\varrho' w''} \cong -g\,\bar{\varrho}\,\overline{\psi'' w''} \cong -g\,\varrho\,\overline{\psi'' w''} \tag{40 a}$$

and

$$\sigma_e(s_m) \cong -c_p\,\overline{\varrho\,\psi''\mathbf{v}''}.\nabla \hat{\psi} - \frac{c_p - c_v}{\bar{p}}\frac{\partial \bar{p}}{\partial y}\,\overline{\varrho\,\psi'' v''} - \frac{L_v}{(\hat{T})^2}\,\overline{\varrho\,\varepsilon''_v\mathbf{v}''}.\nabla \hat{T}. \tag{47}$$

BJERKNES (1951) and WHITE (1951) have shown that $\overline{\varrho\,\psi'' v''} > 0$; consequently, the second term in (47) represents a positive contribution to the entropy production. Less is known regarding the flux of "latent" heat $\overline{\varrho\,\varepsilon''_v\mathbf{v}''}$, but it seems not unreasonable to assume that the last term represents also a positive contribution. Both correlations $\overline{\varrho\,\psi'' v''}$ and $\overline{\varrho\,\psi'' w''}$ being positive, the sign of the first term depends upon the slope of the meridional eddy-motion (v'', w'') with respect to the isentropic surfaces $\hat{\Theta} =$ constant or $\hat{\psi} =$ constant. When the large-scale eddy motion in the meridional planes takes place within the angle between the geopotential surfaces and the isentropic surfaces the first term represents also a positive contribution to the entropy production. Indeed, in the atmosphere, as a rule,

$$\operatorname{tg}\alpha = \frac{w''}{v''} > 0 \quad \text{and} \quad \operatorname{tg}\beta = -\frac{\partial \hat{\Theta}}{\partial y} : \frac{\partial \hat{\Theta}}{\partial z} = -\frac{\partial \hat{\psi}}{\partial y} : \frac{\partial \hat{\psi}}{\partial z} > 0;$$

hence,

$$-c_p\,\overline{\varrho\,\psi''\mathbf{v}''}.\nabla \hat{\psi} = \frac{c_p}{\hat{\Theta}}\frac{\partial \hat{\Theta}}{\partial z}\,\overline{\varrho\,\psi'' w''\left(\frac{\operatorname{tg}\beta}{\operatorname{tg}\alpha} - 1\right)} > 0,$$

when $\alpha < \beta$, the correlation between the fluctuations of temperature and vertical velocity being positive, $(\overline{\varrho\,\psi'' w''} > 0)$.

EADY (1949) has shown the existence of unstable cyclone waves such that, during their growth, potential energy is transformed into kinetic energy, the above mentioned condi-

tion for the meridional eddy motion (v'', w'') being fulfilled. Thus, we may conclude that the growth of cyclone waves is accompanied by a conversion of potential energy into kinetic energy and simultaneously, with a production of entropy.

Acknowledgement

I wish to express my sincere thanks and appreciation to Prof. C. G. Rossby who invited me to visit the Institute of Meteorology of the University of Stockholm. Many stimulating discussions with colleagues of different countries have made my stay in Sweden a very profitable experience.

REFERENCES

Bjerknes, J., 1951: The maintenance of the zonal circulation of the atmosphere. *Ass. de Météor. (UCGI.) Procès-Verbaux de Bruxelles*, II (in print).

Charney, J. G., 1948: On the scale of atmospheric motions. *Geof. Publ.*, **17**, 2, 14—37.

Eady, E. T., 1949: Long waves and cyclone waves. *Tellus*, **1**, 3, 33—52.

Fjørtoft, R., 1951: Stability properties of large-scale atmospheric disturbances. *Comp. of Meteor.*, Boston, Mass., pp. 454—463.

Jeffreys, H., 1926: On the dynamics of geostrophic winds. *Quart. J. R. Meteor. Soc.*, **52**, 85—104.

— 1933: The function of cyclones in the general circulation. *Ass. de Météor. (UGGI.) Procès-Verbaux de Lisbonne*, II, 219—229.

Kuo, H. L., 1951: A note on the kinetic energy balance of the zonal wind systems. *Tellus*, **3**, 205—207.

Miller, J. E., 1950: Energy transformation functions. *J. of Meteor.*, **7**, 152—159.

Priestley, C. H. B., 1949: Heat transport and zonal stress between latitudes. *Quart. J. R. Meteor. Soc.*, **75**, 28—40.

Starr, V. P., 1948: On the production of kinetic energy in the atmosphere. *J. Meteor.*, **5**, 193—196.

Starr, V. P., 1949: Transport of kinetic energy in the atmosphere, *J. Meteor.*, **6**, 160.

Van Mieghem, J., 1949 a: Production et redistribution de la quantité de mouvement et de l'énergie cinétique dans l'atmosphère. Application à la circulation atmosphérique générale. *J. Sc. de la Météor.*, I, 53—67.

— 1949 b: Les équations générales de la mécanique et de l'énergétique des milieux turbulents en vue des applications à la météorologie. *Inst. Roy. Météor. de Belgique, Mém.* **34**, 1—59.

— 1950 a: Comment on the global energy balance of the atmosphere. *Centenary Proc. R. Meteor. Soc.*, 173—175.

— 1950 b: L'équation aux dérivées partielles de la pression de perturbation associée aux ondulations de grande longueur d'onde du courant géostrophique zonal. *Inst. Roy. Météor. de Belgique, Mém.* **39**, 1—45.

— 1951: Hydrodynamic instability. *Comp. of Meteor.*, Boston, Mass. See p. 436.

Van Mieghem, J., et Dufour, L., 1948: Thermodynamique de l'atmosphère. Bruxelles. Off. Int. de Librairie (see pp. 160—167).

White, R. M., 1951: The meridional eddy flux of energy. *Quart. J. R. Meteor. Soc.*, **77**, 188—199.

Starr's Invariant

By GEORGE W. PLATZMAN, University of Chicago

(Manuscript received 22 April 1952)

In a recent communication to this Journal, STARR (1950) pointed out that for two-dimensional flow of an inviscid incompressible fluid between parallel rigid walls (which coincide, say, with latitude circles) on a sphere, the integral

$$\int \delta\zeta \oint \frac{1}{2}\, \varepsilon^2\, \delta\lambda \qquad (1)$$

is invariant, and from this, commented on the stability of such flows, in particular on results obtained earlier by FJØRTOFT (1950).

The notation is as follows: λ is the longitude, ζ the (absolute) vorticity; the integration covers the entire *cyclic* region occupied by fluid, and this region is regarded as composed of strips cut out by lines of equal vorticity ζ, $\zeta + \delta\zeta$, etc.; the line integral follows a line of equal vorticity, and

$$\gamma \equiv a^2 \sin \Phi$$
$$\varepsilon \equiv \gamma - \bar{\gamma},$$

where a in the radius of the sphere, Φ the latitude, and

$$\bar{\gamma} \equiv \frac{1}{2\pi} \oint \gamma\, \delta\lambda \qquad (2)$$

is the average value of γ for all particles composing a given line of equal vorticity.

It is tacit in Starr's discussion that each line of equal vorticity encircles the sphere, as pictured in figure 1 a. Accordingly, $\bar{\gamma}$ corresponds to the mean latitude of the ζ-line, and ε to the departure of a particle from this mean position. A curve of the type pictured in figure 1 a divides the whole doubly-connected region of fluid into two subregions, each doubly connected; we will call this a *cyclic* type of curve.

To provide for more general species of two-dimensional flow, we may consider three other distinct types of curves (vorticity lines); these are illustrated in figures 1 b, c, d. The following "topological" classification of vorticity lines is implied:

	Original space divided into:
a. Cyclic type	— two doubly-connected regions
b. Closed type	— one simply, one triply-connected region
c. Boundary type I	— one simply, one doubly-connected region
d. Boundary type II	— one simply-connected region.

Since vorticity is conserved, and assuming particles never leave or enter the boundaries, the topological classification of any vorticity line is invariant with respect to all dynamically and kinematically possible motions of the fluid.

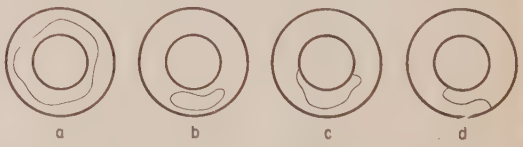

Fig. 1. Each of the four schematic illustrations represents a polar stereographic projection of the spherical sheet of fluid, in which the flow is contained in the zone between two latitude circles. The lightly-drawn curve in each case depicts one of the four topologically distinct types of curves of equal vorticity.

Under these conditions, it is not difficult to prove that the integral in (1) is invariant also when the more general types of vorticity lines, classified above, are permitted, provided $\bar{\gamma}$ in (2) is suitably defined.

For what we have called the *cyclic* type of curve, the line integral (2) is determined by the area between this curve and the pole. Since the fluid is incompressible and vorticity is conserved, $\bar{\gamma}$ thus defined is invariant for any vorticity line of this type. Likewise, for the *closed* type of curve (fig. 1 b), the line integral (2) is determined by the area enclosed by the curve, so for the same reasons $\bar{\gamma}$ is invariant.

We start with the general statement that

$$\iint \gamma\zeta \, dS \tag{3}$$

is invariant (FJØRTOFT, 1950), where dS is an element of surface area of the sphere; for, it can be shown that this integral is determined by the total angular momentum of the fluid. Thus, let ψ denote the stream function and write $\zeta = \operatorname{div} \nabla\psi$ so that

$$\gamma\zeta = \operatorname{div} (\gamma \nabla\psi) - \nabla\gamma \cdot \nabla\psi.$$

If this identity is integrated over a region between two latitude circles corresponding to γ_2 (on the north) and γ_1 (on the south), we get the result (STARR, 1950) that (3) is equal to $\gamma_1 \Gamma_1 - \gamma_2 \Gamma_2 +$ {total angular momentum}, where Γ_1 and Γ_2 are the fluid circulations along the boundaries. The latter, as well as the total angular momentum, are conserved.[1]

Consider first a flow in which the "boundary types" of vorticity lines are excluded, and the boundaries coincide with lines of equal vorticity. Imagine the entire region divided into strips by vorticity lines ζ, $\zeta + \delta\zeta$, etc., and then into elementary parallelograms by meridians λ, $\lambda + \delta\lambda$, etc. (figure 2). The element of area ds is then $\delta\gamma\delta\lambda$, and the contribution of one of these vorticity strips to (3) is[2]

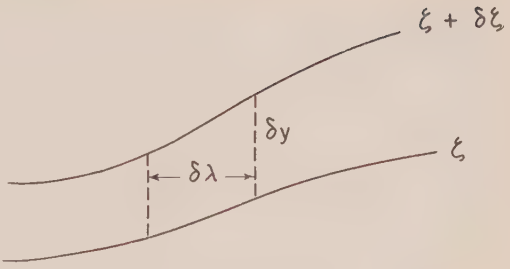

Fig. 2. The strip between vorticity lines ζ and $\zeta + \delta\zeta$ is divided into elementary parallelograms by meridians λ and $\lambda + \delta\lambda$.

$$\zeta\gamma \, \delta\gamma \, \delta\lambda = \oint \oint \delta \left(\frac{1}{2} \, \gamma^2 \zeta \right) \delta\lambda -$$

$$\delta\zeta \oint \frac{1}{2} \, \gamma^2 \, \delta\lambda.$$

In adding the contributions from each strip we can integrate the first term on the right partially for a fixed value of λ, from wall to wall (γ_1 to γ_2), and get the result that *minus* (3) is equal to

$$\frac{1}{2} \, \gamma_1^2 \oint \zeta_1 \, \delta\lambda - \frac{1}{2} \, \gamma_2^2 \oint \zeta_2 \, \delta\lambda + \tag{4}$$

$$+ \int \delta\zeta \oint \frac{1}{2} \, \gamma^2 \, \delta\lambda. \tag{5}$$

In (5) substitute $\gamma = \bar{\gamma} + \varepsilon$; the line integral is then equal to

$$\frac{1}{2} \, \bar{\gamma}^2 \oint \delta\lambda + \bar{\gamma} \oint \varepsilon \, \delta\lambda + \tag{6}$$

$$+ \oint \frac{1}{2} \, \varepsilon^2 \, \delta\lambda. \tag{7}$$

In view of the definition of $\bar{\gamma}$ in (2), we find

$$\oint \varepsilon \, \delta\lambda = 2\pi\bar{\gamma} \, (1 - \tau), \text{ where}$$

$$\tau \equiv \frac{1}{2\pi} \oint \delta\lambda = \begin{matrix} 1 \text{ for cyclic curve} \\ 0 \text{ for closed curve.} \end{matrix}$$

It follows that (6) is equal to

$$2\pi\bar{\gamma}^2 \left(1 - \frac{1}{2} \, \tau \right).$$

[1] The boundary effects disappear when the flow covers the entire sphere; or when viscosity is invoked to provide no slip at the boundaries (in which case, of course, the total angular momentum may not be conserved).

[2] Note that $\delta\zeta$ must be taken in such a sense that the corresponding $\delta\gamma$ is positive wherever $\delta\lambda$ is positive, because $\delta\gamma\,\delta\lambda = dS$ is inherently positive.

Collecting these results, we see that *minus* (3) is equal to

$$\frac{1}{2}\gamma_1^2 \oint \zeta_1 \delta\lambda - \frac{1}{2}\gamma_2^2 \oint \zeta_2 \delta\lambda + \quad (4)$$

$$+ 2\pi \int \bar{\gamma}^2 \left(1 - \frac{1}{2}\tau\right) \delta\zeta + \quad (8)$$

$$+ \int \delta\zeta \oint \frac{1}{2}\varepsilon^2 \delta\lambda. \quad (1)$$

If all vorticity strips are either cyclic or closed, the boundaries must coincide with vorticity lines; in this case each term in (4) is invariant. Further, (8) is invariant in any case because not only are ζ and $\bar{\gamma}$ conservative quantities, but also τ is conservative because of the invariant character of the topological classification of ζ-lines. The invariance of (4) and (8) therefore leads directly to the invariance of (1).

The preceding argument depends upon exclusion of "boundary types" of vorticity lines, since otherwise (4) is not invariant in general. For such curves the integral defining $\bar{\gamma}$ in (2) must be interpreted as a *closed* line integral (for example, for "boundary type I") by arbitrarily incorporating a segment of the boundary joining the two end points of the vorticity line. The integral in (2) is then determined by the area occupied by the fluid thus enclosed, and therefore $\bar{\gamma}$ still is a conservative quantity. With this provision it can be proved that the contribution to (3) represented by (4) *vanishes* if the line integral in (1) is interpreted as traversing in each case a closed curve, by including, where necessary, appropriate portions of the boundary. The invariance of (1) then follows from the invariance of (8).[3]

Of the three conclusions formulated by Starr from the invariance of (1), the first particularly calls for some discussion. He states, in effect, that if the vorticity distribution is *montone*, so that $\delta\zeta$ is everywhere positive or everywhere negative, then "zonal flow cannot develop into disturbed motion." This inference is based on the idea that while (1) vanishes for zonal flow, it cannot vanish for a disturbed monotone vorticity distribution unless $\varepsilon \equiv 0$; but then there can be no disturbance.

If this statement were taken at face value, it would reduce to an obvious truism because zonal flow can never "develop" into disturbed motion unless a disturbance of some kind is supplied; for, regardless of *stability*, zonal flow is an equilibrium state and therefore cannot change without the action of a disturbance. But if a disturbance is postulated, the flow is automatically disturbed *ab initio*.

Evidently, the statement must be interpreted as an inference regarding the *stability* of zonal equilibrium flow, implying, in other words, that if the postulated zonal flow is slightly disturbed, then in some sense (suitably defined) the disturbance will not grow. Since (1) is not restricted in any way to *small* disturbances, it is essential to use the word "stability" with caution. The harmonic-time-dependent perturbation method provides clear-cut analytical procedures for investigating this question, and at the same time establishes a precise operational basis for a *definition* of stability (a definition that cannot, however, be abstracted readily from its operational context).

If the term is used in this sense, the statement in question coincides with the well-known Rayleigh criterion; but it is not evident that there is an equivalence between the concept of stability involved in Rayleigh's criterion and that which is tacit in Starr's statement.

A rather general formal stability criterion in accord with intuition is as follows. Let P and Q be suitable parameters characteristic of the *deformation* of an equilibrium state and let P_0 be the initial value of P corresponding to a prescribed initial disturbance.

> The equilibrium state is *stable* if, regardless of the initial *form* of the disturbance, it is always possible to assign a finite value to P_0 that will make Q smaller than *any* preassigned value *for all time*.

In principle the qualification "for all time" is essential (as intuition suggests), yet this proviso probably prohibits the use of perturbation theory, or in fact any approximation theory whose validity is inherently limited to a restricted interval of time. Since we are dealing with a nonlinear system, the preceding formal definition of stability suggests an investigation of the integral invariants of the system.

[3] If the lateral boundaries are dispensed with and the flow covers the entire sphere, the "boundary types" of vorticity curves do not occur and the integral (1) requires no further elaboration.

The properties P and Q need not be distinct; for example, both may be identified with the energy of the disturbance. It should also be remarked that the choice of P and Q may to some extent restrict the scope of the criterion; in other words stability with respect to one pair of parameters may not always imply stability with respect to a different pair. For example, in connection with the Rayleigh criterion, FJØRTOFT (1950) has stressed that stability can be proved only if P is identified with disturbance *vorticities* (assuming Q is identified with the sum of squares of meridional displacements).

Returning to an interpretation of Starr's inference from the invariance of (1), suppose we identify (1) with the parameter P, and Q with the kinetic energy of the disturbance. This means that we must establish a connection between (1) and the disturbance energy, in such a way as to satisfy the stability criterion. A rigorous proof of stability in this sense would be of considerable interest from the standpoint of theoretical fluid mechanics.

One of the perplexities of this problem arises from the consideration that there may be *certain* parameters Q with respect to which stability can never be proved. Possibly one such inherently "unstable" parameter is the magnitude $|\nabla\zeta|$ of the vorticity gradient. Apart from highly exceptional cases (for example, steady wave propagation), it seems probable that by and large, within the nonlinear framework of the vorticity equation, a given initial flow will evolve toward greater and greater complexity: the vorticity distribution, at least in some regions of the flow, must become progressively distorted, individual lines exhibiting more and more involved convolutions and tending to "fill the space." It seems inevitable that in certain critical regions vorticity gradients must ultimately attain large values (for which viscosity may begin to dominate), regardless of any considerations of the *stability* of the system.[4]

To the writer, an exacting and highly idealized criterion such as involved in the preceding formal definition of stability does not seem to be especially relevant in connection with the behavior of large-scale atmospheric flow. Probably no equilibrium states exist in the atmosphere; and because of the complexity of this system, the inherent oversimplifications in any model render extremely dubious any attempt to investigate the behavior of the model *for all time*.

Starr's invariant is a highly ingenious formulation of the momentum principle for two-dimensional flows; an integral invariant of the hydrodynamical equations, it is of interest *per se*. The writer hopes that the remarks made above will call attention to the need for clarifying some of the inferences made by Starr in his note.

[4] It may be of interest to point out that because it is responsible for the transference of vorticity between fluid particles, viscosity will render nonconservative the "topological" parameter τ defined above. Each such nonconservative event, altering the connectivity of a vorticity strip, corresponds to a transition of τ from 1 to 0 (or vice versa).

REFERENCES

FJØRTOFT, R., 1950: Application of integral theorems in deriving criteria of stability for laminar flows and for the baroclinic circular vortex. *Geof Publ.*, **17**, 6, 52 pp.

STARR, V. P., 1950: Note on recent study of stability by R. FJØRTOFT. *Tellus*, **2**, 321—323.

A Baroclinic Model of the Atmosphere Applicable to the Problem of Numerical Forecasting in Three Dimensions.[1] I

By G. ÁRNASON
University of Stockholm

(Manuscript received 5 July 1952, revised manuscript received 25 September 1952)

Abstract

A three-dimensional baroclinic model of the atmosphere is presented. This model is completely determined by 4 parameters, three of which specify the field of temperature. The main difference between this model and other models so far published is that it allows for a non-uniform temperature lapse-rate in the horizontal. Moreover, it takes into account the observed division of the atmosphere into a troposphere and a stratosphere.

A simplification is introduced by utilizing the synoptic experience that the horizontal temperature gradient is usually reversed when traversing the tropopause. This essentially reduces the number of parameters to three.

This simplified version of the model is used for integrating the vorticity equation along the vertical, and the coefficients of the resulting two-dimensional equation are discussed in some detail. Examination of the coefficients give some valuable information regarding the levels of mean wind and non-divergence.

The main results are that in middle latitudes the level of mean wind may vary from 2.5—6.5 km and that the level of of non-divergence is always higher than the former, the difference amounting to 0.5—3.0 km. On the average, the level of mean wind lies below and the level of non-divergence above the 500 mb surface. One is therefore lead to the conclusion that this surface might be used to approximate each of the two levels mentioned.

The consequence of this for the practical procedures for numerical forecasting is that the height changes at this particular level could alternatively be predicted in the two following ways:

a) By use of the barotropic vorticity equation, thereby assuming that the level of non-divergence can be replaced by the 500 mb surface.
b) By use of an integrated vorticity equation applicable to the level of mean wind. In this case one replaces the level of mean wind with the 500 mb surface.

1. Introduction

The remarkable fact that temperature is nearly a linear function of height is used in this paper as a guiding principle for constructing an atmospheric model which is believed to take into account the essential features of the actual atmosphere. The main divisions, the troposphere and the stratosphere, are kept in the model, but the numerous irregularities in the observed soundings are eliminated through a smoothing procedure. An objective smoothing may be achieved by approximating an observed temperature height curve through a polynomial in z in

[1] This work has been made possible by a grant from the Knut and Alice Wallenberg Foundation, Stockholm.

which the coefficients are functions of x, y and t. Any required degree of accuracy can be obtained in this way; however, because of the well established linearity in temperature with height, a first order polynomial is thought to be sufficient and has been chosen for the model presented in this paper.

Models based upon simplifications in the theoretical representation of the field of temperature are certainly not uncommon; to the contrary, such simplifications are found explicitly or implicitly in a number of papers. We may mention the advective model of ROSSBY (1942), CHARNEY's (1947) and EADY's (1949) basic current models, and the model underlying the forecasting method developed by the Russian meteorologist J. A. Kibel in the early forties [see IZVEKOW (1946) and HAURWITZ (1946)]. Moreover, we will mention the so-called $2^1/_2$ dimensional models presented by SUTCLIFFE (1947), FJÖRTOFT (see CHARNEY 1951), PHILLIPS (1951), EADY (1952) and ELIASSEN (1952).

Common to most of the works referred to above is the assumption that the horizontal temperature gradient is independent of height. The model presented in this paper goes one step further inasmuch as it contains a tropospheric temperature gradient which varies linearly with height in accordance with the equation

$$\nabla\tau = \nabla\tau_0 - z\nabla k \qquad (1, 1)$$

Here $-\nabla\tau_0$ is the horizontal temperature gradient at $z=0$, and $-\nabla k$ the horizontal gradient in the temperature lapse-rate. It is firmly believed that the introduction of a non-uniform lapse-rate in the field of temperature is a considerable improvement over models based on a temperature gradient which is independent of height. This improvement appears clearly when one deals with the adiabatic equation. In the case of temperature gradient independent of height this equation admits only a trivial solution for the vertical velocity, whereas the linear temperature gradient gives a parabolic distribution of the vertical velocity with height. Moreover, an application of the model to numerical forecasting has shown that local changes in the average (with respect to height) temperature lapse rate may contribute considerably to the local pressure changes.

Section 2 of this paper is devoted to the detailed presentation of the equations describing the fields of pressure, geostrophic wind and geostrophic vorticity corresponding to the smoothed field of temperature. The knowledge of the functional relationship of these elements with respect to the height z makes the model particularly well suited for integration of the vorticity equation along a vertical.

The integration of this equation is dealt with in sections 3 and 4, and rather definite information regarding the levels of mean wind and non-divergence is gained. It turns out that these two levels are primarily determined by the vertical structure of the atmosphere, and that the particular distribution of temperature and pressure is not essential for their determination. A considerable influence upon the height of these levels is exerted, however, by the horizontal distribution of temperature in the stratosphere.

A continuation of this article, to be published in a later issue of Tellus, will be devoted to the application of the model to numerical prediction of the fields of temperature and pressure.

2. Specification of the model with respect to height

The field of temperature. The model consists of a troposphere, in which the temperature τ is given as function of the height z by the equation:

$$\tau = \tau_0 - kz \qquad (2, 1)$$

and a stratosphere where the temperature is independent of height. In equ. (2, 1) k is the temperature lapse-rate and is independent of z. Both τ_0 (surface temperature) and k are functions of the horizontal coordinates x, y and the time t. Since the stratosphere by definition is characterized by isothermal conditions in the z-direction, its temperature is obviously obtained from (2, 1) by putting $z = h$, where h is the height of the tropopause, which may vary with x, y and t. Thus:

$$\tau_s = \tau_h = \tau_0 - kh \qquad (2, 2)$$

where the subscripts s and h refer to the values of τ in the stratosphere and at the tropopause level respectively.

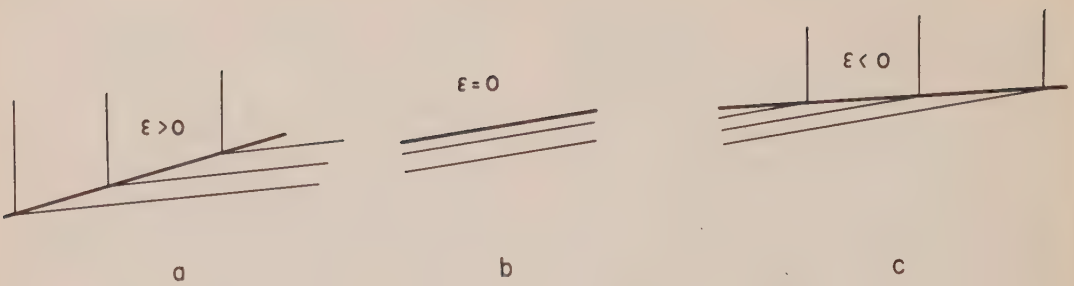

Fig. 1. The thick line is the tropopause and the thin lines are isotherms. In a) the slope of the tropopause is greater than that of the isotherms in the troposphere and the tropospheric and the stratospheric temperature gradients have opposite directions. In b) the isotherms and the tropopause have the same slope and $\nabla \tau_s = 0$, and in c) the two temperature gradients have the same direction.

From (2, 1) and (2, 2) the following expressions for $\nabla \tau$ — the horizontal temperature ascendent in the troposphere — and $\nabla \tau_s$ — the horizontal temperature ascendent in the stratosphere — are obtained through derivation:

$$\nabla \tau = \nabla \tau_0 - z \nabla k \qquad (2, 3)$$

$$\nabla \tau_s = \nabla \tau_0 - \nabla (kh) = (\nabla \tau)_{z=h} - k \nabla h \qquad (2, 4)$$

Three-dimensional nabla operators will not occur in this paper, and the symbol ∇ will therefore be used throughout to denote the two-dimensional nabla operator referring to a horizontal surface.

It is obvious from (2, 4) that knowledge of the topography of the tropopause is needed in order to determine the jump in the horizontal temperature gradient, when passing from the troposphere to the stratosphere.

For later reference and for comparison with the model, the general expression for the relationship between the tropospheric and the stratospheric temperature gradients is given below:

$$(\nabla \tau_s)_{z=h} = (\nabla \tau)_{z=h} - (k - k) \nabla h \qquad (2, 5)$$

where k_s is the stratospheric temperature lapse-rate at the level of the tropopause and k is the tropospheric one at the same level. Putting $k_s = 0$ and assuming k and $\nabla \tau_0$ to be independent of z, equ. (2, 5) becomes identical with (2, 4).

It is frequently observed that, at least in middle latitudes, the direction of the horizontal temperature gradient is reversed when passing through the tropopause. This implies that $(k - k_s) \nabla h$ has the same direction as $(\nabla \tau)_{z=h}$ and is greater in magnitude. Moreover, experience indicates that a strong tropospheric temperature gradient is positively correlated to a great slope of the tropopause. Since the details of the stratospheric field of temperature are presumably of minor importance for the solution of a great many problems in dynamic and synoptic meteorology, these empirical findings will be used to simplify the model. This is done by replacing equ. (2, 4) by the simpler one:

$$\nabla \tau_s = -\varepsilon (\nabla \tau)_{z=h} \qquad (2, 6)$$

where ε is a parameter of the model, the value of which, however, is sofar unknown. Fig. 1 is a vertical cross-section showing how the slope of the tropopause in relation to that of the isotherms of the troposphere depends upon the sign of ε. By use of the daily tropopause charts published by the British Meteorological Office, London, and the associated aerological data, values of the parameter ε have been computed and their variability studied to a certain extent. The results will be discussed in some detail further below.

Returning to equ. (2, 3), the tropospheric temperature gradient is obviously a linear function of height since ∇k is independent of z. An observed temperature gradient alternatively veering and backing with height could therefore not be approximated through (2, 3). Observations indicate that such a variation with height is not very common, and the average veering or backing with height can always be accounted for by the model, since ∇k is independent of $\nabla \tau_0$.

It is convenient to distinguish between the following special cases:

a) $\nabla k = 0$ The horizontal temperature gradient is independent of height. As will appear below this implies a linear variation in the geostrophic wind with height.

b) $\nabla k = \varkappa \triangle \tau_0$. The direction of $\triangle \tau$ is the same throughout the troposphere, with a possible exception for a change of 180 degrees. The magnitude will decrease or increase with height depending on the sign of the proportionality factor $\varkappa$.

c) $\nabla k = \varkappa \nabla \tau_0 \times \mathbf{k}$ where $\mathbf{k}$ is a unit vector directed along the positive vertical. In this case the temperature gradient rotates at a constant rate throughout the troposphere.

The field of pressure. Having expressed the temperature and the temperature gradient as known functions of height, the pressure field is easily determined from the hydrostatic equation, which integrated is most conveniently used in the form:

$$p_2 = p_1 \cdot e^{-\frac{g}{R}\int_{z_1}^{z_2} \frac{dz}{\tau}} \qquad (2,\ 7)$$

where g is the acceleration of gravity and R the gas constant per unit mass.

Applied to the model equ. (2, 7) gives the following expressions for the pressure, the horizontal pressure gradient and the density:

$$p = p_0 \left(\frac{\tau}{\tau_0}\right)^n; \quad \varrho = \varrho_0 \left(\frac{\tau}{\tau_0}\right)^{n-1} \qquad (2,\ 8)$$

$$\nabla p = \left(\frac{\tau}{\tau_0}\right)^n \left[\nabla p_0 + \frac{g\varrho_0}{\tau} z \left(\nabla \tau_0 - \frac{z}{2} \nabla k\right)\right] \qquad (2,\ 9)$$

$$p_s = p_h \cdot e^{-mz_s}; \quad \varrho_s = \varrho_h e^{-mz_s} \qquad (2,\ 10)$$

$$\nabla p_s = e^{-mz_s} \left(\nabla p_h + \frac{g\varrho_h}{\tau_h} z_s \nabla \tau_s\right) \qquad (2,\ 11)$$

where $n = \frac{g}{Rk}$ and $m = \frac{g}{R\tau_h}$

Equations (2, 8) and (2, 9) apply to the troposphere and (2, 10) and (2, 11) to the stratosphere. A slight approximation has been made in (2, 9).

Applying the geostrophic equation we arrive at the following expressions for the geostrophic wind in the troposphere and the stratosphere respectively:

$$\mathbf{v} = \frac{\tau}{\tau_0} \mathbf{v}_0 + \mathbf{v}' z - \mathbf{v}'' z^2 \qquad (2,\ 12)$$

$$\mathbf{v}_s = \mathbf{v}_h + \mathbf{v}'_s z_s \qquad (2,\ 13)$$

where $\mathbf{v}' = \frac{g}{f\tau_0} \mathbf{k} \times \nabla \tau_0$, $\quad \mathbf{v}'' = \frac{g}{2f\tau_0} \mathbf{k} \times \nabla k$,

$\mathbf{v}_s' = \frac{g}{f\tau_h} \mathbf{k} \times \nabla \tau_s$, and f is the Coriolis parameter.

In virtue of (2, 6),

$$\mathbf{v}_s' = -\varepsilon \frac{\tau_0}{\tau_h} (\mathbf{v}' - 2h\mathbf{v}'') \qquad (2,\ 14)$$

which inserted in (2, 13) gives:

$$\mathbf{v}_s = \mathbf{v}_h - \varepsilon \frac{\tau_0}{\tau_h} (\mathbf{v}' - 2h\mathbf{v}'') z_s \qquad (2,\ 15)$$

It follows from (2, 12) that the wind in the troposphere is a polynomial of second order in z. There is no relationship between the constant vectors $\mathbf{v}_0$, $\mathbf{v}'$ and $\mathbf{v}''$ and the wind may decrease or increase with height and change direction as well. In the stratosphere the wind is a linear function of height only, corresponding to the simpler field of temperature.

Fig. 2 gives a sample of possible wind profiles in the case of uniform wind direction with height. It may of course also be interpreted as the profile of the wind component in a certain direction.

Neglecting the variation in $\frac{\tau}{\tau_0}$, $\frac{1}{\tau_0}$ and $\frac{1}{\tau_h}$ compared with that of $\mathbf{v}_0$, $\nabla \tau_0$, ∇k and $\nabla \tau_s$ respectively, the following expressions for the relative vorticity of the troposphere and the stratosphere are obtained from (2, 12) and (2, 13):

$$\zeta = \frac{\tau}{\tau_0} \zeta_0 + \zeta' z - \zeta'' z^2 \qquad (2,\ 16)$$

$$\zeta_s = \zeta_h + \zeta'_s z_s \qquad (2,\ 17)$$

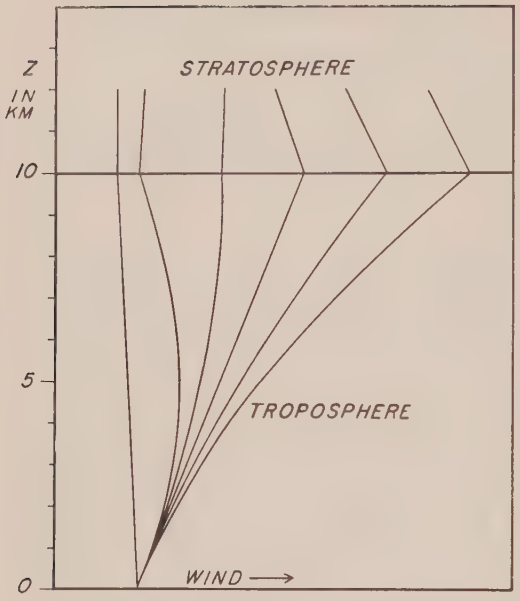

Fig. 2. Examples of possible wind profiles in the model. The first profile from the left corresponds to no temperature gradient and the fourth profile corresponds to a constant temperature gradient throughout the troposphere.

where

$$\zeta_0 = \frac{1}{f\varrho_0}\nabla^2 p_0,\ \zeta' = \frac{g}{f\tau_0}\nabla^2\tau_0,\ \zeta'' = \frac{g}{2f\tau_0}\nabla^2 k,$$

$$\zeta_s' = \frac{g}{f\tau_h}\nabla^2\tau_s \qquad (2,\ 18)$$

and ∇^2 is a two-dimensional Laplacian referring to a horizontal surface. The expressions for the wind and the relative vorticity are analogous, and the profiles depicted in fig. 2 may therefore just as well represent a sample of vorticity profiles.

Derivating equ. (2, 6) and neglecting the variation in h and ε compared with that of $\nabla\tau_0$ and ∇k, we may write

$$\nabla^2\tau_s = -\varepsilon\,(\nabla^2\tau_0 - h\nabla^2 k) \qquad (2,\ 19)$$

This inserted in the expression for ζ_s' gives:

$$\zeta_s' = -\varepsilon\frac{\tau_0}{\tau_h}(\zeta' - 2h\zeta'') \qquad (2,\ 20)$$

Substituting for ζ_s' in (2, 17) we then arrive at the following expression for the stratospheric vorticity:

$$\zeta_s = \zeta_h - \varepsilon\frac{\tau_0}{\tau_h}(\zeta' - 2h\zeta'')z_s \qquad (2,\ 21)$$

The assumptions underlying equation (2, 6) may for some purposes prove to be too crude. We will therefore go back to (2, 4) and give the corresponding expressions for the wind and relative vorticity of the stratosphere:

$$\mathbf{v}_s = \mathbf{v}_h + \left[\frac{\tau_0}{\tau_h}(\mathbf{v}' - 2h\mathbf{v}'') - \frac{gk}{f\tau_h}\mathbf{k}\times\nabla h\right]z_s \qquad (2,\ 22)$$

$$\zeta_s = \zeta_h + \left[\frac{\tau_0}{\tau_h}(\zeta' - 2h\zeta'') - \frac{gk}{f\tau_h}\nabla^2 h\right]z_s \qquad (2,\ 23)$$

In deriving (2, 23) from (2, 22) similar approximations have been done as in the derivation of (2, 16) and (2, 17).

It is clear from (2, 22) and (2, 23) that the topography of the tropopause gives rise to stratospheric wind and vorticity. When replacing the atmosphere by this model, this contribution of the tropopause can be measured from a chart of tropopause contours in the same way as is geostrophic wind and vorticity measured from ordinary upper air maps.

Computed values of the parameter ε based on observations. On the preceding pages the fields of temperature, pressure, geostrophic wind and geostrophic vorticity have been described in terms of quantities, the magnitude and range of variability of which are well known from surface and upper air observations. The single exception is the parameter ε, which is not readily obtained from current data.

In order to investigate the magnitude and variability of this parameter some studies have been made based on the tropopause maps and the aerological data in the Daily Aerological Record, published by the Meteorological Office, London. One value of ε was computed for nearly each day of a period covering the months Febr., July, Aug. 1950 and Nov., Dec. 1951.

As mentioned earlier the horizontal temperature gradient of the stratosphere at $z = h$ is related to that of the troposphere at the same level and the gradient of the contour lines of the tropopause in accordance with the following equation:

$$(\nabla\tau_s)_{z=h} = (\nabla\tau)_{z=h} - (k - k_s)\nabla h \qquad (2,\ 5)$$

The British material quoted above shows that in the majority of cases the three gradients in this equation are approximately directed along the same line. With this in mind two sounding stations were chosen such that their line of connection, as far as possible, was perpendicular to the contour lines of the tropopause, and tropospheric and stratospheric temperature differences were computed as sketched in fig. 3.

Altogether 147 values of ε were computed, and the results are given in table 1 and fig. 4.

As one might expect, the two temperature gradients are in general of the opposite direction. The recorded exceptions were associated with very weak temperature gradient in the layer 500—300 mb and the same applies to the cases with high positive values of ε. It is obvious from (2, 5) that when $(\nabla \tau)_{z=h}$ is zero, $(\nabla \tau_s)_{z=h}$ is proportional to $-\nabla h$. The latter may of course differ from zero, in which case ε approaches $\pm \infty$. Study of the tropopause charts in relation to the relative thickness lines 500—300 mb have shown that the proportionality between the tropospheric and the stratospheric temperature gradients in the vicinity of the tropopause is rather well established, whenever the temperature distribution is not too far from the normal one. The parameter ε is then positive. When, however, the temperature distribution is greatly disturbed, the direction of the two temperature gradients may form a rather arbitrary angle and the assumption of proportionality breaks down. In such cases there will be regions with a very weak temperature gradient in the troposphere, whereas the slope of the tropopause may be rather pronounced, giving rise to a stratospheric temperature gradient which has no simple relationship to the tropospheric one. Determination of ε will then give values within a very great range.

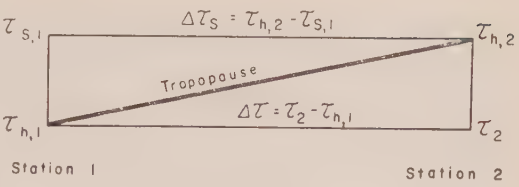

Fig. 3. A vertical cross-section at approximately right angle to the contour lines of the tropopause. The components in this plane of the tropospheric and the stratospheric horizontal temperature gradients at the tropopause are represented through $\Delta\tau$ and $\Delta\tau_s$ respectively. Subscript h refers to the tropopause level, and subscript s to the stratosphere.

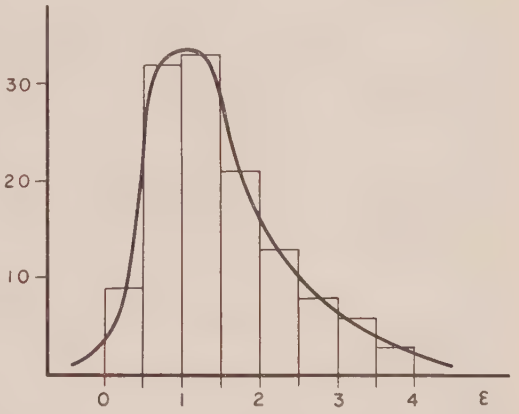

Fig. 4. Frequency distribution for ε. The number of cases within each of the intervals 0.0—0.5, 0.5—1.0 etc. up to 3.5—4.0 are given by means of a histogram. The total number of cases is 147.

In the model one has assumed that the stratospheric temperature gradient is independent of height, whereas the magnitude of the observed one in general decreases with height, and a change in direction may also occur. This actual decrease in magnitude can be accounted for in the model by proper choice

Table 1. Mean values of the parameter ε

Month	Total number of cases	Number of cases with:			Mean values
		$0 \leq \varepsilon \leq 3.99$	$\varepsilon \geq 4.00$	$\varepsilon < 0$	$0 \leq \varepsilon \leq 3.99$
Febr. 1950	28	23	0	5	1.23
July »	29	26	2	1	1.26
Aug. »	30	28	1	1	1.67
Nov. 1951	29	25	1	3	1.50
Dec. »	31	23	4	4	1.48
Period	147	125	8	14	1.43

of the parameter ε. In order to study this decrease to a certain extent, the temperature difference at 100 mb between the two stations in fig. 3 — whenever available — was computed. In the average this difference was 40 % of that at the tropopause level. Altogether 137 cases were treated and in 15 of these, change in the sign of the temperature difference was observed. In 3 cases it increased with height. These 18 cases were associated with weak to moderate temperature differences.

In spite of the very limited region (the British Isles and the two British weather ships in the Atlantic), to which the aerological material used here refers, the results are presumably valid for middle latitudes. In high latitudes negative values of ε will — at least in wintertime — occur more frequently than in middle latitudes, and the assumption of proportionality between the two temperature gradients may turn out to be in less agreement with observations.

3. Integration of the vorticity equation along the vertical

The integrated vorticity equation. When friction is neglected the vorticity equation may be written as follows:

$$\frac{\partial \eta}{\partial t} + \mathbf{v} \cdot \nabla \eta =$$

$$-\left(\eta \operatorname{div} \mathbf{v} + \frac{f}{\varrho} \mathbf{v}_g \cdot \nabla \varrho + w \frac{\partial \zeta}{\partial z} + \nabla w \times \frac{\partial \mathbf{v}}{\partial z} \cdot \mathbf{k}\right)$$

where $\mathbf{v}$ is the horizontal wind vector, $\eta = \zeta + f$ the absolute vorticity component along the vertical, w the vertical velocity, and $\mathbf{v}_g$ the geostrophic wind. Elimination of div $\mathbf{v}$ by use of the equation of continuity

$$\varrho \operatorname{div} \mathbf{v} + \frac{\partial}{\partial z} \varrho w + \mathbf{v} \cdot \nabla \varrho + \frac{\partial \varrho}{\partial t} = 0$$

gives:

$$\varrho \frac{\partial \eta}{\partial t} + \varrho \mathbf{v} \cdot \nabla \eta = \eta \left[\frac{\partial}{\partial z} \varrho w + \mathbf{v} \cdot \nabla \varrho + \frac{\partial \varrho}{\partial t}\right] -$$

$$- f \mathbf{v}_g \cdot \nabla \varrho - \varrho w \frac{\partial \zeta}{\partial z} - \varrho \nabla w \times \frac{\partial \mathbf{v}}{\partial z} \cdot \mathbf{k}$$

It is generally assumed that the last term on the right hand side is comparatively small, and it is therefore neglected here. Furthermore the terms $\eta \mathbf{v} \cdot \nabla \varrho$ and $\eta \frac{\partial \varrho}{\partial t}$ are small compared with the terms $\varrho \mathbf{v} \cdot \nabla \eta$ and $\varrho \frac{\partial \eta}{\partial t}$ because the relative change $\frac{\triangle \varrho}{\varrho}$ in the density is in all cases of practical interest very much smaller than the relative change $\frac{\nabla \eta}{\eta}$ in the absolute vorticity. In virtue of this the vorticity equation is reduced to:

$$\varrho \frac{\partial \eta}{\partial t} + \varrho \mathbf{v} \cdot \nabla \eta = \eta \frac{\partial}{\partial z}(\varrho w) - \varrho w \frac{\partial \zeta}{\partial z} = \eta^2 \frac{\partial}{\partial z}\left(\frac{\varrho w}{\eta}\right) \qquad (3, 1)$$

Equation (3, 1) will now be integrated with respect to z for the boundary conditions $w = 0$ for $z = 0$ and $\varrho = 0$ for $z = \infty$ ($\frac{w}{\eta}$ finite at infinity) by use of the model described in the preceding section. This implies that $\mathbf{v}$ and η are to be interpreted as the geostrophic wind and the geostrophic vorticity of the model. Moreover, we will assume that the integrated contribution due to the variation in η^2 with height is so small that it can be neglected. This together with the boundary conditions makes the right hand side of (3, 1) disappear when integrated from $z = 0$ to $z = \infty$, and we obtain:

$$\int_0^\infty \varrho \frac{\partial \zeta}{\partial t} dz + \beta \int_0^\infty \varrho v dz + \int_0^\infty \varrho \mathbf{v} \cdot \nabla \zeta dz = 0 \qquad (3, 2)$$

where $\beta = \frac{df}{dy}$ and $v = \frac{1}{f\varrho} \frac{\partial p}{\partial x}$ is the y-component of the geostrophic wind. It is possible to make a certain statement regarding the sign of the error introduced by neglecting the variation in η^2 with height. Fig. 5 gives a schematic picture of η^2, $\frac{\varrho w}{\eta}$, and $\frac{\partial}{\partial z}\left(\frac{\varrho w}{\eta}\right)$ as functions of z.

Obviously, η^2 decreasing with height will make the $\int_0^\infty \eta^2 \frac{\partial}{\partial z}\left(\frac{\varrho w}{\eta}\right) dz$ positive when associated with positive vertical velocity and negative when associated with negative vertical velocity. This statement is to be reversed when η^2 increases with height. Apart from this qualitative consideration we will not at this stage try to evaluate the integrated contribution of the right hand side of (3, 1), but it is assumed to be comparatively small in most of cases.

Substituting in (3, 2) for ϱ, $\mathbf{v}$ and ζ the expressions given in the preceding section, the integration can be carried out by elementary methods; but, since a considerable amount of calculation is involved, the details are not given here. From the expressions quoted it can be seen that all the integrals to be evaluated are of the two types $\int_0^h \left(\frac{\tau}{\tau_0}\right)^n z^q dz$ and $\int_0^\infty e^{-mz} z^q dz$ where m, n and q are independent of z, τ is the temperature at the height z and τ_0 the temperature at the zero level.

Having carried out the integration of (3, 2) the following equation is obtained:

$$A_1\frac{\partial \zeta_0}{\partial t} + A_2\frac{\partial \zeta'}{\partial t} - A_3\frac{\partial \zeta''}{\partial t} + \frac{\beta}{f}\left(\frac{1}{\varrho_0}A_1\frac{\partial p_0}{\partial x} + \right.$$
$$\left. + \frac{g}{\tau_0}A_2\frac{\partial \tau_0}{\partial x} - \frac{g}{2\tau_0}A_3\frac{\partial k}{\partial x}\right) + \mathbf{v}_0 \cdot (A_4 \nabla \zeta_0 +$$
$$+ A_5 \nabla \zeta' - A_6 \nabla \zeta'') + \mathbf{v}' \cdot (A_5 \nabla \zeta_0 + A_7 \nabla \zeta' -$$
$$- A_8 \nabla \zeta'') - \mathbf{v}'' \cdot (A_6 \nabla \zeta_0 + A_8 \nabla \zeta' - A_9 \nabla \zeta'') = 0 \qquad (3, 3)$$

The coefficients $A_1, A_2, \ldots A_9$ are in general positive and are functions of the parameters k, h, ε, p_0 and τ_0 of the model. Except for A_1 and A_4, which do not contain ε, each of the coefficients depends upon all the parameters. This functional relationship will be discussed at some length later on.

The considerable number of terms makes (3, 3) somewhat unattractive to deal with, and before attempting a general discussion two special cases will be mentioned:

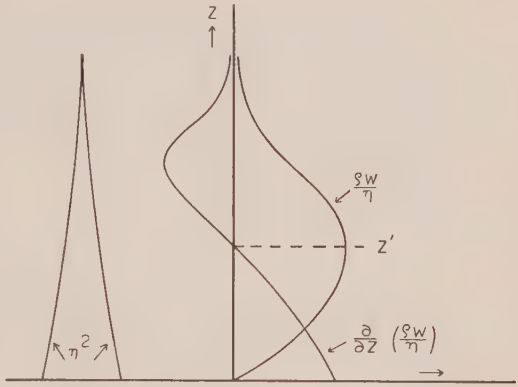

Fig. 5. A schematic picture of the curves η^2, $\frac{\varrho w}{\eta}$ and $\frac{\partial}{\partial z}\left(\frac{\varrho w}{\eta}\right)$. The area between the $\frac{\partial}{\partial z}\left(\frac{\varrho w}{\eta}\right)$ curve and the z-axis is divided in two equal parts by the level $z = z'$.

a. No horizontal temperature gradient, i.e. $\nabla \tau = \nabla k = 0$. Equation (3, 3) reduces to:

$$\frac{\partial \zeta_0}{\partial t} + \mathbf{v}_0 \cdot \nabla f + \frac{A_4}{A_1}\mathbf{v}_0 \cdot \nabla \zeta_0 = 0 \text{ where } \frac{\beta}{f\varrho_0}\frac{\partial p_0}{\partial x} \qquad (3, 4)$$

has been replaced by $\mathbf{v}_0 \cdot \nabla f$. Except for the factor $\frac{A_4}{A_1}$, (3, 4) is identical with the barotropic vorticity equation

$$\frac{\partial \zeta}{\partial t} + \mathbf{v} \cdot \nabla (f + \zeta) = 0 \qquad (3, 5)$$

where $\mathbf{v}$ and ζ are independent of height. While in the baroropic case it is assumed that the vertical velocity is identically zero, no such assumption underlies the derivation of equ. (3, 4). This difference, however, is only of academic interest, since an identically vanishing temperature gradient is physically not compatible with non-vanishing vertical velocity, except in connection with adiabatic processes in an atmosphere with adiabatic temperature lapse-rate.

The ratio $\frac{A_4}{A_1}$ depends practically on the lapse-rate k only; it is equal to unity for $k = 0$ and drops to 0.86 for $k = 0.75 \cdot 10^{-2}$ °C/meter. The difference between the case considered

here ($\nabla\tau=0$) and the barotropic one is explained by the fact that in the latter case the temperature is constant along a pressure surface while in the former it is prescribed to stay constant in a horizontal plane. Only for $k=0$, or when the pressure surfaces are horizontal, are these two cases identical.

b. Uniform temperature lapse-rate, i.e. $\nabla k=0$. In this case equation (3, 3) reduces to:

$$A_1\frac{\partial\zeta_0}{\partial t}+A_2\frac{\partial\zeta'}{\partial t}+\frac{\beta}{f}\left(\frac{A_1}{\varrho_0}\frac{\partial p_0}{\partial x}+\frac{g}{\tau_0}A_2\frac{\partial\tau_0}{\partial x}\right)+\mathbf{v}_0\cdot$$
$$\cdot(A_4\nabla\zeta_0+A_5\nabla\zeta')+\mathbf{v}'\cdot(A_5\nabla\zeta_0+A_7\nabla\zeta')=0 \qquad (3,\ 6)$$

The geostrophic wind is now a linear function of height, and as is well known, models with this property have been used by many authors when dealing with small perturbations, and with considerable success. In a paper not yet published equ. (3, 6) has been applied to investigate the speed, vertical velocity, and, to a certain extent, the stability of spherical harmonic wave disturbances superimposed upon a uniform basic current. The results were promising and it would seem that (3, 6) is an approximation good enough to give reasonably correct answers to certain types of problems.

Discussion of the coefficients of the integrated vorticity equation in relation to the parameters of the model. Returning to the integrated vorticity equation (3, 3) we will now insert $\frac{1}{f\varrho_0}\nabla^2 p_0$, $\frac{g}{\tau_0}\nabla^2\tau_0$ and $\frac{g}{2f\tau_0}\nabla^2 k$ for ζ_0, ζ' and ζ'' respectively. After the substitution and a multiplication of all the terms with the Coriolis parameter f, equ. (3, 3) takes the form:

$$B_1\nabla^2\frac{\partial p_0}{\partial t}+B_2\nabla^2\frac{\partial\tau_0}{\partial t}-B_3\nabla^2\frac{\partial k}{\partial t}+\beta\left(B_1\frac{\partial p_0}{\partial x}+\right.$$
$$\left.+B_2\frac{\partial\tau_0}{\partial x}-B_3\frac{\partial k}{\partial x}\right)+\mathbf{v}_0\cdot(B_4\nabla\nabla^2 p_0+$$
$$+B_5\nabla\nabla^2\tau_0-B_6\nabla\nabla^2 k)+\mathbf{v}'\cdot$$
$$\cdot\left(\frac{\tau_0}{g\varrho_0}B_5\nabla\nabla^2 p_0+B_7\nabla\nabla^2\tau_0-B_8\nabla\nabla^2 k\right)-$$
$$-\mathbf{v}''\left(\frac{2\tau_0}{g\varrho_0}B_6\nabla\nabla^2 p_0+2B_8\nabla\nabla^2\tau_0-\right.$$
$$\left.-B_9\nabla\nabla^2 k\right)=0 \qquad (3,\ 7)$$

The relation between the two sets of coefficients is as follows:

$$\frac{f\cdot A_1}{B_1}=\frac{f\cdot A_4}{B_4}=\varrho_0;\ \frac{f\cdot A_2}{B_2}=\frac{f\cdot A_5}{B_5}=\frac{f\cdot A_7}{B_7}=\frac{\tau_0}{g};$$
$$\frac{f\cdot A_3}{B_3}=\frac{f\cdot A_6}{B_6}=\frac{f\cdot A_8}{B_8}=\frac{f\cdot A_9}{B_9}=\frac{2\tau_0}{g} \qquad (3,\ 8)$$

Each of the coefficients B_1, B_2, ... B_9 is a function of all the parameters k, h, ε, p_0 and τ_0 except for B_1 and B_4, which do not contain ε.

Analytical expressions for the coefficients in terms of the parameters of the model are found in the appendix.

We will now investigate to what extent the coefficients are sensitive for variation in the parameters, since this is a question of great practical importance when applying the equation (3, 7). It appears when studying the expressions for the coefficients, that p_0 is a common factor for all of them expect B_1 and B_4, where we, however, can introduce p_0 by replacing $R\tau_0$ by $\frac{p_0}{\varrho_0}$. Thus a change in the surface pressure does not directly influence the relative magnitude of the coefficients in (3, 7). After division with the common factor p_0, B_1 and B_4 and the coefficients for $\mathbf{v}'\cdot\nabla\nabla^2 p_0$ and $\mathbf{v}''\cdot\nabla\nabla^2 p_0$ are proportional to the surface value $\alpha_0=\frac{1}{\varrho_0}$ of the specific volume and will therefore vary in the same manner. The relative change in α_0 is, however, so small, that for practical purposes it may generally be neglected.

The relation to the surface temperature τ_0 is considerably more complicated and cannot easily be surveyed without making computations for different values of τ_0. This has therefore been done for $\tau_0=255$, 270, 285 and 300 degrees absolute, keeping the parameters k, h and ε constant and equal to $0.65\cdot10^{-2}$ °C/meter, 10 km and 0.50 respectively. The results are given in table 2, where values of all the coefficients in equ. (3, 7) have been computed for the four different values of τ_0 and for $p_0=1{,}000$ mb. For 15° C variation in τ_0 the percental change in the coefficients is from 2—10 %. It is worth-while to notice that some of the coefficients increase with increasing τ_0 while others decrease. Although all the terms of equ. (3, 7) are of the same

Table 2. Values of the coefficients of equ. (3, 7) for four different values of τ_0, and for k, p_0, h and ε equal to 0.65 · 10^{-2} °C/m, 1,000 mb, 10 km and 0.50 respectively

	$\tau_0 = 255°$	$\tau_0 = 270°$	$\tau_0 = 285°$	$\tau_0 = 300°$
$B_1 \cdot 10^{-4}$	0.6457	0.6862	0.7270	0.7679
$B_2 \cdot 10^{-4}$	0.1759	0.1677	0.1596	0.1520
$B_3 \cdot 10^{-8}$	0.0472	0.0434	0.0395	0.0359
$B_4 \cdot 10^{-4}$	0.5647	0.6017	0.6392	0.6769
$B_5 \cdot 10^{-4}$	0.1439	0.1384	0.1330	0.1277
$B_6 \cdot 10^{-8}$	0.0380	0.0354	0.0327	0.0301
$\frac{\tau_0}{g\varrho_0} \cdot B_5 \cdot 10^{-8}$	0.2736	0.2952	0.3160	0.3362
$B_7 \cdot 10^{-8}$	0.1176	0.1139	0.1103	0.1074
$B_8 \cdot 10^{-12}$	0.0439	0.0431	0.0424	0.0423
$\frac{2\tau_0}{g\varrho_0} \cdot B_6 \cdot 10^{-12}$	0.1444	0.1510	0.1556	0.1583
$B_9 \cdot 10^{-16}$	0.0459	0.0475	0.0495	0.0525

order of magnitude it turns out that those with B_1, B_2, B_4 and B_5 are in general the most important. These coefficients show a variation of around 1 % for a 5° C change in τ_0, but for B_1 and B_4 the variation is opposite to that of B_2 and B_5.

Next we shall consider variations merely due to the lapse-rate k. Table 3 gives the values of the B:s for $k = 0.55$, 0.65 and $0.75 \cdot 10^{-2}$ °C/meter. The other parameters τ_0, p_0, h and ε have been asigned the values: 285° absolute, 1,000 mb, 10 km and 0.50 respectively.

Within this range of k none of the coefficients shows a variation exceeding 5 %. Some of the coefficients, however, increase whereas other decrease for the same change in k.

The last column in table 3 gives the values of the coefficients in the case of isothermalcy in the z-direction. This very special case implies no tropopause and consequently no discontinuity in the derivatives of the temperature. The values given correspond to $\tau = 220$ degrees absolute. Analytical expressions for the B:s in this special case are given in the appendix.

Finally the sensitivity with regard to variation in h and ε will be discussed. It appears when one compares reasonable ranges for the parameters that the sensitivity of the coefficients is somewhat greater for changes in h and ε than for changes in the parameters discussed so far. As earlier B_1 and B_4 change in a way different from the rest of the coefficients.

Values of all the coefficients for $h = 8$, 10, 12, 14 and 16 km and $\varepsilon = 1.00$, 0.75, 0.50, 0.25, 0.0, − 0.25, − 0.50, − 0.75 and − 1.00 are given in the appendix. The remaining parameters have been chosen as follows: $\tau_0 = 285°$ absolute, $p_0 = 1{,}000$ mb, $k = 0.65 \cdot 10^{-2}$ °C/meter. B_1 and B_4 have been computed for three values of k.

Above there has been given a brief discussion of the coefficients of the integrated vorticity equation in relation to the parameters of the model. For practical reasons, and also to be consistent with the basic equations describing the model, one will when applying equ. (3, 7) have to work with certain mean values for the parameters p_0, τ_0, k, h and ε. Obviously this implies a certain inaccuracy in the results, since the coefficients vary with the parameters as shown above. Although this investigation regarding the sensitivity of the coefficients with respect to the parameters is somewhat incomplete, it is quite clear that a proper choice of the parameters h and ε is important. This applies particularly to the latter, the variability of which, in space and time, imposes a considerable restriction upon the applicability of equ. (3, 7). Applied to a

Table 3. Values of the coefficients of equ. (3, 7) for $k = 0.55, 0.65, 0.75 \cdot 10^{-2}$ °C/meter and for τ_0, p_0, h and ε equal to 285°, 1,000 mb, 10 km and 0.50 respectively. The last column gives the coefficients in the case of isothermalcy in the vertical ($\tau = 220°$ abs.)

k	$0.55 \cdot 10^{-2}$	$0.65 \cdot 10^{-2}$	$0.75 \cdot 10^{-2}$	0.00
$B_1 \cdot 10^{-4}$	0.7429	0.7270	0.7112	0.6436
$B_2 \cdot 10^{-4}$	0.1598	0.1596	0.1596	0.2926
$B_3 \cdot 10^{-8}$	0.0394	0.0395	0.0399	0.1883
$B_4 \cdot 10^{-4}$	0.6657	0.6392	0.6138	0.6436
$B_5 \cdot 10^{-4}$	0.1371	0.1330	0.1290	0.2926
$B_6 \cdot 10^{-8}$	0.0337	0.0327	0.0320	0.1883
$\frac{\tau_0}{g\varrho_0} \cdot B_5 \cdot 10^{-8}$	0.3258	0.3160	0.3065	0.4143
$B_7 \cdot 10^{-8}$	0.1110	0.1103	0.1101	0.3766
$B_8 \cdot 10^{-12}$	0.0429	0.0424	0.0423	0.1818
$\frac{2\tau_0}{g\varrho_0} \cdot B_6 \cdot 10^{-12}$	0.1599	0.1556	0.1519	0.5332
$B_9 \cdot 10^{-16}$	0.0505	0.0495	0.0491	0.1560

limited region and using carefully chosen mean values of the parameters the errors involved can certainly in most cases be kept below 20 %. In favourable cases the error may amount to a few per cent only.

4. The levels of mean wind and non-divergence

The level of mean wind. It is common when dealing with numerical forecasting to replace the actual atmosphere by a barotropic one, which has the same horizontal pressure distribution as the former when averaged with respect to height. These mean conditions will in general be found to be the same as those observed at some middle level — for inst. 500 mb — and the problem is thereby reduced to two dimensions.

It is of great practical importance to investigate to what extent the level representing the mean conditions depend upon the particular distribution of temperature and pressure, and whether or not it can be assumed to be approximately at a constant height or a constant pressure in time and space. If such a constancy is found to exist, it may be a great advantage in the theory of three-dimensional numerical forecasting to choose this level as a level of reference, rather than the earths surface or some other levels. This particular level will here be referred to as the *level of mean wind.*

Study of observed wind profiles (CHARNEY 1947) has revealed that the zonal wind at around 600 mb is in the average equal to the mean zonal wind defined by the equation:

$$\bar{U} = \frac{1}{p_0} \int_0^{p_0} U dp \qquad (4, 1)$$

where U is the zonal wind component, and the bar refers to an average with respect to a vertical coordinate. Applying this concept of a mean wind to the geostrophic wind of our model, we will now attempt to determine a tropospheric level, at which the wind is equal to a mean wind defined in accordance with equ. (4, 1).

Utilizing expressions for $\mathbf{v}$ as a function of z given earlier in this paper, the integration is easily carried out, and the following result is obtained:

$$\bar{\mathbf{v}} = \frac{g}{p_0} \left(\varrho_0 B_1 \mathbf{v}_0 + \frac{\tau_0}{g} B_2 \mathbf{v}' - \frac{2\tau_0}{g} B_3 \mathbf{v}'' \right) \qquad (4, 2)$$

Table 4. Computed values for z (in km) in equ. (4, 4) for $\tau_0 = 285°$ and $k = 0.65 \cdot 10^{-2}$ °C/meter, and h and ε ranging from 8—16 km and 1.00 to —1.00 resp.

	h / ε	1.00	0.75	0.50	0.25	0.00	— 0.25	— 0.50	— 0.75	— 1.00
$z_2 = \frac{\tau_0}{p_0} \cdot B_2$	8 km	2.1	2.9	3.6	4.3	5.0	5.7	6.5	7.2	7.9
	10 »	3.5	4.0	4.6	5.1	5.6	6.2	6.7	7.2	7.8
	12 »	4.5	4.9	5.3	5.7	6.1	6.5	6.8	7.2	7.6
	14 »	5.3	5.5	5.8	6.1	6.4	6.7	6.9	7.2	7.5
	16 »	5.8	6.0	6.2	6.4	6.6	6.8	7.0	7.2	7.4
$z_3 = \sqrt{\frac{2\tau_0}{p_0} \cdot B_3}$	8 km	Not real		3.1	4.7	5.8	6.7	7.5	8.2	8.9
	10 »	1.1	3.4	4.7	5.8	6.6	7.4	8.1	8.7	9.3
	12 »	4.4	5.1	5.9	6.7	7.3	7.9	8.5	9.0	9.5
	14 »	5.6	6.2	6.8	7.4	7.9	8.3	8.8	9.2	9.6
	16 »	6.6	7.1	7.5	7.9	8.3	8.6	9.0	9.3	9.6

where the notations are the same as used earlier.

Assuming that there is at least one level within the troposphere at which the wind is equal to $\bar{\mathbf{v}}$, this level is in virtue of (2, 12) determined from:

$$\left(\frac{\tau}{\tau_0} - \frac{g\varrho_0}{p_0} B_1\right) \mathbf{v}_0 + \left(z - \frac{\tau_0}{p_0} B_2\right) \mathbf{v}' - \left(z^2 - \frac{2\tau_0}{p_0} B_3\right) \mathbf{v}'' = 0 \qquad (4, 3)$$

where z is the height of this level and τ the corresponding temperature. If all the coefficients of (4, 3) are zero for the same z, this is independent of the particular distribution of pressure and temperature; if not, the level of mean wind will be different from one case to another depending upon the special features of the fields of pressure and temperature.

Putting the coefficients in (4, 3) equal to nought, the following three independent equations for determining z are obtained:

$$\frac{\tau}{\tau_0} = 1 - \frac{k}{\tau_0} z = \frac{g}{R\tau_0} B_1; \quad z = \frac{\tau_0}{p_0} B_2; \quad z^2 = \frac{2\tau_0}{p_0} B_3 \qquad (4, 4)$$

It appears from the expressions for B_1, B_2 and B_3 given in the appendix that z is independent of p_0 and from earlier discussion on the B:s that for practical purposes variation in τ_0 and k may be neglected. The first equation (4, 4) gives $z = 5.0$ km for $h = 8$ km and increasing almost linearly to 6.6 km for $h = 16$ km (B_1 is indep. of the parameter ε).

The values of z in km obtained from the second and third equation of (4, 4) are given in table 4 as z_2 and z_3. It is interesting to note that these two are for most values of h and ε rather close to each other, the latter being (in general by $^1/_2$—1 km) the highest.

Although the three equ. (4, 4) do not give identically the same values for z, we still may conclude, that the particular horizontal distribution of temperature and pressure is rather unimportant for the determination of this level. Obviously the level of mean wind is highest when the horizontal temperature gradient is caused by non-uniformity in lapse-rate only. In the case of reasonably strong and uniform temperature gradient this level is very close to the level given by z_2, which is the lowest one of those three determined from (4, 4).

The results given here are in very close agreement with the value 4.0—4.5 km for mean zonal wind at middle latitudes given by CHARNEY (1947).

Due to the increase in the height of the tropopause from the pole to the equator, one would expect that the level of mean wind increases in height towards low latitudes. The parameter ε, however, presumably decreases towards higher latitudes and this effects the height in an opposite direction. Assuming h and ε to be 14 km and 0.75 respectively at 30° latitude and $h = 9$ km and $\varepsilon = 0.25$ at 70° latitude the level of the mean wind will be around only 1 km higher at 30° than at 70° lat. This corresponds approximately to the slope of the 500 mb surface.

The mean relative vorticity $\bar{\zeta}$ is obviously given by an equation analogous to (4, 2), namely:

$$\bar{\zeta} = \frac{g}{p_0}\left(\varrho_0 B_1 \zeta_0 + \frac{\tau_0}{g} B_2 \zeta' - \frac{2\tau_0}{g} B_3 \zeta''\right) \quad (4, 5)$$

Taking the level of mean wind as our level of reference, the wind velocity $\mathbf{v}$ and the relative vorticity ζ may be expressed as follows:

$$\mathbf{v} = \bar{\mathbf{v}} + \mathbf{v}^\star \text{ and } \zeta = \bar{\zeta} + \zeta^\star \quad (4, 6)$$

where $\mathbf{v}^\star$ and $\zeta^\star$ are the deviations from the respective means. If this is introduced into the vorticity equation (3, 2) it is possible to compute the vorticity advection $\overline{\mathbf{v}^\star \cdot \nabla \zeta^\star}$. Obviously,

$$\overline{\mathbf{v}^\star \cdot \nabla \zeta^\star} = \overline{\mathbf{v} \cdot \nabla \zeta} - \bar{\mathbf{v}} \cdot \nabla \bar{\zeta} \quad (4, 7)$$

The first term on the right hand side of this equation is known from (3, 3) and inserting for $\bar{\mathbf{v}}$ and $\bar{\zeta}$ from (4, 2) and (4, 5) resp. the following expression for $\overline{\mathbf{v}^\star \cdot \nabla \zeta^\star}$ is arrived at:

$$\overline{\mathbf{v}^\star \cdot \nabla \zeta^\star} = \mathbf{v}_0 \cdot (C_4 \nabla \zeta_0 + C_5 \nabla \zeta' - C_6 \nabla \zeta'') + \\ + \mathbf{v}' \cdot (C_5 \nabla \zeta_0 + C_7 \nabla \zeta_1 - C_8 \nabla \zeta'') - \mathbf{v}'' \cdot \\ \cdot (C_6 \nabla \zeta_0 + C_8 \nabla \zeta' - C_9 \nabla \zeta'') \quad (4, 8)$$

Expressions for $\bar{\mathbf{v}} \cdot \nabla \zeta$ and the coefficients $C_4, \ldots C_9$ in terms of $B_1, \ldots B_9$ are given in the appendix. Having computed all the C:s comparison is made between $\overline{\mathbf{v}^\star \cdot \nabla \zeta^\star}$ and $\bar{\mathbf{v}} \cdot \nabla \bar{\zeta}$ written in a form analogous to (4. 8). We find then that C_4 is practically zero and that C_5 and C_6 amount to approximately 5 % and 10 % resp. of the corresponding coefficients in the expression for $\bar{\mathbf{v}} \cdot \nabla \bar{\zeta}$. The corresponding figures for C_7, C_8 and C_9 are 50 %, 100 % and 100—500 % resp.

In the case of uniform lapse-rate ($\nabla k = 0$) the vorticity advection would seem to be determined mainly by the advection of mean vorticity by the mean wind, but the more complicated the temperature distribution becomes, the more important becomes the "eddy" term $\overline{\mathbf{v}^\star \cdot \nabla \zeta^\star}$. When judging, however, the importance of this compared with $\bar{\mathbf{v}} \cdot \nabla \bar{\zeta}$, the relative magnitude of the various terms in (4, 8) or the corresponding expression for $\bar{\mathbf{v}} \cdot \nabla \bar{\zeta}$, has to be taken into consideration. Rather often is it so, that the terms containing a derivative of the temperature lapse-rate are considerably smaller than the others.

We will now neglect the terms with C_4, C_5 and C_6 in the expression for $\overline{\mathbf{v}^\star \cdot \nabla \zeta^\star}$, which is then reduced to:

$$\overline{\mathbf{v}^\star \cdot \nabla \zeta^\star} = C_7 \mathbf{v}' \cdot \nabla \zeta' - C_8 \mathbf{v}' \cdot \nabla \zeta'' - C_8 \mathbf{v}'' \cdot \\ \cdot \nabla \zeta' + C_9 \mathbf{v}'' \cdot \nabla \zeta'' \quad (4, 9)$$

and try to determine a coefficient γ such that

$$\overline{\mathbf{v}^\star \cdot \nabla \zeta^\star} = \gamma \, \mathbf{v}_T(\bar{z}) \cdot \nabla \zeta_T(\bar{z})$$

where $\bar{z}$ is the level of mean wind and $\mathbf{v}_T$ and ζ_T the thermal wind and the thermal relative vorticity respectively for the layer $z =$ 0 to $z = \bar{z}$. But,

$$\mathbf{v}_T(\bar{z}) \cdot \nabla \zeta_T(\bar{z}) = \bar{z}^2 \mathbf{v}' \cdot \nabla \zeta' - \bar{z}^3 \mathbf{v}' \cdot \nabla \zeta'' - \\ \bar{z}^3 \mathbf{v}'' \cdot \nabla \zeta' + \bar{z}^4 \mathbf{v}'' \cdot \nabla \zeta''$$

Comparison with (4, 9) shows that γ will somewhat depend upon the particular distribution of temperature and pressure. In the case of uniform lapse-rate, i.e. $\mathbf{v}'' = \zeta'' = 0$ γ is determined from: $\gamma = \frac{C_7}{\bar{z}^2}$

One finds that γ is nearly constant within a reasonable range of the parameters h and ε of the model and can in the average be put equal to 0.5.

In the very special case of a horizontal temperature distribution which is exclusively due to non-uniformity in the temperature lapse-rate, γ is determined by the following equation:

$$\gamma = \frac{C_9}{\bar{z}^4}$$

For the most common values of h and ε, γ is within the range 1—4. As an overall value for γ in the general case we will suggest the number 0.6.

The integrated vorticity equation may then be written

$$\frac{\partial \bar{\zeta}}{\partial t} = -\bar{\mathbf{v}} \cdot \nabla \bar{\eta} - 0.6 \cdot \mathbf{v}_T \cdot \nabla \zeta_T \quad (4, 10)$$

The second term on the right hand side of (4, 10) is sometimes called the "development

term". By this is meant that this term admits non-conservative changes of the vorticity in the mean motion. In practice one may possibly identify the level of mean wind with the 500 mb surface. From (4, 10) we then learn that the tendency at this level can be computed by means of two maps, namely the 500 mb map and the map for the relative topography 1,000—500 mb.

The level of non-divergence. Besides the level of mean wind, the so-called level of non-divergence plays an important role in numerical forecasting. By definition, the barotropic vorticity equation

$$\frac{\partial \eta}{\partial t} + \mathbf{v} \cdot \nabla \eta = 0$$

shall apply at the latter level, and consequently the left hand side of equ. (3, 1) has to be nought there.

Because of the great simplification the knowledge of this level means to the theory and practical procedures for numerical forecasting, an attempt will be made to gather some information regarding this level by consideration similar to that given above for the level of mean wind.

Substituting for the wind velocity and relative vorticity from (2, 12) and (2, 16) p. . . . into $\frac{\partial \zeta}{\partial t} + \beta v + \mathbf{v} \cdot \nabla \zeta = 0$ and comparing with the integrated vorticity equation (3, 3), the following equation for determining the height z of the level of non-divergence is arrived at:

$$\left(A_1 - \frac{p_0}{g}\frac{\tau}{\tau_0}\right)\frac{\partial \zeta_0}{\partial t} + \left(A_2 - \frac{p_0}{g}z\right)\frac{\partial \zeta'}{\partial t} -$$

$$\left(A_3 - \frac{p_0}{g}z^2\right)\frac{\partial \zeta''}{\partial t} + \frac{\beta}{\varrho_0 f}\left(A_1 - \frac{p_0}{g}\frac{\tau}{\tau_0}\right)\frac{\partial p_0}{\partial x} +$$

$$+ \frac{\beta}{f}\cdot\frac{g}{\tau_0}\left(A_2 - \frac{p_0}{g}z\right)\frac{\partial \tau_0}{\partial x} - \frac{\beta}{f}\cdot\frac{g}{2\tau_0}\left(A_3 -\right.$$

$$\left. - \frac{p_0}{g}z^2\right)\frac{\partial k}{\partial x} + \left(A_4 - \frac{p_0}{g}\left(\frac{\tau}{\tau_0}\right)^2\right)\mathbf{v}_0 \cdot \nabla \zeta_0 +$$

$$+ \left(A_5 - \frac{p_0}{g}\frac{\tau}{\tau_0}z\right)\mathbf{v}_0 \cdot \nabla \zeta' - \left(A_6 - \frac{p_0}{g}\frac{\tau}{\tau_0}z^2 \cdot\right)$$

$$\cdot \mathbf{v}_0 \cdot \nabla \zeta'' + \left(A_5 - \frac{p_0}{g}\frac{\tau}{\tau_0}z\right)\mathbf{v}' \cdot \nabla \zeta_0 +$$

$$+ \left(A_7 - \frac{p_0}{g}z^2\right)\mathbf{v}' \cdot \nabla \zeta' - \left(A_8 - \frac{p_0}{g}z^3\right)\mathbf{v}' \cdot$$

$$\cdot \nabla \zeta'' - \left(A_6 - \frac{p_0}{g}\frac{\tau}{\tau_0}z^2\right)\mathbf{v}'' \cdot \nabla \zeta_0 -$$

$$- \left(A_8 - \frac{p_0}{g}z^3\right)\mathbf{v}'' \cdot \nabla \zeta' + \left(A_9 - \frac{p_0}{g}z^4\right) \cdot$$

$$\cdot \mathbf{v}'' \cdot \nabla \zeta'' = 0 \qquad (4, 11)$$

By putting all the coefficients in (4, 11) equal to nought the following 9 independent equations for determinating z are obtained:

$$\frac{\tau}{\tau_0} = 1 - \frac{k}{\tau_0}z = \frac{g}{R\tau_0}B_1; \quad z = \frac{\tau_0}{p_0}B_2$$

$$z^2 = \frac{2\tau_0}{p_0}B_3; \quad \left(\frac{\tau}{\tau_0}\right)^2 = \frac{g}{R\tau_0}B_4$$

$$\frac{\tau}{\tau_0}z = \frac{\tau_0}{p_0}B_5; \quad \frac{\tau}{\tau_0}z^2 = \frac{2\tau_0}{p_0}B_6; \quad z^2 = \frac{\tau_0}{p_0}B_7$$

$$z^3 = \frac{2\tau_0}{p_0}B_8; \quad z^4 = \frac{2\tau_0}{p_0}B_9 \qquad (4, 12)$$

where the A:s have been replaced by B:s from (3, 8). The three first equations are identical with (4, 4) and the corresponding values of z were given in table 4 above.

The values for the remaining z:s are not given here, but it appears from them that the level of non-divergence is somewhat higher than the level of mean wind. How much, depends upon the particular horizontal distribution of temperature and pressure. When non-uniformity in the lapse-rate is the predominant feature of the field of temperature, the height difference between these two levels is slightly larger than in the case of uniform lapse-rate.

In fig. 6 we have given the height of the level of mean wind and the above mentioned height difference for the latter case. It appears from the figure that in middle latitudes, the level of non-divergence is from 0.7 to 3.0 km higher than the level of mean wind, and that the most frequent values for this height difference are below 1.5 km. Since ε is usually positive in middle latitudes and the most frequent values of k lie between 9 and 11 km, it is obvious from figure 6 that the level of mean wind is generally somewhat below the 500 mb surface and the

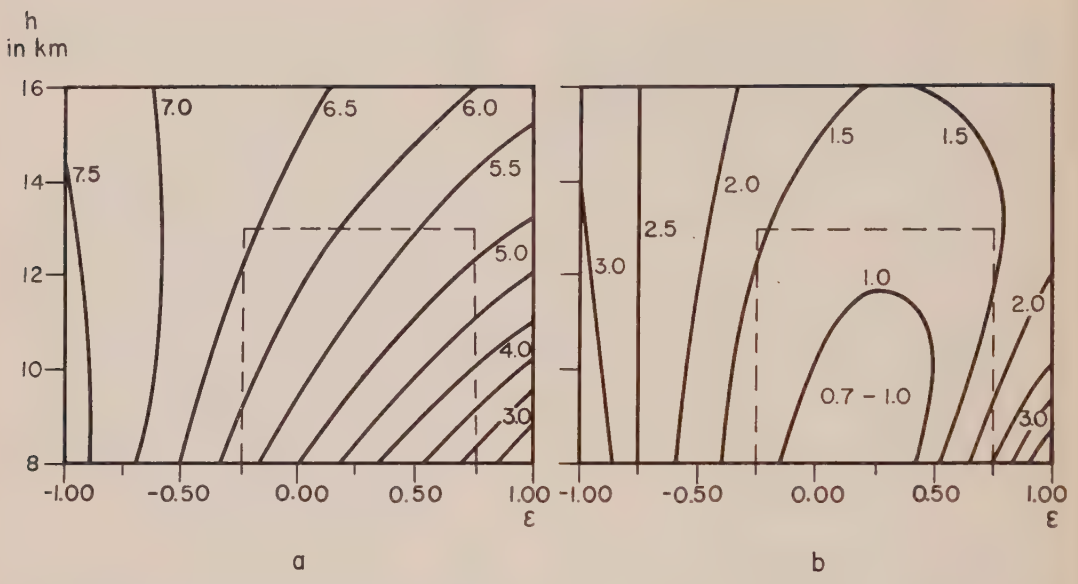

Fig. 6. The curved lines in a) are isopleths for the level of mean wind for the case of uniform lapse-rate. In b) the curves show how much the level of non-divergence is higher than the level of mean wind, also for the case of uniform lapse-rate. The numbers refer to km as a unit. The dashed rectangle gives the range of h and ε which is thought to cover middle latitudes.

level of non-divergence slightly above the same. *This is of considerable practical interest, since the 500 mb level may be used as an approximation for both of them.*

The results given here are in fair agreement with the statement (CHARNEY, FJÖRTOFT, v. NEUMANN, 1950) that the level of non-divergence is in the average between 400—500 mb.

So far considerations have only been given to the dynamical aspects connected with the model. In a following article the thermodynamics will be consulted, and a complete set of equations for the purpose of numerical forecasting of the fields of temperature and pressure will be derived.

APPENDIX

A. Expressions for the coefficients B_1, B_2 . . . . . B_9 of the equation (3, 7) p . . . in terms of the parameters of the model:

$$B_1 = \frac{R\tau_0}{g} \cdot \frac{n}{n+1}\left[1 + \frac{1}{n}\left(\frac{\tau_h}{\tau_0}\right)^{n+1}\right]$$

$$B_2 = \frac{p_0}{\tau_0}\left[\int_0^h \left(\frac{\tau}{\tau_0}\right)^n dz - \varepsilon\frac{R\tau_0}{g}\left(\frac{\tau_h}{\tau_0}\right)^n\right]$$

$$B_3 = \frac{p_0}{\tau_0}\left[\int_0^h \left(\frac{\tau}{\tau_0}\right)^n z\,dz - \varepsilon h \cdot \frac{R\tau_0}{g} \cdot \left(\frac{\tau_h}{\tau_0}\right)^n\right]$$

$$B_4 = \frac{R\tau_0}{g} \cdot \frac{n}{n+2}\left[1 + \frac{2}{n}\left(\frac{\tau_h}{\tau_0}\right)^{n+2}\right]$$

$$B_5 = \frac{p_0}{\tau_0}\left[\frac{n}{n+1}\int_0^h \left(\frac{\tau}{\tau_0}\right)^{n+1} dz + \left(\frac{h}{n+1} - \varepsilon\frac{R\tau_0}{g}\right) \cdot \left(\frac{\tau_h}{\tau_0}\right)^{n+1}\right]; \quad B_6 = \frac{p_0}{\tau_0}\left[\frac{n}{n+1}\int_0^h \left(\frac{\tau}{\tau_0}\right)^{n+1} \cdot z\,dz + h\left(\frac{h}{2(n+1)} - \varepsilon\frac{R\tau_0}{g}\right)\left(\frac{\tau_h}{\tau_0}\right)^{n+1}\right]$$

$$B_7 = \frac{2p_0}{\tau_0}\left[\int_0^h \left(\frac{\tau}{\tau_0}\right)^n z\,dz - \varepsilon\frac{R\tau_0}{g}\left(h - \varepsilon\frac{R\tau_0}{g}\right) \cdot \left(\frac{\tau_h}{\tau_0}\right)^n\right]; \quad B_8 = \frac{3}{2}\frac{p_0}{\tau_0}\left[\int_0^h \left(\frac{\tau}{\tau_0}\right)^n z^2 dz - \varepsilon\frac{R\tau_0}{g} \cdot h\left(h - \frac{4}{3}\varepsilon\frac{R\tau_0}{g}\right)\left(\frac{\tau_h}{\tau_0}\right)^n\right]$$

$$B_9 = \frac{2p_0}{\tau_0}\left[\int_0^h \left(\frac{\tau}{\tau_0}\right)^n z^3 dz - \varepsilon\frac{R\tau_0}{g}h^2 \cdot \right.$$
$$\left. \cdot \left(h - 2\varepsilon\frac{R\tau_0}{g}\right)\left(\frac{\tau_h}{\tau_0}\right)^n\right] \qquad (1)$$

The notations are the same as earlier. The integrals involved in the expressions for the coefficients are easily evaluated by use of the recurrence formula:

$$I_{n,q} = \int_0^h \left(\frac{\tau}{\tau_0}\right)^n z^q dz = \frac{\tau_0}{k(n+1)}\left[qI_{n+1,\,q-1} - \right.$$
$$\left. - h^q\left(\frac{\tau_h}{\tau_0}\right)^{n+1}\right] \qquad (2)$$

together with

$$I_{n,0} = \int_0^h \left(\frac{\tau}{\tau_0}\right)^n dz = \frac{\tau_0}{k(n+1)}\left[1 - \left(\frac{\tau_h}{\tau_0}\right)^{n+1}\right] \qquad (3)$$

B. Expressions for the coefficients B_1, B_2, ... B_9 in the case of isothermalcy in the z-direction.

$$B_1 = B_4 = \frac{R\tau_0}{g}, \quad B_2 = B_5 = \frac{Rp_0}{g}$$
$$B_3 = B_6 = B_2 \cdot B_1, \quad B_7 = 2B_6 = 2B_2 \cdot B_1 \qquad (4)$$
$$B_8 = \frac{3}{2}B_3 \cdot B_1 = \frac{3}{2}B_2 \cdot B_1^2, \quad B_9 = 2B_2 \cdot B_1^3$$

C. Numerical values for the coefficients B_1, B_2, ... B_9.

The tables 5 and 6 below give the values of B_1 and B_4 for $p_0 = 1{,}000$ mb, $\tau_0 = 285°$ absolute, the three k-values $0.55 \cdot 10^{-2}$, $0.65 \cdot 10^{-2}$ and $0.75 \cdot 10^{-2}$ °C/meter and $h = 8$, 10, 12, 14 and 16 km. The remaining coefficients are given in table 7 for the same p_0, τ_0 and h values, for $k = 0.65 \cdot 10^{-2}$ °C/meter only and ε ranging from -1.00 to $+1.00$.

Table 5. Computed values for $B_1 \cdot 10^{-4}$

h \ k	$0.55 \cdot 10^{-2}$	$0.65 \cdot 10^{-2}$	$0.75 \cdot 10^{-2}$
8 km . . .	0.7527	0.7383	0.7241
10 » . . .	5.7429	0.7270	0.7112
12 » . . .	0.7355	0.7186	0.7019
14 » . . .	0.7302	0.7126	0.6954
16 » . . .	0.7263	0.7083	0.6909

Table 6. Computed values for $B_4 \cdot 10^{-4}$

h \ k	$0.55 \cdot 10^{-2}$	$0.65 \cdot 10^{-2}$	$0.75 \cdot 10^{-2}$
8 km . . .	0.6820	0.6573	0.6335
10 » . . .	0.6657	0.6392	0.6138
12 » . . .	0.6541	0.6266	0.6006
14 » . . .	0.6461	0.6181	0.5919
16 » . . .	0.6406	0.6126	0.5866

D. Expressions for the term $\bar{\mathbf{v}} \cdot \nabla\bar{\zeta}$ and the coefficients C_4 . . . . . C_9 in equ. (4, 8)

$$\bar{\mathbf{v}} \cdot \nabla\bar{\zeta} = \left(\frac{g}{p_0}\right)^2\left[\varrho_0 B_1 \mathbf{v}_0 + \frac{\tau_0}{g}B_2\mathbf{v}' - \frac{2\tau_0}{g}B_3\mathbf{v}''\right] \cdot$$
$$\cdot \nabla\left[\varrho_0 B_1\zeta_0 + \frac{\tau_0}{g}B_2\zeta' - \frac{2\tau_0}{g}B_2\zeta''\right] =$$
$$= \mathbf{v}_0 \cdot \left[\left(\frac{g}{R\tau_0}\right)^2 B_1^2 \nabla\zeta_0 + \left(\frac{g}{R\tau_0}B_1\right) \cdot \right.$$
$$\left. \cdot \left(\frac{\tau_0}{p_0}B_2\right)\nabla\zeta' - \left(\frac{g}{R\tau_0}B_1\right) \cdot \left(\frac{2\tau_0}{p_0}B_3\right)\nabla\zeta''\right]$$
$$+ \mathbf{v}' \cdot \left[\left(\frac{g}{R\tau_0}B_1\right)\left(\frac{\tau_0}{p_0}B_2\right)\nabla\zeta_0 + \left(\frac{\tau_0}{p_0}B_2\right)^2\nabla\zeta' - \right.$$
$$\left. - \left(\frac{\tau_0}{p_0}B_2\right)\left(\frac{2\tau_0}{p_0}B_3\right)\nabla\zeta''\right]$$
$$- \mathbf{v}'' \cdot \left[\left(\frac{g}{R\tau_0}B_1\right)\left(\frac{2\tau_0}{p_0}B_3\right)\nabla\zeta_0 + \left(\frac{\tau_0}{p_0}B_2\right) \cdot \right.$$
$$\left. \cdot \left(\frac{2\tau_0}{p_0}B_3\right)\nabla\zeta' - \left(\frac{2\tau_0}{p_0}B_3\right)^2\nabla\zeta''\right] \qquad (5)$$

Comparing with (3, 3) and utilizing (3, 8) the coefficients C_4 . . . . . C_9 in (4, 8) are found to be:

$$C_4 = \frac{g}{R\tau_0}B_4 - \left(\frac{g}{R\tau_0}B_1\right)^2$$
$$C_5 = \frac{\tau_0}{p_0}B_5 - \frac{g}{R\tau_0}B_1 \cdot \frac{\tau_0}{p_0}B_2$$
$$C_6 = \frac{2\tau_0}{p_0}B_6 - \frac{g}{R\tau_0}B_1 \cdot \frac{2\tau_0}{p_0}B_3$$
$$C_7 = \frac{\tau_0}{p_0}B_7 - \left(\frac{\tau_0}{p_0}B_2\right)^2$$
$$C_8 = \frac{2\tau_0}{p_0}B_8 - \frac{\tau_0}{p_0}B_2 \cdot \frac{2\tau_0}{p_0}B_3$$
$$C_9 = \frac{2\tau_0}{p_0}B_9 - \left(\frac{2\tau_0}{p_0}B_3\right)^2 \qquad (6)$$

Table 7. Computed values for B_2, B_3, B_5, ... B_9

	h \ ε	1.00	0.75	0.50	0.25	0.00	— 0.25	— 0.50	— 0.75	— 1.00
$B_2 \cdot 10^{-4}$	8 km	0.0746	0.1000	0.1254	0.1507	0.1761	0.2015	0.2269	0.2522	0.2776
	10 »	0.1220	0.1408	0.1596	0.1783	0.1971	0.2159	0.2346	0.2534	0.2722
	12 »	0.1581	0.1717	0.1853	0.1990	0.2126	0.2262	0.2398	0.2534	0.2670
	14 »	0.1850	0.1946	0.2043	0.2140	0.2237	0.2333	0.2430	0.2527	0.2624
	16 »	0.2046	0.2113	0.2180	0.2247	0.2315	0.2382	0.2449	0.2516	0.2583
$B_3 \cdot 10^{-8}$	8 km	− 0.0229	− 0.0026	0.0177	0.0380	0.0583	0.0786	0.0989	0.1192	0.1395
	10 »	0.0020	0.0207	0.0395	0.0583	0.0771	0.0958	0.1146	0.1334	0.1522
	12 »	0.0287	0.0450	0.0613	0.0777	0.0940	0.1104	0.1267	0.1430	0.1593
	14 »	0.0542	0.0678	0.0813	0.0948	0.1084	0.1219	0.1355	0.1490	0.1626
	16 »	0.0770	0.0877	0.0985	0.1092	0.1200	0.1308	0.1415	0.1523	0.1630
$B_5 \cdot 10^{-4}$	8 km	0.0666	0.0873	0.1080	0.1288	0.1495	0.1703	0.1910	0.2117	0.2325
	10 »	0.1040	0.1185	0.1330	0.1475	0.1620	0.1764	0.1909	0.2054	0.2199
	12 »	0.1301	0.1400	0.1499	0.1598	0.1697	0.1796	0.1895	0.1994	0.2092
	14 »	0.1479	0.1545	0.1611	0.1677	0.1743	0.1808	0.1874	0.1940	0.2006
	16 »	0.1596	0.1639	0.1682	0.1725	0.1767	0.1810	0.1853	0.1896	0.1938
$B_6 \cdot 10^{-8}$	8 km	− 0.0177	− 0.0011	0.0155	0.0321	0.0487	0.0653	0.0819	0.0985	0.1151
	10 »	0.0038	0.0183	0.0327	0.0472	0.0617	0.0762	0.0907	0.1052	0.1197
	12 »	0.0248	0.0367	0.0485	0.0604	0.0723	0.0841	0.0960	0.1079	0.1197
	14 »	0.0434	0.0526	0.0618	0.0711	0.0803	0.0895	0.0987	0.1080	0.1172
	16 »	0.0586	0.0654	0.0723	0.0791	0.0859	0.0927	0.0996	0.1064	0.1133
$\frac{\tau_0}{gQ_0} B_5 \cdot 10^{-8}$	8 km	0.1582	0.2075	0.2567	0.3060	0.3553	0.4046	0.4538	0.5031	0.5524
	10 »	0.2471	0.2816	0.3160	0.3504	0.3849	0.4192	0.4537	0.4881	0.5225
	12 »	0.3093	0.3328	0.3563	0.3797	0.4032	0.4267	0.4503	0.4738	0.4972
	14 »	0.3514	0.3670	0.3827	0.3984	0.4141	0.4297	0.4453	0.4610	0.4767
	16 »	0.3793	0.3895	0.3996	0.4098	0.4199	0.4301	0.4402	0.4504	0.4605
$B_7 \cdot 10^{-8}$	8 km	0.1235	0.0900	0.0778	0.0866	0.1166	0.1678	0.2401	0.3335	0.4482
	10 »	0.1291	0.1119	0.1103	0.1244	0.1541	0.1995	0.2605	0.3371	0.4294
	12 »	0.1481	0.1411	0.1453	0.1610	0.1880	0.2263	0.2761	0.3371	0.4095
	14 »	0.1729	0.1718	0.1787	0.1937	0.2168	0.2479	0.2871	0.3343	0.3897
	16 »	0.1988	0.2007	0.2082	0.2213	0.2400	0.2643	0.2943	0.3298	0.3709
$B_8 \cdot 10^{-12}$	8 km	0.0801	0.0452	0.0273	0.0263	0.0422	0.0749	0.1247	0.1913	0.2749
	10 »	0.0800	0.0534	0.0424	0.0471	0.0674	0.1034	0.1550	0.2223	0.3051
	12 »	0.0867	0.0684	0.0637	0.0727	0.0953	0.1315	0.1814	0.2448	0.3219
	14 »	0.0998	0.0888	0.0890	0.1005	0.1233	0.1574	0.2028	0.2595	0.3275
	16 »	0.1178	0.1122	0.1156	0.1280	0.1493	0.1796	0.2189	0.2670	0.3243
$\frac{2\tau_0}{gQ_0} B_6 \cdot 10^{-12}$	8 km	− 0.0832	− 0.0050	0.0737	0.1526	0.2315	0.3102	0.3891	0.4679	0.5468
	10 »	0.0180	0.0869	0.1556	0.2245	0.2933	0.3622	0.4311	0.4999	0.5688
	12 »	0.1179	0.1743	0.2306	0.2870	0.3434	0.3999	0.4563	0.5126	0.5690
	14 »	0.2061	0.2500	0.2938	0.3377	0.3815	0.4254	0.4693	0.5131	0.5570
	16 »	0.2783	0.3108	0.3434	0.3759	0.4082	0.4407	0.4733	0.5058	0.5383
$B_9 \cdot 10^{-16}$	8 km	0.1445	0.0757	0.0340	0.0194	0.0318	0.0713	0.1379	0.2315	0.3523
	10 »	0.1623	0.0903	0.0495	0.0401	0.0620	0.1152	0.1997	0.3155	0.4526
	12 »	0.1764	0.1090	0.0743	0.0723	0.1030	0.1664	0.2625	0.3912	0.5527
	14 »	0.1922	0.1345	0.1086	0.1143	0.1515	0.2204	0.3210	0.4532	0.6170
	16 »	0.2126	0.1671	0.1506	0.1626	0.2033	0.2727	0.3708	0.4975	0.6532

REFERENCES

Bolin, B. and Charney, J. G., 1951: Numerical tendency computations from the barotropic vorticity equation. *Tellus*, **3**, 4, 248—257.

Charney, J. G., 1947: The dynamics of long waves in a baroclinic westerly current. *J. Meteor.*, **4**, 5, 135—162.

Charney, J. G. and Eliassen, A., 1949: A numerical method for predicting the perturbations of the middle latitude westerlies. *Tellus*, **1**, 2, 38—54.

Charney, J. G., Fjörtoft, R. and v. Neumann, J., 1950: Numerical integration of the barotropic vorticity equation. *Tellus*, **2**, 4, 237—254.

Charney, J. G., 1951: Dynamic forecasting by numerical process. *Compendium of Meteorology*, 470—482.

Eady, E. T., 1949: Long waves and cyclone waves. *Tellus*, **1**, 3, 33—52.

— 1952: Note on weather computing and the so-called $2^1/_2$ dimensional model. *Tellus*, **4**, 3.

Eliassen, A., 1952: Simplified dynamic models of the atmosphere, designed for the purpose of numerical weather prediction. *Tellus*, **4**, 3.

Haurwitz, B., 1946: An investigation of Kibel's method of forecasting. *Bull. Am. Soc.*, **27**, 9, 499—508.

Izvekov, B. I., 1946: Professor I. A. Kibel's theoretical method of weather forecasting. *Bull. Am. Soc.*, **27**, 9, 488—498.

Phillips, A. N., 1951: A simple three-dimensional model for the study of large-scale extratropical flow patterns. *J. Meteor.*, **8**, 6, 381—394.

Rossby, C.-G., 1942: Kinematic and hydrostatic properties of certain long waves in the westerlies. *Univ. Chicago, Misc. Reports No. 5.*

Staff Members, University of Stockholm, 1952: Preliminary report on the prognostic value of barotropic models in the forecasting of 500 mb height changes. *Tellus*, **4**, 1, 21—30.

Sutcliffe, R. C., 1947: A contribution to the theory of development. *Quart. Journal*, **73**, 370—383.

Numerical Solution of Elliptic Difference Equations by Matrix Methods

By OLLE KARLQVIST, Swedish Board of Computing Machinery, Stockholm

(Manuscript received 1 October 1952)

Abstract

A non-iterative method for solving boundary value problems of elliptic difference equations is developed that is based on the simple structure of the triangular matrices obtained by applying the well-known elimination procedure of Gauss to the matrix of the difference equation. It is proved that the procedure is numerically stable, i. e., there is no tendency to error-growth. The method seems to be particularly suited to such problems as weather forecasting on high-speed computing machines where one has to solve the same equations (e. g., Poisson's or Helmholtz's) a great number of times with the same net but different right member and boundary values. The number of stored constants as well as the computational work in the application of the method is only a fractional part of that required when using the inverse matrix (Green's function). Poisson's equation for a rectangular region is given a close study, but the method can be applied to irregular regions and to equations of higher order.

1. Introduction

For numerical solution of boundary value problems it is usual to replace the differential equation by a difference equation of the same or higher order. If the differential equation is linear we obtain a system of linear equations to solve that generally is of very high order. The methods for solving this system can be divided into iterative and direct methods (Bodewig, 1947). To the former are counted the Liebmann process (Stiefel, 1952), relaxation (Southwell, 1946), and steepest descent (Stiefel, 1952). The direct methods consist either in forming the inverse matrix or in splitting the original matrix into triangular matrices according to Gauss or Choleski; the last-mentioned method can only be applied to symmetric matrices. Variants of the methods of Gauss and Choleski are given in the literature but common to for them all is some kind of elimination procedure.

The matrices appearing in connection with ordinary and partial differential equations have a simple structure. A splitting of the original matrix can be done once for all for a given region. Below it will be shown how this splitting process can be done and that the amount of work for calculating the unknowns from the triangular matrices often is considerably less than for calculating the unknowns from the inverse matrix. Both the decomposition procedure and the solving of the unknowns are extremely well suited for electronic computers, even those having a fixed binary point. From the tabulation point of view it is more economical to tabulate triangular matrices than inverse matrices.

2. Arrangement of the matrix of the Poisson's equation

Because Poisson's equation

$$\nabla^2 u = J(x, y), \qquad \nabla^2 = \frac{\partial^2}{\partial x^2} + \frac{\partial^2}{\partial y^2} + \frac{\partial^2}{\partial z^2} \quad (1)$$

has both general and meteorological interest this equation will be treated in detail. This equation occurs in the barotropic case where J essentially is a Jacobian of the absolute vorticity and the pressure height (CHARNEY, FJØRTOFT, VON NEUMANN, 1950).

Now we consider the corresponding difference equation of second order in two dimensions and with the u-values given on the boundary. The difference equation for quadratic nets with the mesh length h is

$$\triangle_x{}^2 u + \triangle_y{}^2 u = h^2 \cdot J(x, y) \qquad (2)$$

where $\triangle^2$ means central differences of the second order. We want a solution of (2) satisfying the boundary conditions. This is called the first boundary value problem and has been treated for difference equations from a purely mathematical standpoint by COURANT, FRIEDRICHS and LEWY (1928).

In a rectangular region (fig. 1) with r inner rows and s inner points per row the notation u_{jk} means u at $\varrho = j$ and $\sigma = k$. Using these subscripts we can form the following equations. (σ corresponds to the x-direction and ϱ to the y-direction).

$\varrho = 1$

$$\begin{aligned}
4u_{11} - u_{12} - u_{21} &= u_{01} + u_{10} - h^2 \cdot J_{11} \\
-u_{11} + 4u_{12} - u_{13} - u_{22} &= u_{02} - h^2 \cdot J_{12} \\
-u_{12} + 4u_{13} - u_{14} - u_{23} &= u_{03} - h^2 \cdot J_{13} \\
&\cdots \\
-u_{1,s-1} + 4u_{1s} - u_{2s} &= u_{0s} + u_{1,s+1} - h^2 \cdot J_{1s}
\end{aligned}$$

$\varrho = 2$

$$\begin{aligned}
-u_{11} + 4u_{21} - u_{22} - u_{31} &= u_{20} - h^2 \cdot J_{21} \\
-u_{12} - u_{21} + 4u_{22} - u_{23} - u_{32} &= -h^2 \cdot J_{22} \\
&\cdots \\
-u_{1s} - u_{2,s-1} + 4u_{2s} - u_{3s} &= u_{2,s+1} - h^2 \cdot J_{2s}
\end{aligned}$$

etc.

The equations above can be written in matrix notation

$$\mathbf{G} \cdot \mathbf{u} = \mathbf{t} \qquad (3)$$

where $\mathbf{u}$ is a column matrix partitioned in r columns $\mathbf{u}_1, \mathbf{u}_2, \ldots, \mathbf{u}_r$ each holding the s u-values of row $1, 2, \ldots, r$.

$$\mathbf{u}_1 = \begin{bmatrix} u_{11} \\ u_{12} \\ u_{13} \\ \vdots \\ u_{1s} \end{bmatrix} \quad \mathbf{u}_2 = \begin{bmatrix} u_{21} \\ u_{22} \\ u_{23} \\ \vdots \\ u_{2s} \end{bmatrix} \quad \ldots \quad \mathbf{u}_r = \begin{bmatrix} u_{r1} \\ u_{r2} \\ u_{r3} \\ \vdots \\ u_{rs} \end{bmatrix}$$

In the same way the column matrix $\mathbf{t}$ formed by the boundary values and the function J is partitioned.

$$\mathbf{t}_1 \quad \begin{bmatrix} -h^2 J_{11} + u_{01} + u_{10} \\ -h^2 J_{12} + u_{02} \\ -h^2 J_{13} + u_{03} \\ \vdots \\ -h^2 J_{1s} + u_{0s} + u_{1,s+1} \end{bmatrix},$$

$$\mathbf{t}_2 = \begin{bmatrix} -h^2 J_{21} + u_{20} \\ -h^2 J_{22} \\ -h^2 J_{23} \\ \vdots \\ -h^2 J_{2s} + u_{2,s+1} \end{bmatrix} \ldots$$

$$\mathbf{t}_r = \begin{bmatrix} -h^2 J_{r1} + u_{r+1,1} + u_{r0} \\ -h^2 J_{r2} + u_{r+1,2} \\ -h^2 J_{r3} + u_{r+1,3} \\ \vdots \\ -h^2 J_{rs} + u_{r+1,s} + u_{r,s+1} \end{bmatrix}$$

The matrix **G** is partitioned in r^2 submatrices each of the order s.

$$\mathbf{G} = \begin{bmatrix} \mathbf{D} & -\mathbf{I} & \mathbf{O} & \mathbf{O} \ldots & & \\ -\mathbf{I} & \mathbf{D} & -\mathbf{I} & \mathbf{O} \ldots & & \\ \mathbf{O} & -\mathbf{I} & \mathbf{D} & -\mathbf{I} \ldots & & \\ & & \cdots & & & \\ \mathbf{O} & \mathbf{O} & \mathbf{O} & \mathbf{O} \ldots & -\mathbf{I} & \mathbf{D} \end{bmatrix} \quad (4)$$

Here **I** denotes the unit matrix of the order s and the zeros are zero matrices of the same order. The submatrix **D** is defined as

$$\mathbf{D} = \begin{bmatrix} 4 & -1 & 0 & 0 \ldots & & \\ -1 & 4 & -1 & 0 \ldots & & \\ 0 & -1 & 4 & -1 \ldots & & \\ & & \cdots & & & \\ 0 & 0 & 0 & 0 \ldots & -1 & 4 \end{bmatrix} \quad (5)$$

From the structure of the matrix **G** it is clear that it is symmetric and contains at most 5 non-vanishing elements per row and that these are collected in diagonals, the outer lies s diagonals from the head diagonal.

3. General theory for splitting up a matrix into triangular matrices

Because of the symmetry of the matrix **G** in (4) this matrix can be split either according to Gauss or Choleski, but as the main procedure is the same in both cases, we treat the former method only. Gauss' method consists in forming a triangular matrix by elimination from which the unknowns can be solved by recurrence formula. Banachiewicz has shown that the matrix can be split up directly into two triangular matrices, a procedure called in German literature "Gauss' abgekürzte Verfahren" (ZURMÜHL, 1950). For manual solution this procedure is preferable to the pure elimination procedure because less writing is required. For electronic computers, however, the elimination is more suitable. The inverse matrix can be computed from triangular matrices. The number of arithmetic operations is the same for the two methods.

Fig. 1. Numbering in a rectangular region.

We now split up a *symmetric* matrix **A** into two triangular matrices **B** and **C**. Hence

$$\mathbf{A} = \mathbf{B} \cdot \mathbf{C} \quad (6)$$

Here we have a certain freedom in the choice of the diagonal elements of the matrices **B** and **C**. In this case the following arrangement seems to be convenient, for all elements except the diagonal elements in the important case of Poisson's equation will be positive.
Set

$$\mathbf{B} = \begin{bmatrix} b_{11} & 0 & 0 & 0 \ldots & 0 \\ b_{12} & b_{22} & 0 & 0 \ldots & 0 \\ b_{13} & b_{23} & b_{33} & 0 \ldots & 0 \\ & & \cdots & & \\ b_{1s} & b_{2s} & b_{3s} & b_{4s} \ldots & b_{ss} \end{bmatrix},$$

$$\mathbf{C} = \begin{bmatrix} -1 & c_{12} & c_{13} & c_{14} \ldots & c_{1s} \\ 0 & -1 & c_{23} & c_{24} \ldots & c_{2s} \\ 0 & 0 & -1 & c_{34} \ldots & c_{3s} \\ & & \cdots & & \\ 0 & 0 & 0 & 0 \ldots & -1 \end{bmatrix}$$

We identify the two members in (6) and compute the elements b_{jk} and c_{jk} from the following relations

$$\begin{aligned} b_{1k} &= -a_{1k} && k = 1, 2, \ldots, s \\ c_{1k} &= -b_{1k}/b_{11} && k = 2, 3, \ldots, s \\ b_{2k} &= -a_{2k} + c_{12} \cdot b_{1k} && k = 2, 3, \ldots, s \\ c_{2k} &= -b_{2k}/b_{22} && k = 3, 4, \ldots, s \end{aligned} \quad (7)$$

— — —

$$b_{jk} = -a_{jk} + \sum_{n=1}^{j-1} c_n \cdot b_{nk} \quad k = j, j+1, \ldots, s$$

$$c_{jk} = -b_{jk}/b_{jj} \qquad k = j+1, j+2, \ldots, s$$

For checking purposes we can use a relation for the sum of the computed elements b_{jk} in the j_{th} column.

$$\sum_{n=j}^{s} b_{jn} = -\sum_{n=1}^{s} a_{nj} + \sum_{n=1}^{j-1} c_{nj} \cdot q_n$$

$$q_n = \sum_{m=n}^{s} b_{nm}$$

When the matrix **A** is symmetric as here, the matrix — **C** has originated from **B** by multiplying the transposed **B** by a diagonal matrix formed by the inverted values of **B**'s diagonal elements.

4. Splitting up the matrix G into triangular matrices

It is easy now to form triangular matrices for the matrix defined by (4). **G** is symmetric and beyond the $(s+1)$:th diagonal (the head diagonal is numbered one) **G**'s elements are zero.
We thus form

$$\mathbf{G} = \mathbf{B} \cdot \mathbf{C} \qquad g_{jk} = g_{kj}$$

The elements of the triangular matrices are computed from (7). In general

$b_{1k} \neq 0$ for $k = 1, 2, \ldots, s+1$

but

$b_{1k} = 0$ for $k > s+1$

In the next b-column we have

$b_{2k} \neq 0$ for $k = 2, 3, \ldots, s+2$

$b_{2k} = 0$ for $k > s+2$

etc.

Generally we have

$b_{jk} \neq 0$ for $k = j, j+1, \ldots, j+s$

$b_{jk} = 0$ for $k > j+s$

From this we conclude the essential property of the triangular matrix **B** is that its diagonals $1, 2, \ldots, s+1$ (numbering as above) have non-vanishing elements but, the other diagonals contain zero elements only. For the matrix **C** we get similar results, but the non-vanishing diagonals lie to the right of the head diagonal.

The conclusions above are valid for general difference equations of any order in which the letter s does not mean the number of points per row in fig. 1. The difference equation can originate from ordinary or partial differential equations. The region need not to be rectangular, in non-rectangular regions let s denote the diagonal, usually not filled, beyond which we have zero elements only, then no non-vanishing elements will lie outside the s^{th} diagonal in the triangular matrix.

In Poisson's equation for a rectangular region the triangular matrices contain about rs^2 elements each, but the inverse matrix contains r^2s^2 elements, where r denotes the number of rows and s the number of points per row in the region. The triangular matrix has besides another delightful property, viz. we can add extra rows to the region without affecting the preceding elements in the triangular matrix. The inverse matrix on the other hand changes every element when one adds an extra row to the region. See also section 8.

5. Solution of the unknowns from the triangular matrices

In order to solve the function **u** from the equation

$$\mathbf{B} \cdot \mathbf{C} \cdot \mathbf{u} = \mathbf{t} \tag{8}$$

we first solve an auxiliary function **v** defined by

$$\mathbf{B} \cdot \mathbf{v} = \mathbf{t} \tag{9}$$

Then **u** is solved from

$$\mathbf{C} \cdot \mathbf{u} = \mathbf{v} \tag{10}$$

The function **v** is solved recurrently from (9) beginning with v_{11}.

$$v_{11} = \frac{1}{b_{11}} \cdot t_{11}$$

$$v_{12} = \frac{1}{b_{22}} (t_{12} - v_{11} \cdot b_{12}) \tag{11}$$

$$v_{13} = \frac{1}{b_{33}} (t_{13} - v_{11} \cdot b_{13} - v_{12} \cdot b_{13})$$

etc.

Now we can solve **u** from (10) beginning with u_{rs}.

$$u_{rs} = -v_{rs}$$

$$u_{r,s-1} = -v_{r,s-1} + u_{rs} \cdot c_{rs-1,rs}$$

$$u_{r,s-2} = -v_{r,s-2} + u_{rs} \cdot c_{rs-2,rs} + u_{r,s-1} \cdot c_{rs-2,rs-1}$$

etc.

6. The work for solving Laplace's and Poisson's equations

As a measure for the work for solving u we take the number of multiplications and additions that must be made. We consider rectangular regions but we can get an upper bound for the work for irregular regions if s denotes the maximum number of points in a row of the region.

To form the triangular matrices we need about $rs^3/2$ multiplications and additions (cf. sec. 8), and to solve u from these matrices this number is about $2\,rs^2$. Thus we ought to turn the region so that r will be greater than s.

The difference between Laplace's equation and Poisson's equation from the numerical point of view lies in the right member of (1), and the work to solve them with triangular matrices will be about the same, i.e., $2\,rs^2$ multiplications and additions. We compare this with the number we get in computing u from the inverse matrix. For Laplace's equation we need $rs^2 + r^2s$ multiplications and additions. For Poisson's equation this number is r^2s^2, because every u value demands $r \cdot s$ multiplications and additions. The work for solving u from the triangular matrices is thus equivalent to compute two rows by the inverse matrix.[1]

However, when using the inverse matrix we can reduce the work considerably by computing two adjacent rows with the inverse matrix and computing next row by the formula

$$u_{3k} = 4\,u_{2k} - u_{2,k-1} - u_{2,k+1} - u_{1k} \qquad k = 1, 2, \ldots, s$$

[1] Poisson's eq. in a rectangular region can also be solved by using finite Fourier analysis and synthesis (cf. e. g. Charney, Fjørtoft, von Neumann, 1950). The work is about $2\,rs^2 + 2\,r^2s$ multiplications and additions.

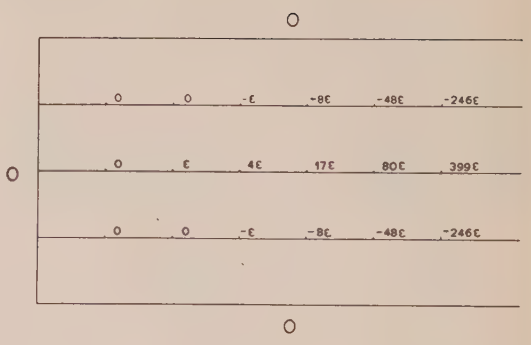

Fig. 2. The error-growth in the step-ahead process.

When the third row has been computed we compute the fourth and so on. The process, however, is unstable, which theoretically has been shown by HYMAN (1952). The following ε-scheme (COLLATZ, 1951) establishes the error-growth in which we have an error ε in the middle row (see fig. 2).

Hyman calls this process step-ahead and shows that the loss after stepping 13 rows is 10 decimal figures. According to our experience the step-ahead process is favourable only when the boundary values have such a character that the solution is of exponential order in which case the relative error is constant. In other cases the error-growth very soon causes trouble and computing fresh rows with the inverse is necessary. Below will be shown that the triangular procedure is stable and an error (for example a rounding-off) will be damped. Besides, the gain with the step-ahead is none for Poisson's equation if we must compute with the inverse the u-values in more than two rows in the region.

7. The inverse matrix regarded as a function of the matrix D

For rectangular regions we can choose an alternative method (cf. section 8) for solving the u-values instead of that given by equations (11) and (12). The computation of the triangular matrices by this method has been replaced by the computation of a submatrix of the inverse matrix, and we now derive some matrix relations for the inverse matrix. By introducing allied Chebyshev polynomials for the inverse matrix we are led to expressions that are nicer than Hyman's for numerical purposes.

For Poisson's equation our expressions contain simple sums while Hyman's contain double sums corresponding directly to Green's function of the continuous case (see below equation 21). LAASONEN (1948) gives for Laplace's equation the same relations as we do.

The determinant of $\mathbf{D}$ can be put in a closed form (RUTHERFORD, 1946). Denote the determinant to the matrix $\mathbf{D}$ of the s^{th} order by D_s. Expanding D_{s+1} after the first row we have the recurrence relation

$$D_{s+1} = 4 \cdot D_s - D_{s-1} \qquad (13)$$

Now we introduce a polynomial $S_n(a)$ of the n^{th} degree defined by the relations

$$S_{n+1}(a) = a \cdot S_n(a) - S_{n-1}(a);\ S_0(a) = 1;$$
$$S_1(a) = a \qquad (14)$$

Thus,

$$S_s(4) = D_s$$

The difference equation (14) has the solution

$$S_n(a) = \sin(n+1)x/\sin x \quad 2\cos x = a \qquad (15)$$

which is a polynomial allied to the Chebyshev polynomials. The eigenvalues d_k of $\mathbf{D}$ are derived immediately from (15).

$$d_k = 4 - 2 \cdot \cos\frac{\pi \cdot k}{s+1} \qquad k = 1, 2 \ldots s \qquad (16)$$

Because a > 2 we put (15) in the more convenient form

$$S_n(a) = \sinh(n+1)x/\sinh x \quad 2\cosh x = a \qquad (17)$$

The eigenvector matrix (transformation matrix) of $\mathbf{D}$ is

$$\left\{ \sin\frac{jk\pi}{s+1} \right\}$$

We denote the normalized eigenvector matrix by $\mathbf{T}$.

$$\mathbf{T} = \sqrt{\frac{2}{s+1}} \cdot \left\{ \sin\frac{jk\pi}{s+1} \right\}$$

With the knowledge of $\mathbf{T}$ we can according to a known theorem of the matrix algebra compute an arbitrary matrix polynomial of $\mathbf{D}$ by the formula ($\mathbf{D}$ and $\mathbf{T}$ are symmetric).

$$F(\mathbf{D}) = \mathbf{T} \cdot \{ F(d_k) \} \cdot \mathbf{T}$$

where $\{ F(d_k) \}$ is a diagonal matrix formed by the values $F(d_k)$ where d_k are defined by (16).

The inverse matrix is decomposed in r^2 submatrices each of the order s.

$$\mathbf{G}^{-1} = \{ \mathbf{G}_{jk} \} \qquad \mathbf{G}_{jk} = \mathbf{G}_{kj}$$

Since

$\mathbf{G} \cdot \mathbf{G}^{-1} =$ unit matrix of the order $r \cdot s$, we can for the submatrices $\mathbf{G}_{1k}$ write the relations

$$\begin{aligned} \mathbf{D}\,\mathbf{G}_{11} - \quad \mathbf{G}_{12} &= \quad \mathbf{I} \\ -\mathbf{G}_{11} + \mathbf{D}\,\mathbf{G}_{12} - \quad \mathbf{G}_{13} &= \mathbf{O} \\ - \quad \mathbf{G}_{12} + \mathbf{D}\,\mathbf{G}_{13} - \mathbf{G}_{14} &= \mathbf{O} \qquad (18) \\ - \quad - \quad - & \\ - \mathbf{G}_{1,r-1} + \mathbf{D} \cdot \mathbf{G}_{1r} &= \mathbf{O} \end{aligned}$$

(18) satisfies in matrix notation the same difference equation as the polynomial $S_n(a)$.

We thus write the solution of (18) in the form

$$\mathbf{G}_{1k} = \text{constant} \cdot S_{r-k}(\mathbf{D})$$

because $\mathbf{G}_{1k}$ decreases with increasing k.

The constant is determined from the first equation of (18).

Hence,

$$\mathbf{G}_{1k} = S_{r-k}(\mathbf{D}) \cdot S_r^{-1}(\mathbf{D})$$

but since both factors are functions of $\mathbf{D}$ no ambiguity results if we write

$$\mathbf{G}_{1k} = S_{r-k}(\mathbf{D})/S_r(\mathbf{D}) \qquad k = 1, 2 \ldots r \qquad (19)$$

which will be used in the following.

We multiply $\mathbf{G}$ by the next column of its inverse and have the relations

$$\begin{aligned} \mathbf{D}\,\mathbf{G}_{12} - \quad \mathbf{G}_{22} &= \mathbf{O} \\ -\mathbf{G}_{12} + \mathbf{D}\,\mathbf{G}_{22} - \mathbf{G}_{23} &= \mathbf{I} \\ - \quad \mathbf{G}_{22} + \mathbf{D} \cdot \mathbf{G}_{23} - \mathbf{G}_{24} &= \mathbf{O} \\ - \quad - \quad - & \\ - \mathbf{G}_{2,r-1} + \mathbf{D}\,\mathbf{G}_{2r} &= \mathbf{O} \end{aligned}$$

To solve this we make the same attempt and the constant is determined by the second of the equations above. We have

$$\mathbf{G}_{2k} = S_1(\mathbf{D}) \cdot S_{r-k}(\mathbf{D})/S_r(\mathbf{D}) \quad k = 2, 3 \ldots r$$

By induction we obtain the general formula

$$\mathbf{G}_{jk} = S_{j-1}(\mathbf{D}) \cdot S_{r-k}(\mathbf{D}) \cdot /S_r(\mathbf{D}) \quad j \leq k \quad (20)$$

From (20) we easily derive formulas for computing the inverse matrix for half open regions, e.g., $r = \infty$, s finite. If we let s approach infinity in the formulas, the elements in the inverse matrix yield integrals that correspond to relations established by STÖHR (1950).

For comparison we establish the solutions of the continuous case. We divide the solution in two parts, one due to the boundary values denoted $f(\sigma)$, and an other part due to the function $J(x, y)$. Then, the solution of Poisson's equation

$$\nabla^2 u = J(x, y)$$

can be written in the form

$$u(x, y) = \int \frac{\partial K}{\partial n} \cdot f(\sigma) \cdot d\sigma -$$

$$- \iint_{\text{region}} K(x, y; \xi, \eta) \cdot J(\xi, \eta) \cdot d\xi \cdot d\eta$$

where $K(x, y; \xi, \eta)$ is Green's function. The first integral is taken round the boundary. In the particular case when having a rectangle with the vertices (0, 0), $(a, 0)$, (a, b) and $(0, b)$, the normal derivative of Green's function for the side $y = 0$ and $0 \leq x \leq a$ is

$$\frac{\partial K}{\partial n} = \frac{2}{a} \sum_{n=1}^{\infty} \frac{\sinh n \cdot \frac{\pi}{a}(b - y)}{\sinh n \cdot \frac{\pi}{a} \cdot b} \cdot$$

$$\cdot \sin n \frac{\pi x}{a} \cdot \sin n \frac{\pi \xi}{a}$$

and Green's function itself if expressed in Fourier series is

$$K = -\frac{4}{\pi^2 a \cdot b} \sum_{m=1}^{\infty} \sum_{n=1}^{\infty} \frac{\sin n \frac{\pi x}{a} \cdot \sin m \frac{\pi y}{b} \cdot \sin n \frac{\pi \xi}{a} \cdot \sin m \frac{\pi \eta}{b}}{\frac{m^2}{b^2} + \frac{n^2}{a^2}} \quad (21)$$

Now we write the solution in matrix notation for the difference equation (2). Let $u = 0$ for $\sigma = 0$ and for $\sigma = s + 1$. We put

$$\mathbf{t} = \mathbf{t}' + \mathbf{t}''$$

where $\mathbf{t}'$ is due to the boundary values and $\mathbf{t}''$ is due to the function $J(x, y)$. Then,

$$\mathbf{u}_j = \mathbf{G}_{1j} \cdot \mathbf{t}_1' + \mathbf{G}_{jr} \cdot \mathbf{t}_r' + \sum_{k=1}^{r} \mathbf{G}_{jk} \cdot \mathbf{t}_k''$$

$\mathbf{G}_{jk}$ is defined by (19) and $\mathbf{t}$ is the right member of (3). If $J \equiv 0$ we only need the submatrices $\mathbf{G}_{1k}$, for $\mathbf{G}_{jr} = \mathbf{G}_{1, r-j+1}$. When comparing our matrix solution with the continuous solution we find that the normal derivative of Green's function corresponds to the "boundary matrices" $\mathbf{G}_{1k}$ and that Green's function mainly corresponds to the "kernel matrices" $\mathbf{G}_{jk}$, $jk \neq 1$.

We also consider the inverse matrix for rectangular nets. The eigenvalues of $\mathbf{D}$ will be changed but the eigenvector matrix $\mathbf{T}$ will be unchanged. If we denote the quotient between the mesh length of ϱ- and σ- directions by p, the new eigenvalues are then given by

$$d_j' = 2(1 + p^2) - 2p^2 \cdot \cos \frac{j\pi}{s + 1}$$

$$j = 1, 2, \ldots, s$$

The mesh length h occurring in some equations will now mean the mesh length in the ϱ-direction.

8. A matrix method for solving u from the triangular matrices

A slight modification of the procedure indicated by equations (11) and (12) will give a convenient procedure to compute the u-values of Poisson's equation for a *rectangular* region. We split the partitioned matrix $\mathbf{G}$ into quasi-triangular matrices consisting of quadratic submatrices of the order s. Now

the elements b_{jk} and c_{jk} derived from formulas (7) will become submatrices in the triangular matrices **B** and **C**. By induction we find that the **B** and **C** matrices can be written

$$\mathbf{B} = \begin{bmatrix} -S_1 & \mathbf{O} & \mathbf{O} & \mathbf{O} \dots & & & \\ \mathbf{I} & -\frac{S_2}{S_1} & \mathbf{O} & \mathbf{O} \dots & & & \\ \mathbf{O} & \mathbf{I} & -\frac{S_3}{S_2} & \mathbf{O} \dots & & & \\ & & & - - - & & & \\ & & & \dots & \mathbf{I} - \frac{S_j}{S_{j-1}} & \mathbf{O} \dots & \mathbf{O} \\ & & & & & - - - & \\ & & & & & & \mathbf{I} - \frac{S_r}{S_{r-1}} \end{bmatrix}$$

$$\mathbf{C} = \begin{bmatrix} -\mathbf{I} & \frac{\mathbf{I}}{S_1} & \mathbf{O} & \mathbf{O} \dots & & & \\ \mathbf{O} & -\mathbf{I} & \frac{S_1}{S_2} & \mathbf{O} \dots & & & \\ \mathbf{O} & \mathbf{O} & -\mathbf{I} & \frac{S_2}{S_3} \dots & & & \\ & & & - - - & & & \\ & & & \dots & -\mathbf{I} & \frac{S_{j-1}}{S_j} & \mathbf{O} \dots \\ & & & & & - - - & \\ & & & & & & -\mathbf{I} \end{bmatrix}$$

For abbreviation the polynomial $S_n(\mathbf{D})$ is written S_n.
We introduce a matrix $\mathbf{H}_j$ defined by

$$\mathbf{H}_j = \frac{S_{j-1}}{S_j} = \sinh j\mathbf{X}/\sinh (j+1)\mathbf{X} \qquad (22)$$

where $2 \cdot \cosh \mathbf{X} = \mathbf{D}$

We form an arbitrary row in **B** and obtain a difference equation for the matrix $\mathbf{H}_j$.

$$\mathbf{H}_j + \mathbf{H}_{j+1}^{-1} = \mathbf{D} \qquad (23)$$

Now, equation (22) expresses the first submatrix $\mathbf{G}_{11}$ in the partitioned inverse matrix of a region of j rows according to equation (19).

To solve u from the partitioned triangular matrices **B** and **C** we first form an auxiliary function **z** that corresponds to **v** in equation (9). Thus we have

$$\begin{aligned} \mathbf{z}_1 &= \mathbf{H}_1 \cdot \mathbf{t}_1 \\ \mathbf{z}_{j+1} &= \mathbf{H}_{j+1} \cdot (\mathbf{z} + \mathbf{t}_{j+1}) \quad j = 1, 2, \dots, r \end{aligned} \qquad (24)$$

To solve u from

$$\mathbf{C} \cdot \mathbf{u} = -\mathbf{z}$$

we easily find from the partitioned matrix **C**

$$\begin{aligned} \mathbf{u}_r &= \mathbf{z}_r \\ \mathbf{u}_j &= \mathbf{z}_j + \mathbf{H}_j \cdot \mathbf{u}_{j+1} \quad j = r-1, r-2, \dots, 2, 1. \end{aligned} \qquad (25)$$

If we solve u according to the equations (24) and (25) we need $\mathbf{H}$ and $\mathbf{z}$ only. We also can apply the usual checking procedure for matrices when solving u in this way. We thus have transfered our problem to tabulate $\mathbf{G}_{11}$ for $r = 1, 2, 3, \ldots$ and these matrices can be computed free from each other. The eigenvalues of $\mathbf{H}_j$ denoted h_{jk} can be computed recurrently from (23) which gives a stable procedure.[1]

$$h_{jk} = \frac{1}{d_k - h_{j-1,\,k}} \qquad d_k = 4 - 2 \cdot \cos \frac{\pi k}{s+1}$$

The number of stored constants for solving Poisson's equation in a rectangular region is $r(s+1)$ using $\mathbf{H}_j$ matrices. For we have

$$\mathbf{H}_j = \frac{2}{s+1}\left\{\sum_{n=1}^{s} \sin \mu \frac{\pi n}{s+1} \cdot \sin \nu \frac{\pi n}{s+1} \cdot h_{jn}\right\}$$

$$= \frac{1}{s+1}\left\{\sum_{n=1}^{s} \left(\cos(\mu - \nu)\frac{\pi n}{s+1} - \right.\right.$$

$$\left.\left. - \cos(\mu + \nu)\frac{\pi n}{s+1}\right) \cdot h_{jn}\right\}$$

This implies that every $\mathbf{H}_j$ matrix demands $2s$ constants. But using congruence properties we find that $s+1$ constants are enough. Hence, having r rows we need $r(s+1)$ constants. But, as we have seen, $r(s+1)$ constants can be used to solve Poisson's equation in r regions. The first region contains 1 row, the second 2 rows and the last region contains r rows. Using inverse matrices we should need for these r regions considerably more constants. The work to compute the r $\mathbf{H}$ matrices is about rs^2.

In irregular regions it is sometimes convenient to split up the original matrix into triangular matrices that are partitioned in submatrices. See also § 11.

9. Stability

A stability investigation is now easy to perform on the equations (24) and (25), for an error will satisfy the same equations as $\mathbf{z}$ and $\mathbf{u}$ do. The error will be increased if an eigenvalue $\mathbf{H}_j$ is greater than 1, but will be decreased if it is less than 1. From (22) we immediately have the expression for h_{jk}, the eigenvalues of $\mathbf{H}_j$.

$$h_{jk} = \sinh jx / \sinh(j+1)x$$

$$\cosh x = 2 - \cos \frac{\pi k}{s+1}$$

from which equation we conclude that the eigenvalues must be less than 1.

10. Numerical considerations

To illustrate the foregoing paragraphs we give an example of triangular matrices for $s = 2$, shown in table 1. The space only allows one matrix to be written and this is written in columns. The first column should be regarded as the head diagonal of the triangular matrix $\mathbf{B}$. In this case the elements are stationary after 8 rows if rounded off to 5 decimals. Moskovitz (1944) has tabulated parts of the inverse matrix for $r = 1$, 2 and 3 so these tables can be used in special cases.

For computations on BARK, the Swedish relay-computer, the triangular matrices have been formed by direct elimination because the "shorter" method has some drawbacks. At the preliminary planning of program for BESK, the Swedish electronic computer under construction, we also have used Gauss' method, and normally no difficulties arise in forming the triangular matrix because of the fixed binary point. Having rectangular regions, the forming of necessary matrices is an extremely simple procedure. Very large systems can have their matrices stored on the magnetic drum, which is favourable. In meteorological computations we can use information from preceding steps and compute corrections instead of the function itself. This will reduce the computational work.

[1] The formulas (24) and (25) can be expressed in T and diagonal matrices formed by h_{jk}. This means a finite Fourier analysis of the function f in the x-direction. In this case the elements h_{jk} only need to be tabulated.

Table 1. The triangular matrix B for $s = 2$

r	Head Diagonal	2	3
1	— 4.00000	—	—
	— 3.75000	1.00000	—
2	— 3.73333	0.25000	1
	— 3.42857	1.06667	1
3	— 3.70833	0.28571	1
	— 3.39185	1.08333	1
4	— 3.70518	0.29214	1
	— 3.38679	1.08612	1
5	— 3.70474	0.29314	1
	— 3.38606	1.08655	1
6	— 3.70467	0.29329	1
	— 3.38596	1.08662	1
7	— 3.70466	0.29331	1
	— 3.38594	1.08663	1
8	— 3.70466	0.29331	1
	— 3.38594	1.08663	1

11. Poisson's equation for non-rectangular regions

The method of triangular matrices can be applied, of course, to irregular regions. In these cases the submatrices in the diagonal of the partitioned matrix **G** will have their order given by the number of inner points in an actual row. Still we can add extra rows to the region without affecting the preceding elements in the triangular matrices.

12. Other elliptic problems in two dimensions

We first consider Helmholtz's equation

$$\nabla^2 u - \lambda \cdot u = J(x, y)$$

an equation which has interest in certain atmospheric models. If the λ-values are given, this equation can be solved in the same way as Poisson's equation. In a rectangular region the only difference from a numerical point of view is that the eigenvalues d_k in equation (16) will be replaced by the new expression

$$d_k = 4 + \lambda \cdot h^2 - 2 \cdot \cos \frac{\pi k}{s+1} \qquad k = 1, 2, \ldots s$$

h denotes the mesh length.

The second boundary value problem where we have the derivative of u instead of u itself given on the boundary can also be solved by triangular matrices. The original matrix for this problem has the same simple structure as the **G** matrix.

Elliptic equations with variable coefficients give variable elements in the matrix which in general will be non-symmetric. The work for solving the function from the triangular matrices will be the same as for Poisson's equation. Self-adjoint equations give a symmetric matrix if the variable coefficients are tabulated in the half-points. Let the equation be

$$(a \cdot u_x)_x + (b \cdot u_y)_y = 0 \qquad u_x = \frac{\partial u}{\partial x} \text{ etc.}$$

where the functions a and b are functions of x and y only. Then, the corresponding difference equation is

$$\begin{aligned} &- b_{j-1,k} \cdot u_{j-1,k} - a_{j,k-1} \cdot u_{j,k-1} + \\ &+ (b_{j-1,k} + a_{j,k-1} + a_{jk} + b_{jk}) \cdot u_{jk} - \\ &- a_{jk} \cdot u_{j,k+1} - b_{jk} \cdot u_{j+1,k} = 0 \end{aligned}$$

Fig. 3 explains the index notation.

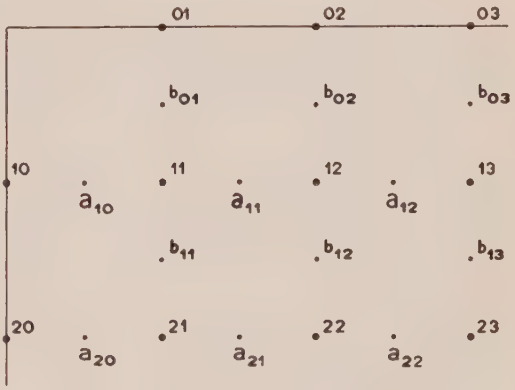

Fig. 3. Numbering for self-adjoint equations.

The biharmonic equation is an example of an equation of the fourth order that can be solved conveniently by triangular matrices. The corresponding difference equation gives $2s + 1$ non-vanishing diagonals where, as usual, s denotes the number of points per row.

13. *n*-dimensional problems

The matrix **G** will for Poisson's equation contain twice as many non-vanishing diagonals around the head diagonal as there are dimensions. For example, the matrix for a parallelepiped of cubic net is

$$\mathbf{G}_3 = \begin{bmatrix} \mathbf{G}_2 - \mathbf{I}_2 & \mathbf{O} & \mathbf{O} & \dots & & \\ -\mathbf{I}_2 & \mathbf{G}_2 - \mathbf{I}_2 & \mathbf{O} & \dots & & \\ \mathbf{O} & -\mathbf{I}_2 & \mathbf{G}_2 - \mathbf{I}_2 & \dots & & \\ & & - - - & & & \\ \mathbf{O} & \mathbf{O} & \mathbf{O} & \mathbf{O} & \dots & -\mathbf{I}_2\ \mathbf{G}_2 \end{bmatrix}$$

where $\mathbf{I}_2$ is a unit matrix of the r^{th} order and $\mathbf{G}_2$ means the matrix

$$\mathbf{G}_2 = \begin{bmatrix} \mathbf{D}_2 - \mathbf{I}_3 & \mathbf{O} & \mathbf{O} & \dots & & \\ -\mathbf{I}_3 & \mathbf{D}_2 - \mathbf{I}_3 & \mathbf{O} & \dots & & \\ \mathbf{O} & -\mathbf{I}_3 & \mathbf{D}_2 - \mathbf{I}_3 & \dots & & \\ & & - - - & & & \\ \mathbf{O} & \mathbf{O} & \mathbf{O} & \mathbf{O} & \dots & -\mathbf{I}_3\ \mathbf{D}_2 \end{bmatrix}$$

where $\mathbf{I}_3$ is a unit matrix of the s^{th} order and $\mathbf{D}_2$ means a matrix related to **D**.

$$\mathbf{D}_2 = \begin{bmatrix} 6 & -1 & 0 & 0 & \dots & & \\ -1 & 6 & -1 & 0 & \dots & & \\ 0 & -1 & 6 & -1 & \dots & & \\ & & - - & - & & & \\ 0 & 0 & 0 & 0 & \dots & -1 & 6 \end{bmatrix}$$

The inverse can be derived in a similar way as we did for rectangular regions. We also can find a procedure for solving u that corresponds to equations (24) and (25).

14. Non-linear equations

For non-linear equations we often can use a linearized solution as a first approximation. Then, we add successive corrections to this approximation by solving a linearized perturbation. This equation gives matrices of the kind we have considered.

Acknowledgment

The writer wishes to acknowledge the benefit he has received from many stimulating discussions about these problems with mr G. Dahlquist at the Swedish Board of Computing Machinery.

REFERENCES

Bodewig, E., 1947: Bericht über die verschiedenen Methoden zur Lösung eines Systems linearer Gleichungen mit reellen Koeffizienten. *Proc. Kon. Ned. Akad. v. Wetensch.* vol. L, nr 8, pp. 930—941, nr 9, pp. 1105—1116.

Charney, J. G., Fjørtoft, R., and v. Neumann, J., 1950: Numerical integration of the barotropic vorticity equation. *Tellus*, **2**, pp. 237—254.

Collatz, L., 1951: *Numerische Behandlung von Differentialgleichungen.* Berlin, Springer-Verlag. p. 205 ff. and p. 269 ff.

Courant, R., Friedrichs, K., und Lewy, H., 1928: Über die partiellen Differenzengleichungen der mathematischen Physik. *Math. Ann.*, 100, pp. 32—74.

Hyman, M., 1952: Non-iterative numerical solution of boundary-value problems. *Appl. Sci. Res.*, **2** (B), nr 5, pp. 325—351.

Laasonen, P., 1948: Über die erste und zweite Randwerteaufgabe der präharmonischen und harmonischen Funktionen. *Ann. Acad. Sci. Fennicae*, ser. A, nr 40, 28 pp.

Moskovitz, D., 1944: The numerical solution of Laplace's and Poisson's equations. *Quart. of Appl. Math.*, **2** pp. 148—163.

Platzman, G., 1952: Some remarks on high-speed automatic computers and their use in meteorology. *Tellus*, **4**, pp. 168—178.

Rutherford, D. E., 1946: Some continuant determinants arising in physics and chemistry. *Proc. Roy. Soc. Edinburgh*, **62** sec. A, pp. 229—236.

Southwell, R. V., 1946: *Relaxation methods in theoretical physics.* Oxford. Clarendon Press, 248 pp.

Stiefel, E., 1952: Ueber einige Methoden der Relaxationsrechnung. *Zeitsch. für Angew. Math. und Physik*, **3**, pp. 1—33.

Stöhr, A., 1950: Über einige lineare partielle Differenzengleichungen mit konstanten Koeffizienten. *Mathematische Nachrichten*, **3**; Erster Teil pp. 208—242. Zweiter Teil pp. 295—315. Dritter Teil pp. 330—357.

Turing, A. M., 1948: Rounding-off errors in matrix processes. *Quart. J. of Mech. and Appl. Math.*, **1**, pp. 287—308.

Zurmühl, R., 1950: *Matrizen.* Berlin. Springer-Verlag. pp. 248—285.

Letters to the Editor

Jet Streams and Clear Air Turbulence

Dear Sir,

Dr Berggren (1952) has given interesting frontal analyses of three occasions of jet stream over western Europe and has put forward the hypothesis that most occurrences of clear air turbulence in the upper troposphere and lower stratosphere are associated with fronts.

Frontal analyses are necessarily subjective and influenced by the personal views of the analyst and it is, therefore, not surprising that I do not agree with some aspects of Berggren's analyses. For example, the level of the tropopause over Downham Market in Berggren's figure 6 does not agree with that published in the Upper Air Section of the British Daily Weather Report, where it is given as 260 mb; the fall of temperature between 319 and 260 mb, i.e. above Berggren's tropopause, was 7.9° C. giving a temperature gradient of — 5.8° C. per kilometre, which would seem tropospheric rather than stratospheric. There are other minor points of disagreement.

Frontal analysis in the upper troposphere is difficult, as has been pointed out by Murray and Johnson (1952). Thus, though the idea of tracing the frontal zone into the stratosphere is attractive, yet because the evidence for such zones rests on one, or at most two, radiosonde ascents in each case and because of the subjective element in the analysis illustrated above, I prefer to await the promised publication of the complete analysis before accepting the stratospheric fronts as significant.

There is no doubt that clear air turbulence in the upper troposphere is sometimes associated with frontal zones. Hislop (1951) in his table I lists four cases which were definitely so associated and there may well have been others among the number listed as "doubtful". In analysing other occurrences of turbulence I have recognized many as occurring in frontal zones (Bannon, 1952). Undoubtedly, however, turbulence may occur outside such frontal zones. A good example is the Flight VR60 of Hislop's table I where part of the turbulent layer was in a frontal zone and part above it in the strong vertical shear under a jet stream core.

Berggren's extension of the front through the tropopause entails a definition of front in that region by strong horizontal shear. His hypothesis, that most cases of clear air turbulence are associated with a frontal zone, therefore implies with his definitions that the clear air turbulence is associated with either vertical or horizontal shear or both. This does not seem to me to be any advance on previous ideas (Harrison, 1950; Bannon, 1951, a, b, c). "Front" is merely a name given to a boundary zone; it does not imply any increased tendency towards turbulence except as such a zone is associated with the usual turbulence-producing agencies, shear and convection.

For a proper investigation of the causes of clear air turbulence it is not sufficient, except perhaps as a demonstration of a possible forecasting tool, merely to associate the phenomenon with a loosely-defined attribute of the meteorological variables called a "front". Even if the great majority of occasions of turbulence were found to be associated with fronts, which is not the case, it would still be necessary to study the fundamental features of each occasion, viz. vertical and horizontal shear and lapse rate of temperature. As Hislop (1951, Section 6.4) has pointed out, it is the relative scarcity of observations of clear air turbulence and the lack of adequate measures of the meteorological parameters, shear and temperature lapse rate, which are restraining progress in this field.

I should like to draw attention to a misprint in the footnote on page 50 of Berggren's paper. The dimensions of eddies causing bumps to Spitfire and Mosquito aircraft are thought to be from 15—150 metres and not 15—500 metres, as stated.

Yours faithfully,

T. K. Bannon

Harrow, Middlesex

September 15, 1952

REFERENCES

Bannon, J. K., 1951:

a) Meteorological Aspects of Turbulence affecting Aircraft at High Altitude. *Met. Office London, Prof. Notes*, No. 104, 16 pp.

b) Severe Turbulence encountered by Aircraft near Jet Streams, *Met. Mag.*, **80**, pp. 262—269.

c) Turbulence at High Altitude: Further Meteorological Analysis. *Met. Mag.*, **80**, pp. 331—332.

BANNON, J. K., 1952. Weather Systems associated with some occasions of Severe Turbulence at High Altitude. *Met. Mag.*, **81**, pp. 97—102.

BERGGREN, R., 1952. The Distribution of Temperature and Wind connected with active tropical air in the High Troposphere and some remarks concerning Clear Air Turbulence at High Altitude. *Tellus*, **4**, pp. 43—53.

HARRISSON, 1950. Some characteristics of the Upper Level Low and Jet Streams. *United Air Lines Circular*, No. 34.

HISLOP, G. S., 1951. Clear Air Turbulence over Europe. *Journal of the Roy. Aero. Soc.*, **55**, pp. 185—225.

MURRAY, R. and JOHNSON, D. H., 1952: Structure of the upper Westerlies; a Study of the Wind Field in the Eastern Atlantic and Western Europe in September 1950. *Q. J. Roy. Met. Soc.*, **78**, pp. 186—199.

Reply

Dr Bannon emphasizes that it is necessary to study the fundamental features of each occasion with clear air turbulence, viz. vertical and horizontal shear and lapse rate of temperature. I agree completely with him in this respect, and that is the reason why I have mentioned this special phenomenon in my paper. As is pointed out there the distance between the stations of the present radiosonde networks is often not of the same order as that of the phenomenon one is investigating. For that reason it is—for the time being—necessary to use some sort of a model. Here the concept of front enters the picture. If we study the frontal model in detail when the available material is most favourable and make as many generalizations as are justified by the data, then we may use the frontal model to advantage in such cases where the material is sparse. A specific example may clarify what I mean.

It is generally accepted—as can also be seen in Bannon's letter—that horizontal wind shear is of great importance in many cases with clear air turbulence. In his paper BANNON (1951 a) tries to correlate the appearance of these two items and is taking the horizontal shear given by the wind-observing stations in Great Britain. I dare say that my paper (as well as many others)—and a second one which will soon appear as "band I, nr 24", of "Arkiv för Geofysik"—has made it clear that the wind distribution is anything but linear over such great distances as those ordinarily existing between radiosonde stations. We have no possibility whatsoever to get the true value of the shear by linear interpolation between stations, but—and this is one of the main points in the second part of my paper—the frontal model gives a possibility to get better values, even if not the right ones. Furthermore it is easier—for instance in a vertical cross-section—to extrapolate or interpolate the wind field with the help of a model then to do it without one. It is certainly rather dangerous to do so, but if one is well aware of this fact, the danger can be diminished.

Bannon mentions a paper by MURRAY and JOHNSON (1952) stating that frontal analysis in the upper troposphere is difficult. I certainly agree with that statement, but this gives us no reason not to use the concept of front also in this analysis. The fact that the frontal analysis may be carried through also in the upper troposphere is well established by many writers, among others by PALMÉN (1951) and GODSON (1951).

It is right that table I in Hislop's paper gives only 4 cases with clear air turbulence connected with fronts. But the table gives only 6 cases where it is definitely stated that no front was associated. For the remaining 10 cases the connection is stated as 'doubtful'. Considering the difficulty of analysing fronts in the upper troposphere one is justified to assume that a number of front-cases are hidden in this group, as Bannon also does.

It do not quite understand Bannon's statement in paragraph four. First he says that clear air turbulence in the upper troposphere is *sometimes* associated with frontal zones, and then he states that he has recognized *many* such cases as occurring in frontal zones. I certainly agree with his last statement.

As to the connection with fronts I would like to review a remark made by Farquharson in a discussion meeting held in London February 1952, on "Meteorology and the operation of jet aircraft" (see *Quart. Journ.* vol. **78** no. 337 p. 451). He states that in the forecasting of clear air turbulence the Meteorological Office at Dunstable succeeded in 22 cases out of 24 by using the observed connection between clear air turbulence and the jet stream. Is it not so, however, that talking about the displacement and the behaviour of the jet stream is equivalent in many (most?) cases with the use of the frontal model?

It was not the purpose of my paper to touch directly the question of the *causes* of clear air turbulence. I wanted primarily to discuss the treatment of the involved meteorological parameters.

As far as I can see, the difference of opinion concering the height of the tropopause in my fig. 6 is not an important question. It is quite right that the layer immediately above the tropopause in my case shows a vertical temperature gradient

of $-5.8°$ C km^{-1}, but the gradient in the layer below the tropopause is $-7.3°$ C km^{-1}. It is thus a marked difference between the layers. It must not be forgotten that the definition of the tropopause used by the Meteorological Office in the daily service is to some extent arbitrary and formal and may sometimes lead to wrong conclusions.

Finally I want to thank Dr Bannon for the interest he has shown in my paper and I am glad that a discussion has arisen out of it.

ROY BERGGREN

REFERENCES

PALMÉN, E., 1951: The Aerorology of Extratropical Cyclones. Compendium of Meteorology, *Am. Met. Soc.*, Boston, p. 599—620.

GODSON. W. L., 1951: Synoptic Properties of Frontal Surfaces, *Q. J. Roy. Met. Soc.*, **77**. pp. 633—653.

Dear Sir,

The article "The Distribution of Temperature and Wind Connected with Active Tropical Air in the Higher Troposphere and Some Remarks Concerning Clear Air Turbulence at High Altitude" by Roy Berggren in the February 1952 issue of Tellus, has recently been drawn to my attention.

I do not wish to comment here on Mr Berggren's claim that clear air turbulence is essentially associated with the presence of a frontal system in the upper air, as I understand that this will be covered in a separate communication from Mr Bannon.

However, I would like to point out that in my view figure 10 in my paper to the Royal Aeronautical Society (mentioned on page 52 of Mr Berggren's paper) does not give the impression that the turbulent area is associated with anticyclonic wind shear. In fact, my interpretation of the figure is that, if anything, the shear is cyclonic. In any case, no mention of the character of the wind shear is mentioned in the text. The figure shown is merely illustrative of typical conditions and rather than show a chart which we might have prepared specially, I preferred to use the chart as published in the Daily Weather Report.

Yours faithfully,
G. S. HISLOP.
Ruislip, Middlesex
11 September 1952

Reply

Dr Hislop is opposing to my comments on one of his figures of the paper cited by me. I do not quite understand his objections and for this reason I shall give a short discussion of the sign of the horizontal wind shear on his figure.

The radiosonde station Liverpool (03322) gives the wind 200° 129 knots at 300 mb at a height of 29,200 feet. Station Larkhill (03743) gives 200° 115 knots and the height 29,700 feet. Isotach analyses by many authors (e.g. NEWTON, PHILLIPS, CARSON, and BRADBURY, 1951) give as a rule the jet centre quasi-parallel to the isohypses, in cases without strong accelerations. Thus, in this case, the centre of the strong winds must pass to the west of the indicated turbulent area. In any case, I consider it impossible to get cyclonic shear through this area.

The most serious objection, however, to the discussed figure is the time difference between the chart and the observation of clear air turbulance. As I pointed out in my paper the chart time is 0300 GCT, while the observation was made at 1300 GCT. Studying the change of the wind from 0300 to 1500 GCT one gets the following interesting values. At 350 mb the Liverpool wind changed from 200° 122 knots to 230° 78 knots, while the corresponding values for Larkhill were 200° 111 knots and 200° 102 knots, respectively. The Downham Market (03476) sounding gave at 1500 GCT 210° 109 knots (unfortunately the 0300 GCT sounding did not reach the 350 mb level).

This distribution of the wind makes it quite clear that the horizontal (isobaric) wind shear was cyclonic at the time of observation over the area where clear air turbulence was observed.

I cannot quite understand the reason to publish a 0300 GCT chart to illustrate the conditions at 1300 GCT, when there are soundings made at 1500 GCT. I know that the 300 mb charts for that time were not published in the Upper Air Section, but that is not a sustainable explanation for the choice.

It is quite true that nothing specific is said in Hislop's paper about the sign of the shear, but this question has been brought up in later papers. For that reason I considered it important to make these remarks, as Hislop's paper will be classic in this field and is and will be read by many persons.

ROY BERGGREN.

REFERENCE

NEWTON, C. W., PHILLIPS, N. A., CARSON, J. E. and BRADBURY, D. L., 1951: Structure of Shear Lines near the Tropopause in Summer. *Tellus*, **3**, p. 154—171.

Direct observation of upward leaders from the earth during a thunderstorm in South Africa

Dear Sir,

The following observation was made at Hluhlune, Zululand, Souh Africa, December 11, 1951, and might be of interest to you.

Around six o'clock in the afternoon a very severe thunderstorm began. As usual in South Africa the storm came very suddenly, she sky turned black and the lightning strokes came with very short intervals from all directions. They blinded one's eyes completely. A very heavy shower followed with big hailstones. We were living up on a hill and there are mountains and hills all around the horizon: the northern parts of big Dragon-mountains. I was standing at the window watching, when the storm culminated around seven o'clock. Suddenly I saw a series of lightning strokes, that seëmed to come straight up from te earth. It looked exceedingly strange. I saw them absolutely clearly and they seemed to be broader at the base and became more narrow upwards. Then a very intense lightning strokes blinded me completely and when I looked out again afterwards, the lightning strokes from the earth had disappeared.

Yours sincerely

KARIN FJÄLLBÄCK HOLMGREN

NOTE

During the week of October 13—18, 1952, a meteorological conference was held at the Institute of Meteorology, University of Stockholm under the leadership of professor C.-G. Rossby. The purpose of this conference was twofold. First it was felt important to retain close contacts with other groups in Europe and the USA in the field of numerical forecasting, which has been the main research subject of the institute during the last year. Secondly, the conference represented an attempt to make a survey of the present stage of our knowledge in the fields of cloud physics and the cycle of fixed nitrogen in the atmosphere, in order to formulate preliminary research programs in these two fields. It is hoped that those two subjects will be taken up for detailed study in a near future at the institute and in close collaboration with other institutions.

The titles of the lectures are listed below. Some of them are published in this issue, others will appear in later issues of Tellus.

LECTURES

Section I. Synoptic-aerological problems.

Prof. E. Palmén, University of Helsinki: Comments on the cyclone problem.

Dr C. W. Newton, University of Chicago: Structure of the wind field over the United States in a summer situation.

Section II. Numerical Forecasting.

Dr J. Charney, Institute for Advanced Study, Princeton: The numerical forecasting program in Princeton.

Dr R. C. Sutcliffe, Meteorological Office, Dunstable: Some preliminary experiments in numerical computations at the meteorological office, Dunstable.

Dr E. Eady, Imperial College of Science, London: Some problems of numerical forecasting.

Dr A. Eliassen, Institutt for vaer- og klimaforskning, Blindern, Oslo: Tendency computations by means of a $2^1/_2$-dimensional model.

Dr E. Lingelbach, German Weather Service, Bad Kissingen: A report on some 3-dimensional computations performed at Bad Kissingen.

Fil. lic. B. Bolin, University of Stockholm: Comments on the testing of atmospheric models.

Dr J. Charney, Institute for Advanced Study, Princeton: Remarks on three and four parameter models.

Prof. J. van Mieghem, University of Brussels: Energy conversions in the atmosphere on the scale of the general circulation. Problems of the International Year 1957—58 and the spacing of aerological stations.

Civilingenjör O. Karlqvist, Computor Project, Stockholm: A noniterative method for solving elliptic boundary value problems.

Fil. lic. G. Arnason, University of Stockholm: Example of temperature and pressure tendency computations for the troposphere with a simplified baroclinic model.

Section III. Cloud Physics.

Dr V. Schaefer, General Electric Company, Schenectady: I. Clouds in the laboratory and in the sky.

Dr N. Herlofson, Royal Institute of Technology, Stockholm: Report on Australian researches in cloud physic- and cloud modification.

Dr Whittle, University of Uppsala: Statistical methods for evaluation of cloud seeding operations.

Mr F. H. Ludlam, Imperial College of Science, London: Natural and artificial showers.

Dr C. Junge, Universitätsinstitut für Meteorologie und Geophysik, Frankfurt am Main: Particle-size distribution of condensation and sublimation nucleii.

Prof. T. Bergeron, University of Uppsala: Rain mechanisms in the temperate zone and the possibility of influencing them.

Dr C. W. Newton, University of Chicago: Effect of vertical wind shear on thunderstorm and tornado formation.

Dr V. Schaefer, General Electric Company, Schenectady: II. The modification of clouds in the free atmosphere.

Dr V. Schaefer, General Electric Company, Schenectady: III. An experimental approach to the study of the lower atmosphere.

Section IV. The Nitrogen Cycle in the Atmosphere.

Laborator H. Egner, Royal Institute of Agriculture, Ultuna: On the role of the atmosphere in the circulation of nutrient elements.

Agr. lic. E. Erikson, Royal Institute of Agriculture, Ultuna: On the origin of atmospheric salts.

Dr C. Junge, Universitätsinstitut für Meteorologie und Geophysik, Frankfurt am Main: Concentration of various aerosols in the atmosphere.

Dr A. Ångström, Swedish Meteorological and Hydrological Institute, Stockholm: On the fixed nitrogen content in precipitation, its geographical distribution and seasonal variation in Sweden.

Fil. lic. W. Schytt, University of Stockholm: On the fixed nitrogen content of ice samples from Antarctica and from a Norwegian glacier.

Dr O. Arrhenius, Grödinge: Chemical denudation and soil destruction in Sweden.

INDEX

Italics indicate titles of articles or shorter contributions. Asterisks indicate notes and correspondence.

ALAKA, M. A.: *On the Budget of Angular Momentum in the Zone between Equator and 30° N*, 324.

ÅNGSTRÖM, A.: *On the Content of Nitrogen (NH_4-N, and NO_3-N) in atmospheric precipitation*, 31.

ÅNGSTRÖM, A.: *On the Content of Nitrogen in Atmospheric Precipitation*, 271.

Anntenna, rotating, Hellgren, Meos, 249

ÁRNASON, G.: *A Baroclinic Model of the Atmosphere Applicable to the Problem of Numerical Forecasting in three Dimensions*, 356.

ARRHENIUS, O.: *The Chemical Denudation of the Soil*, 307.

VON ARX, W.: *Notes on the Surface Velocity Profile and Horizontal Shear across the Width of the Gulf Stream*, 211.

VON ARX, W.: *A Laboratory Study of the Wind-driven Ocean Circulation*, 311.

Aurorae, localization, Hellgren, Meos, 249.

*BANNON, T. K.: *Jet Streams and Clear air Turbulence*, 385.

BERGGREN, R.: *The Distribution of Temperature and Wind Connected with Active Tropical Air in the Higher Troposphere and Some Remarks Concerning Clear Air Turbulence at High Altitude*, 43.

*BERGGREN, R.: *Jet Streams and clear Air Turbulence, Reply*, 386, 387.

BOLIN, B.: *Report on a Conference on the Application of Numerical Methods in Forecasting Atmospheric Flow Patterns*, 141.

BREIER, G. W.: *Forty-Year Sea Level Pressure and Sunspots*, 262.

Chlorid, content in precipitation, Eriksson, 280.

Circulation, atmospheric, van den Dungen, Cox, van Mieghem, 1; van Mieghem, 334.

Circulation, ocean, von Arx, 311.

Clear Air Turbulence, Berggren, 43; *Bannon, 385; *Berggren, 386; *Hislop, 387; *Berggren, 387.

Clouds, convection, Starr Malkus, 71.

Clouds, nuclei, Ogiwara, Okita, 233.

Computer, high-speed, Platzman, 168.

*Conference, meteorological, 141; 389.

Configuration, upper mean flow, Wippermann, 112.

Convection, clouds, Starr Malkus, 71.

Convection, from boundary source, Rouse, Yih, Humphreys, 201.

Convection, gravitational, Rouse, Yih, Humphreys, 201.

COX, J. F.: *Les fluctuations saisonnières de la rotation du globe terrestre et la circulation atmosphérique générale*, 1.

Denudation, soil, Arrhenius, 307.

Development, atmospheric disturbances, McVittie, 8.

Difference equation, elliptic, Karlqvist, 374.

VAN DEN DUNGEN, F. H.: *Les fluctuations saisonnières de la rotation du globe terrestre et la circulation atmosphérique générale*, 1.

EADY, E. T.: *Note on Weather Computing and the so-called 2 1/2-dimensional Model*, 157.

Earth, gravity, Saxov, 137.

Earth, rotation, Cox, van den Dungen, van Mieghem, 1.

ELIASSEN, A.: *Simplified Models of the Atmosphere, Designed for the Purpose of Numerical Weather Prediction*, 145.

Energy, conversion, van Mieghem, 334.

Energy, kinetic, van Mieghem, 68; Kuo, 70.

ERIKSSON, E.: *Composition of Atmospheric Precipitation*, I, 215.

ERIKSSON, E.: *Composition of Atmospheric Precipitation*, II, 280.

Filaments, sun, Öhman, Lodén, 241.

FJØRTOFT, R.: *On a Numerical Method of Integrating the Barotropic Vorticity Equation*, 179.

Flare, sun, Öhman, Lodén, 241.
Flow, mean, Wippermann, 112.
Flux, angular momentum, Starr, White, 118; Palmén, Alaka, 324; Starr, White, 332.
Forecasting, numerical, Staff members, University of Stockholm, 21; *Bolin, Newton, 141; Eliassen, 145; Eady, 157; Fjørtoft, 179; Lönnqvist, 195; Árnason, 356.

Gravity, variation, Saxov, 137.

Hellgren, G.: *Localization of Aurorae with 10 m High Power Radar Technique, using a Rotating Antenna*, 249.
*Hislop, G. S.: *Jet Streams and Clear Air Turbulence*, 387.
Högberg, L.: *On the Content of Nitrogen (NH_4-N, and NO_3-N) in atmospheric precipitation*, 31.
Högberg, L.: *On the Content of Nitrogen in atmospheric Precipitation in Sweden*, II, 271.
Hovmöller, E.: *A Comparison between Observed and Computed Winds with Respect to Their Applicability for Vorticity Computations*, 126.
Hultqvist, B.: *Calculation of the Ionization due to Radioactive Substances in the Ground*, 54.
Humphreys, H. W.: *Gravitational Convection from a Boundary Source*, 201.

Iodine, content in precipitation, Eriksson, 280.
Ionization, Hultqvist, 54.

Jet stream, *Bannon, 385; *Hislop, 387; *Berggren, 386, 387.

Karlqvist, O.: *Numerical Solution of Elliptic Difference Equation by Matrix Methods*, 374.
Kinetic energy, *van Mieghem, 68; *Kuo, 70.
*Kuo, H. L.: *Comment on a note on the Kinetic Energy Balance of Zonal Wind Systems, Reply*, 70.

Landmark, B.: *Determination of the Sense of Polarization of the Magnetio-Ionic z-Component*, 319.
Lehnert, B.: *Experiments on Non-Laminar Flow of Mercury in Presence of a Magnetic Field*, 63.
Lodén, L. O.: *Sunspot Areas, Flares and Filaments observed at the Stockholm Observatory in the years 1950 and 1951*, 241.
Lönnqvist, O.: *To the Comparison between Numerical Methods and Methods Now in Use for Forecasting Meteorological Charts*, 195.

Magnetic field, flow, Lehnert, 63.
Magneto-Ionic z-component, Landmark, 319.
Matrix methods, Karlqvist, 374.
McVittie, G. C.: *Theory of Development and of Thickness Patterns*, 8.
Meos, J.: *Localization of Aurorae with 10 m High Power Radar Technique, using a Rotating Antenna*, 249.
Van Mieghem, J.: *Les fluctuations saisonnières de la rotation du globe terrestre et la circulation atmosphérique générale*, 1.
*Van Mieghem, J.: *Comment on a Note on the Kinetic Energy Balance of Zonal Wind Systems*, 68.
Van Mieghem, J.: *Some Remarks on the Angular Momentum Balance in the Atmosphere*, 135.
Van Mieghem, J.: *Energy Conversions in the Atmosphere on the Scale of the General Circulation*, 334.
Model, barotropic, Staff members, University of Stockholm, 21; Fjørtoft, 179.
Model, baroclinic, Eliassen, 145; Eady, 157; Árnason, 356.
Model, numerical, forecasting, Staff members, University of Stockholm 21; Eliassen, 145; Eady, 157; Fjørtoft, 179; Árnason, 356.
Momentum, balance, Van Mieghem, 135; Palmén, Alaka, 324.
Momentum, flux, Starr, White, 118; Palmén, Alaka, 324; Starr, White, 332.

*Newton, H.: *Report on a Conference on the Application of Numerical Methods in Forecasting Atmospheric Flow Patterns*, 141.
Nitrogen, content of precipitation, Ångström, Högberg, 31; Eriksson, 215; Ångström, Högberg, 271; Eriksson, 280.
Nitrogen, cycle, Virtanen, 304.
Nitrogen, fixation, Virtanen, 304.
Non-laminar flow, Lehnert, 63.
Nuclei, cloud, Ogiwara, Okita, 233.
Nuclei, fog, Ogiwara, Okita, 233.

Ocean, circulation, von Arx, 311.
Ogiwara, S.: *Electron-Microscope Study of Cloud and Fog Nuclei*, 233.
Öhman, Y.: *Sunspot Areas, Flares and Filaments observed at the Stockholm Observatory in the Years 1950 and 1951*, 241.
Okita, T.: *Electron-Microscope Study of Cloud and Fog Nuclei*, 233.

Palmén, E.: *On the Budget of Angular Momentum in the Zone between Equator and 30° N*, 324.
Platzman, G. W.: *Some Remarks on High-Speed Automatic Computers and their Use in Meteorology*, 168.

PLATZMAN, G. W.: *Starr's Invariant*, 352.
Polarization, Landmark, 319.
Precipitation, Composition, Eriksson, 215; Eriksson, 280.
Precipitation, Nitrogen content, Ångström, Högberg, 31; Ångström, Högberg, 271.
Pressure, sea-level, Brier, 262.

QUENEY, P.: *Les ondes atmosphériques considérées comme associées aux discontinuités du tourbillon*, 88.

Radar, for aurorae, Hellgren, Meos, 249.
Radioactive substance, Hultqvist, 54.
Rotation, earth, Cox, van den Dungen, van Mieghem, 1.
ROUSE, H.: *Gravitational Convection from a Boundary Source*, 201.

SAXOV, S.: *The Variation of Gravity within the Earth*, 137.
Shear, Gulf Stream, von Arx, 211.
Soil denudation, Arrhenius, 307.
STARR, V. P.: *Meridional Flux of Angular Momentum in the Tropics*, 118.
STARR, V. P.: *Two Years of Momentum Flux Data for 31° N*, 332.
STARR MALKUS, J.: *Recent Advances in the Study of Convectic Clouds and their Interaction with the Environment*, 71.
Starr's Invariant, Platzman, 352.
Sulfur, content in precipitation, Eriksson, 280.
Sunspot, Öhman, Lodén, 241.
Sunspot, meterological effects, Brier, 262.

Temperature, higher troposphere, Berggren, 43.
Thickness pattern, McVittie, 8.
Tropical air, Berggren, 43.
Turbulence, clear air, Berggren, 43; *Bannon, 385; *Berggren, 386; *Hislop, 387; *Berggren, 387.
Turbulence, discontinuities, Queney, 88.

UNIVERSITY OF STOCKHOLM, STAFF MEMBERS: *Preliminary Report on the Prognostic Value of Barotropic Models in the Forecasting of 500 mb Height Changes*, 21.

Velocity profile, Gulf Stream, von Arx, 211.
VIRTANEN, A. I.: *Molecular Nitrogen Fixation and Nitrogen Cycle in Nature*, 304.
Vorticity, computation, Hovmöller, 126; Fjørtoft, 179.
Vorticity equation, Staff members, 21; Fjørtoft, 179.

Waves, atmospheric, Queney, 88.
WHITE, R. M.: *Meridional Flux of Angular Momentum in the Tropics*, 118.
WHITE, R. M.: *Two Years of Momentum Flux Data for 31° N*, 332.
Wind, computed, Hovmöller, 126.
Wind, high troposphere, Berggren 43.
Wind, observed, Berggren, 43; Hovmöller, 126.
WIPPERMANN, F.: *Die Konfiguration mittlerer Höhenströmungsfelder und ihre Ursachen*, 112.

YIH, C. S.: *Gravitational Convection from a Boundary Source*, 201.